

Investigating Nucleoside Analogue Inhibition of Coronavirus Replication

By

Maria Lucia-Karwoski Agostini

Dissertation

Submitted to the Faculty of the
Graduate School of Vanderbilt University
in partial fulfillment of the requirements
for the degree of

DOCTOR OF PHILOSOPHY

in

Microbiology and Immunology

October 31, 2019

Nashville, Tennessee

Approved:

Kristen M. Ogden, Ph.D.

Eric P. Skaar, Ph.D., M.P.H.

F. Peter Guengerich, Ph.D.

John Karijolich, Ph.D.

Mark R. Denison, M.D.

To Margaret Rose, the one who taught me to persist against all odds.

ACKNOWLEDGEMENTS

I have learned so much throughout the course of my graduate studies, but these lessons have not come from books and experiments alone. Indeed, much of my personal and professional growth is a direct result of the people I have met along the way. Each and every person I have interacted with has shaped this journey, and I am extremely fortunate to have had the opportunity to learn and grow from so many outstanding people. This accomplishment, in part, belongs to each of you, and I will forever be thankful for the roles you have played in this adventure.

First, to the members of the Denison lab. These people have served as my scientific family over the past few years. The friendships I have shared with you have made the rough days that much easier to handle, and I can't thank you enough. To Michelle, thank you for managing the lab and always sharing your love of Nashville. To Erica, thank you for your never-ending kindness, your unwavering support, and for shared dietary choices. To Clint, thank you for always taking the time to answer my questions, being the staple behind lab lunches, and gracing me with the knowledge of the story basket. To Litton, thank you for teaching me about mentorship and for your impeccable social planning. To Xiaotao, your institutional knowledge and magic hands keep this place afloat, and I can't thank you enough for always being there to support all of the graduate students without complaints. To Nicole, thank you for always taking the time to show me that I was never alone and for letting some of your feisty spirit rub off on me. To Brett, thank you for your guidance and lava. To Kevin, thank you for sharing the suffering and for your lessons on

kilts. To Jennifer, thank you for teaching me your “geek” ways and for taking on the mantle of the young one. To Laura, thank you for believing I existed, keeping the sass alive, and teaching me countless things about professionalism. To Tia, thank you for taking on some of the challenges this project had to offer and for taking time to listen to my advice. To Andrea, thank you for your organization, keeping my eyes open to possibilities, and showing me how to properly peel an orange. To Jim, thank you for your careful preparation and your willingness to always provide suggestions that were the product of considerable thought. To Selene and Thayer, thanks for keeping things light and reminding me of the undergraduate struggles in the most hilarious of ways. Specific thanks are in order to Clint and Erica, as this dissertation work would not have been possible without your initial efforts to get this project off the ground.

The Denison lab would not be the Denison lab without my mentor, Dr. Mark Denison. I can’t thank you enough for the opportunity to work on such collaborative projects with extensive implications. I’ve learned so much from these interactions, and I appreciate your trust in me to move these projects forward. But, most importantly, thank you for your infectious enthusiasm for science; on my most pessimistic days, I definitely needed it. You’ve pushed me to think in ways that do not come naturally to me and were not comfortable, and that has only helped me to grow personally and professionally.

I am fortunate to have worked with many wonderful scientists to advance these projects. First, I want to thank the various departments I have been affiliated with during my time

at Vanderbilt University. The Vanderbilt Institutes for Chemical Biology, the Pathology Microbiology and Immunology Department, and the Vanderbilt Institute for Infection, Immunology, and Inflammation have each served to enhance my training. Special thanks to the Pediatric Infectious Diseases Group for your comradery. I also want to thank the multiple collaborators that have worked on this project; this work is only possible because of your contributions. To my collaborators at Gilead Sciences: my interactions with each of you have taught me something new. I particularly want to thank Joy and Rob for walking me through experimental design and analysis during the early years of my graduate training. Much of what I know about drug discovery and development has come from interfacing with your expertise. To my collaborators at the University of North Carolina-Chapel Hill, thank you for all of your help and for always welcoming me into your circles at antiviral conferences. Last, but certainly not least, thank you to my collaborators at the Emory Institute for Drug Development. You have continued to expand my understanding and perspective of drug discovery and development. I have learned so much by working with each and every one of you, and I am extremely lucky to have had your guidance along the way.

This work would not have been possible without the funding that has supported it. Thank you to the Antiviral Drug Discovery and Development Center 5U19AI109680 (MRD), 1U19AI142759 (MRD) as well as HHSN272201500008C, F31AI133952 (MLA), R01AI108197 (MRD) and R01AI132178 (MRD) all funded by the National Institutes of Health. I want to thank the Chemical Biology of Infectious Diseases training grant

5T32AI089554 (MLA) along with its director Dr. Eric Skaar for granting me the unique opportunity to spend two months interning at Gilead Sciences. I particularly want to thank Rob Jordan for your instrumental role in setting up this opportunity. I can't thank you enough for the time and effort you put into researching how to make this internship happen. You, along with the rest of the Discovery Virology team, made the experience truly worthwhile and served as excellent mentors to facilitate my growth and understanding of the drug development process.

To my early research mentors, thank you for taking on an inexperienced undergraduate and making sure I was competent in some new way when I left you. Each of these research experiences have shaped who I am as a scientist, and I cannot thank you enough. My first lab experience was in the laboratory of Dr. Sreenivasa Chinni at Wayne State University. During the course of the summer I was there, I learned a tremendous amount about the successes and failures that are integral to scientific research. Thank you to this group, for taking me in despite my lack of experience, and providing me with a great base that has helped me to move forward. While I never performed research in the laboratory of Dr. Kathy Spindler, I am extremely grateful to have served as part of the lab team. I learned so much about virology, and the tightknit group showed me just how much fun I could have doing scientific research. I was also very fortunate to join the Walter Lab as an undergraduate. It was here that I began to develop independence in research and writing. I was blessed with so many amazing mentors from my undergraduate research

endeavors, and your encouragement taught me what I needed to know to move forward in a scientific career.

I have been lucky to be surrounded by wonderfully talented scientists. Thank you to my thesis committee members both past and present- Dr. Kristen Ogden, Dr. Eric Skaar, Dr. F. Peter (Fred) Guengerich, Dr. John Karijolich, and Dr. Earl Ruley- for your guidance and helpful suggestions along the way. Your suggestions and your involvement have truly pushed me to be a better, more adventurous scientist.

Graduate school is a bit like running a marathon. The journey requires a remarkable amount of endurance and you always end up running a little bit more than you expected. I have been fortunate to have had friends and family along for the literal and figurative (half) marathons I have embarked on during this journey. Thank you to my East Nasty running family, especially Alison and Caroline, for being great listeners and for helping to make the stressful times so much more enjoyable. Thank you to my IGP ladies Cherie, Karin, and Susan for being an awesome and punny lunch crew. At every step along this journey, you have been there to show me, regardless of the problem at hand, that I was never alone. Thank you to Julie, Katie, Laura, and Andrea for staying by my (figurative) side for so long despite the distance between us and making fun of the southernisms I brought home.

To Nathan, my darling fiancé, I'm sure it would have been easier for you to pursue your own dreams without having to consider mine along the way. I can't thank you enough for moving to Nashville and for the unconditional love and support you provided along the way. I wish you so many guitars, banjos, international adventures, and bikes to reward you for your efforts. To Margaret Rose, your presence and excitement at every stage of my life pushed me to get to this point. You may have only seen part of this journey, but I know I never would have made it this far without your encouragement and enthusiasm in the process. To my parents, I couldn't have achieved any of this without your love and support. I'm convinced I wouldn't be here writing this if you hadn't stressed the importance of education and hard work from an early age (and giving me Cocoa to be my support team while I was studying). Thank you for pushing me to set lofty goals, but, more importantly, thanks for always being there when things didn't quite work out as expected. Your encouragement made this journey possible, and I am forever grateful.

TABLE OF CONTENTS

	Page
DEDICATION	ii
ACKNOWLEDGEMENTS	iii
LIST OF TABLES	xiii
LIST OF FIGURES	xiv
Chapter	
I. BACKGROUND AND LITERATURE REVIEW	1
Introduction.....	1
Coronavirus disease and emergence	2
Current standard of care and clinically available therapeutic options.....	4
Coronavirus taxonomy, genome organization, and replication	5
Coronavirus antiviral strategies	14
Host targets.	16
CoV structural protein targets.	18
CoV nonstructural protein targets.	20
Clinically approved direct-acting antivirals	24
Human Immunodeficiency Virus	24
Hepatitis C Virus.....	25
Hepatitis B Virus.....	26
Herpesviruses	27
Respiratory Syncytial Virus.....	28
Influenza Virus.....	28
Nucleoside analogue antivirals	29
Chain termination.....	30
Lethal mutagenesis.	33
Additional mechanisms.	33
Summary.....	35
II. CORONAVIRUS SUSCEPTIBILITY TO THE ANTIVIRAL REMDESIVIR (GS-5734) IS MEDIATED BY THE VIRAL POLYMERASE AND THE PROOFREADING EXORIBONUCLEASE.....	37
Introduction.....	37
GS-441524 and remdesivir inhibit MHV replication.....	39
GS-441524 and remdesivir potently inhibit SARS-CoV and MERS-CoV in HAE cells	40
Remdesivir acts at early times post-infection to decrease viral RNA levels.....	42
Viruses lacking ExoN-mediated proofreading are more sensitive to treatment with remdesivir	44
Two mutations in the RdRp mediate partial resistance and restoration of RNA levels in the presence of remdesivir.....	44

Remdesivir resistance mutations impair competitive fitness of MHV	48
Mutations identified in remdesivir-resistant MHV also confer resistance in SARS-CoV	48
Remdesivir-resistant SARS-CoV is attenuated <i>in vivo</i>	50
Discussion.....	52
Potential remdesivir mechanism of action in CoVs.....	52
Mechanism of resistance to remdesivir.....	56
Remdesivir resistance is associated with a fitness cost <i>in vitro</i> and attenuation <i>in vivo</i>	59
Conclusion	59
III. β-D-N^4-HYDROXYCYTIDINE: A MUTAGEN ACTIVE AGAINST A PROOFREADING-INTACT CORONAVIRUS WITH A HIGH GENETIC BARRIER TO RESISTANCE.....	61
Introduction.....	61
NHC inhibits MHV and MERS-CoV replication with minimal cytotoxicity	62
NHC inhibition profile in CoVs is consistent with mutagenesis	65
NHC treatment increases transition mutations present across the MHV genome, particularly the proportion of G:A and C:U transitions	65
NHC inhibition is modestly enhanced in the absence of ExoN proofreading	67
Passage in the presence of NHC yields low-level resistance associated with multiple transition mutations.....	69
Discussion.....	74
Utility of the broad-spectrum antiviral NHC as a pan-CoV therapeutic.....	76
NHC inhibition may circumvent ExoN-mediated proofreading.....	77
NHC mutagenesis may hinder emergence of robust resistance to NHC.....	78
Conclusion	80
IV. INHIBITORY EFFECTS OF A PANEL OF NUCLEOSIDE ANALOGUES DURING CORONAVIRUS INFECTION	81
Introduction.....	81
Nucleoside analogues decrease viral titer and genomic RNA levels.....	83
Nucleoside analogue inhibition in WT MHV is MOI-dependent.....	85
Effect of exogenous ribonucleoside addition on nucleoside analogue inhibition	85
Nucleoside analogues can decrease CoV specific infectivity	87
NHC is the only nucleoside analogue in the panel that induces mutagenesis	90
A qPCR-based approach to detect truncated RNAs after nucleoside analogue treatment	92
RNA species released after infection are altered after treatment with nucleoside analogues	92
Lack of cross-resistance across the nucleoside analogue panel.....	94
Discussion.....	96
Lower viral load enhances CoV inhibition by nucleoside analogues regardless of proposed mechanism.....	96
Nucleoside analogue treatment can alter viral RNA released after infection	98

Lack of cross-resistance between nucleoside analogues indicates their potential to control antiviral resistance.....	101
Conclusion	102
V. MATERIALS AND METHODS.....	103
Cell culture	103
Viruses.....	104
Compounds and cell viability studies.....	104
Compound sensitivity studies and generation of EC ₅₀ curves.....	104
<i>In vitro</i> efficacy in human airway epithelial cells.....	105
Time-of-drug addition assay.....	106
Quantification of viral genomic RNA.....	106
Determination of specific infectivity	107
NGS studies	107
Selection of remdesivir resistance mutations	108
MHV population passage in the presence of NHC	109
MERS-CoV population passage in the presence of NHC	109
Modeling and conservation of resistance mutations in the CoV MHV nsp12 RdRp ..	110
Cloning, recovery, and verification of mutant viruses	110
SARS-CoV remdesivir resistance assessment.....	111
Virus replication assays.....	111
Competitive fitness of mutant viruses.....	112
Assessment of resistant virus virulence <i>in vivo</i>	112
Relative quantification of viral nsp1 and nsp16 RNA	113
Exogenous nucleoside addition assays.....	114
Statistics.....	114
Primers generated for this dissertation research	114
VI. SUMMARY AND FUTURE DIRECTIONS	116
Introduction.....	116
Nucleoside analogues with broad antiviral spectrum potently inhibit CoVs	117
Nucleoside analogues can potently inhibit CoVs by multiple mechanisms of action	120
Nucleoside analogues are important tools for investigating CoV replication	122
Nucleoside analogue combination treatments to prevent and control resistance emergence.....	127
Concluding remarks	128
Appendix	
A: CORONAVIRUS SUSCEPTIBILITY TO THE ANTIVIRAL REMDESIVIR (GS-5734) IS MEDIATED BY THE VIRAL POLYMERASE AND THE PROOFREADING EXORIBONUCLEASE	130
B: THE SMALL MOLECULE ANTIVIRAL β-D-<i>N</i>⁴-HYDROXYCYTIDINE INHIBITS A PROOFREADING-INTACT CORONAVIRUS WITH A HIGH GENETIC BARRIER TO RESISTANCE	140

C: MUTATIONS IN PASSAGED VIRUSES	153
C.1 MHV p30.1 mutations ^a	180
C.2 MHV p30.2 mutations ^a	185
C.3 MHV p19.1 mutations ^a	188
C.4 MHV p19.2 mutations ^a	189
C.5 MERS-CoV p30.1 mutations ^a	191
C.6 MERS-CoV p30.2 mutations ^a	192
D: COPYRIGHT PERMISSIONS	194
D.1. Ferrer-Orta et al., 2006, reproduced in Figure 5	194
D.2. de Wit et al., 2016, reproduced in Figure 6	201
REFERENCES.....	206

LIST OF TABLES

Table	Page
1. EC ₅₀ and CC ₅₀ values of GS-441524 or remdesivir in MERS-CoV or SARS-CoV infected HAE cultures	45
2. F476L and V553L mutations confer up to 5.6-fold resistance to remdesivir in MHV.	55
3. Cytotoxicity of the nucleoside analogue panel	86
4. Primers generated for this dissertation research	115

LIST OF FIGURES

Figure	Page
1. Coronavirus disease and emergence.....	6
2. Coronavirus virion and genome organization.....	8
3. Coronavirus genome replication and subgenomic mRNA transcription.....	11
4. Model of the coronavirus Replication/Transcription Complex (RTC)	13
5. Viral RNA-dependent RNA polymerases (RdRps) are highly structurally conserved.	15
6. Many processes within the coronavirus replication cycle may be targeted for antiviral development.....	17
7. Chemical structure of the most common natural nucleosides	31
8. Model of chain termination and lethal mutagenesis, the most common mechanisms of inhibition by nucleoside analogues	34
9. GS-441524 and remdesivir inhibit MHV with minimal cytotoxicity	41
10. Antiviral activity of GS-441524 and remdesivir and modeled therapeutic efficacy of remdesivir against SARS-CoV and MERS-CoV in HAE cultures.....	43
11. Remdesivir acts at early times post-infection to decrease viral RNA levels.....	47
12. Viruses lacking ExoN-mediated proofreading are more sensitive to remdesivir inhibition.....	49
13. Two mutations in the predicted fingers domain of the nsp12 RdRp, F476L and V553L, arose after 23 passages in the presence of GS-441524, and these residues are highly conserved across CoVs.....	51
14. The F476L and V553L mutations mediate resistance to remdesivir and are associated with a fitness defect.....	53
15. MHV resistance mutations confer resistance and are attenuated in SARS-CoV.....	57
16. Chemical structure of EIDD-1931, β -D- N^4 -hydroxycytidine (NHC)	63
17. NHC inhibits MHV and MERS-CoV with minimal cytotoxicity.....	64
18. NHC inhibition profile of MHV is consistent with mutagenesis.....	66
19. NHC treatment drives increase in low-frequency G:A and C:U transition mutations in WT MHV during a single infection.....	68
20. Sensitivity of ExoN(-) MHV to inhibition by NHC.....	70
21. Resistance and mutational profile of MHV after 30 passages in the presence of NHC	72

22. Mutational profile and resistance of MHV after 19 passages in the presence of NHC	73
23. Resistance and mutational profile of MERS-CoV after 30 passages in the presence of NHC	75
24. Chemical structures of 2'-C-Methyladenosine, β -D- N^4 -hydroxycytidine, and GS-441524.....	82
25. Treatment of WT MHV with nucleoside analogues decreases viral titer and supernatant viral genomic RNA	84
26. Nucleoside analogues more potently inhibit WT MHV at lower MOI regardless of proposed mechanism of action	88
27. Addition of exogenous nucleosides can restore viral titer after treatment with 2'-C-MeA and NHC but not remdesivir.....	89
28. Treatment with NHC and remdesivir significantly decreases specific infectivity.....	91
29. NHC is the only nucleoside analogue in the panel that increases low-frequency mutations spread across the WT MHV genome compared with the vehicle control.....	93
30. Change in levels of nsp16 relative to nsp1 after nucleoside analogue treatment	95
31. Sequencing coverage is more variable in the absence of poly(A) library selection after nucleoside analogue treatment.....	97
32. Dose-dependent change in sequencing coverage variability without poly(A) library selection after remdesivir treatment.....	99
33. Resistance to a single nucleoside analogue does not confer broad cross-resistance.	100

CHAPTER I

BACKGROUND AND LITERATURE REVIEW

Introduction

From the smallpox and yellow fever epidemics of the 16th and 17th centuries to the latest Ebola outbreak in 2019, infectious diseases have shaped human history. Currently, the World Health Organization (WHO) classifies 19 diseases as pandemic, epidemic threats. Viruses cause 15 of these diseases, demonstrating the risk they pose to human health. As people continue to increase their global travel and expand into previously uninhabited rural areas, the list of viral diseases threatening humans will likely grow as well (World Health Organization, 2018). Unfortunately, the United States Food and Drug Administration (FDA) has approved direct-acting antivirals to mitigate only one of the viral diseases of epidemic concern (De Clercq and Li, 2016a). In the absence of direct-acting antivirals to treat these infections, public health workers have implemented measures, such as surveillance and quarantine, to control the spread of these diseases (House, 2005; Svoboda et al., 2004). However, these practices take a toll on workers and are difficult to achieve in rural and low-income areas (Delamou et al., 2017). This is especially evident in recent Ebola epidemics in Africa, where weak health infrastructure and social instability have hampered control efforts. Thus, the growing magnitude and frequency of these outbreaks has emphasized the urgency of developing therapeutics to combat emerging viral diseases of international concern.

This dissertation research is aimed at identifying and understanding direct-acting antiviral compounds able to combat coronaviruses, a family of viruses that have emerged into human hosts from animal reservoirs to cause severe and lethal disease twice in the last twenty years and pose continuing threats for new zoonotic diseases.

Coronavirus disease and emergence

In late 2002, a man in the Guangdong province of China fell ill with an unknown ailment that caused pneumonia-like symptoms. Within 9 months, the illness, named severe acute respiratory syndrome (SARS), infected over 8,000 people in 29 countries and killed approximately 800 people (WHO) (Fig. 1A). A coronavirus (CoV), SARS-CoV, was ultimately identified as the culprit of SARS disease (Ksiazek et al., 2003). However, with the lack of direct-acting antivirals against this CoV, public health measures such as contact tracing and quarantine were crucial to prevent further spread (James et al., 2006; Klinkenberg et al., 2006). These methods were ultimately successful as the global epidemic was contained in July 2003, and the last case of SARS was reported in 2004. Up until this point, only two human CoVs (HCoVs), HCoV-229E and HCoV-OC43, had been identified, and they were known to cause mild to moderate respiratory disease associated with the common cold (McIntosh et al., 1970). So, the SARS epidemic served as the introduction to the pandemic potential and disease severity of CoVs.

However, SARS-CoV is not the only CoV that has caused global concern. In 2012, the first case of Middle East respiratory syndrome coronavirus (MERS-CoV) was reported in Saudi Arabia (Zaki et al., 2012). While MERS-CoV has not spread as rapidly as SARS-CoV, the virus has infected over 2,000 people and killed over 800 people in 27 countries thus far, and MERS-CoV

continues to cause new cases in humans (Fig. 1B). MERS-CoV outbreaks have primarily been localized to the Middle East, but large outbreaks have occurred outside of this region, including in South Korea. While MERS-CoV outbreaks have not persisted in the human population at detectable levels, new MERS-CoV cases continue to be reported. These new MERS-CoV cases may represent continued introduction of MERS-CoV into human populations or that MERS-CoV subsists in human populations sub-clinically (Alshukairi et al., 2018; Dudas et al.).

So, where did these viruses come from? The emergence of SARS-CoV into human populations prompted a search for its origin and ultimately resulted in the discovery of two other human CoVs, HCoV-NL63 and HCoV-HKU1 (van der Hoek et al., 2004; Woo et al., 2005). This search also identified a proposed route of transmission into humans from a reservoir species, horseshoe bats, through an intermediate host, palm civets (Li et al., 2006). The origins of MERS-CoV also trace to bats, with dromedary camels serving as intermediate hosts (Anthony et al., 2017; Azhar et al., 2014; Han et al., 2016). In fact, there is evidence that supports that all human CoVs have zoonotic origins, and bat reservoirs are particularly common for these viruses (Anthony et al., 2017; Drexler et al., 2014; Hu et al., 2015). Thus, the search for related CoVs that may emerge into human populations has focused on bats, and multiple CoVs that have been identified in bats are poised for human emergence (Ge et al., 2013; Menachery et al., 2015; 2016; Woo et al., 2018). However, CoVs infect a wide range of species. CoVs such as infectious bronchitis virus, transmissible gastroenteritis virus, and bovine CoV, have critical implications in agriculture, as they infect livestock such as chickens, pigs and cattle (Cavanagh, 2007; Oma et al., 2016; Paarlberg, 2014; Wang et al., 2019). CoVs also infect common household pets such as dogs, cats, and rodents (Licitra et al., 2014; Monchatre-Leroy et al., 2017; Myrrha et al., 2011).

Importantly for this dissertation work, murine hepatitis virus (MHV) infects mice and serves as a model virus invaluable in understanding CoV replication and biology (Lavi et al., 1987; Yount et al., 2002). Interactions between humans and animals may represent an additional zoonotic source, emphasizing the potential for CoVs to emerge by multiple routes.

In total, there are six CoVs currently known to infect humans. HCoVs-229E, OC43, HKU1, NL63 are endemic within human populations; they primarily infect the upper respiratory tract and typically cause mild to moderate respiratory symptoms (Gaunt et al., 2010; Pyrc et al., 2007; Walsh et al., 2013; Zeng et al., 2018). SARS-CoV- and MERS-CoV-infected individuals typically present with nonspecific respiratory symptoms of fever, chills, coughing, headache, malaise, and myalgia, within 13 days of exposure (de Wit et al., 2016). Severe disease in SARS and MERS likely results from direct virologic damage and subsequent immunopathology in the lower respiratory tract. SARS-CoV and MERS-CoV replicate to high titers in respiratory epithelial cells early during infection (Channappanavar et al., 2016; Oh et al., 2016). However, delayed and overexuberant immune responses may impair viral clearance and lead to acute respiratory distress syndrome (ARDS), the primary cause of death from severe CoV disease (Channappanavar and Perlman, 2017; Gralinski and Baric, 2015; Peiris et al., 2003). Poor disease outcomes in both SARS and MERS patients are associated with comorbidities, such as advanced age, diabetes mellitus, hypertension, cancer, and co-infections (Alqahtani et al., 2019; Chan et al., 2003; Moni and Pietro Liò, 2014; Yang et al., 2017).

Current standard of care and clinically available therapeutic options. When CoVs first emerged to cause severe disease in 2002, initial efforts were focused on using currently available

drugs that would inhibit SARS. Thus far, repurposing existing therapeutics has had little clinical benefit for treating either SARS or MERS patients (Arabi et al., 2019; Cheng et al., 2013; Stockman et al., 2006). However, one clinical trial is currently ongoing in Saudi Arabia to treat MERS-CoV infected patients with repurposed human immunodeficiency virus (HIV) protease inhibitors lopinavir and ritonavir in a fixed combination (Kaletra) along with human type I interferon (IFN) (And the MIRACLE trial group et al., 2018). Nevertheless, no specific antiviral treatment regimen is approved or recommended for MERS-CoV patients currently.

Coronavirus taxonomy, genome organization, and replication

According to the International Committee on Taxonomy of Viruses, the family *Coronaviridae* exists within the order *Nidovirales*. *Coronaviridae* is divided into the subfamilies *Orthocoronavirinae* and *Letovirinae*. All of the viruses discussed in this dissertation are classified within the *Orthocoronavirinae* subfamily and will be referred to as coronaviruses (CoVs) throughout this text. The *Orthocoronavirinae* subfamily is further subdivided into four genera: *Alphacoronavirus*, *Betacoronavirus*, *Deltacoronavirus*, and *Gammacoronavirus*. The *Betacoronavirus* genus consists of four lineages: A-D (Woo et al., 2007). All identified HCoVs fall within either the *Alphacoronavirus* (HCoV-229E, HCoV-NL63) and *Betacoronavirus* (HCoV-HKU1, HCoV-OC43, SARS-CoV, MERS-CoV) genera. Both SARS- CoV and MERS-CoV fall within the *Betacoronavirus* genus, though they are classified within distinct lineages, B and C, respectively (de Groot et al., 2013; Lau et al., 2013). MHV is classified as a lineage A *Betacoronavirus*, along with HCoV-OC43 and HCoV-HKU1, making it an excellent and relevant model for study (Woo et al., 2009).

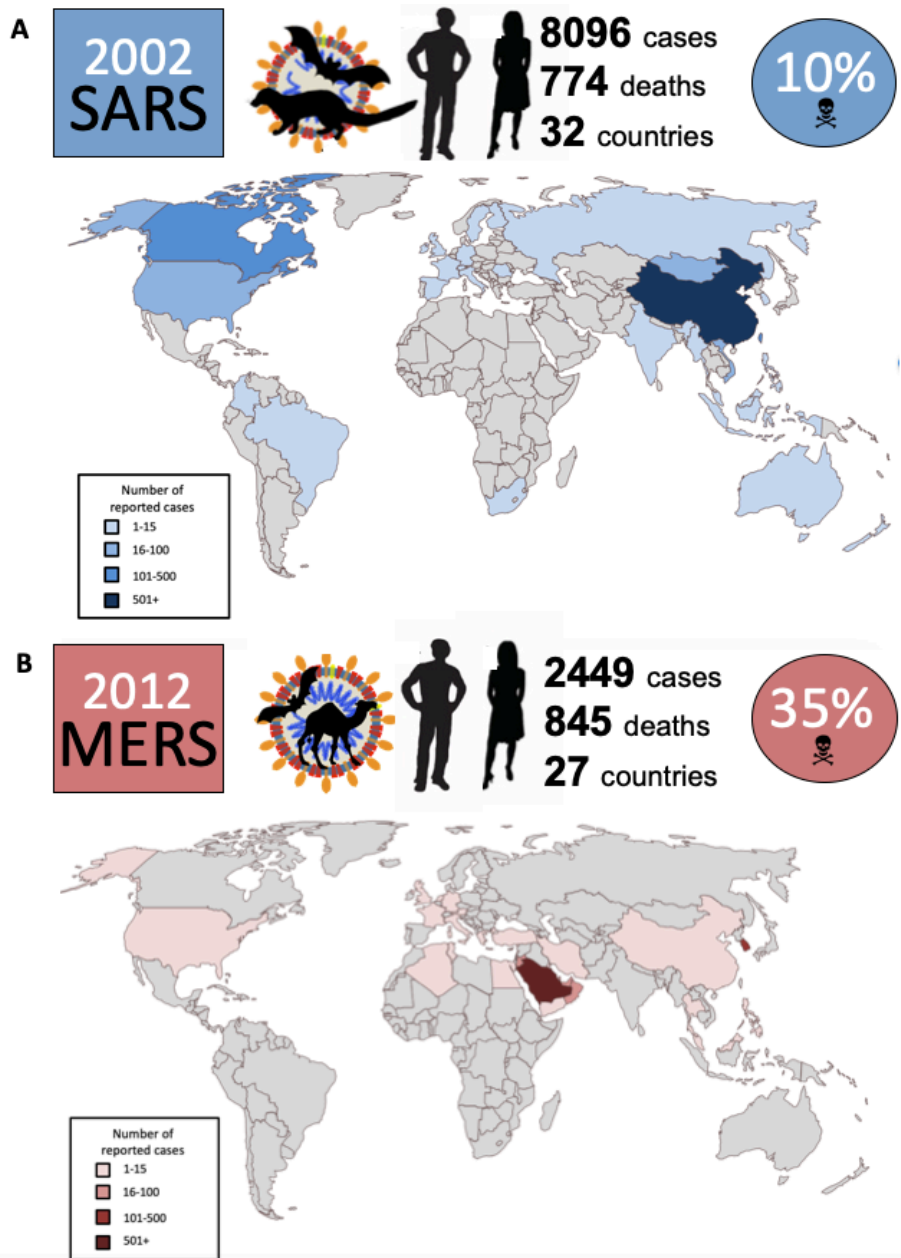


Figure 1. Coronavirus disease and emergence.

(A) SARS-CoV emerged in human populations in 2002 as the causative agent of SARS. The virus likely originated from bat reservoirs and was introduced into humans primarily from palm civets. Overall, the virus spread to 32 countries and had a case fatality rate (CFR) of 10% based on confirmed cases. (B) MERS-CoV emerged into humans in 2012 and is the causative agent of MERS. The virus has origins in bats and camels and, since emerging into humans, has an approximately 35% CFR based on reported cases across 27 countries. Numbers are current as of July 31, 2019 (WHO).

CoVs are enveloped viruses with large RNA genomes. CoVs contain four main structural proteins: spike (S), envelope (E), membrane (M), and nucleocapsid (N) (Fehr and Perlman, 2015) (Fig. 2A). A subset of β-CoVs encode a hemagglutinin esterase (HE) that is not essential for replication but appears to be important for infection in the host (Kazi et al., 2005; Lissenberg et al., 2005). The S, E, and M proteins are anchored in the membrane of the CoV virion (Bárcena et al., 2009). These viral proteins perform several vital functions, including facilitating viral entry into and release from the cell (Belouzard et al., 2012; Fehr and Perlman, 2015; Siu et al., 2008). Inside the virion lies the viral genome. The CoV genome is a large single-stranded positive-sense RNA, up to 36 kilobases (kb) in length, and the *Nidovirales* order contains the largest known RNA genomes, up to 41.1 kb (Saberi et al., 2018). The nucleocapsid (N) binds the viral genome, aiding in virion assembly (McBride et al., 2014). The genome itself mimics cellular messenger RNAs, as it has a 5' cap and 3 poly A tail (Lai and Stohlman, 1978; 1981; Lai et al., 1982; Lomniczi, 1977; Macnaughton and Madge, 1978). These features allow the RNA to be directly translated into protein by host cell ribosomes in the cytoplasm (Nakagawa et al., 2016). CoV RNA is composed of multiple open reading frames (ORFs) (Perlman and Netland, 2009). The first ORF (ORF1ab) encompasses approximately two-thirds of the genome and encodes 16 nonstructural proteins (nsps) involved in genome replication (Fehr and Perlman, 2015). This ORF is translated as two polyproteins (pp1a and pp1ab) where the second polyprotein (pp1ab) is generated as the result of a -1 frameshift during translation due to an RNA structural element (Baranov et al., 2005; Brierley et al., 1989). The last third of the genome encodes a variable, virus-specific number of ORFs that encode viral structural and accessory proteins that are translated from a nested set of subgenomic mRNAs (de Wit et al., 2016; Fehr and Perlman, 2015; Masters, 2006; Perlman and Netland, 2009) (Fig. 2B).

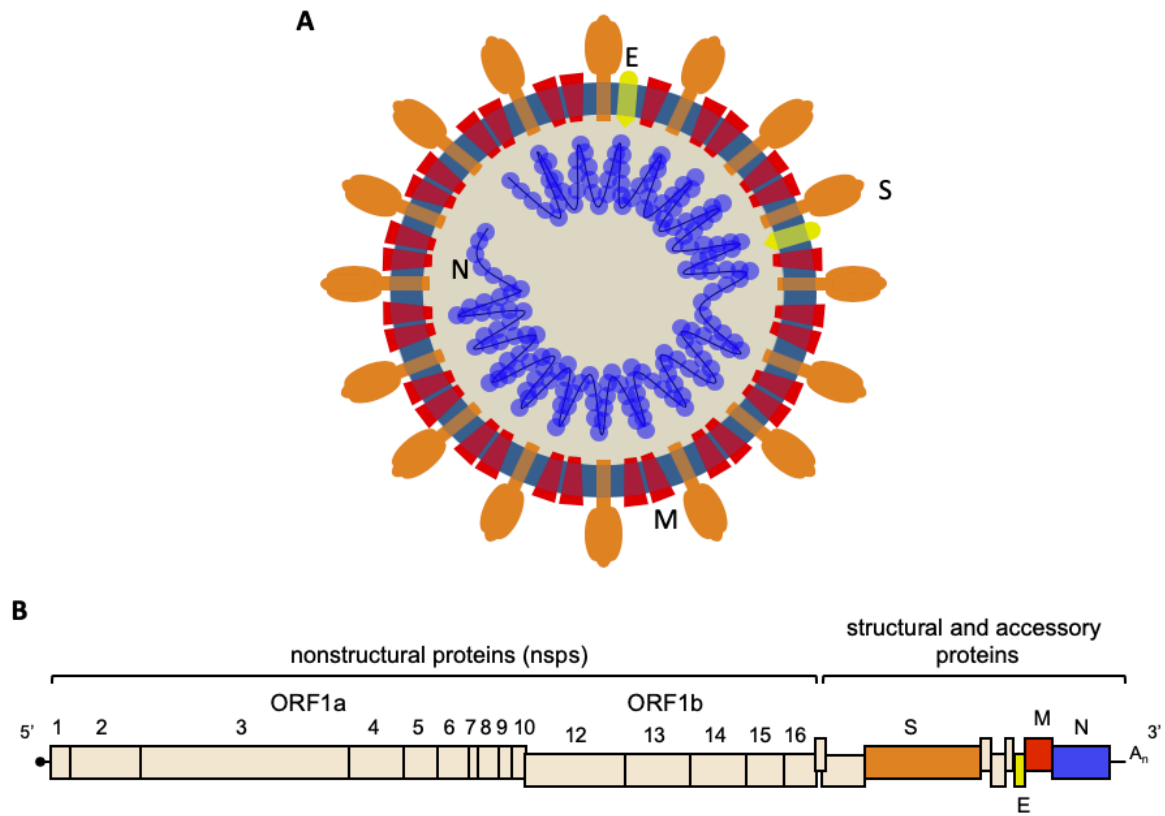


Figure 2. Coronavirus virion and genome organization.

(A) Schematic representation of a CoV virion. Four structural proteins: spike (S), envelope (E), membrane (M) and nucleocapsid (N) are indicated in orange, yellow, red, and blue, respectively. (B) Genome organization of murine hepatitis virus (MHV). The MHV genome is 31.4 kilobases in length. The 5' two-thirds of the genome encode 16 nonstructural proteins in ORF1ab. The last one-third of the genome encodes structural and accessory proteins. The location of the structural proteins highlighted in (A) are colored as above in the genome.

CoV infection commences with the interaction between the viral S protein and its cognate host receptor to facilitate cell entry. The host receptors for SARS-CoV, MERS-CoV, MHV are angiotensin-converting enzyme 2 (ACE2), dipeptidyl peptidase 4 (DPP4), and carcinoembryonic adhesion molecule 1a (CEACAM1a), respectively (Hirai et al., 2010; Li et al., 2003; Raj et al., 2013). Upon entry into the cell by either direct fusion at the plasma membrane or receptor-mediated endocytosis, the virion is uncoated to reveal the viral genome (Masters, 2006). Once uncoated, host ribosomes in the cytoplasm translate the genome, producing viral polyproteins pp1a and pp1ab. Viral proteases encoded within nsp3 and nsp5 cleave the polyproteins into individual components (Gorbatenko et al., 2000). These proteins then assemble to form replication complexes. Data suggest that nsp3, nsp4, and nsp6 co-opt and reorganize host membranes to form double membrane vesicles that serve as the site of viral genome replication (Knoops et al., 2008). Several nsps likely cooperate to form the viral replication/transcription complex (RTC) that performs genome replication (Smith et al., 2014; Subissi et al., 2014). The viral RTC must synthesize a negative-sense RNA intermediate from the positive-strand genomic template. This negative-strand RNA then serves as a template to generate positive-sense genome RNA molecules (Sawicki et al., 2007). Subgenomic mRNAs are generated by the RTC through transcription of negative-sense RNAs, which are products of discontinuous synthesis led by recognition of short transcriptional regulatory sequences (TRSs) and serve to amplify structural and accessory proteins (Sawicki and Sawicki, 1998) (Fig. 3). Ultimately, progeny virions assemble on membranes that bud into the endoplasmic reticulum-Golgi intermediate compartment (ERGIC) and are trafficked to the cell surface where they are released to infect other cells (de Haan and Rottier, 2005; de Wit et al., 2016).

While nearly all RNA viruses encode their own polymerase and many encode a helicase to replicate their genomes (Lai, 2005), CoVs encode several nonstructural proteins within their large RNA genomes that aid in replication and transcription of the viral genome. Based on interactions between these proteins (Brunn et al., 2007; Smith et al., 2014; Subissi et al., 2014) (Fig. 4), the CoV RTC is proposed to consist of the following: a viral processivity factor encoded within nsp7 and nsp8 (Imbert et al., 2006; Kirchdoerfer and Ward, 2019; Subissi et al., 2014; Velthuis et al., 2012; Zhai et al., 2005), a single stranded RNA binding protein encoded within nsp9 (Egloff et al., 2004), the viral RNA-dependent RNA polymerase (RdRp) and nidovirus-RdRp associated nucleotidyltransferase encoded within nsp12 (Cheng et al., 2005; Lehmann et al.; Xu, 2003)

The central enzyme of the CoV RTC is the viral RdRp. This enzyme performs elongation, which is comprised of NTP binding, active site closure, catalysis, and translocation that are proposed to occur in six sequential steps (Shu and Gong, 2016). Several regions of the polymerase play a role in this process. Their roles are discussed more below.

Across viral families, RdRps fold into a structure that resembles a cupped right hand composed of fingers, thumb and palm domains (Ferrer-Orta et al., 2006; Ng et al., 2008) (Fig. 5). Generally, the fingers domain is involved in template and nucleotide entry, the thumb domain contacts exiting nascent RNA, and the palm domain contains the three catalytic residues (Venkataraman et al., 2018; Velthuis, 2014). Despite little sequence conservation among RdRps, they contain conserved motifs A-G (Bruenn, 2003; Venkataraman et al., 2018). Motifs A-E are located within the palm domain, while Motifs F and G are located within the fingers domain

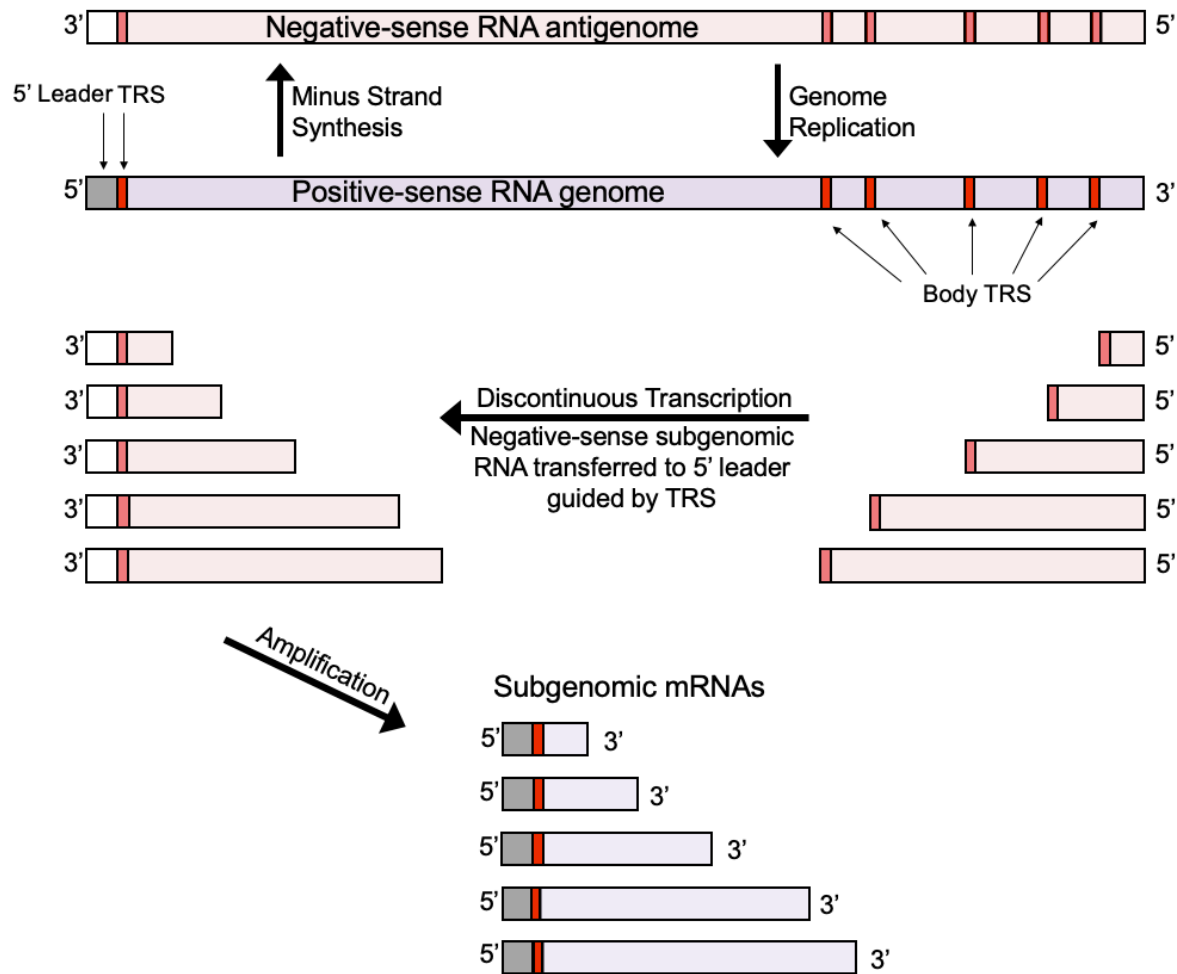


Figure 3. Coronavirus genome replication and subgenomic mRNA transcription.

The negative-sense RNA antigenome is synthesized by the coronavirus replication/transcription complex (RTC) from a positive-sense RNA genome. This negative-sense RNA also serves as a template for generating positive-sense genome RNA during genome replication. Negative-sense subgenomic RNAs are generated from positive-sense RNA through discontinuous transcription where the RTC relocates between body transcriptional regulatory sequences (TRS) and the 5' leader TRS. These negative-sense subgenomic RNAs are transcribed to yield subgenomic mRNAs that aid in amplifying structural and accessory protein production.

(Velthuis, 2014). Motif C is one of the most conserved and contains the xDD catalytic residues important for metal ion coordination in catalysis (Arnold et al., 1999; Jablonski and Morrow, 1995; Ng et al., 2008; Poch et al., 1989). Motif A houses a less conserved DX₂₋₄D catalytic motif that, along with motif B, assists in substrate discrimination (Garriga et al., 2013; Gorbalenya et al., 2002; Velthuis, 2014). Motif D is one of the most dynamic and is involved in several functions, including nucleotide selection and conformational changes (Jácome et al., 2015). Motif E aids in primer positioning. Motif F is involved in nucleotide selection, and motif G interacts with the template and priming NTPs (Jácome et al., 2015). In general, these motifs cooperate to facilitate genome replication by recognizing the nucleoside that correctly pairs with the template strand and catalyzing its addition (Ng et al., 2008). Thus, residues throughout the polymerase may influence the ability of the polymerase to select the correct nucleotide and play a role in regulating replication fidelity and nucleotide selectivity (Campagnola et al., 2015; Ferrer-Orta et al., 2007). Indeed, many studies in several viruses have identified polymerase mutations that impact the fidelity of genome replication (Pfeiffer and Kirkegaard, 2003a; Smith et al., 2014b). In CoVs, previous studies have modeled the CoV RdRp structure based on other viral RdRps (Sexton et al., 2016; Xu, 2003), but several specific details of CoV RdRp catalysis remain unclear (Ahn et al., 2012; Cheng et al., 2005; Subissi et al., 2014; Velthuis et al., 2009). The SARS-CoV polymerase structure has recently been reported in complex with nsp7 and nsp8 and will aid in further understanding details of the CoV RdRp (Kirchdoerfer and Ward, 2019).

While fidelity of genome replication in other RNA viruses has been primarily associated with how faithfully the RdRp copies the viral genome, CoVs encode additional fidelity regulators. Several studies have implicated the 3'-5' exoribonuclease (ExoN) as a proofreading enzyme

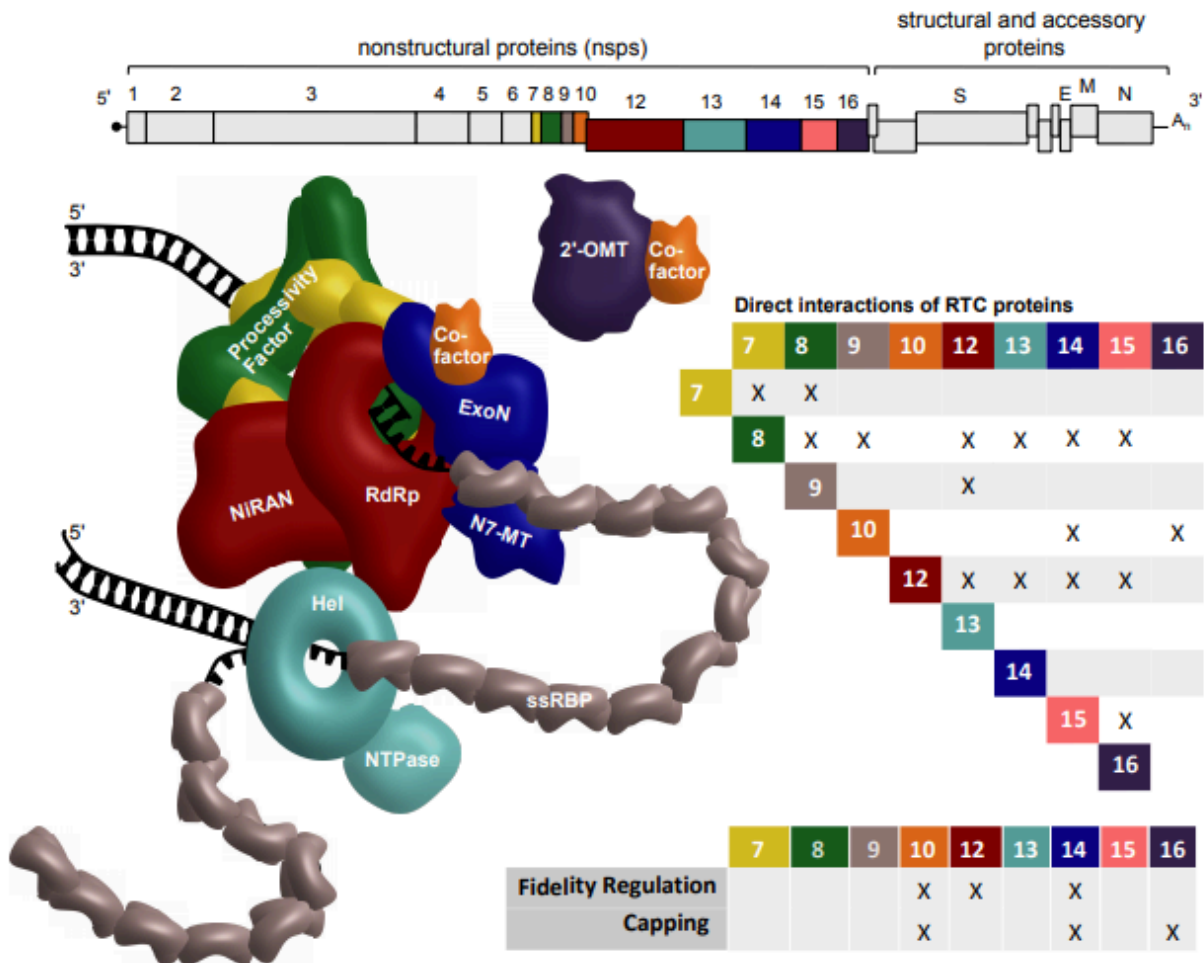


Figure 4. Model of the coronavirus Replication/Transcription Complex (RTC).

CoVs encode multiple replicase proteins that likely assemble into a larger Replication/Transcription Complex (RTC). Based on biochemical and genetic studies, the core of this complex is proposed to include the RNA-dependent RNA polymerase (RdRp) in nsp12, the helicase and NTPase in nsp13, and the processivity factors in nsp7 and nsp8. Additional functionalities of the RTC include the single stranded binding protein in nsp9, which has been shown to interact with nsp8, and the nidovirus RdRp-associated nucleotidyltransferase in nsp12. In addition to the RdRp in nsp12, fidelity regulation is achieved by the nsp14 3'-5' exoribonuclease in conjunction with its nonenzymatic cofactor nsp10, likely through direct interactions. However, nsp10 may also bind the 2'-O-methyltransferase in nsp16 that, along with the *N*⁷-methyltransferase in nsp14, is involved in capping. The culmination of these interactions may ultimately affect the composition of the RTC. This figure is reproduced from Sexton, 2017, with permission.

during RNA synthesis (Eckerle et al., 2007; 2010; Ferron et al., 2017; Minskaia et al., 2006; Sexton et al., 2016; Smith et al., 2013). In addition, the non-enzymatic co-factor nsp10 also modulates fidelity, likely through interactions with nsp14 (Smith et al., 2015). Thus, given the direct interactions of the RdRp with nsp7, 8, and 13 as well as their importance for catalysis *in vitro* (Subissi et al., 2014), it is plausible that several members of the RTC work together to regulate viral replication fidelity (Graepel et al., 2017; Sexton et al., 2016) (Fig. 4). Indeed, the helicase acts as a fidelity regulator in alphaviruses (Stapleford et al., 2015), further supporting the hypothesis that CoV fidelity modulation may be regulated by additional RTC proteins.

Coronavirus antiviral strategies

Currently, there are no drugs approved to treat CoV infections, but several antiviral targets have been identified within the CoV replication cycle (Fig. 6). Given that CoVs continue to circulate in several animal populations and that they have a demonstrated ability to transcend species barriers into humans (Peck et al., 2015), it is important to identify strategies that will aid in combating any CoV that may emerge. The best approach to broadly inhibit CoVs would be to develop antivirals that are targeted toward processes that are both conserved and essential during viral replication. Some of the CoV antiviral targets under investigation have been chosen based on their success in treating other viral infections; however, some targets are unique to the large CoV genome. As such, CoV antivirals may be repurposed previously identified compounds or newly identified and developed compounds. Combining multiple antiviral approaches and targets may also be necessary to prevent emergence of viruses that are resistant to specific antiviral treatments or approaches (Pirrone et al., 2011). While active vaccination remains an important

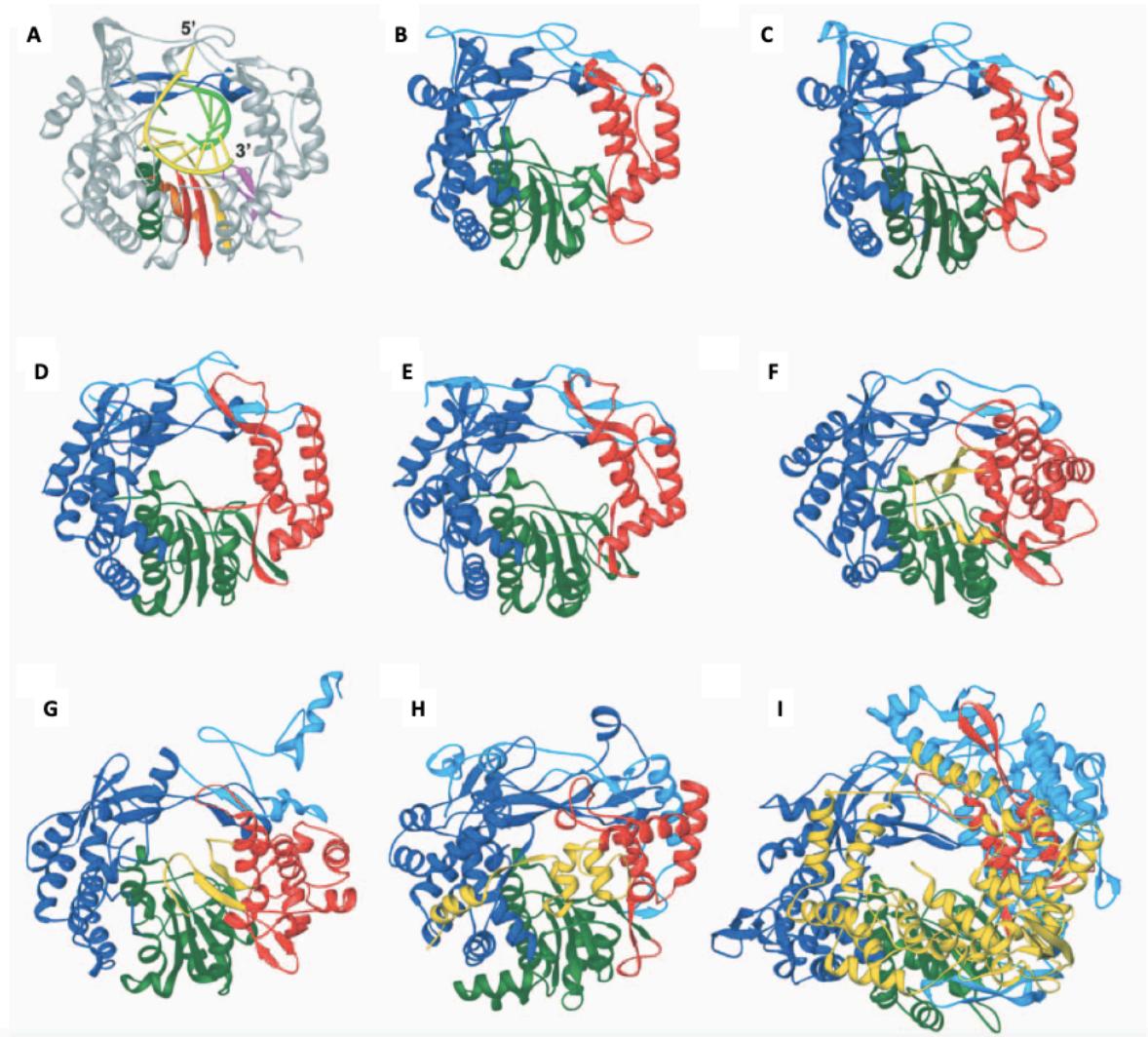


Figure 5. Viral RNA-dependent RNA polymerases (RdRps) are highly structurally conserved.

Structures of the RdRps from (A) foot and mouth disease virus, (B) poliovirus, (C) human rhinovirus 16, (D) rabbit hemorrhagic disease virus, (E) Norwalk Virus, (F) hepatitis C virus (HCV), (G) Bovine viral diarrhea virus, (H) bacteriophage $\phi 6$, and (I) reovirus $\lambda 3$. Each of these RdRps show a high degree of structural conservation and fold into a conserved structure resembling a cupped right hand with fingers, palm, and thumb domains. These domains are shown in blue, green, and red, respectively. This figure is reproduced from (Ferrer-Orta et al., 2006), with permission.

preventative strategy to combat CoV infection, this section focuses on some of the antiviral strategies proposed to treat CoV infections and outlines their utility in pan-CoV inhibition.

Host targets. One pan-CoV antiviral strategy is to inhibit cellular processes that CoVs use during replication. Since this strategy would target the host and does not target the virus directly, viral mutations that mediate drug resistance are less likely to emerge. However, this antiviral strategy also requires, regardless of the host target, extensive safety tests.

Because both SARS and MERS disease severity are partly mediated by immunopathology, several host-centric antiviral strategies revolve around modulating the host immune response. Several studies have focused on the antiviral activity of IFN, an immunomodulatory molecule that serves as the first line of defense against invading pathogens (Fensterl and Sen, 2009). These molecules act by inducing proteins that interfere and restrict viral replication and spread (Stark et al., 1998). Several recombinant IFNs have been approved to treat various viral infections (Lin and Young, 2014). These IFNs have also demonstrated antiviral activity against CoVs, suggesting their utility as CoV therapeutics (Cinatl et al., 2003; Falzarano et al., 2013; Haagmans et al.; Hart et al., 2014; Tan et al., 2004). Clinically, IFNs have been used to treat SARS and MERS patients with limited effectiveness, potentially due to late administration (Stockman et al., 2006; Totura and Bavari, 2019). However, other potentially immunomodulatory compounds such as cyclosporin A (CsA) also inhibit CoVs, and showed positive combinatorial effects when combined with IFN (de Wilde et al., 2011; Li et al., 2018). Immunomodulatory agents are not without risk, as corticosteroids were used to treat SARS and MERS patients with little benefit and possible deleterious effects. However, they remain an appealing antiviral strategy for CoVs,

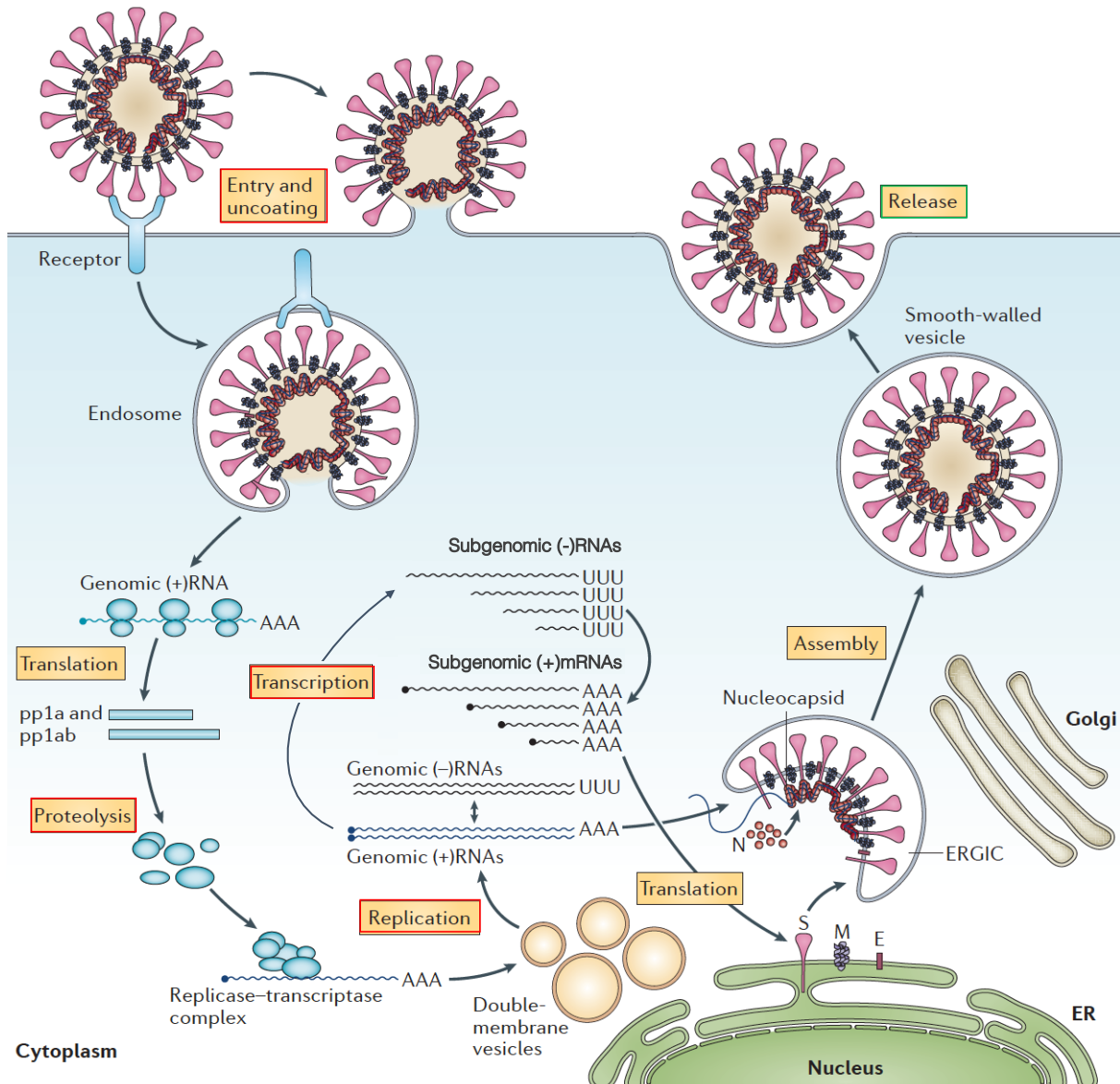


Figure 6. Many processes within the coronavirus replication cycle may be targeted for antiviral development.

CoV spike proteins recognize the host receptor to facilitate viral entry. The virion is uncoated in the cytoplasm and the released genomic RNA is translated by host ribosomes. The resulting polypeptides are cleaved by viral proteases into individual nonstructural proteins (nsps). The nsps assemble to form the RTC, which replicates genomic RNA and transcribes subgenomic mRNAs (sgmRNAs) on virus-induced double-membrane vesicles. CoV structural proteins are translated from these sgmRNAs. Structural proteins and genomic RNA assemble into full virions in the endoplasmic reticulum golgi-intermediate complex (ERGIC). Ultimately, the resulting progeny virions are trafficked and released by non-lytic exocytic pathways. Some of the CoV antiviral targets discussed here are outlined in red. Antiviral targets discussed here that have been successful for other viruses but are not discussed for CoVs are outlined in green. This figure is adapted from (de Wit et al., 2016), with permission.

considering the immunologically driven pathophysiology of severe SARS- and MERS-CoV infections.

CoVs rely on multiple host factors during viral replication (de Wilde et al., 2017; Lim et al., 2016). Rational antiviral design against host factors have focused primarily on proteases like TMPRSS2 that assist with viral entry, but, due to the variability of proteases used by individual CoVs, this strategy may require a cocktail of inhibitors for pan-CoV inhibition (Simmons et al., 2005; Totura and Bavari, 2019; Zhou et al., 2016). Some reports have suggested that exocytic pathways could be inhibited to block viral release, but few studies have extensively investigated this proposition (Holmes, 2003). Additional studies have screened approved drugs in hopes of repurposing them as CoV antivirals and have identified compounds that may target host proteins and processes essential for viral replication (Coleman et al., 2016; de Wilde et al., 2014; Dyall et al., 2014; Frieman et al., 2011; Müller et al., 2018). Overall, further studies are warranted to better investigate the use of host-targeted strategies for developing pan-CoV antivirals.

CoV structural protein targets. Structural proteins perform essential functions during viral replication. They are the structural components of the virion and their interactions with host proteins ultimately facilitate entry into the cell. While these proteins make excellent antiviral targets, they are generally not well conserved across CoVs, complicating pan-CoV antiviral strategies directed at these proteins.

The clinical success of monoclonal antibodies (mAbs) for treatment of both viral and non-viral diseases (Singh et al., 2018) has fueled interest in their utility as an antiviral strategy for CoVs.

Neutralizing mAbs that inhibit viral infections principally target viral surface proteins to block infection (Crowe, 2017). In CoVs, neutralizing mAbs can be targeted toward multiple different regions of the CoV S glycoprotein to prevent viral infection (Du et al., 2017; Pallesen et al., 2017; Wang et al., 2018). These mAbs may be derived from multiple sources, including human survivors of infection or experimentally infected animals (Han et al., 2018; Wang et al., 2018; 2015a). Several groups have identified mAbs that inhibit SARS-CoV or MERS-CoV and ameliorate disease *in vivo* (Houser et al., 2016; Johnson et al., 2016; Pascal et al., 2015; Zhu et al., 2007). Some of these mAbs targeting MERS-CoV, REGN3048 and REGN3051, have completed Phase I clinical trials, further emphasizing their potential as CoV therapeutics (NCT03301090). However, S is less than 50% conserved across CoVs (Sheahan et al., 2017; Stadler et al., 2003), and mAbs are generally not cross-reactive across CoVs (Agnihothram et al., 2014), complicating mAbs as a pan-CoV antiviral strategy.

While small molecule inhibitors of E protein ion channels have been identified (Wilson et al., 2006), antiviral development targeting structural proteins has primarily focused on inhibiting viral entry and fusion by S protein (Xia et al., 2014; Zumla et al., 2016). Small molecule, peptide, and RNA-based inhibitors have been identified and proposed to block various stages of viral entry and fusion (Adedeji and Sarafianos, 2014; Liang et al., 2018; Zumla et al., 2016). Some of the antivirals under development aim to target entry and fusion in CoVs in a similar manner as therapeutics that have been successful for other viral infections, particularly HIV (Gao et al., 2013; Kilby et al., 1998; Lu et al., 2014), and some even have broad-spectrum antiviral activity (Xia et al., 2019; Zhao et al., 2016). Viral entry and fusion facilitated by structural proteins are essential processes in viral replication and highly desirable antiviral targets.

However, as has been mentioned previously, the entry and fusion mechanisms vary across CoVs, which can complicate this strategy for pan-CoV antiviral discovery and development.

CoV nonstructural protein targets. Several nonstructural proteins are indispensable for viral replication. Further, this region of the genome shares the most sequence identity across distantly related CoVs (Sheahan et al., 2017; Stadler et al., 2003), making several nonstructural proteins excellent targets for pan-CoV antiviral development.

The CoV polyproteins are cleaved into individual proteins at conserved sites primarily by the 3C-like protease (3CLpro) in nsp5 with additional cleavage performed by the papain-like protease(s) (PLpro) in nsp3 in some CoVs (Gorbalenya et al., 2000; Perlman and Netland, 2009). Given the essential role of proteases in viral protein processing, several studies have reported compounds to inhibit these targets. The activity of some protease inhibitors, such as the repurposed alcohol aversion therapy drug disulfiram, only have demonstrated activity against PLpro (Lin et al., 2018), while compounds, such as polyphenols, inhibit both PLpro and 3CLpro (Park et al., 2017). However, most antiviral development for CoV proteases has remained focused on 3CLpro. Small molecules such as GC376 and N3 potently inhibit across CoVs (Kim et al., 2016; 2012; Yang et al., 2005). The development of these and other inhibitors have benefited from the solved 3CLpro structure, and some studies have even rationally designed inhibitors using docking studies (Galasiti Kankanamalage et al., 2018; Niu et al., 2008; Xue et al., 2008; Yang et al., 2005). Complementary efforts have focused on repurposing existing compounds as CoV protease inhibitors. The combination of lopinavir and ritonavir was first developed to inhibit HIV, but further testing has demonstrated its antiviral activity in CoVs

targeting 3CLpro both *in vitro* and *in vivo* (Wu et al., 2004). Other compounds that may be repurposed to inhibit 3CLpro include neuraminidase and enterovirus peptidomimetic 3Cpro inhibitors (Kumar et al., 2017; 2016). Overall, several 3CLpro inhibitors displayed broad-spectrum inhibition of CoV activity, making them important leads for pan-CoV antivirals.

The cap structure of the viral RNA helps prevent the virus from being recognized by innate immune sensors and is important for viral genome translation (Ramanathan et al., 2016). These features make targeting enzymes involved in viral capping an exciting antiviral target (Ferron et al., 2012). CoVs encode multiple proteins that play a role in capping the viral genome that could be targeted, such as the *N*⁷-methyltransferase in nsp14, the 2'-*O*-methyltransferase in nsp16, and the nonenzymatic cofactor in nsp10 that interacts with both of these proteins (Chen and Guo, 2016). Initial studies have reported inhibitors that target capping in CoVs (Sun et al., 2014; Wang et al., 2015), though specificity for viral targets over host molecules remain a concern for these inhibitors (Aouadi et al., 2017). Future studies are warranted to further investigate this potential pan-CoV antiviral strategy.

CoVs reorganize membranes to replicate their genomes. Targeting these proteins may represent an additional anti-CoV strategy. Indeed, K22 is a broad-spectrum CoV inhibitor that acts by disrupting membrane-bound viral RNA synthesis (Lundin et al., 2014) and warrants further exploration.

CoVs encode a nidoviral uridylylate-specific endoribonuclease (NendoU) in nsp15 (Ivanov et al., 2004a). This protein is a unique and identifying feature of the *Nidovirales* order (Fehr and

Perlman, 2015; Snijder et al., 2003), making it a target that could specifically target these viruses. Recent studies have demonstrated the importance of NendoU in innate immune evasion during viral replication (Deng et al., 2017). Previous reports have recognized the potential to develop antivirals against this target in CoVs (Xu et al., 2006), but identification of inhibitors have focused on the structural similarity of NendoU to ribonuclease A (RNase A) (Treatment2010). Future studies may focus on novel CoV NendoU inhibitors or further repurposing inhibitors of RNase A or cellular endoribonucleases based on structural similarities (Deng and Baker, 2018; Ragno et al., 2011), though careful safety studies are a priority with these approaches.

The proofreading 3'-5' exoribonuclease activity is another unique functionality of CoVs that could be targeted for antiviral development. Outside of the *Nidovirales* order, the only other RNA virus family to encode a 3'-5' exoribonuclease (ExoN) is arenaviruses (Qi et al., 2010). While both the CoV and arenavirus ExoN play a role in the innate immune response (Case et al., 2016; Qi et al., 2010), the CoV ExoN also has demonstrated proofreading activity (Ferron et al., 2017; Minskaia et al., 2006; Smith et al., 2013). No CoV ExoN inhibitors have been identified, but ATA and PV6R have demonstrated biochemical antiviral activity against the arenavirus ExoN (Huang et al., 2016). These compounds present the opportunity to inhibit a signature factor of CoV replication. Future studies would be necessary to assess the ability of these compounds to inhibit CoVs as well as their toxicity.

Another antiviral target within the CoV RTC is the helicase and NTPase activity within nsp13. Along with nsp12, nsp13 shows the most sequence conservation across CoVs (Stadler et al.,

2003), making it a desirable target for development of pan-CoV antivirals. This protein uses the energy of nucleoside triphosphate (NTP) hydrolysis to separate double-stranded nucleic acid to facilitate viral replication (Adedeji and Lazarus, 2016; Ivanov et al., 2004b; Tanner et al., 2003; Adedeji 2004). Some compounds, such as myricetin and scutellarein, selectively inhibit the NTPase activity of nsp13 (Yu et al., 2012), whereas compounds such as aryl diketoacids and SSYA10-001 and its derivatives, selectively inhibit the unwinding activity (Adedeji et al., 2012; Lee et al., 2009). Further, some compounds, such as bananin, 5-hydroxychromone and their derivatives were shown to inhibit both the NTPase and unwinding activities of SARS-CoV nsp13 (Kim et al., 2011; Tanner et al., 2005). SSYA10-001 has demonstrated broad-spectrum CoV activity (Adedeji et al., 2014), further emphasizing nsp13 as a pan-CoV antiviral target. However, the major hurdle to nsp13 inhibitors is specificity for viral targets due to the large number of cellular helicases that could be affected to consequently result in drug-related toxicity (Adedeji and Sarafianos, 2014).

Given the critical role of polymerases in viral genome replication, they are attractive targets for antiviral development. The CoV polymerase is an obvious pan-CoV antiviral target because the amino acid sequence identity is approximately 70% conserved across divergent CoVs (Sheahan et al., 2017). Polymerase inhibitors are classified in two major categories: nucleoside and non-nucleoside inhibitors. Nucleoside inhibitors directly compete for the polymerase active site with natural nucleosides for incorporation into viral genomes (Sofia et al., 2012). Non-nucleoside inhibitors inhibit polymerases, but are not competitive inhibitors as they often inhibit a site distinct from the catalytic domain of the polymerase (Wang et al., 2003). Prior to this dissertation work, CoV polymerase inhibitors had not been investigated in depth.

Clinically approved direct-acting antivirals

Given all of the targets and strategies for discovering and developing CoV antivirals discussed above, it is important to understand antiviral strategies that have been successful for other viral infections. Learning from these successes can help inform design of CoV antivirals.

The first direct-acting antiviral compound, idoxuridine, was approved by the FDA to treat herpes simplex virus (HSV) in 1963 (De Clercq and Li, 2016a). Now, more than 100 antiviral regimens have been formally approved in the United States to treat human viral infections. Direct-acting antivirals have been approved against DNA viruses, RNA viruses, and retroviruses (De Clercq and Li, 2016a), and some compounds have been approved to treat multiple viral infections. The following is an overview of approved direct-acting antiviral drugs.

Human Immunodeficiency Virus. HIV is the causative agent of acquired immune deficiency syndrome (AIDS) and was first discovered in 1983 (Gallo and Montagnier, 2003). HIV is a retrovirus, an RNA virus that replicates through a DNA intermediate that inserts into the host genome (Baron and Cloyd, 1996). HIV is a chronic disease, and HIV therapeutics focus on controlling infection and preventing progression to AIDS (Deeks et al., 2013; Detels et al., 1998). Compounds approved to treat HIV target many aspects of viral replication and fall into these main categories: nucleoside reverse transcriptase inhibitors (NRTIs), non-nucleoside reverse transcriptase inhibitors (NNRTIs), protease inhibitors (PIs), integrase strand transfer inhibitors (INSTIs), and entry inhibitors (EIs) (De Clercq and Li, 2016a).

The first HIV inhibitor, azidothymidine (AZT) was approved in 1987 (Fischl et al., 1987). This compound is classified as an NRTI, a group of compounds that target the viral reverse transcriptase by mimicking nucleosides that that viral polymerase would typically recognize. Drug resistance to AZT quickly emerged after treatment began with this compound, suggesting a low barrier to resistance and demonstrating the need for additional HIV antivirals (Larder et al., 1989; Rooke et al., 1989; Wainberg et al., 1991). Further investigation identified multiple distinct NRTI inhibitors that have been approved in the United States (Cihlar and Ray, 2010). However, other classes of compounds target the virus differently and have also been essential in the fight against HIV. NNRTIs also inhibit reverse transcriptase, but their chemical structure is different, allowing them to inhibit at a site distinct from the active site (de Béthune, 2010). PIs inhibit the viral protease, and INSTIs inhibit HIV integration into the host genome (Hazuda et al., 2000; Lv et al., 2015). EIs may inhibit viral entry into host cells by targeting multiple steps, including interactions of HIV envelope protein gp120 with the CD4 T cell receptor or CCR5/CXCR4 co-receptors (Kuritzkes, 2009; Qian et al., 2009). Due to the large number of HIV inhibitors now available and the likelihood of resistance development to a single therapeutic, HIV drugs are now primarily administered in combination as highly active antiretroviral therapy (HAART), though NRTIs still serve as a backbone in several of these combinations (Dybul et al., 2002; Pau and George, 2014). When used properly, HAART controls infection and opposes progression to AIDS, though none of these approved drugs cure HIV-infected patients (Detels et al., 1998; Sankaranantham, 2019).

Hepatitis C Virus. Hepatitis C virus (HCV) was first discovered in 1989 as a causative agent of hepatitis (Choo et al., 1989). HCV is a positive-sense RNA virus (Chevaliez et al.). There are

eight distinct genotypes and several subtypes of HCV (Borgia et al.; Smith et al., 2014a), with genotype 1 being the most common around the world (Messina et al., 2015). In the absence of direct-acting antivirals, the standard of care for HCV patients included ribavirin (RBV) and interferon (IFN). However, patients experienced severe side effects from these treatments and the cure rates on these regimens peaked at 80% only for specific genotypes after 24-48 weeks (Antaki et al., 2010; Fried et al., 2002), underscoring the importance of continued drug development. Protease inhibitors boceprevir (BOC) and telaprevir (TVR) were among the first direct-acting antivirals approved to treat HCV in combination with RBV and IFN. As more direct-acting antivirals were developed, the FDA ultimately approved the first treatment regimen that did not require RBV or IFN. Common combination regimens included the modified uridine prodrug sofosbuvir and the protease inhibitor ledipasvir (De Clercq and Li, 2016a). Overall, several treatment regimens are now approved to treat HCV infection, though they are still largely genotype specific (Burstow et al., 2017). The cure rate for HCV with the direct-acting antivirals is now approximately 95% within 12 weeks of starting the treatment (Dahiya et al.).

Hepatitis B Virus. Hepatitis B virus (HBV) is a DNA virus that was first discovered in 1963 and is one of the causative viral agents of hepatitis (Blumberg, 1997). While HBV and HCV are members of different virus families, they cause similar clinical symptoms and may lead to hepatocellular carcinoma (Bartosch, 2010). HBV can cause acute or chronic disease (Liang et al., 2018). While antiviral treatment is typically not indicated for treatment of acute disease caused by HBV (Terrault et al., 2018), all direct-acting antiviral agents for chronic HBV can be classified as nucleoside analogues (De Clercq et al., 2010). The first direct-acting antiviral approved to treat HBV was lamivudine (3TC), a cytidine analogue, that also inhibits HIV (De

Clercq and Li, 2016a). This compound is rarely used alone now because of the high occurrence of resistance (Thompson et al., 2007). Other antivirals approved to treat chronic HBV infection include tenofovir, adefovir, entecavir, and telbivudine (De Clercq and Li, 2016a). Tenofovir and adefovir are acyclic adenine analogues, where entecavir and telbivudine are deoxyguanosine and deoxythymidine analogues, respectively. Unlike the HCV treatments discussed above, HBV antivirals are not cures; they merely suppress viral replication (Tang et al., 2014). Because of the nature of transmission of HIV, HCV, HBV, and some herpes viruses, several individuals are co-infected with combinations of these viruses (Soriano et al., 2010), making therapeutics that can inhibit across these viral infections highly appealing.

Herpesviruses. Herpesviruses are DNA viruses that can cause a wide range of clinical symptoms. One characteristic feature of these infections is that they can latently infect a person for life and reactivate to cause disease (Grinde, 2013). Of the more than 100 known herpesviruses, eight infect humans (Baron and Whitley, 1996). The FDA has approved antivirals to treat three of the viruses within the *Herpesviridae* family: human cytomegalovirus (CMV), varicella zoster virus (VZV), and herpes simplex virus (HSV). Many of the herpesvirus therapeutics are approved to treat more than one of the infections listed above (De Clercq and Li, 2016a). This is unsurprising, as many of these antivirals target aspects of viral replication conserved across the virus family. Most of the direct acting antivirals that combat herpesvirus infection target the polymerase (De Clercq, 2014). Many of the polymerase inhibitors can be classified as nucleoside analogues, though structurally these may take many forms (Vere Hodge and Field, 2013). For example, nucleosides such as acyclovir require activation by the viral thymidine kinase, aiding in their specificity for herpesviruses (Elion, 1982).

Respiratory Syncytial Virus. Respiratory syncytial virus (RSV) is an RNA virus that causes respiratory disease, and these infections can be particularly serious for infants and older adults (Collins et al., 2013). Each year, RSV infection leads to approximately 3 million hospitalizations and 60,000 deaths in children less than 5 years old (Shi et al., 2017). Currently, mAb therapies, such as palivizumab, are approved, though this is only indicated as an immunoprophylaxis for high risk children and does not provide benefit when administered after infection (Alansari et al., 2019; American Academy of Pediatrics Committee on Infectious Diseases American Academy of Pediatrics Bronchiolitis Guidelines Committee, 2014). Several studies have identified RSV inhibitors, and multiple clinical trials are underway to assess RSV treatment options (Xing and Proesmans, 2019).

Influenza Virus. Evidence of influenza outbreaks stretch back to as early as the 12th century (Hirsch, 1883). Influenza is also the culprit of the large pandemic that occurred in 1918-1919 that killed an estimated 21-50 million people worldwide (Johnson and Mueller, 2002). Influenza virus is a segmented RNA virus that typically causes acute respiratory disease outbreaks each year during the winter months (Finkelstein et al., 2007; Moghadami, 2017). These outbreaks lead to as many as 650,000 deaths per year worldwide (Iuliano et al., 2018). There are currently six antivirals approved to treat influenza infections in the United States, but additional antiviral drugs have been approved in Japan (Centers for Disease Control and Prevention (CDC), 2019; De Clercq and Li, 2016a; Principi et al., 2019). Influenza inhibitors are grouped into four classes: neuraminidase inhibitors, endonuclease inhibitors, matrix 2 protein inhibitors, and polymerase inhibitors (Centers for Disease Control and Prevention (CDC), 2019). The neuraminidase

inhibitors target viral release from host cells and are the most common flu drugs (Moscona, 2005). While antivirals targeted against the influenza matrix 2 protein, which is involved in viral entry, have been approved, they are not currently recommended to treat patients because resistance widely circulates (Cady et al., 2009; Centers for Disease Control and Prevention (CDC), 2019). One endonuclease inhibitor was approved in 2018, making it the only recommended influenza drug approved in the US that does not target neuraminidase (Dziewiatkowski et al., 2019; Hayden et al., 2018; Jones et al., 2016). Favipiravir, a nucleobase that inhibits the viral RNA polymerase, is approved in Japan and inhibits influenza A and B strains even if they are resistant to other classes of inhibitors (Furuta et al., 2017).

Nucleoside analogue antivirals

As discussed above, targeting viral genome replication through use of nucleoside analogues has been a successful antiviral strategy for nearly all viral infections with approved therapeutics. Nucleoside analogues have also been explored as anti-cancer agents (Galmarini et al., 2002). Given the clinical success of these compounds and the sequence conservation of the CoV polymerase, this dissertation research focuses on nucleoside analogues as pan-CoV antivirals.

The five most common nucleosides found in nature are adenosine (A), guanosine (G), cytidine (C), thymidine (T), and uridine (U), and the ribonucleosides A, G, C, and U are the building blocks of RNA (Fig. 7). A and G are purines, while C and U are pyrimidines. These nucleosides consist of a sugar moiety of either ribose (RNA) or deoxyribose (DNA) and a nucleobase; they are considered nucleotides when they contain a phosphate group at the 5' position. Nucleoside analogues refer to structurally modified versions of traditional, naturally occurring purine and

pyrimidine nucleosides. Chemically, they take many forms. Modifications may be made at multiple positions on the sugar scaffold or the nucleobase (Seley-Radtke and Yates, 2018) (Fig. 7). When used as therapeutics, nucleoside analogues aim to mimic naturally occurring nucleosides to inhibit enzymatic processes. Since polymerases recognize NTPs as substrates (Choi, 2012), nucleoside analogues often need to be metabolized into triphosphates after entry into the cell to exert their antiviral activity (Eyer et al., 2017).

Prior to this dissertation work, some studies had reported the inability of previously identified ribonucleoside and base analogues, such as RBV, to potently inhibit CoVs (Centers for Disease Control and Prevention (CDC), 2003; Ströher et al., 2004), and this inactivity has been attributed to the proofreading capacity of ExoN (Ferron et al., 2017; Smith et al., 2013). However, some nucleoside analogues, such as 6-azauridine, β -D- N^4 -hydroxycytidine, and mizoribine, have been reported to inhibit CoVs (Pyrc et al., 2006; Saijo et al., 2005). During the course of this dissertation work, galidesivir (BCX4430), remdesivir (GS-5734), fleximer nucleosides, and gemcitabine hydrochloride have also shown efficacy against CoVs (Dyall et al., 2014; Peters et al., 2015; Pruijssers and Denison, 2019; Warren et al., 2016; 2015), though the inhibition of CoVs by many of these nucleoside analogues has not been explored in depth.

Nucleoside analogues may have multiple mechanisms of action that can work independently or together to inhibit a particular virus. Among the most common mechanisms are chain termination and mutagenesis. Regardless of mechanism of inhibition, viruses must select for mutations that enhance fitness in the presence of the inhibitor to survive. These resistance

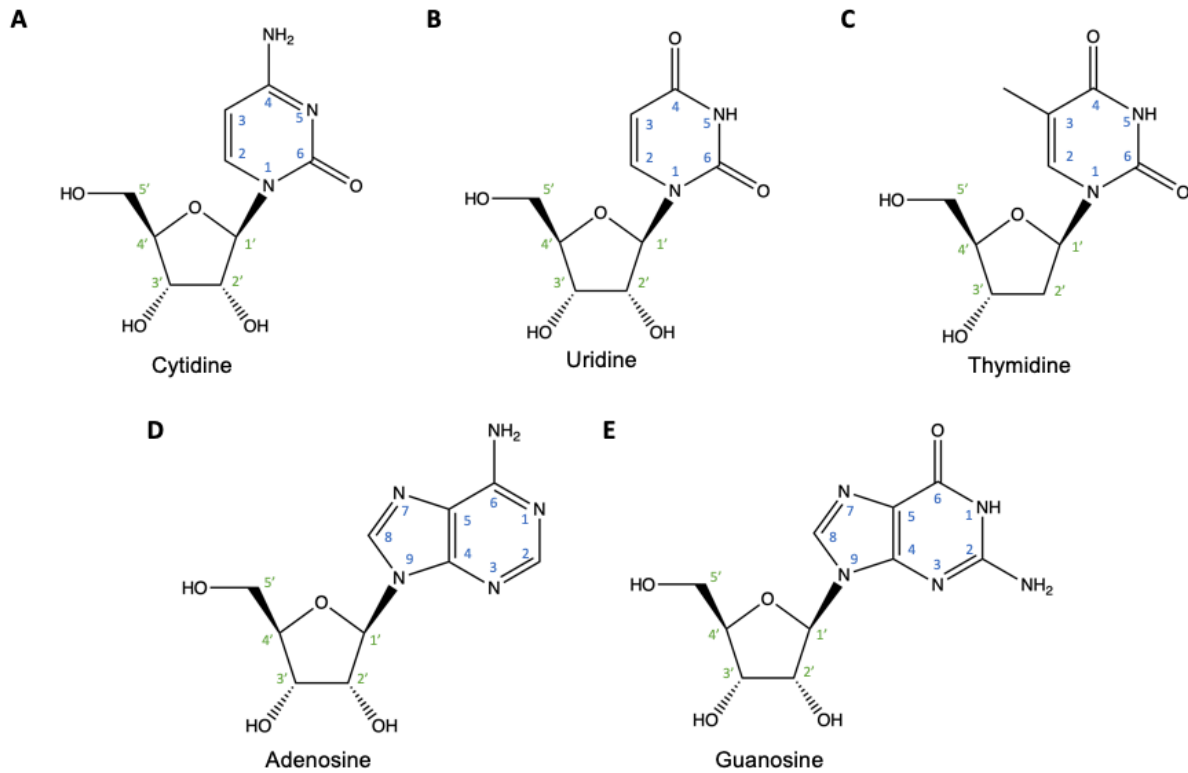


Figure 7. Chemical structure of the most common natural nucleosides.

(A) Cytidine is a pyrimidine nucleoside. (B) The pyrimidine ribonucleoside uridine has a 2' OH group on the sugar moiety. (C) Thymidine, a pyrimidine deoxyribonucleoside, lacks a 2' OH group. The purine nucleosides (D) adenosine and (E) guanosine. Numbers in green and blue represent the positions on the sugar and nucleobase moieties, respectively.

mutations can enhance our understanding of the interactions necessary for inhibition by these compounds that can ultimately help guide future drug discovery and design while maintaining the potential to reveal important aspects of viral biology and genome replication. Thus, some of the mechanisms of inhibition and resistance to these compounds are explored more below.

Chain termination. Chain termination is a common mechanism of action amongst approved nucleoside analogue antivirals, and it is typically achieved following analogue incorporation by the viral polymerase and cessation of strand elongation (Fig. 8A). Nucleoside analogues that act by chain termination may be classified as obligate or non-obligate (Eltahla et al., 2015). This designation is determined by the absence or presence of the 3' OH on the nucleoside, respectively, and thus refers to the necessity of termination based on the ability to add an additional nucleoside after incorporation (De Clercq and Neyts, 2009). Many nucleosides terminate nucleic acid synthesis on the primary strand. However, others may inhibit second strand synthesis; that is, they have an effect once the strand containing the compound serves as the template (Deval, 2009). Little has been directly shown about the precise reasons for non-obligate chain termination. Some studies, particularly with compounds modified at the 2' OH position, have attributed chain termination to a potential steric clash with the incoming NTP (Ma et al., 2007; Vernekar et al., 2014; De Clercq, 2007). Viral resistance to these compounds has primarily been reported in the active site of the polymerase (Eyer et al., 2018; Migliaccio et al., 2003), suggesting that these resistance mutations may alter the polymerase active site to better discriminate against the nucleoside analogue. Despite the chain termination mechanism of herpesvirus inhibitors, these compounds often select for resistance in the viral thymidine kinase required to metabolize them to nucleotides (Frobert et al., 2005; Piret and Boivin, 2011).

Lethal mutagenesis. Viral polymerases erroneously incorporate nucleosides during polymerization providing a genetic platform for viral adaptation in various environments (Domingo et al., 2012; Holland et al., 1982). However, there is a limit to the number of mutations that genomes can tolerate while maintaining function, and this mutation rate limit is referred to as the error threshold (Tejero et al., 2016). Since viruses naturally replicate near this error threshold (Lauring and Andino, 2010), nucleoside analogues that inhibit by lethal mutagenesis take advantage of this limit. In the case of lethal mutagenesis, the virus goes extinct by accumulation of mutations (Tejero et al., 2016), typically during subsequent rounds of replication following incorporation of the nucleoside (Fig. 8B). Viral resistance to lethal mutagenesis may be achieved by modulating either replication fidelity (Pfeiffer and Kirkegaard, 2003a) or mutational robustness (Graci et al., 2012), a measure of the ability of a virus to buffer deleterious mutations (Visher et al., 2016).

Additional mechanisms. While most nucleoside analogues show evidence of incorporation and subsequent biological activity, they may also inhibit viral replication by additional mechanisms. For example, RBV inhibits inosine monophosphate dehydrogenase (IMPDH) (Leyssen et al., 2005; Streeter et al., 1973), which can result in altered nucleoside pools (Wray et al., 1985), and 5-azacytidine can lead to demethylation (Biktasova et al., 2017; Robertson et al., 1995). As for additional mechanisms that involve the polymerase, one nucleoside analogue likely causes backtracking by the polymerase (Dulin et al., 2017). Nucleosides may also have other viral targets, such as the helicase/NTPase (Borowski et al., 2003; 2002) or the N^7 -methyltransferase (Vernekar et al., 2015). Recently, a nucleoside analogue was reported to inhibit multiple viruses

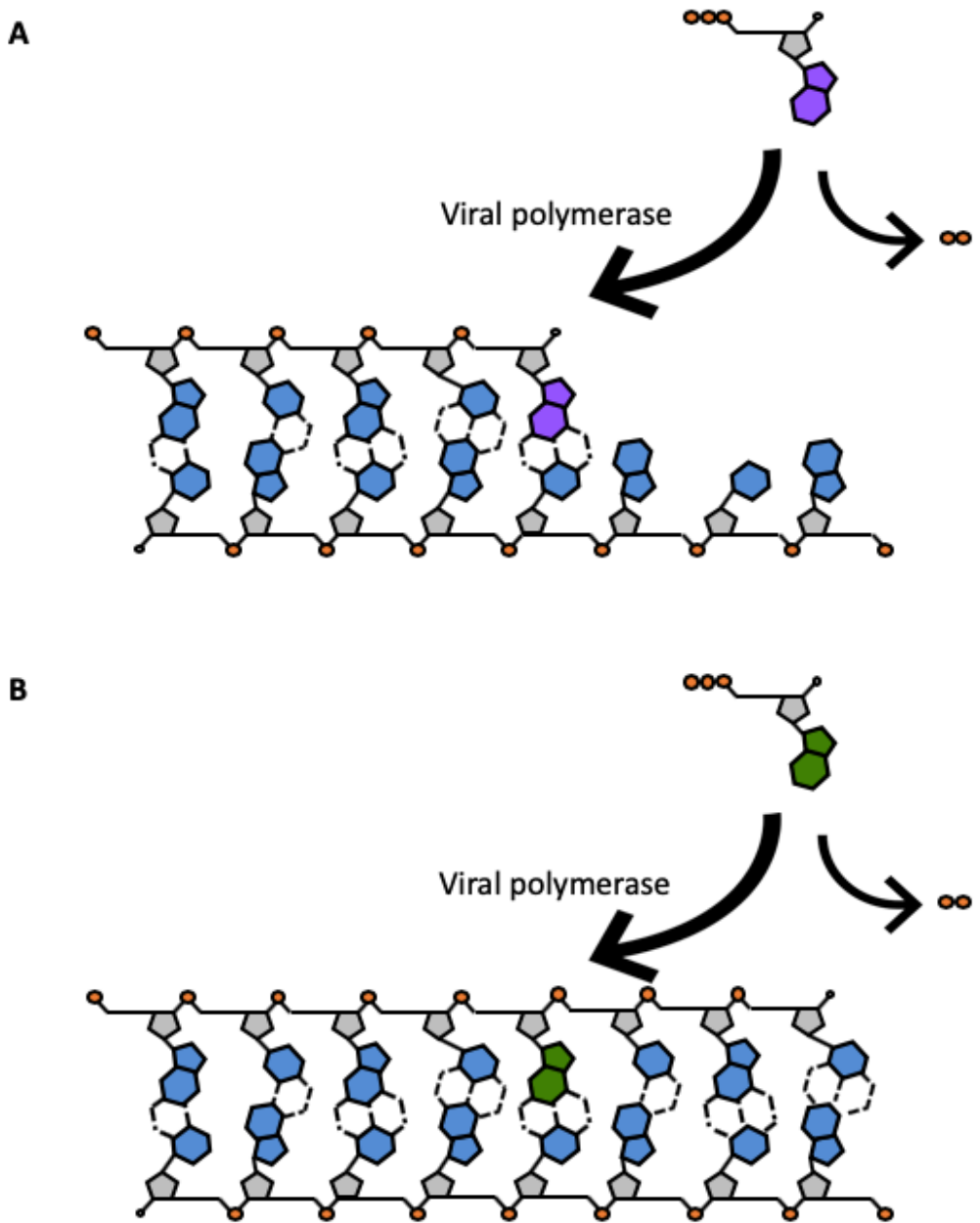


Figure 8. Model of chain termination and lethal mutagenesis, the most common mechanisms of inhibition by nucleoside analogues.

(A) Model of a chain termination mechanism of action. The chain terminator nucleoside analogue is shown in purple. Incorporation of this nucleoside into the nucleic acid strand halts replication either immediately or after the addition of a few nucleotides. (B) Model of a mutagenic mechanism of action. The mutagenic nucleoside analogue, shown in green, is incorporated into the nucleic acid. Elongation continues, and mispairing upon subsequent rounds of replication cause mutations that may lead to loss of genetic information.

by targeting S-adenosyl-L-homocysteine hydrolase to disrupt viral RNA capping (Yoon et al., 2019). In some cases, these mechanisms may be in addition to their activity on the viral polymerase and may help mitigate viral resistance (Eyer et al., 2018).

Summary

Emerging infections continue to pose a threat to human health. However, direct-acting antivirals have not been approved to treat emerging viruses, emphasizing the importance of antiviral development to combat these diseases. CoVs are included within this classification, as two CoVs with pandemic potential have emerged into humans over the past twenty years to cause severe disease. CoVs encode multiple proteins within their large RNA genomes, and several of these proteins have been investigated as potential antiviral targets. Since two distinct CoVs have been the culprits for severe disease in humans thus far, antivirals directed toward CoVs should inhibit essential yet conserved functions during replication. The CoV polymerase is a particularly enticing target, as it performs an essential function during viral genome replication and is among the most highly conserved proteins across CoVs. Further, all polymerases are highly structurally conserved, allowing for potential broad-spectrum inhibitors not only across CoVs, but potentially across viral families. Polymerase inhibitors have been successful antiviral targets for multiple viral infections and primarily come in two flavors: nucleoside and non-nucleoside inhibitors. Nucleoside inhibitors mimic naturally occurring nucleosides that the polymerase recognizes for synthesis while non-nucleoside inhibitors targets are often distant from the active site that may be less conserved. This dissertation work investigates the use of broad-spectrum nucleoside analogue antivirals in the inhibition of CoVs.

In Chapter II, I investigate the antiviral activity of the adenosine analogue GS-441524 and its phosphoramidate prodrug remdesivir (GS-5734) in CoVs through identifying resistance mutations and their implications on fitness. In Chapter III, I probe the antiviral activity of the cytidine analogue, β -D- N^4 -hydroxycytidine (NHC), in CoVs. Chapter IV explores similarities and difference in CoV inhibition and replication across nucleoside analogues with different proposed mechanisms. Chapter V outlines the materials and methods used throughout this dissertation research. In Chapter VI, I highlight the implications of this work and outline areas for future investigation. Overall, this dissertation research identifies two nucleoside analogues that potently inhibit CoVs that also provide insight into the intricacies of CoV replication.

CHAPTER II

CORONAVIRUS SUSCEPTIBILITY TO THE ANTIVIRAL REMDESIVIR (GS-5734) IS MEDIATED BY THE VIRAL POLYMERASE AND THE PROOFREADING EXORIBONUCLEASE

Introduction

While nucleoside analogues have been approved to treat several viral infections, few nucleoside therapeutics had been reported to inhibit emerging infections prior to this dissertation work. The Ebola epidemic of 2014 in West Africa reignited fear of a global pandemic and underscored the need for broadly active antivirals to combat emerging viral infections (Ravi et al.). Many studies began revisiting compounds that demonstrated efficacy against other viral infections to repurpose them for infections with pandemic potential.

GS-441524 is a C-nucleoside analogue that was first reported to inhibit RNA viruses such as HCV (Cho et al., 2012). The designation C-nucleoside refers to the carbon-carbon linkage between the heterocyclic nucleobase and sugar as opposed to the carbon-nitrogen bond present in classical nucleosides. Well known C-nucleosides include pseudouridine, a natural component of RNA (Charette and Gray, 2000) and showdomycin, an antibiotic (Böttcher and Sieber, 2010; Nishimura et al., 1964). While no C-nucleosides are currently approved as antiviral therapies, C-nucleosides such as GS-6620 and galidesivir (BCX4430) have recently been reported to inhibit viral infections (Feng et al., 2014; Taylor et al., 2016; Eyer et al., 2017; Julander et al., 2017). These compounds have renewed interest in C-nucleosides as antivirals, especially since

traditional N-nucleosides are subject to enzymatic and acid-catalyzed hydrolysis, where C-nucleosides are more stable (Boutureira et al.).

Upon cell entry, most nucleosides need to undergo stepwise metabolism by cellular kinases to their triphosphate form to exert antiviral activity. Typically, the rate-limiting step of this process is the first phosphorylation step (Sinokrot et al., 2017; Van Rompay et al., 2000). Since nucleoside phosphates are inefficiently taken up due to their charged nature, prodrug strategies have been developed and implemented to circumvent this problem (Hecker and Erion, 2008; Pradere et al., 2014). The phosphoramidate strategy, where the nucleoside monophosphate is masked by other moieties that are non-toxic when cellularly cleaved, has been employed to combat this inefficiency (Mehellou et al., 2009). Remdesivir (GS-5734) is the monophosphoramidate prodrug of the nucleoside GS-441524 (Slusarczyk et al., 2018). Metabolism of this compound by cellular enzymes will result in GS-441524 monophosphate, which kinases can act upon to ultimately result in GS-441524 triphosphate (Warren et al., 2016).

During this dissertation research, the body of work supporting the use of remdesivir as a broad-spectrum antiviral has continued to grow. Remdesivir was first reported to potently inhibit Ebola virus, but further studies have reported activity against multiple viruses, including but not limited to, hepatitis C virus, Nipah virus, Lassa fever virus, and respiratory syncytial virus (RSV) (Cho et al., 2012; Lo et al., 2019; 2017a; Warren et al., 2016). Importantly, remdesivir potently inhibits diverse CoVs, suggesting its utility as a pan-CoV antiviral (Brown et al., 2019; Sheahan et al., 2017). Biochemical studies with polymerases from RSV, Nipah virus, and Ebola virus have demonstrated that remdesivir inhibits through delayed chain termination in these systems

(Jordan et al., 2018; Tchesnokov et al., 2019; Warren et al., 2016). Clinically, remdesivir has been used in two compassionate use cases and both patients have survived (Dörnemann et al., 2017; Jacobs et al., 2016). Remdesivir clinical trials have also been undertaken to test efficacy in Ebola infected patients (Nakkazi, 2018) and Ebola survivors (NCT02818582).

In this study, I sought to understand the inhibition of CoVs by remdesivir. Here, I describe the only reported resistance mutations for remdesivir during viral infection and begin to identify the impact of these mutations on viral replication. I also work toward understanding the mechanism by which remdesivir inhibits CoVs. I performed all experiments and final analyses for the data in this chapter with the exceptions listed below. Erica Andres helped perform cytotoxicity assays for remdesivir and GS-441524, began the passage of WT MHV in the presence of GS-441524, engineered the polymerase mutations into MHV, and performed initial sensitivity tests with remdesivir resistant mutants. Xiaotao Lu provided technical support to sequence the entire p23 genome. Amy Sims performed the HAE experiments. Rachel Graham engineered the SARS-CoV F480L+V557L virus and assessed its resistance to remdesivir. Tim Sheahan performed the SARS-CoV animal studies.

GS-441524 and remdesivir inhibit MHV replication

GS-441524, a 1'cyano 4-aza-7,9-dideazaadenosine C-nucleoside (Fig. 9A), has been shown to inhibit multiple virus families *in vitro* (Cho et al., 2012; Lo et al., 2017b). To determine if GS-441524 inhibited the model β-2a CoV, murine hepatitis virus (MHV), I infected DBT cells with MHV and treated with increasing concentrations of drug. I observed a dose-dependent reduction in viral titer with up to a 6-log₁₀ decrease at 11.1 μM GS-441524 (Fig. 9B). The half-maximum

effective concentration (EC_{50}) value resulting from GS-441524 treatment was 1.1 μM (Fig. 9C). We observed minimal detectable cytotoxicity within the tested range, with the concentration resulting in 50% cytotoxicity (CC_{50}) $> 300 \mu\text{M}$ (Fig. 9D). This resulted in a therapeutic index (CC_{50}/EC_{50}) of > 250 . Having demonstrated the inhibition of MHV by GS-441524, I next tested its monophosphoramidate prodrug remdesivir (Fig. 9E). Treatment with increasing concentrations of remdesivir resulted in up to a 6-log₁₀ decrease in viral titer, and virus was undetectable by plaque assay at concentrations above 0.5 μM remdesivir (Fig. 9F). Remdesivir inhibited MHV more potently than GS-441524, with an EC_{50} value of 0.03 μM (Fig. 9G), consistent with higher cellular permeability and more efficient metabolism of the prodrug into the active nucleoside triphosphate by bypassing the rate-limiting first phosphorylation step (Murakami et al., 2008; Warren et al., 2016). We also observed minimal cytotoxicity at concentrations required for antiviral activity of remdesivir, with a CC_{50} value of 39 μM (Fig. 9H), resulting in a therapeutic index of > 1000 . These results expand the breadth of GS-441524 and remdesivir inhibition of CoVs to include the model β -CoV MHV.

GS-441524 and remdesivir potently inhibit SARS-CoV and MERS-CoV in HAE cells

Primary human airway epithelial cell cultures (HAE) are among the most clinically relevant *in vitro* models of the lung, recapitulating the cellular complexity and physiology of the epithelium in the human conducting airway (Sims et al., 2005). Previous results have demonstrated that remdesivir inhibits viral titer of multiple CoVs in this model but did not assess the potency or the effect of delaying treatment with compound (Sheahan et al., 2017). Thus, we determined the EC_{50} values after treatment with GS-441524 and remdesivir in SARS-CoV and MERS-CoV-

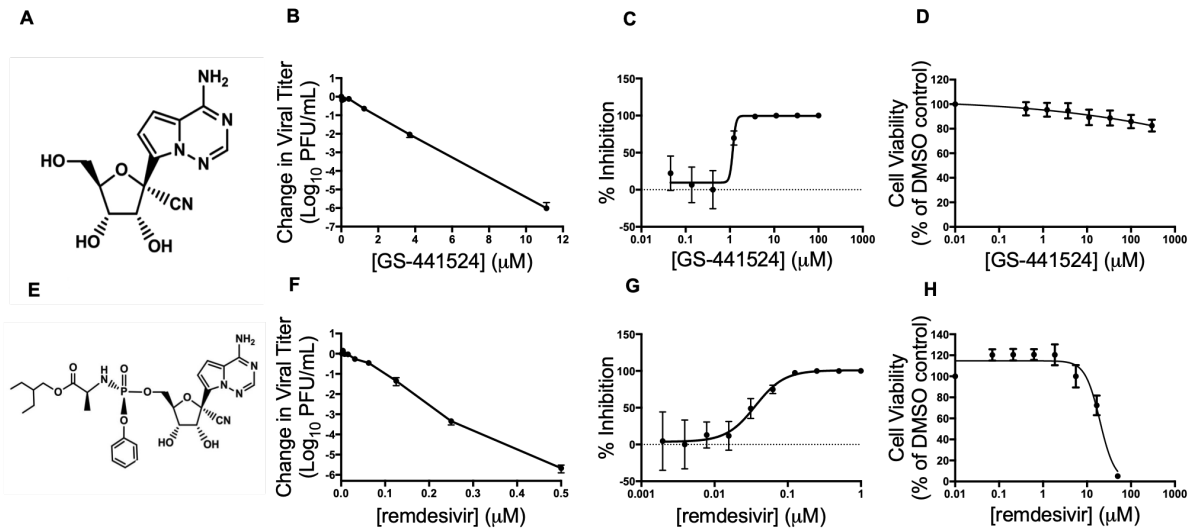


Figure 9. GS-441524 and remdesivir inhibit MHV with minimal cytotoxicity.

(A) GS-441524 is a 1'-cyano 4-aza-7,9-dideazaadenosine C-adenosine nucleoside analogue. (B) Change in viral titer of MHV compared to vehicle control after treatment with GS-441524. The data represent the results from 2 independent experiments, each with 3 replicates. Error bars represent standard error of the mean (SEM). (C) Viral titer data from panel B presented as the percentage of uninhibited control. The EC₅₀ of GS-441524 was calculated to be 1.1 μM. (D) Cell viability normalized to the vehicle control after treatment with GS-441524. The data represent the results from 3 independent experiments, each with 3 replicates. Error bars represent SEM. (E) Remdesivir is a monophosphoramidate prodrug of GS-441524. (F) Change in viral titer of MHV compared to vehicle control after treatment with remdesivir. The data represent the results from 4 independent experiments, each with 3 replicates. Error bars represent SEM. (G) Viral titer data from panel F presented as the percentage of uninhibited control. The EC₅₀ of remdesivir was calculated to be 0.03 μM. (H) Cell viability normalized to vehicle control after treatment with remdesivir. The data represent the results from 3 independent experiments, each with 3 replicates. Error bars represent SEM.

infected HAE cultures. Mean EC₅₀ values for both viruses were approximately 0.86 μM for GS-441524 and 0.074 μM for remdesivir (Fig. 10A). Further, delaying addition of remdesivir until 24 hours post-infection resulted in decreased viral titer in HAE cultures for both SARS-CoV (Fig. 10B) and MERS-CoV (Fig. 10C) at 48- and 72-hours post-infection. No measurable cellular toxicity was observed in HAE cultures for either compound (Table 1). These results demonstrate a similar high potency of remdesivir across divergent CoVs, supporting the utility of the model MHV system to study remdesivir inhibition and resistance.

Remdesivir acts at early times post-infection to decrease viral RNA levels

The predicted mechanism of action of remdesivir is through incorporation of the active triphosphate into viral RNA (Warren et al., 2016). I therefore tested the hypothesis that remdesivir would inhibit CoVs at early steps in replication by inhibiting viral RNA synthesis. To determine which stage in the viral replication cycle remdesivir inhibited CoVs, I infected cells with MHV at an MOI of 1 PFU/cell and treated with 2 μM remdesivir (>50x EC₅₀ value) at 2 hour intervals from 2 hours pre-infection to 10 hours post-infection. I observed maximal inhibition when remdesivir was added between 2 hours pre-infection and 2 hours post-infection. Less inhibition was detected when remdesivir was added between 4- and 6-hours post-infection and no inhibition was observed when remdesivir was added after 8-hours post-infection (Fig. 11A). These results demonstrate that remdesivir inhibits CoVs at early steps during infection. Because viral RNA is synthesized early in infection and remdesivir is implicated in inhibiting viral RNA synthesis (Daelemans et al., 2011; Fehr and Perlman, 2015; Warren et al., 2015), I next determined the level of viral RNA present in cellular monolayers after treatment with remdesivir by qRT-PCR. Treatment with increasing concentrations of remdesivir resulted in

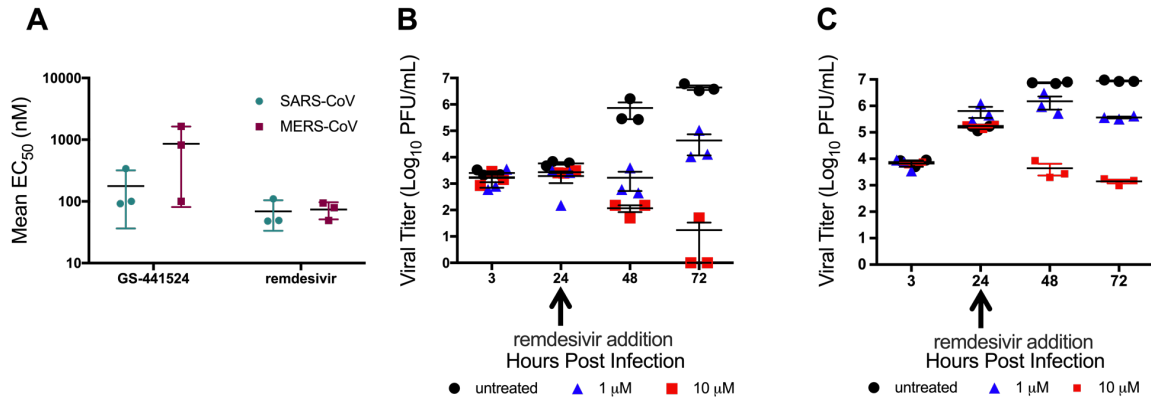


Figure 10. Antiviral activity of GS-441524 and remdesivir and modeled therapeutic efficacy of remdesivir against SARS-CoV and MERS-CoV in HAE cultures.

(A) Mean EC₅₀ values of SARS-CoV and MERS-CoV-infected HAE cultures from three different patient isolates treated with GS-441524 or remdesivir. (B) Viral titers of SARS-CoV-infected HAE cultures when treated with various doses of remdesivir 24 h post-infection. (C) Viral titers of MERS-CoV-infected HAE cultures when treated with various doses of remdesivir 24 h post-infection.

decreased viral RNA levels that correlated with the decrease in titer I observed (Fig. 11B). These results suggest that remdesivir inhibits CoVs early after infection by interfering with viral RNA levels.

Viruses lacking ExoN-mediated proofreading are more sensitive to treatment with remdesivir

The resistance of CoVs to inhibition by the nucleoside and base analogues RBV and 5-FU has been attributed to the proofreading ExoN in nsp14, as engineered ExoN(-) mutant MHV and SARS-CoV are profoundly more sensitive to these compounds (Smith et al., 2013). I therefore compared the sensitivity of WT and ExoN(-) MHV to remdesivir. ExoN(-) MHV demonstrated up to a 100-fold greater reduction in virus titer at 0.25 μ M remdesivir compared to WT (Fig. 12A), and the calculated EC₅₀ for ExoN(-) in this experiment was 0.019 μ M, a 4.5-fold decrease compared to the WT EC₅₀ of 0.087 μ M (Fig. 12B). Similarly to other nucleoside analogues tested in CoVs, ExoN(-) virus demonstrates an increased sensitivity to remdesivir and suggests that, if remdesivir is incorporated into viral RNA, it can likely be removed, albeit inefficiently, by ExoN. However, the results also suggest there is a fundamentally different relationship of remdesivir with the CoV replicase compared with RBV or 5-FU, since remdesivir potently inhibits CoVs with intact proofreading (Smith et al., 2013).

Two mutations in the RdRp mediate partial resistance and restoration of RNA levels in the presence of remdesivir

We next sought to identify the target(s) of remdesivir inhibition. WT MHV was serially passaged in the presence of increasing concentrations of GS-441524, and, after 23 passages, we observed

Table 1. EC₅₀ and CC₅₀ values of GS-441524 or remdesivir in MERS-CoV or SARS-CoV infected HAE cultures^a

Virus	GS-441524		remdesivir	
	EC ₅₀ ± SD (μM)	CC ₅₀ ± SD (μM)	EC ₅₀ ± SD (μM)	CC ₅₀ ± SD (μM)
MERS	0.86 ± 0.78	>100	0.074 ± 0.023	>10
SARS	0.18 ± 0.14	>100	0.069 ± 0.036	>10

^aValues represent the average (mean ± SD) from HAE cultures from at least three donors.

an increased ability of the passaged virus to replicate in the presence of GS-441524 as determined by increased viral CPE. Full genome sequencing of passage 23 (p23) viral RNA revealed 6 non-synonymous mutations in four viral protein-coding regions (Fig 13A): the nsp13 helicase (A335V); the ns2 2',5' phosphodiesterase (Q67H); the spike glycoprotein (A34V, I924T); and the nsp12 RdRp (F476L and V553L) (Fig. 13B). Molecular modeling of the MHV RdRp predicts that both the F476 and V553 residues reside within the predicted fingers domain of the conserved right-hand structure of the RdRp (Fig. 13C) (Sexton et al., 2016; Xu, 2003), and this is also the case in the SARS-CoV RdRp (Kirchdoerfer and Ward, 2019). In addition, both the F476 and V553 residues are identical across sequenced α , β , and γ CoVs (Fig. 13D). Based on the known role of polymerase mutations in resistance to nucleoside analogues for other viruses (Coffey et al., 2011; Migliaccio et al., 2003; Miller et al., 1998; Pfeiffer and Kirkegaard, 2003b), and the previous work describing inhibition of the RSV polymerase by remdesivir (Warren et al., 2016), we first engineered and recovered recombinant MHV encoding the F476L and V553L RdRp mutations. We then tested if these mutations were necessary and sufficient for the observed resistance phenotype of the passage 23 (p23) virus population. Recombinant MHV containing either F476L or V553L individually was less sensitive to remdesivir inhibition than WT MHV, but still more sensitive than the p23 virus population across a broad range of concentrations. In contrast, MHV encoding both F476L and V553L demonstrated a resistance pattern indistinguishable from p23 (Fig. 14A). Neither the p23 virus population nor any of the recombinant viruses were completely resistant to remdesivir; all viruses remained sensitive to higher but non-toxic concentrations of remdesivir. Compared to WT MHV, the F476L virus showed 2.4-fold resistance to remdesivir, V553L demonstrated 5-fold resistance to remdesivir while combined mutations mediated 5.6-fold resistance to remdesivir based on EC₅₀ values

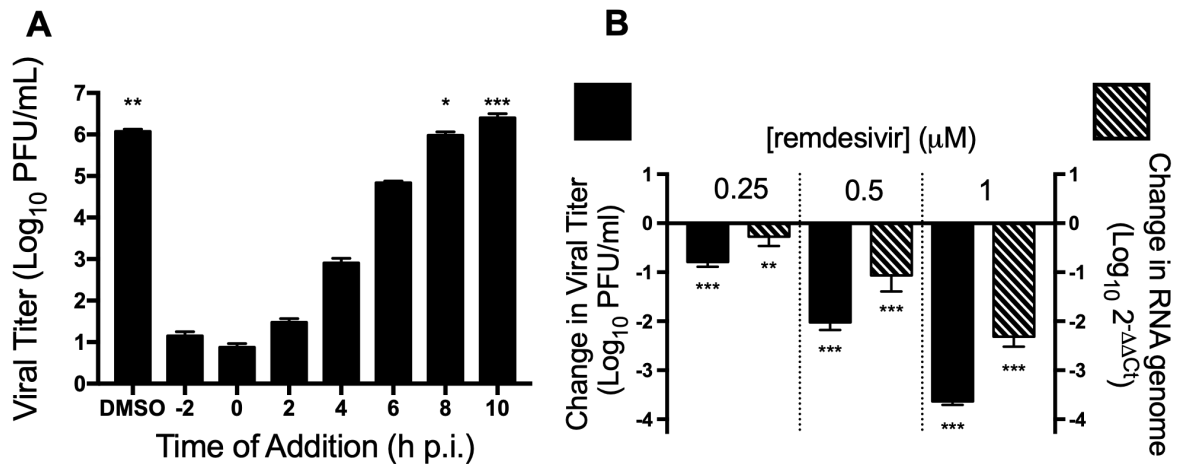


Figure 11. Remdesivir acts at early times post-infection to decrease viral RNA levels.

(A) MHV viral titer after single-cycle infection and treatment with 2 μ M remdesivir at the indicated times post-infection. The data represent the results from 2 independent experiments, each with 3 replicates. Error bars represent SEM. Statistical significance compared to addition of remdesivir at 0 h post-infection (p.i.) was determined by one-way analysis of variance (ANOVA) with Dunnett's post hoc test for multiple comparisons and is denoted by asterisks: *, $P < 0.05$; **, $P < 0.01$; ***, $P < 0.001$. (B) Change in viral titer (black bars) and viral RNA levels (hatched bars) normalized to vehicle control 10 h post-infection after treatment with remdesivir. The data represent the results from 2 independent experiments, each with 3 replicates. Error bars represent SEM. Statistical significance compared to DMSO-treated samples was determined by one-way ANOVA with Dunnett's post hoc test for multiple comparisons and is denoted by asterisks: **, $P < 0.01$; ***, $P < 0.001$.

(Table 2). Because remdesivir decreases viral RNA levels, I next tested if resistance mutations restored viral RNA levels in the presence of remdesivir. RdRp resistance mutations partially restored RNA levels in the presence of remdesivir, and that the degree of restoration of RNA levels correlated with their fold resistance to remdesivir (Fig. 14B). Together, these results are consistent with a mechanism of action of remdesivir primarily targeting RdRp-mediated RNA synthesis.

Remdesivir resistance mutations impair competitive fitness of MHV

To assess the effect of remdesivir resistance on viral fitness, I first determined the replication capacity of recombinant MHV encoding the F476L, V553L, and F476L + V553L mutations. Each of these viruses replicated similarly to WT MHV, both in replication kinetics and observed peak titer (Fig. 14C). I next tested the competitive fitness of F476L + V553L MHV compared to WT MHV during co-infection over multiple passages. Murine DBT cells were co-infected with WT MHV and F476L + V553L MHV at WT:mutant ratios of 1:1, 1:9 or 9:1 in the absence of remdesivir, and infected culture supernatants were serially passaged 3 times to fresh cell monolayers. By passage 4, F476L + V553L MHV was outcompeted by WT MHV in the population at every input ratio (Fig. 14D), demonstrating a competitive fitness cost of the F476L + V553L mutations in the absence of remdesivir. This competitive fitness cost further suggests that remdesivir resistance mutations will not persist in the absence of treatment.

Mutations identified in remdesivir-resistant MHV also confer resistance in SARS-CoV

Given the high conservation of the F476 and V553 residues across CoVs, we next tested whether substitutions at the homologous SARS-CoV residues (F480L and V557L) could confer

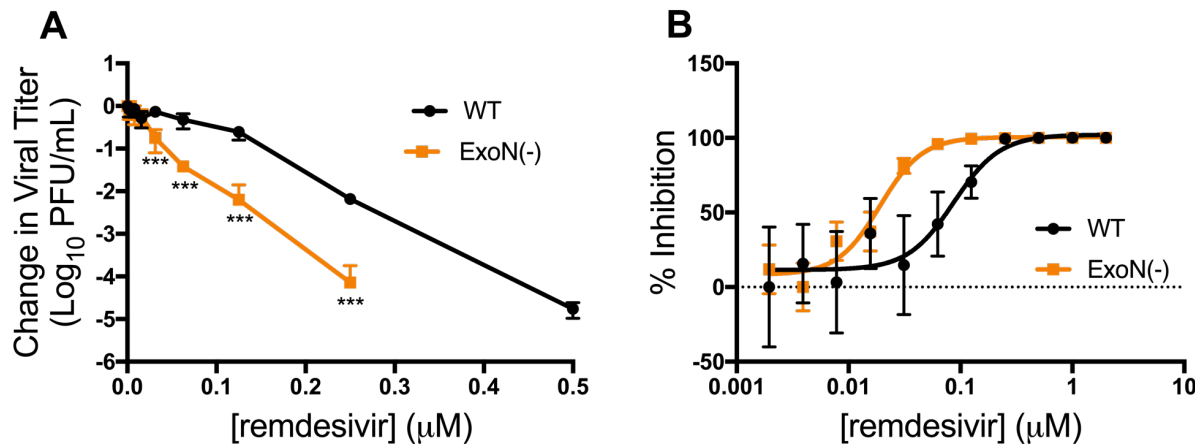


Figure 12. Viruses lacking ExoN-mediated proofreading are more sensitive to remdesivir inhibition.

(A) Change in viral titer of WT and ExoN(-) viruses normalized to vehicle control after treatment with remdesivir. The data represent the results from 2 independent experiments, each with 3 replicates. Error bars represent SEM. Statistical significance compared to WT at each concentration was determined by unpaired *t* test using the Holm-Sidak method to correct for multiple comparisons and is denoted by asterisks: ***, $P < 0.001$. (B) Viral titer reduction from panel A represented as percentage of vehicle control, resulting in a WT EC₅₀ value of 0.087 μM and an ExoN(-) EC₅₀ of 0.019 μM .

resistance to remdesivir. We recovered SARS-CoV encoding the homologous F480L and V557L substitutions and tested recovered mutant viruses for resistance to remdesivir in Calu-3 2B4 cells. WT SARS-CoV demonstrated dose-dependent inhibition by remdesivir with an EC₅₀ of 0.01 μM (Fig 15A). The F480L + V557L recombinant virus was also inhibited by remdesivir. However, the F480L + V557L EC₅₀ value was 0.06 μM, a 6-fold resistance to remdesivir (Fig. 15B), that is nearly identical to the fold-resistance of F476L + V553L MHV. These results support the conclusion that the conserved residues across divergent CoVs reflect conserved functions impaired by remdesivir, potentially implying common pathways to resistance across CoVs.

Remdesivir-resistant SARS-CoV is attenuated *in vivo*

To gain insight into the pathogenic potential of remdesivir resistant viruses, we directly compared WT SARS-CoV and F480L + V557L SARS-CoV following high (10⁴ PFU) and low (10³ PFU) dose inoculation in a well-characterized mouse model of SARS-CoV pathogenesis with disease reminiscent of that observed in humans (Gralinski et al., 2013). Mice infected with a high dose of F480L + V557L SARS-CoV lost significantly less weight ($P < 0.05$) than WT SARS-CoV infected mice (Fig. 15C). At 2 days post-infection, mouse lung viral titers were similarly high between WT and F480L + V557L SARS-CoV, but by 4 days post-infection lung viral titers were significantly reduced ($P < 0.05$) in mice infected with F480L + V557L SARS-CoV (Fig. 15D). Together, these data demonstrate that remdesivir resistant SARS-CoV is likely attenuated in its ability to cause disease and replicates less efficiently than WT virus in robust mouse models of human SARS-CoV disease.

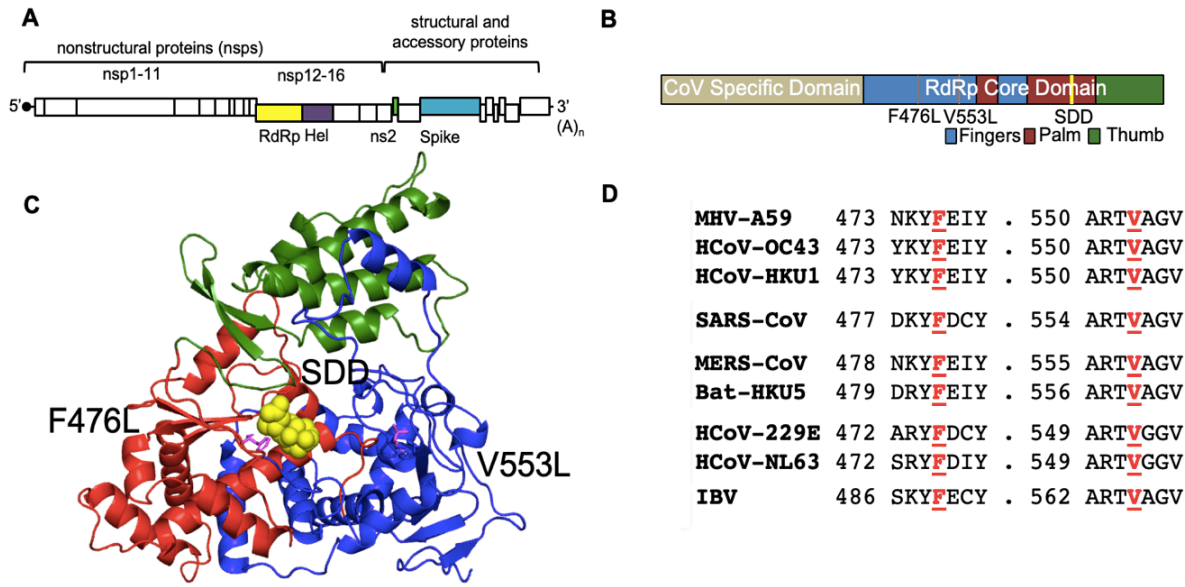


Figure 13. Two mutations in the predicted fingers domain of the nsp12 RdRp, F476L and V553L, arose after 23 passages in the presence of GS-441524, and these residues are highly conserved across CoVs.

(A) Schematic of the MHV genome displaying proteins with mutations identified after passage with GS-441524. The nsp12 RdRp is shown in yellow, nsp13-helicase in purple, ns2 in green, and spike in blue. (B) Linear schematic of nsp12 showing the locations of F476L and V553L within the predicted fingers of the RdRp core domain. (C) A model of the MHV RdRp core domain was determined based on the SARS-CoV polymerase structure (Kirchdoerfer and Ward, 2019) using the Phyre² platform. This model was used to map the predicted locations of the F476L and V553L residues, shown here in magenta. The SDD active site residues are shown in yellow, the palm domain in red, the fingers domain in blue, and the thumb domain in green. (D) Amino acid conservation of F476 and V553 residues across CoVs demonstrating that both of these residues are highly conserved.

Discussion

Broadly active antivirals are needed to treat contemporary human CoVs, including endemic MERS-CoV in the Middle East and potential future zoonotic CoV epidemics. The prophylactic and therapeutic efficacy of remdesivir (GS-5734) was recently demonstrated in a mouse model of SARS-CoV infection, as well as *in vitro* activity against multiple other human and zoonotic CoVs (Sheahan et al., 2017). In this study I began to define the ability of remdesivir to inhibit CoVs in the setting of intact nsp14 proofreading activities. While ExoN(-) MHV is 4.5-fold more sensitive to remdesivir treatment than WT MHV, the potent inhibition of WT CoVs suggests a unique mechanism of inhibition of CoV RNA synthesis that is able to circumvent ExoN surveillance and activity. Further, we report for the first time for any virus inhibited by remdesivir that selection for partial resistance to remdesivir required prolonged passage. Surprisingly, no resistance mutations were selected within ExoN, but rather two mutations of highly conserved residues in the RdRp reduced the sensitivity to remdesivir to a level comparable to the passaged virus. Introduction of the homologous substitutions in SARS-CoV reproduced the fold resistance to remdesivir observed in MHV, demonstrating the potential for common, family-wide drug resistance pathways in the RdRp.

Potential remdesivir mechanism of action in CoVs. Nucleoside analogues can have multiple mechanisms of action, including lethal mutagenesis, obligate or non-obligate chain termination, and perturbation of natural nucleotide triphosphate pools via inhibition of nucleotide biosynthesis (Baranovich et al., 2013; Crotty et al., 2000; Eltahla et al., 2015; Pyrc et al., 2006; Sangawa et al., 2013; Streeter et al., 1973; Te et al., 2007). Remdesivir has been reported to cause premature termination of nascent RNA transcripts in biochemical assay with purified

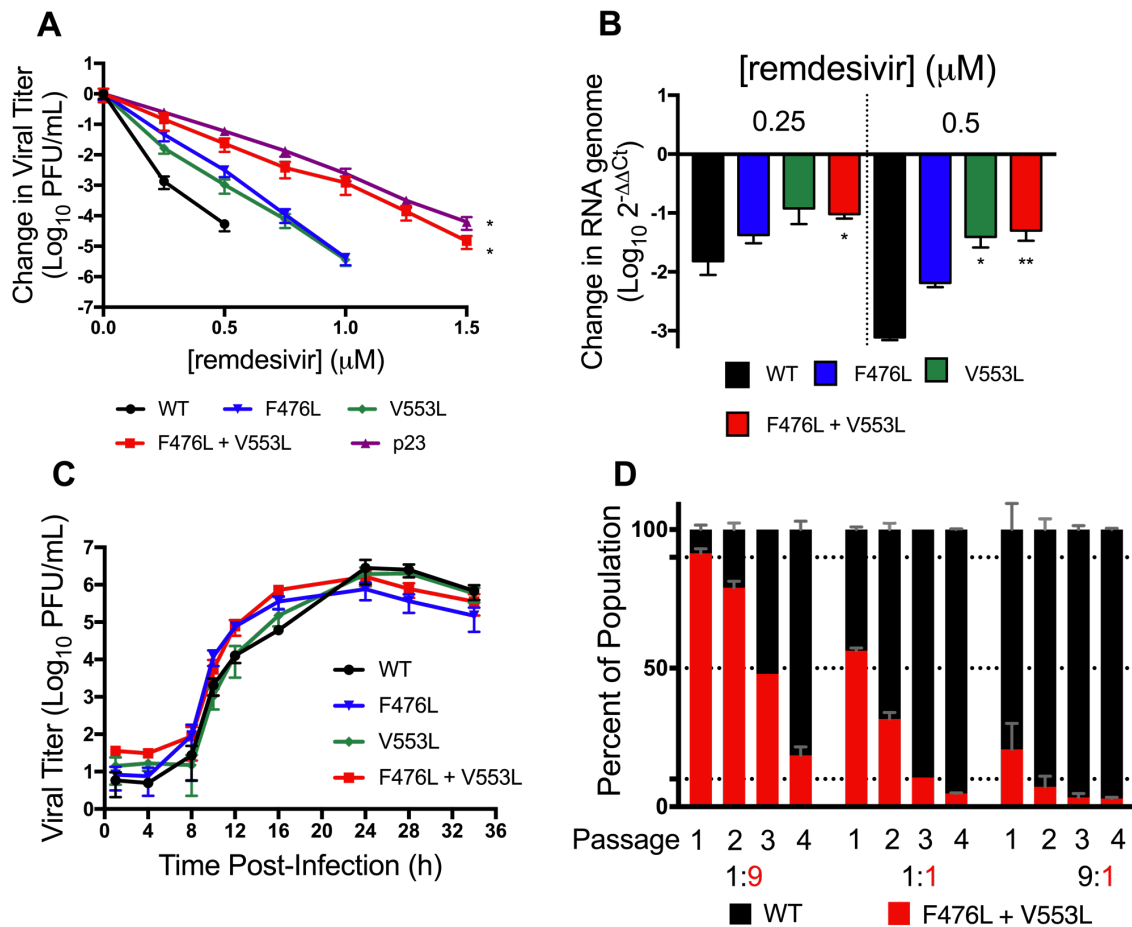


Figure 14. The F476L and V553L mutations mediate resistance to remdesivir and are associated with a fitness defect.

(A) Change in viral titer of WT, F476L, V553L, F476L + V553L, and p23 viruses normalized to the vehicle control after treatment with remdesivir. The data represent 2 independent experiments, each with 3 replicates. Error bars represent SEM. Statistical significance compared to WT was determined by Kolmogorov-Smirnov test and is denoted by asterisks: *, $P < 0.05$. (B) The change in genomic RNA levels of WT, F476L, V553L, and F476L + V553L MHV normalized to vehicle control after treatment with remdesivir. The data represent the results from 2 independent experiments, each with 3 replicates. Error bars represent SEM. Statistical significance compared to WT at each concentration was determined by one-way ANOVA with Dunnett's post hoc test for multiple comparisons and is denoted by asterisks: *, $P < 0.05$; **, $P < 0.01$. (C) Multi-cycle replication kinetics of WT, F476L, V553L, or F476L + V553L MHV. The data represent the results from 2 independent experiments, each with 3 replicates. Error bars represent SEM. (D) Coinfection competition assay of WT and F476L + V553L MHV at the indicated ratios. The percentage of the population of each mutation was assessed after four successive passages. The data are representative of 2 independent experiments each with 2 replicates. Error bars represent standard deviation (SD).

polymerases, but the mechanism of inhibition in CoVs has not been fully explored (Warren et al., 2016). Our data demonstrate that remdesivir acts early in infection and decreases RNA levels in a dose-dependent manner that parallels impairment of viral titer. Further, while remdesivir is highly active against WT CoVs, it is 4.5-fold more active in MHV lacking the proofreading activity of ExoN. Finally, remdesivir is 3-30 times more active than GS-441524 in all of the CoVs tested, suggesting the triphosphate metabolite is the active molecule inhibiting the viral RdRp. All of the above support a mechanism involving incorporation of remdesivir into nascent CoV RNA, but do not discriminate between chain termination and incorporation mutagenesis. In fact, other nucleoside analogues have multiple proposed mechanisms of virus inhibition, including favipiravir in influenza and RBV in HCV (Baranovich et al., 2013; Sangawa et al., 2013; Te et al., 2007). Future studies using deep sequencing and biochemical approaches will allow us to precisely define the remdesivir mechanism(s) of action against CoVs.

Nucleoside analogues have been approved to treat a variety of RNA and DNA viruses, but CoVs have been refractory to inhibition by some nucleoside analogues (Smith et al., 2013). This resistance to potent inhibition by RBV and 5-FU has been attributed to the CoV nsp14 proofreading exoribonuclease. Previous reports have shown that MHV and SARS-CoV lacking the proofreading activity of ExoN [ExoN(-)] were more sensitive to 5-FU and RBV, underscoring the role of ExoN-mediated proofreading in resistance to inhibition by these compounds (Smith et al., 2013). These results suggest that, to effectively inhibit CoVs, nucleoside analogues would need to inhibit ExoN directly, be incorporated so efficiently that the 5'-3' elongation reaction is much faster than the ExoN cleavage reaction, or not be recognized for ExoN-mediated removal. The latter mechanism has been proposed for sensitivity of herpes

Table 2. F476L and V553L mutations confer up to 5.6-fold resistance to remdesivir in MHV^a

Virus	EC ₅₀ (μ M)	Fold resistance
WT	0.024 ± 0.011	1
F476L	0.057 ± 0.040	2.4
V553L	0.12 ± 0.06	5.0
F476L + V553L	0.13 ± 0.06	5.6

^aMean EC₅₀ values ± SD and fold resistance of remdesivir -resistant viruses were calculated using viral titer data following infection of DBT cells with the indicated virus at MOI = 0.01 PFU/cell and treatment with increasing concentrations of remdesivir. Fold resistance was calculated as EC₅₀ of mutant/EC₅₀ of WT. The data represent the results from 3 independent experiments, each with 3 replicates.

simplex virus (HSV) to acyclovir; specifically, that the HSV exonuclease is unable to remove acyclovir (Derse et al., 1981). Here, I show that ExoN(-) MHV is more sensitive than WT MHV to remdesivir treatment. This result suggests that remdesivir is recognized, at least partially, by a functional ExoN, but that the ExoN activity is not sufficient to prevent potent inhibition of CoV replication. One possible explanation is that remdesivir may be recognized and removed by ExoN less efficiently than these mutagens or other incorrect nucleotides, though further studies are needed to fully understand the role of ExoN in remdesivir inhibition of CoVs. Overall, the enhanced activity of the monophosphate prodrug, the increased sensitivity of ExoN(-) viruses to remdesivir inhibition, selected resistance mutations in the modeled RdRp fingers domain, the time-dependent viral inhibition profile, and decreased viral RNA levels support the hypothesis that remdesivir directly inhibits viral RNA synthesis.

Mechanism of resistance to remdesivir. Previous studies have assessed inhibition by remdesivir in multiple viruses, but none have reported resistance mutations during treatment. In this study, passage of MHV in the presence of GS-441524 resulted in selection of 5.6-fold resistance. Sequencing identified consensus non-synonymous F476L and V553L mutations in the nsp12 core polymerase-coding region. A similar level of resistance was observed for the homologous F480L and V557L substitutions in SARS-CoV. As these mutations are not in the immediate vicinity of the RdRp active site, the mechanism of resistance to remdesivir remains to be determined. Both of these residues are conserved across CoVs, suggesting that they mediate conserved functions. Sequence alignment and molecular modeling of the CoV RdRp predicts that V553L lies just outside of motif F of the fingers domain, which forms a channel for

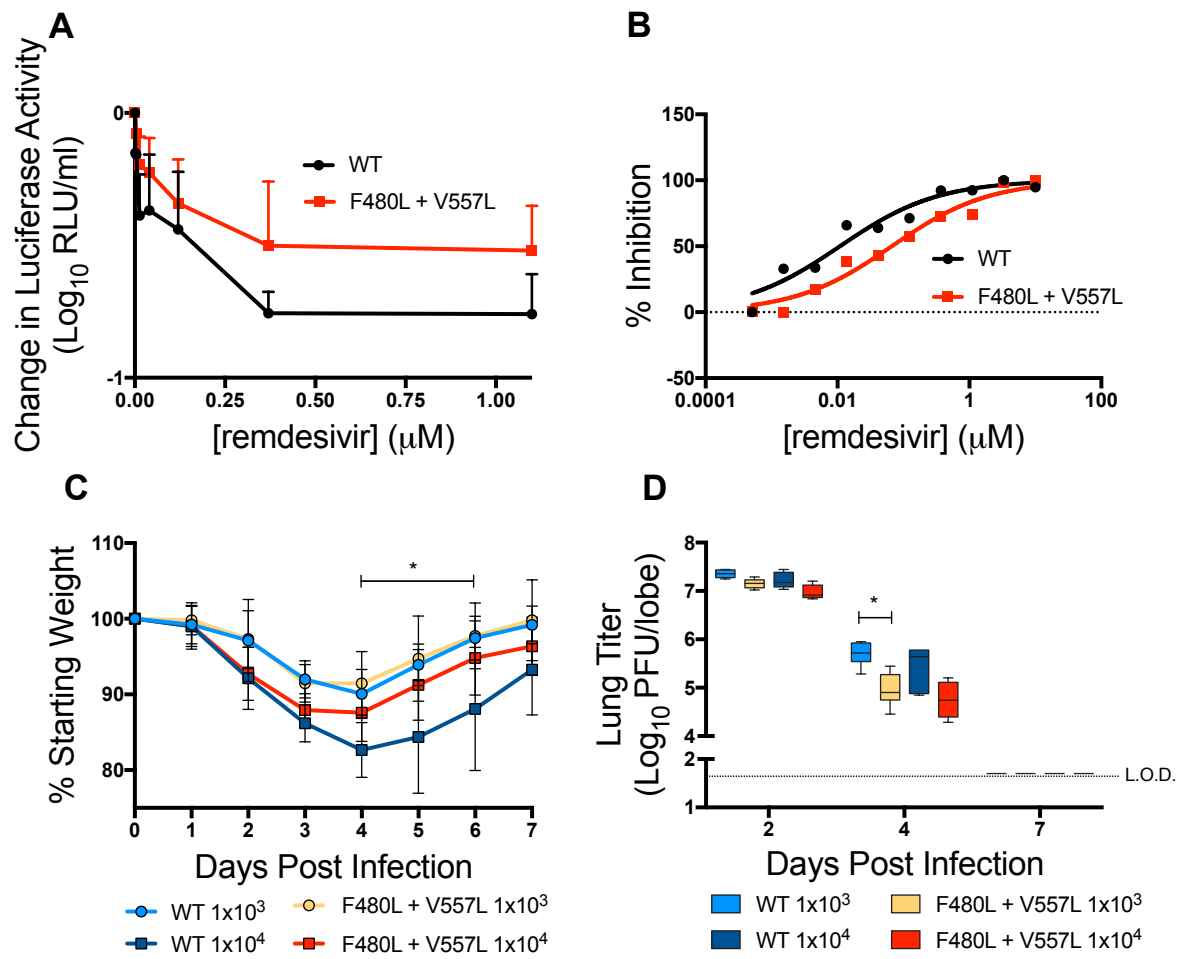


Figure 15. MHV resistance mutations confer resistance and are attenuated in SARS-CoV.

(A) Change in luciferase activity normalized to vehicle control of WT or F480L + V557L SARS-CoV containing the NanoLUC reporter. The data are representative of the results from 2 independent experiments, each with 3 replicates. Error bars represent SEM. (B) Viral titer data from panel A presented as the percentage of vehicle control. This EC₅₀ value was calculated as 0.01 μ M for WT and 0.06 μ M for F480L + V557L virus, which represents a 6-fold increase in resistance. (C) Percent starting weight of BALB/c mice inoculated with WT or F480L + V557L SARS-CoV containing the NanoLUC reporter at 103 or 104 PFU. The data are representative of the results from 2 independent experiments, each with 10 to 12 animals per group. Error bars represent SEM. Statistical significance was determined by 2-way ANOVA and is denoted by asterisks: *, P < 0.05. (D) Lung titers from animals in panel C 2, 4, and 7 days post-infection. The data are representative of the results from 2 independent experiments, each with 3 animals per group. Error bars represent SEM. Statistical significance was determined by Wilcoxon test and is denoted by asterisks: *, P < 0.05.

incoming NTPs and contacts the 5' end of the template, while F476L is not within any defined structural motif but also resides in the fingers domain (Ferrer-Orta et al., 2007; Xu, 2003).

Resistance mutations to nucleoside analogues, including those that lie in the fingers domain, have been implicated in altering replication fidelity as a mechanism of resistance in picornaviruses and HIV (Hsu, 1997; Pfeiffer and Kirkegaard, 2003b; Wainberg et al., 1996). In a previous study, using homology modeling of the CoV RdRp based on the Coxsackie Virus B3 RdRp structure, work by Nicole Sexton in the Denison lab predicted and confirmed that a V553I substitution in the MHV RdRp increases CoV fidelity in ExoN(-) viruses (Sexton et al., 2016), suggesting that viral replication fidelity modulation may also impact susceptibility to remdesivir. This conclusion is supported by the result that remdesivir, while highly active in WT virus, is even more potent in the absence of nsp14-ExoN proofreading activity. However, the CoV replicase encodes many proteins, and these mutations may alter protein-protein interactions among these components. Thus, it will be interesting to determine if F476L and V553L confer class-level resistance to nucleotide analogues, general increased fidelity, changes in specific nucleotide selectivity, alterations in replicase protein interactions, or if they act by other novel mechanisms.

Recombinant MHV containing the F476L and V553L mutations very closely recapitulated the remdesivir resistance phenotype of passage 23 virus population, confirming the importance of these mutations for resistance. However, we also identified additional non-RdRp mutations in the consensus sequence of passage 23 virus, including another component of the MHV replicase, the nsp13 helicase. It will be important to determine if other proteins contribute to resistance, as well

as using remdesivir as a probe to define protein interactions and functions within the viral replicase.

Remdesivir resistance is associated with a fitness cost *in vitro* and attenuation *in vivo*.

Identifying resistance mutations to antiviral compound candidates *in vitro* provides an opportunity to assess the concern that resistance may promote viral fitness, leading to enhanced transmission or greater disease severity. The resistance of MHV to remdesivir was very slow to emerge and only partial, suggesting a high genetic barrier to resistance, similar to that seen for HCV resistance to the nucleotide antiviral sofosbuvir (Svarovskaia et al., 2016). Moreover, although recombinant MHV containing both F476L and V553L replicated similarly to WT in parallel cultures, resistant virus failed to compete with WT MHV during co-infection over multiple passages, demonstrating a fitness cost to the resistance mutations that may limit emergence during treatment. The fitness impairment was further evidenced *in vivo* by attenuation of F480L + V557L in a SARS-CoV mouse model, similar to that reported for other viruses with selected resistance to nucleotide analogues, including HIV and chikungunya virus (Coffey et al., 2011; Paredes et al., 2009; Pfeiffer and Kirkegaard, 2005). This fitness impairment may be due to alterations in RNA replication, fidelity, nucleotide incorporation, or protein stability, but suggests that remdesivir resistance will not lead to more transmissible or pathogenic virus.

Conclusion

In summary, this work provides evidence that remdesivir is highly active against CoVs and that there is a high genetic barrier to achieve resistance. Additionally, resistant virus suffers a loss of competitive fitness *in vitro* and attenuation in animals, suggesting these mutations will not favor disease emergence and are likely to be poorly maintained in nature, particularly during acute

infections. Finally, the results identify potential novel determinants of polymerase function that will guide future studies focused on better understanding polymerase structure-function relationships and remdesivir mechanism. Together, these results argue strongly for the continued clinical development of remdesivir to treat MERS-CoV and demonstrate its potential utility in the broad-spectrum treatment of CoV infections.

CHAPTER III

β-D-N⁴-HYDROXYCYTIDINE: A MUTAGEN ACTIVE AGAINST A PROOFREADING-INTACT CORONAVIRUS WITH A HIGH GENETIC BARRIER TO RESISTANCE

Introduction

β-D-N⁴-Hydroxycytidine (NHC) represents one of the products of the reaction between cytidine and hydroxylamine (Brown and Hewlins, 1968; Brown et al.). This compound is modified solely on the N⁴ position of the cytosine nucleobase compared with its naturally occurring cytidine counterpart. Early work with this compound focused on the mutagenic effects of this compound in multiple bacterial systems (Popowska et al.; Popowska and Janion, 1974; Salganik et al., 1973). However, more recent studies have investigated the antiviral properties of NHC. NHC inhibits multiple RNA virus families, including chikungunya virus, Venezuelan equine encephalitis virus (VEEV), respiratory syncytial virus (RSV), hepatitis C virus (HCV), norovirus, influenza A and B viruses, and Ebola virus (Costantini et al., 2012; Ehteshami et al., 2017; Reynard et al., 2015; Stuyver et al., 2003; Urakova et al., 2017; Yoon et al., 2018). Previous reports have demonstrated an increased introduction of transition mutations in viral genomes after treatment as well as a high genetic barrier to resistance (Stuyver et al., 2003; Urakova et al., 2017; Yoon et al., 2018). Antiviral activity of NHC has also been reported against the human α-CoV HCoV-NL63, as well as the β-CoV SARS-CoV (Barnard et al., 2004; Pyrc et al., 2006). Neither an NHC mechanism of action or resistance have been described for any CoVs to date.

In this chapter, I investigated NHC inhibition and resistance in CoVs. NHC potently inhibits WT MHV and MERS-CoV with minimal cytotoxicity. I demonstrate that MHV ExoN RNA proofreading has a limited, but measurable effect on sensitivity to NHC. In addition, I observed an NHC inhibition profile consistent with a mutagenic mechanism of action featuring an accumulation of transition mutations, indicative of a high genetic barrier to resistance.

I performed all experiments and final analyses for the data in this chapter with the exceptions listed below. Jim Chappell passaged MERS-CoV in the presence of NHC, and Andrea Pruijssers performed all other MERS-CoV NHC experiments. Erica Andres performed DBT-9 cytotoxicity assays. Jennifer Gribble bioinformatically processed deep sequencing mutagenesis data files.

NHC inhibits MHV and MERS-CoV replication with minimal cytotoxicity

NHC (Fig. 16) has potent broad-spectrum antiviral activity against many RNA viral families (Stuyver et al., 2003). We first determined if NHC also inhibited CoV replication using a dose-response experiment with two divergent β-CoVs: the model CoV, MHV, and the epidemically circulating zoonotic CoV, MERS-CoV. NHC treatment resulted in a dose-dependent reduction in viral titer for MHV (Fig. 17A) and MERS-CoV (Fig. 17B). This inhibition resulted in a 50% effective concentration (EC_{50}) of 0.17 μM for MHV (Fig. 17C) and 0.56 μM for MERS-CoV (Fig. 17D). We detected negligible changes in DBT-9 cell viability out to 200 μM (Fig. 17E) and CC_{50} values above 10 μM in Vero cells (Fig. 17F), respectively. Thus, the selectivity index was >1000 for MHV and >20 for MERS-CoV. Together, these results confirm potent inhibition of β-CoVs by NHC.

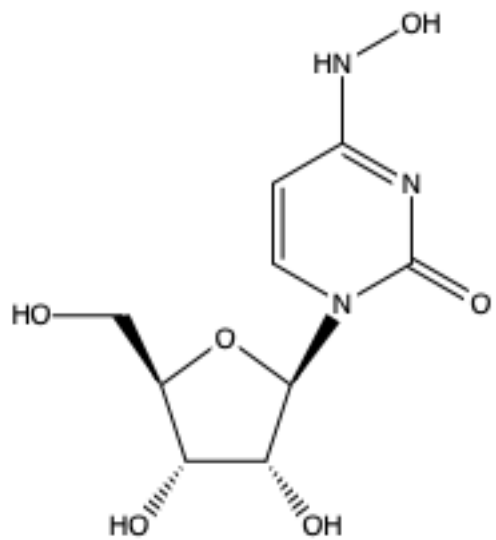


Figure 16. Chemical structure of EIDD-1931, β -D- N^4 -hydroxycytidine (NHC).

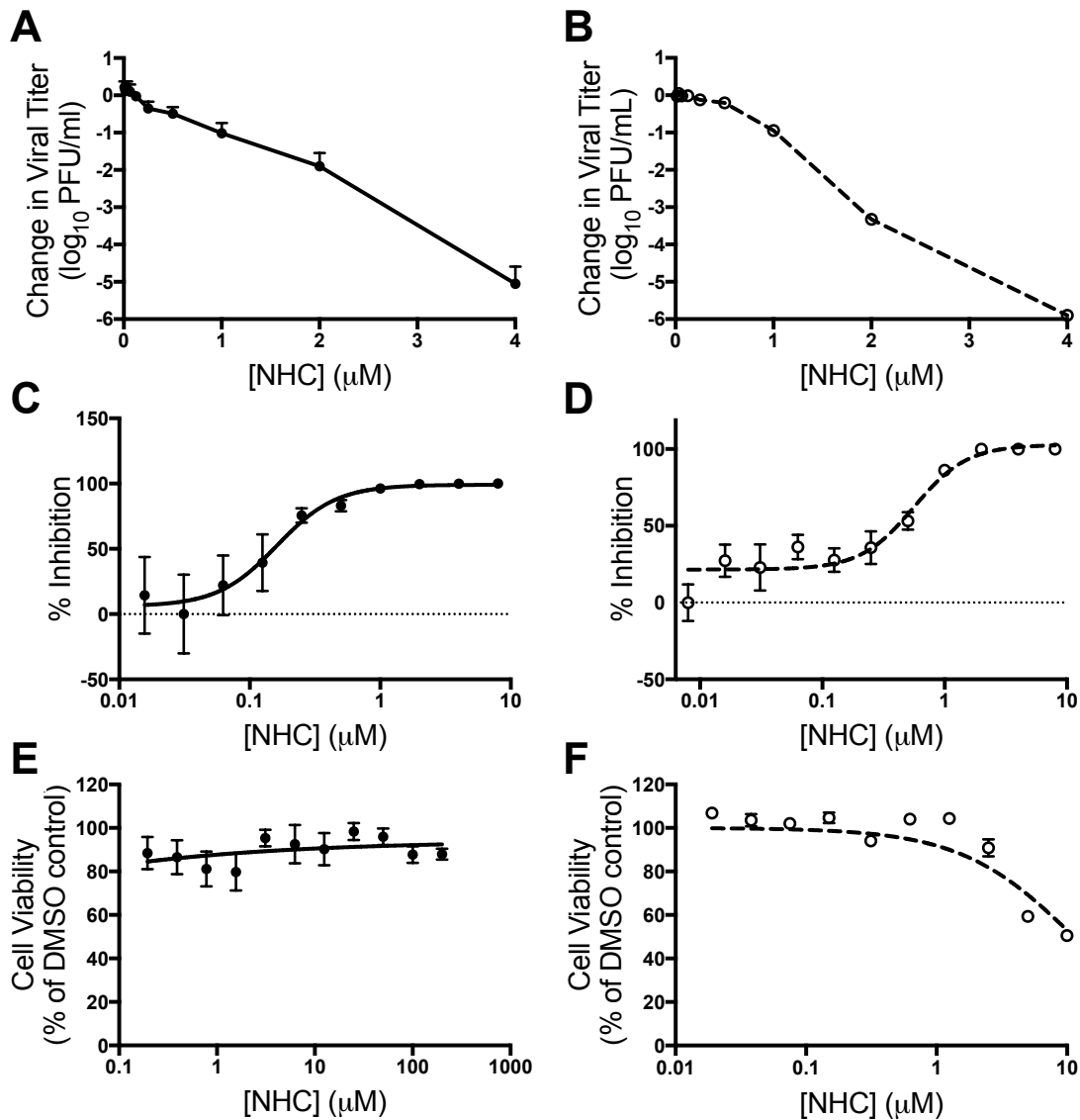


Figure 17. NHC inhibits MHV and MERS-CoV with minimal cytotoxicity.

(A) Change in MHV and (B) MERS-CoV titer relative to vehicle control after treatment with increasing concentrations of NHC. The data represent the results of 2 independent experiments, each with 3 replicates. Error bars represent standard error of the mean (SEM). (C) Change in titer data from (A) represented as percent of vehicle control. WT MHV EC₅₀ = 0.17 μM . (D) Change in titer data from (B) represented as percent of vehicle control. WT MERS-CoV EC₅₀ = 0.56 μM . (E) DBT-9 cell viability as a percent of DMSO control across NHC concentrations. No cytotoxicity was detected up to 200 μM . The data represent the results of 2 independent experiments, each with 2 replicates (MHV). Error bars represent standard error of the mean (SEM). (F) Vero cell viability as a percent of DMSO control across NHC concentrations. Less than 50% cytotoxicity was detected up to 10 μM . The data represent the results of 2 independent experiments, each with 3 replicates. Error bars

NHC inhibition profile in CoVs is consistent with mutagenesis

To better understand the mechanism through which NHC inhibits CoV replication, I performed a time-of-drug addition assay to determine at what point in the viral replication cycle NHC acts (Daelemans et al., 2011). Therefore, I added 16 µM (~100x EC₅₀ concentration) NHC to cells at the indicated times pre- or post-infection with WT MHV at a MOI of 1 PFU/cell and quantified viral replication after a single infectious cycle. Compared to the vehicle (DMSO) control, NHC significantly inhibited MHV replication when added at or before six hours post-infection (Fig. 18A), suggesting that NHC acts at early stages of the viral replication cycle. I next determined the effect of NHC on MHV RNA levels and compared that to its effect on infectious viral titer. RNA levels were reduced by approximately 10-fold at the highest tested concentration of NHC in both MHV-infected cell monolayers (Fig. 18B) and supernatants (Fig. 18C). In contrast, viral titer was reduced up to 5,000-fold at these concentrations. I therefore calculated the ratio of infectious titer per viral RNA genome copy (specific infectivity) after NHC treatment and found that the specific infectivity of WT MHV was reduced in a dose-dependent manner after treatment with increasing concentrations of NHC (Fig. 18D). Together, these data are consistent with a mutagenic mechanism of NHC anti-CoV activity.

NHC treatment increases transition mutations present across the MHV genome, particularly the proportion of G:A and C:U transitions

To directly test the effect of NHC treatment on MHV mutational burden, I treated WT MHV with increasing concentrations of NHC and performed full-genome next-generation sequencing (NGS) on viral populations released after a single infection. My data demonstrate a dose-dependent increase in mutations present at low frequencies (<5 % of viral population)

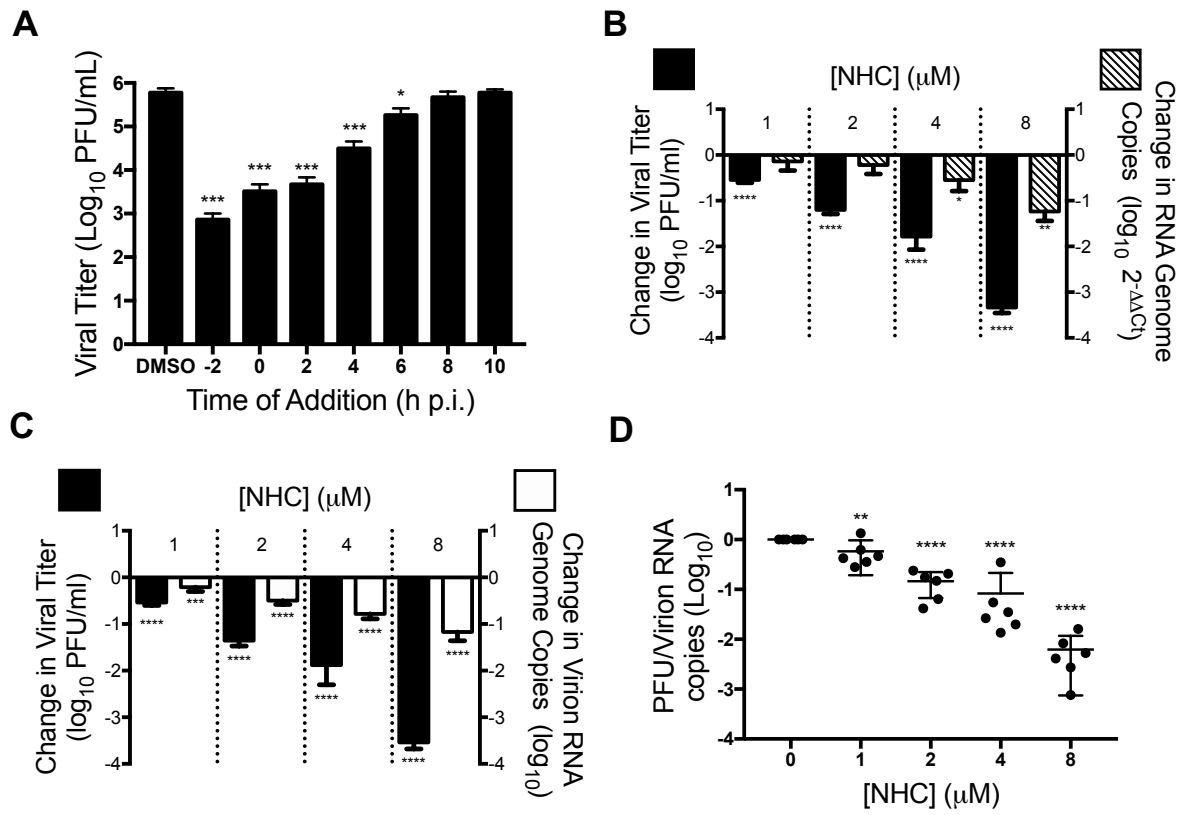


Figure 18. NHC inhibition profile of MHV is consistent with mutagenesis.

(A) Treatment with 16 μM NHC (~100X EC₅₀) significantly inhibits MHV replication during a single infection when added before 6 h p.i. (B) Both MHV titer and monolayer RNA copies decrease after treatment with increasing concentrations of NHC. (C) NHC treatment results in a decrease in supernatant MHV RNA. (D) Data from (C) represented as the ratio of infectious WT MHV to genomic MHV RNA present in supernatant, or specific infectivity, normalized to vehicle control. NHC treatment results in a decrease in specific infectivity of MHV. All data in this figure represent the results of 2 independent experiments, each with 3 replicates. Error bars represent standard error of the mean (SEM). Statistical significance compared to DMSO control was determined by one-way analysis of variance (ANOVA) with Dunnett's *post-hoc* test for multiple comparisons and is denoted *, P < 0.05; **, P < 0.01; ***, P < 0.001; ****, P < 0.0001.

across the genome after treatment with increasing concentrations of NHC (Fig. 19A-C). Further analysis of the types of mutations introduced by NHC revealed an increase in the total number of transition mutations, or mutations resulting in a purine-to-purine or pyrimidine-to-pyrimidine change, with increasing NHC concentrations (Fig. 19D-F). Specifically, the relative proportion of G:A and C:U transitions increased approximately 15% in the presence of 2 μ M NHC and 40% in the presence of 4 μ M NHC compared to the vehicle control (Fig. 19G, H). Conversely, the relative proportion of A:G and U:C transitions decreased with increasing NHC concentrations compared to the vehicle control (Fig. 19G, H). Together, these results demonstrate that NHC treatment during a single round of WT MHV infection introduces predominantly G:A and C:U transition mutations that are detectable at low frequencies across the genome. These data further support a mutagenic mechanism of action for NHC inhibition of WT MHV.

NHC inhibition is modestly enhanced in the absence of ExoN proofreading

Mutagenic nucleoside analogues, such as RBV and 5-fluorouracil (5-FU), have been ineffective at potently inhibiting WT CoVs and this has been attributed to the ExoN proofreading activity (Smith et al., 2013). A proofreading-deficient MHV mutant, ExoN(-), displays increased sensitivity to previously tested nucleoside analogues, indicating that proofreading dampens inhibition by these compounds (Agostini et al., 2018; Graepel et al., 2017; Smith et al., 2013). Thus, I tested the sensitivity of ExoN(-) MHV to NHC inhibition. NHC decreases viral titer of both WT and ExoN(-) MHV in a dose-dependent manner, but ExoN(-) MHV demonstrates a statistically significant increase in sensitivity to NHC inhibition compared to WT MHV (Fig. 20A). However, this difference is reflected in only a modest decrease in EC₉₀ concentration by approximately 2-fold for ExoN(-) (0.72 μ M) compared to WT MHV (1.59 μ M) (Fig. 20B). The

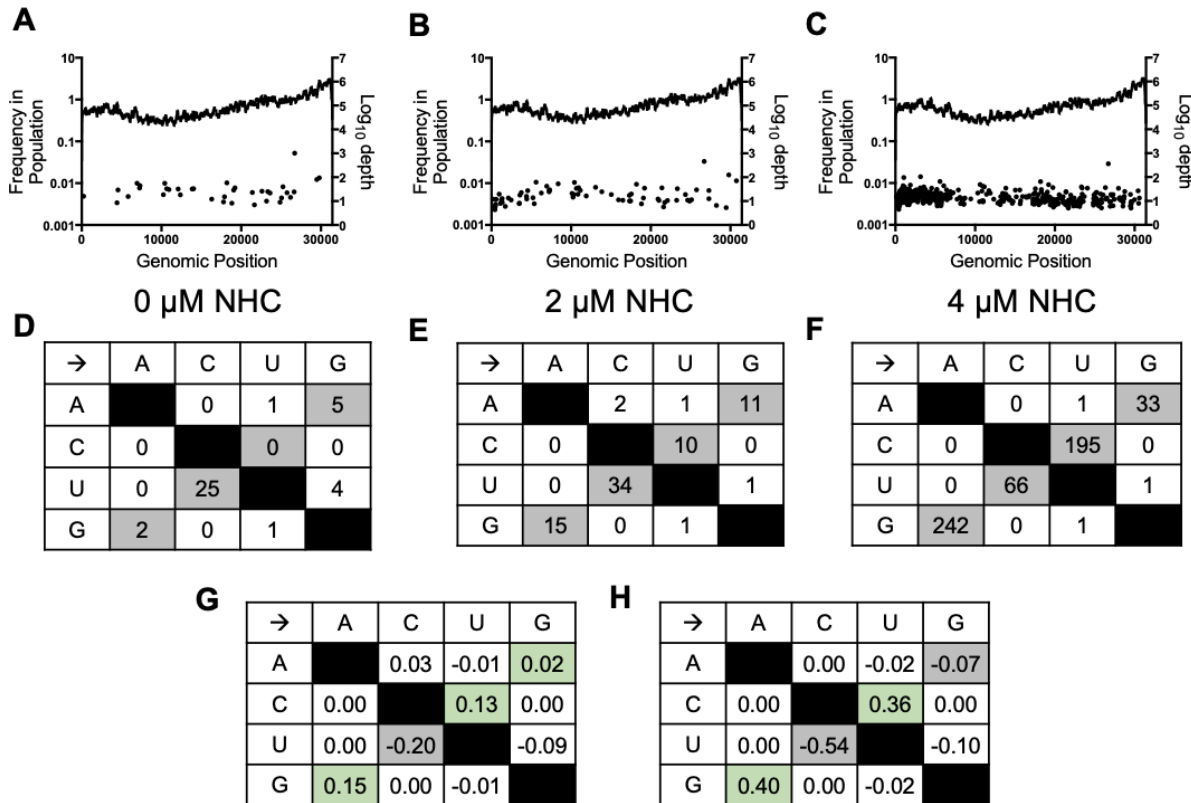


Figure 19. NHC treatment drives increase in low-frequency G:A and C:U transition mutations in WT MHV during a single infection.

(A) Distribution and frequency of variants across the genome detected by NGS after vehicle treatment, (B) 2 μ M NHC treatment, or (C) 4 μ M NHC treatment. Log₁₀ depth of coverage at each genomic position is depicted by the line; frequency of individual mutations spread across the genome are represented by dots. (D) Number of mutations in WT MHV after infection in the presence of (D) vehicle, (E) 2 μ M NHC, or (F) 4 μ M NHC presented by type. Transition mutations are shown in grey and transversion mutations are shown in white. (G) Change in relative proportion of each mutation type after treatment with (G) 2 μ M NHC, or (H) 4 μ M NHC compared to vehicle control. The relative proportions of G:A and C:U transitions increase with increasing concentrations of NHC treatment and are denoted by green shading.

minimal change in sensitivity to NHC observed for ExoN(-) MHV indicates that NHC potency is only marginally affected by ExoN proofreading activity.

Passage in the presence of NHC yields low-level resistance associated with multiple transition mutations

To better understand the development and impact of NHC resistance in CoVs, I passaged WT MHV in two lineages thirty times in the presence of increasing concentrations of NHC. I first tested the sensitivity of passage 30 (p30) MHV populations to NHC inhibition. I found that the lineage 1 (MHV p30.1) viral population showed no change in sensitivity to NHC compared to WT MHV (Fig. 21A). However, lineage 2 (MHV p30.2) did show a decrease in sensitivity to NHC inhibition in a titer-reduction assay, especially at higher concentrations of compound. I observed a modest, approximately 2-fold, increase in EC₉₀ values for MHV NHC passage viruses (MHV p30.1 EC₉₀ = 2.61 μM; MHV p30.2 EC₉₀ = 2.41 μM; WT MHV EC₉₀ = 1.53 μM) (Fig. 21B). This suggests that MHV passage resulted in minimal resistance to NHC. I next sought to determine if passaging WT MHV in the presence of NHC altered the replication capacity of these viruses. I found that both of these lineages showed a delay in replication but ultimately reached similar peak titers as WT MHV (Fig. 21C). This delay in replication suggests that MHV p30 viruses are less fit than WT MHV.

To identify mutations associated with these phenotypes after passage, I sequenced complete genomes of MHV p30.1 and MHV p30.2. Both lineages passaged in the presence NHC had accumulated over 100 consensus mutations distributed across the genome (Fig. 21D, E). By comparison, a previous study reported that WT MHV accumulated only 23 total mutations after

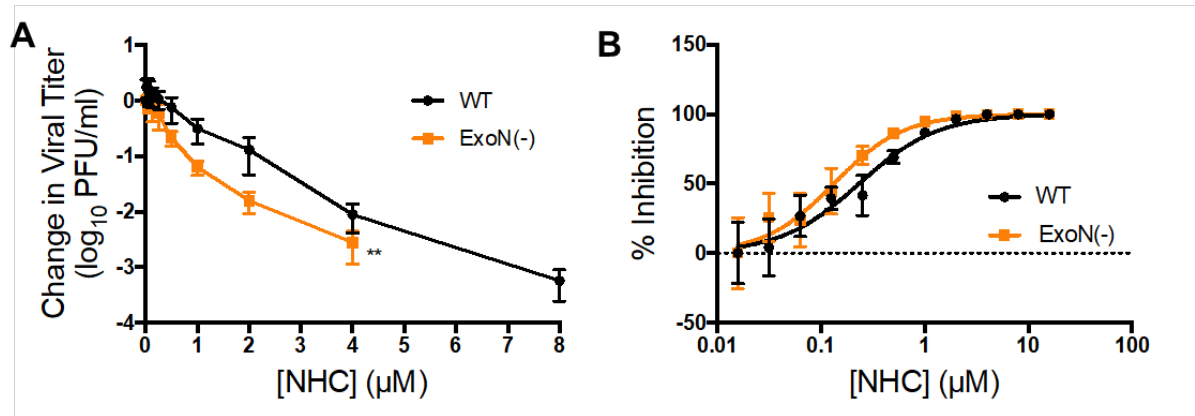


Figure 20. Sensitivity of ExoN(-) MHV to inhibition by NHC.

(A) Change in viral titer for WT MHV and ExoN(-) MHV relative to vehicle control after treatment with NHC. ExoN(-) is more sensitive to NHC than WT. The data represent the results of 3 independent experiments, each with 3 replicates. Error bars represent SEM. Statistical significance compared to WT MHV was determined by Wilcoxon test and is denoted **, $P < 0.01$. (B) Change in viral titer data from (A) represented as percent of vehicle control. WT EC₉₀ = 1.59 μ M, ExoN(-) EC₉₀ = 0.72 μ M. ExoN(-) MHV is approximately 2-fold more sensitive to NHC than WT MHV.

250 passages in the absence of drug (Graepel et al., 2017). Further analysis of the p30 MHV mutational profile demonstrated that slightly more of the total mutations in both lineages were synonymous changes that did not result in an amino acid change as opposed to nonsynonymous changes that did alter amino acid sequence (Fig. 21F). Additionally, the vast majority of mutations in both lineages were transition mutations (Fig. 21G). Both lineages contained only two transversion mutations resulting in a purine-to-pyrimidine or pyrimidine-to-purine change. Though all possible transition mutation types were detected in both viral lineage populations, the majority in both passage lineages were G:A transitions (Fig. 21H), which is consistent with the MHV NGS data (Fig. 19). To determine if the mutational profile at p30 was consistent with an earlier passage, I analyzed the whole genome of both lineage 1 and 2 at passage 19 (p19). Both lineages demonstrated fewer mutations at p19 than at p30, but the profiles of synonymous vs. nonsynonymous changes and the transition mutations were similar (Fig. 22).

To determine whether the lack of robust resistance to NHC was broadly applicable across β -CoVs, we assessed the capacity of MERS-CoV to evolve resistance to NHC. Like MHV, we passaged two lineages of MERS-CoV 30 times in the presence of increasing concentrations of NHC and tested the sensitivity of these lineages to NHC inhibition. Compared to WT MERS-CoV passaged in the absence of drug, both MERS-CoV p30.1 and p30.2 exhibited decreased sensitivity to NHC inhibition (Fig. 23A). This correlated with modestly increased EC₉₀ values for the passage lineages (MERS-CoV p30.1 EC₉₀ = 3.04 μ M; MERS-CoV p30.2 EC₉₀ = 2.12 μ M; WT MERS-CoV EC₉₀ = 1.31 μ M) (Fig. 23B), corresponding to approximately 2-fold resistance. Similar to MHV, we observed no substantial shift in dose response curve for

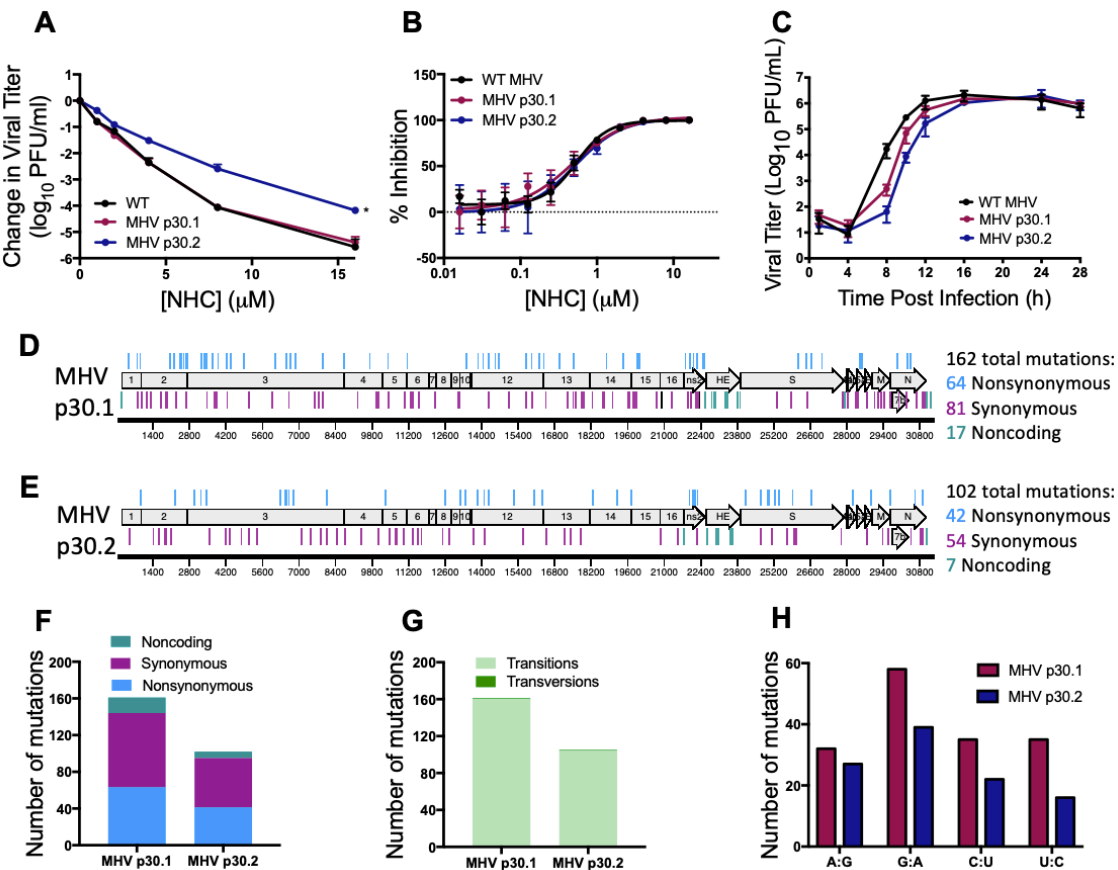


Figure 21. Resistance and mutational profile of MHV after 30 passages in the presence of NHC.

(A) Change in viral titer for WT MHV, MHV NHC passage 30 (p30) lineage 1 (MHV p30.1), and MHV NHC p30 lineage 2 (MHV p30.2) relative to vehicle controls after treatment with NHC. MHV NHC p30.2 is less sensitive to NHC than WT MHV while MHV p30.1 shows no change in sensitivity. The data represent the results of 2 independent experiments, each with 3 replicates. Error bars represent SEM. Statistical significance compared to WT MHV was determined by ratio paired *t* test and is denoted *, $P < 0.05$. (B) Change in viral titer data from (A) represented as percent of vehicle control. WT MHV EC₉₀ = 1.53 μM ; MHV p30.1 EC₉₀ = 2.61 μM , MHV p30.2 EC₉₀ = 2.41 μM . (C) Replication kinetics of NHC passage viruses. MHV p30.1 and p30.2 are delayed in replication compared to WT MHV but ultimately reach similar peak titers. The data represent the results of 2 independent experiments, each with 3 replicates. Error bars represent standard deviation (SD). (D) MHV p30.1 accumulated a total of 162 consensus mutations across the genome detectable by Sanger sequencing. Of these mutations, 81 were synonymous, 64 were nonsynonymous, and 17 were noncoding. (E) MHV p30.2 accumulated 102 total mutations across the genome. Of these mutations, 54 were synonymous, 42 were nonsynonymous, and 7 were noncoding. (F) Each lineage accumulated more synonymous changes than nonsynonymous or noncoding changes over passage. (G) Breakdown of transition and transversion mutations present in each lineage after passage. MHV p30.1 and p30.2 mutations were predominantly transitions. (H) Breakdown of the types of transition mutations present in each lineage across passage. G:A transitions were the most abundant for both MHV p30.1 and p30.2.

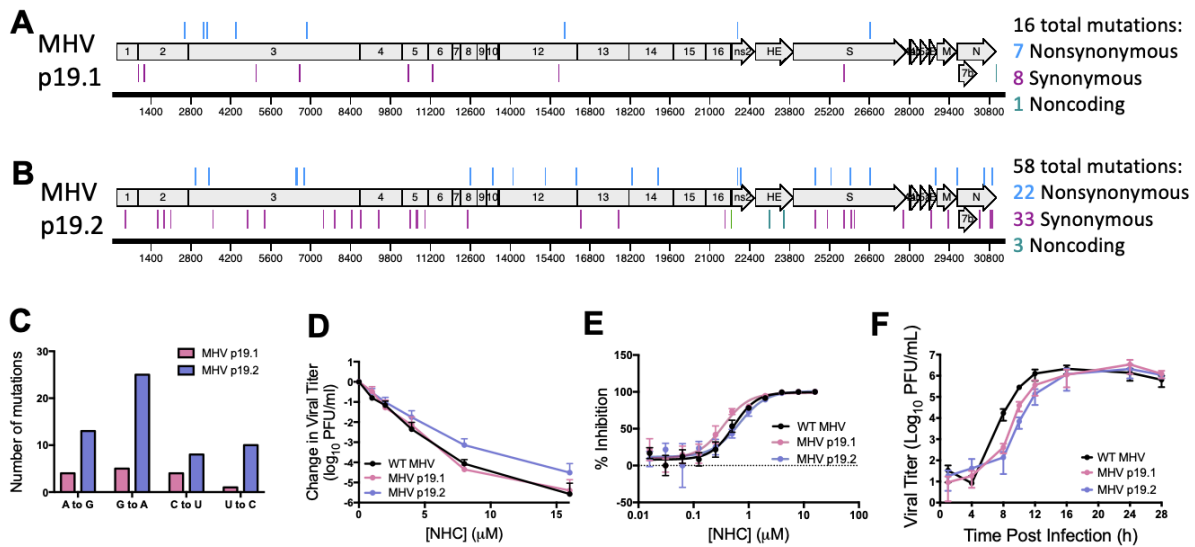


Figure 22. Mutational profile and resistance of MHV after 19 passages in the presence of NHC.

(A) Lineage 1 accumulated a total of 16 mutations across the MHV genome by passage 19, 146 fewer mutations than identified after p30. Of these mutations, 8 were synonymous, 7 were nonsynonymous, and 1 was noncoding. (B) Lineage 2 accumulated 58 mutations by passage 19, 44 fewer mutations than identified after p30. Of these mutations, 33 were synonymous, 22 were nonsynonymous, and 3 were noncoding. (C) The majority of mutations present at p19 were transitions. G:A was the most common type of transition mutation present in both lineages at p19, similar to p30. (D) Change in viral titer for WT MHV and MHV p19.1 and p19.2 relative to vehicle controls after treatment with NHC. MHV p19.2 is less sensitive to NHC than WT while MHV p19.1 shows no change in sensitivity. The data represent the results of 2 independent experiments, each with 3 replicates. Error bars represent SEM. Statistical significance compared to WT MHV was determined by ratio paired *t* test and is denoted *, $P < 0.05$. (E) Change in viral titer data from (D) represented as percent of vehicle control. WT MHV EC₉₀ = 1.53 μ M, MHV p19.1 EC₉₀ = 1.11 μ M, MHV p30.2 EC₉₀ = 2.28 μ M. (F) Replication kinetics of NHC passage viruses. MHV p19.1 and p19.2 are delayed in replication compared to WT MHV, similar to their p30 counterparts. The data represent the results of 2 independent experiments, each with 3 replicates. Error bars represent SD.

MERS-CoV, indicating minimal acquired resistance. However, NHC p30 viruses replicated similarly to WT p30 MERS-CoV (Fig. 23C). We sequenced both lineages of MERS-CoV p30 population virus and detected 27 consensus mutations in MERS-CoV NHC p30.1 (Fig. 23D) and 41 consensus mutations in MERS-CoV NHC p30.2 (Fig. 23E) randomly distributed across the genome. Both MERS-CoV NHC p30.1 and MERS-CoV NHC p30.2 accumulated nonsynonymous and synonymous mutations in roughly equal proportions (Fig. 23F). Like MHV, the mutations detected in MERS-CoV p30 lineages were predominantly transition mutations (Fig. 23G). Further analysis of these mutations revealed that the predominant type of transition was lineage-dependent. The majority of transition mutations in MERS-CoV NHC p30.1 were G:A transitions, as was observed in both p30 MHV lineages, whereas MERS-CoV NHC p30.2 contained a similar number of each type (Fig. 23H). These results indicate that MERS-CoV can achieve low-level resistance to NHC and that development of resistance is associated with the accumulation of multiple transition mutations. Together, our data suggest NHC acts as a mutagen and that it poses a high genetic barrier to resistance for β -CoVs.

Discussion

In this chapter, I present results that demonstrate the potent inhibition of MHV and MERS-CoV, two divergent β -CoVs, by NHC. My results are consistent with a mutagenic mechanism of action for NHC in CoVs, as evidenced by a decrease in specific infectivity and an increase in G:A and C:U transition mutations present at low frequencies across the genome after treatment. We also demonstrate that robust resistance to NHC is difficult to achieve in both MHV and MERS-CoV. Both WT MHV and ExoN(-) MHV are sensitive to NHC inhibition, suggesting that NHC is able

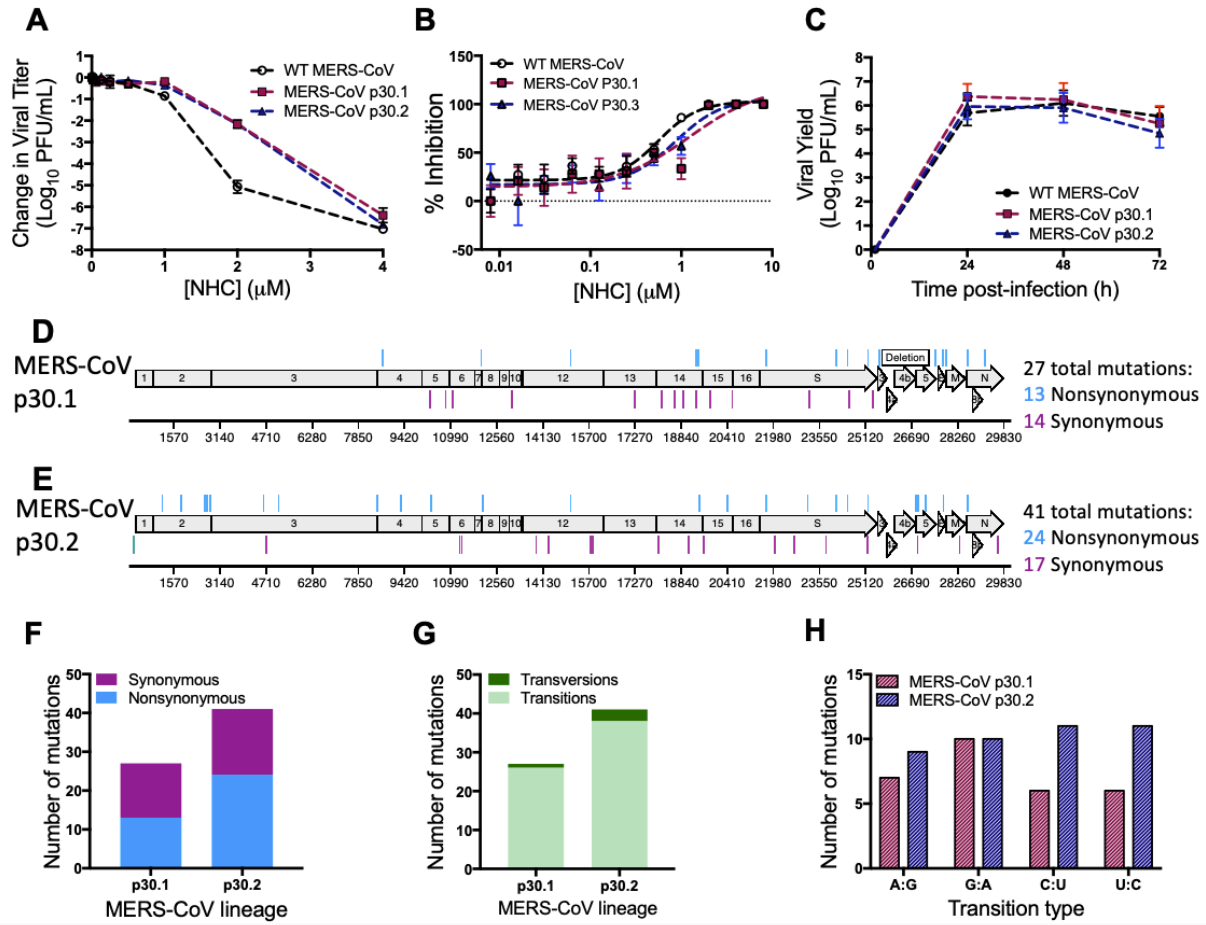


Figure 23. Resistance and mutational profile of MERS-CoV after 30 passages in the presence of NHC.

(A) Change in viral titer relative to vehicle controls after treatment with NHC for WT MERS-CoV passaged 30 times in the absence of drug, MERS-CoV NHC passage 30 lineage 1 (MERS-CoV p30.1), and MERS-CoV NHC passage 30 lineage 2 (MERS-CoV p30.2) relative to vehicle controls after treatment with NHC. Both MERS-CoV p30.1 and p30.2 are less sensitive to NHC than WT MERS-CoV. The data represent the results of 2 independent experiments, each with 3 replicates. Error bars represent SEM. (B) Change in viral titer data from (A) represented as percent of vehicle control. WT MERS-CoV EC₅₀ = 1.31 μM , MERS-CoV p30.1 EC₉₀ = 3.04 μM , MERS-CoV p30.2 EC₅₀ = 2.12 μM . (C) Replication kinetics of NHC passage viruses. WT MERS-CoV, MERS-CoV p30.1, and MERS-CoV p30.2 replicate with similar kinetics and reach similar peak titers. The data represent the results of 2 independent experiments, each with 3 replicates. Error bars represent SEM. (D) MERS-CoV p30.1 accumulated 27 total mutations across the genome. Of these mutations, 14 were synonymous and 13 were nonsynonymous. (E) MERS-CoV p30.2 accumulated 41 total mutations. Of these mutations, 17 were synonymous, and 24 were nonsynonymous. (F) Both MERS-CoV p30.1 and p30.2 accumulated a similar numbers of nonsynonymous and synonymous changes during passage. (G) MERS-CoV p30.1 and p30.2 acquired predominantly transitions. (H) The types of transition mutations present in each lineage across passage. MERS-CoV p30.1 acquired relatively more G:A transitions, whereas MERS-CoV p30.2 acquired similar numbers of each transition type.

to overcome ExoN-mediated proofreading to inhibit WT CoVs and that it interacts with CoVs differently than other previously tested nucleoside analogues.

Utility of the broad-spectrum antiviral NHC as a pan-CoV therapeutic. Early work with NHC focused on the mutagenic effects of this compound in multiple bacterial systems (Popowska et al.; Popowska and Janion, 1974; Salganik et al., 1973). More recently, the antiviral properties of this compound have been reported for multiple RNA viruses, including chikungunya virus, VEEV, RSV, HCV, norovirus, influenza A and B viruses, and Ebola virus (Costantini et al., 2012; Ehteshami et al., 2017; Reynard et al., 2015; Stuyver et al., 2003; Urakova et al., 2017; Yoon et al., 2018). NHC has also been shown to potently inhibit SARS-CoV and HCoV-NL63 (Barnard et al., 2004; Pyrc et al., 2006), suggesting its utility in treating CoV infections (De Clercq, 2014). Based on previous studies, NHC appears to primarily inhibit viral replication by mutagenesis (Urakova et al., 2017; Yoon et al., 2018). Serial passaging in the presence of NHC led to low-level resistance for VEEV, but no detectable resistance for RSV, Influenza A virus, or bovine viral diarrhea virus, indicating a high barrier to resistance (Stuyver et al., 2003; Urakova et al., 2017; Yoon et al., 2018). Consistent with these previous studies, the results in this chapter demonstrate that NHC is mutagenic in CoVs and that passage yields low-level, approximately 2-fold resistance. Low-level resistance has also been observed for remdesivir, another nucleoside analogue that potently inhibits CoVs. Approximately 6-fold resistance to remdesivir is conferred by two mutations in the CoV RdRp (Agostini et al., 2018). This study expands the known antiviral spectrum of NHC to include MHV and MERS-CoV, two genetically divergent β-CoVs and further supports NHC development as a broad-spectrum CoV antiviral.

NHC inhibition may circumvent ExoN-mediated proofreading. NHC is the first mutagenic nucleoside analogue demonstrated to potently inhibit proofreading-intact CoVs. Previous studies have demonstrated that viruses lacking ExoN proofreading activity, or ExoN(-) viruses, are more sensitive to inhibition by nucleoside analogues, especially RBV and 5-FU (Agostini et al., 2018; Graepel et al., 2017; Sexton et al., 2016; Smith et al., 2013). This increased sensitivity has been attributed to an inability of ExoN(-) to efficiently remove incorrect nucleosides (Ferron et al., 2017). However, I observed a minimal change in NHC sensitivity between WT MHV and ExoN(-) MHV, especially by EC₉₀. This suggests that NHC interacts with the CoV replicase differently than these previously tested nucleoside analogues. One explanation of NHC's unique potency is that it may evade removal by the proofreading ExoN. Studies investigating nucleosides that inhibit DNA viruses have suggested an inability of the viral exonuclease to efficiently excise some nucleoside analogues (Chamberlain et al., 2019; Derse et al., 1981). Further, a previous study suggested that the T4 DNA exonuclease activity was incapable of removing NHC (Śledziewska-Gójska and Janion, 1982). While the SARS-CoV ExoN efficiently removes 3' terminal mismatches regardless of type (Bouvet et al., 2012; Ferron et al., 2017), the effect of NHC on this activity has not been investigated. Interestingly, mismatches readily observed during single nucleotide elongation by the SARS-CoV polymerase in the absence of drugs correspond to mismatches that would lead to the G:A and C:U transitions observed after NHC treatment (Ferron et al., 2017). This suggests that the CoV polymerase could be naturally more prone to make these types of errors, which are then magnified by NHC. This could lead to a scenario where ExoN cannot prevent dipping below the error threshold, ultimately resulting in lethal mutagenesis and similar inhibition of both WT and ExoN(-) MHV (Tejero et al., 2016).

However, several nucleosides, including the mutagenic RBV, have multiple demonstrated mechanisms beyond direct incorporation (Biktasova et al., 2017; Crotty et al., 2000; Leyssen et al., 2005). Thus, another explanation for the unique potency of NHC in the presence of an active proofreading ExoN is that it may inhibit viral replication by additional mechanisms beyond mutagenesis. Indeed, previous reports have suggested that NHC may also interfere with the RNA secondary structure or virion release to cause inhibition (Stuyver et al., 2003; Urakova et al., 2017). Further, exogenous C or U in the presence of NHC could rescue viral replication in HCV, chikungunya virus, RSV, and Influenza A virus (Ehteshami et al., 2017; Stuyver et al., 2003; Yoon et al., 2018), indicating that NHC competes with exogenous nucleosides at some stage prior to viral inhibition. These results raise the possibility that NHC could inhibit a process that results in similar inhibition of these viruses by a mechanism unrelated to ExoN. Thus, future studies will be important to investigate the role of proofreading in NHC inhibition of CoVs to shed light on intricacies of NHC inhibition of the CoV replication complex.

NHC mutagenesis may hinder emergence of robust resistance to NHC. The decrease in specific infectivity along with the accumulation of transitions across the CoV genome support a mutagenic mechanism of action for NHC in CoVs. NHC resistance in CoVs was modest and difficult to achieve, as we obtained approximately 2-fold resistance after 30 passages. Resistance was associated with multiple mutations. Interestingly, MERS-CoV accumulated less mutations over 30 passages than MHV. While differences in viral mutation rates could be the driver of this difference, previous studies have suggested that MHV does not have a higher mutation rate than MERS-CoV (Cotten et al., 2014; Hemida et al., 2014; Sanjuan et al., 2010). The differences in

mutation accumulation between MHV and MERS-CoV may be a product of different passage conditions. While MHV was passaged with a consistent transfer volume, MERS-CoV passage volumes were adjusted over time to sustain viral replication under escalating selection for drug resistance. The constant volume passaging conditions may have more severely bottlenecked MHV populations and fixed more mutations in the genome than the variable volume passaging conditions applied to MERS-CoV (Domingo et al., 2012). Alternatively, this difference could also reflect a difference in mutational robustness of the MHV and MERS-CoV genomes, though this proposition would need to be investigated further (Bloom et al., 2007; Fares, 2015). While a portion of the mutations that accumulated over passage likely contribute to NHC resistance, other mutations, such as those in ns2 or nsp2, which encode proteins dispensable for viral replication in cell culture, may be merely tolerated because of their limited effect on viral fitness in the context of our passage conditions (Graham et al., 2005; Schwarz et al., 1990; Zhao et al., 2011). Few common mutations arose in both MHV and MERS-CoV passage series, (Appendix C), suggesting that multiple pathways to low-level NHC resistance exist in CoVs. Both MHV passage lineages replicated less well than WT MHV, suggesting that the accumulation of mutations during passage may impact viral fitness and the ability of MHV to evolve robust resistance to NHC. Interestingly, for both MHV and MERS-CoV, the p30 lineage that demonstrated a greater decrease in sensitivity to NHC was the lineage that had fewer overall mutations (Fig. 21, 23). Further, the MHV lineage that did not change sensitivity to NHC by p30 (MHV p30.1) had fewer mutations present at consensus by p19 than the other lineage (Fig. 22). Thus, mutations promoting NHC resistance may need to arise early during passage to help mitigate the accumulation of excess deleterious mutations. If that is the case, the inability to evade inhibition by NHC may lead to the accumulation of a greater number of NHC-associated

transitions and ultimately a higher mutational burden that negatively impact viral fitness (Lyons and Lauring, 2018; Sanjuán et al., 2004). Consequently, it is possible that the accumulation of deleterious mutations counteracts potential benefits of resistance mutations (Manrubia Cuevas et al., 2010). Together, our results support the hypothesis that establishment of resistance to NHC in CoVs requires a delicate balance of resistance-promoting mutations, viral fitness, and accumulation of deleterious mutations. Thus, defining the roles of individual NHC resistance-associated mutations will be an important goal for future studies.

Conclusion

Overall, these results, in combination with previous reports, demonstrate that NHC inhibits a wide range of RNA viruses, including diverse CoVs. This compound exerts its antiviral function, at least in part, by increasing the number of G:A and C:U transition mutations present in viral RNA. Interestingly, ExoN proofreading only modestly affects inhibition by NHC, suggesting that this compound interacts differently with the CoV replicase than others that have been previously reported. In addition, passage in the presence of NHC results in minimal acquired resistance that is associated with multiple transition mutations, indicating a high genetic barrier to resistance and further supporting mutagenesis as the mechanism of action of NHC in CoVs. Together, these results support further development of NHC as a broad-spectrum CoV antiviral and contribute new insights into important aspects of CoV replication.

CHAPTER IV

INHIBITORY EFFECTS OF A PANEL OF NUCLEOSIDE ANALOGUES DURING CORONAVIRUS INFECTION

Introduction

In the previous chapters, I have demonstrated the potent inhibition of CoVs by two nucleoside analogues: remdesivir (GS-5734) and β -D- N^4 -hydroxycytidine (NHC). While these nucleoside analogues inhibit CoVs independently, many clinically available antiviral therapies are composed of multiple compounds with different mechanisms of action as a combination regimen (Hofmann et al., 2009). Thus, several compounds in combination may be required to effectively treat CoV infections and control the emergence of drug resistance. Advancing our understanding of the similarities and differences between inhibitors may be helpful for determining these types of regimens.

In this chapter, I investigate the inhibition of CoVs by a panel of three nucleoside analogues with distinct proposed mechanisms of action: 2'-C-methyladenosine (2'-C-MeA), NHC, and remdesivir. 2'-C-MeA is structurally identical to adenosine except for the addition of a methyl group at the 2' position on the ribose sugar (Fig. 24A). Modifications at the 2' position have been important components of approved hepatitis C virus (HCV) antivirals and have been shown to cause immediate chain termination (Carroll et al., 2003). As discussed above, NHC (Fig. 24B) is a cytidine analogue with the addition of a hydroxyl group at the N^4 position of the cytosine nucleobase. NHC also inhibits multiple RNA virus families, likely through

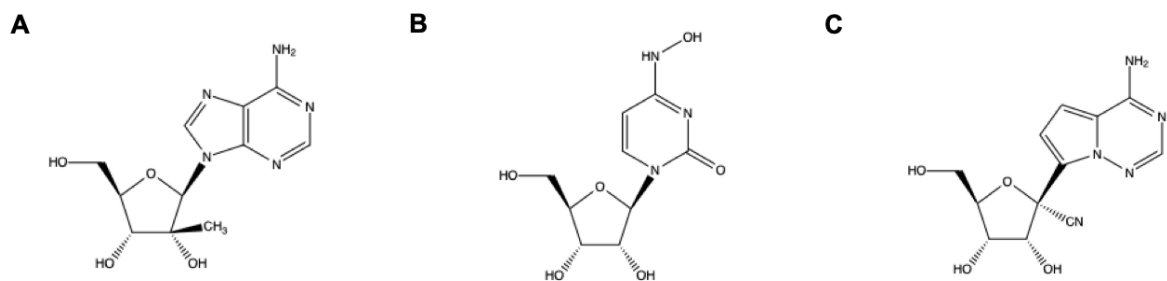


Figure 24. Chemical structures of a panel of three nucleoside analogues.

(A) The adenosine analogue 2'-C-Methyladenosine (2'-C-MeA). (B) The cytidine analogue β -D- N^4 -hydroxycytidine (NHC). (C) The adenosine analogue GS-441524, the 1'cyano 4-aza-7,9-dideazaadenosine parent C-nucleoside of remdesivir.

incorporation into the viral genome and subsequent mutagenesis (Urakova et al., 2017; Yoon et al., 2018). Remdesivir is the monophosphoramidate prodrug of GS-441524 (Fig. 24C), a 1'cyano 4-aza-7,9-dideazaadenosine C-nucleoside with broad-spectrum antiviral activity, and has been shown to cause delayed chain termination (Jordan et al., 2018; Tchesnokov et al., 2019; Warren et al., 2016). The mechanisms of the compounds discussed here have primarily been demonstrated in other RNA viruses; prior to this dissertation work, direct evidence of any of these mechanisms had not been reported in CoVs. Since some nucleoside analogues have distinct mechanisms of action in different viruses (Furuta et al., 2017), I sought to further investigate the inhibition of CoVs using this panel of antiviral nucleoside analogues. In this chapter, I present preliminary data that suggest both similarities and differences between the inhibition of CoVs by these compounds.

I performed all experiments and final analyses for the data presented in this chapter, except that Jennifer Gribble performed bioinformatic processing of NGS data and Tia Hughes performed 2'-C-MeA cytotoxicity assays.

Nucleoside analogues decrease viral titer and genomic RNA levels

To begin assessing the antiviral effect of the nucleoside analogue panel, I first determined WT MHV titers and RNA genome copy levels after treatment with these compounds. WT MHV titers were significantly decreased by all nucleosides tested. Further, each of the nucleoside analogues in this panel reduced viral titer similarly across the concentration range tested (Fig. 25A-C). WT MHV supernatant RNA genome copies were also significantly decreased after treatment with this panel of nucleoside analogues (Fig. 25D-F), but the effects on RNA levels

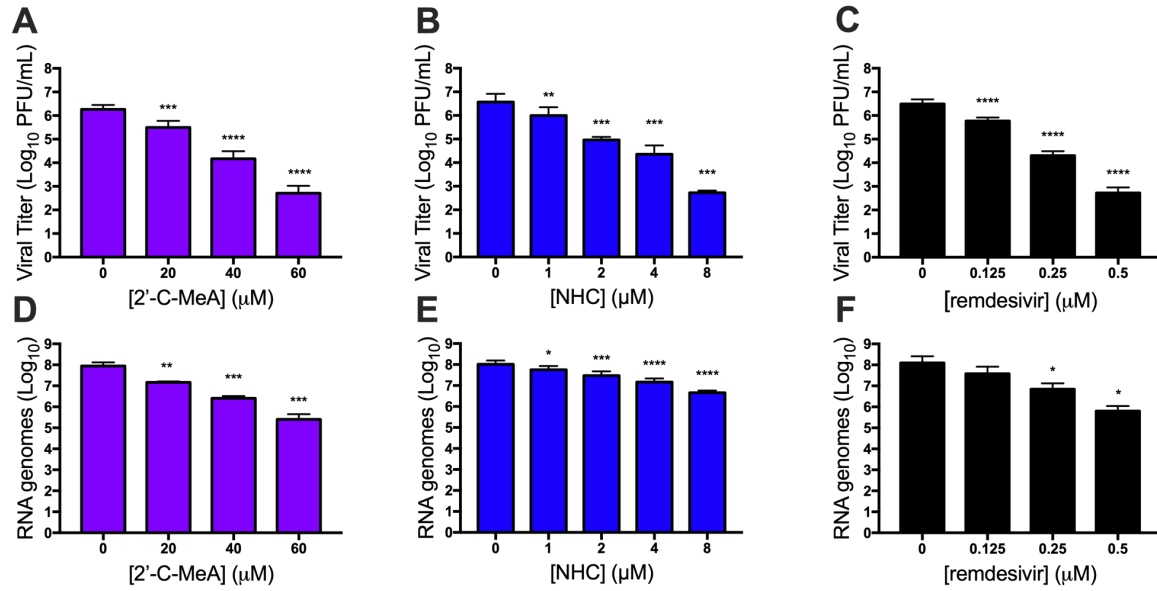


Figure 25. Treatment of WT MHV with nucleoside analogues decreases viral titer and supernatant viral genomic RNA.

(A) MHV titer after treatment with increasing concentrations of 2'-C-MeA, (B) NHC, and (C) remdesivir. Treatment with each of these nucleoside analogues significantly reduces MHV titer. (D) MHV supernatant RNA levels after treatment with 2'-C-MeA, (E) NHC, and (F) remdesivir. Nucleoside analogue treatment also significantly decreases MHV supernatant RNA levels. All data in this figure represent the results of two independent experiments, each with 3 replicates. Error bars represent SEM. Statistical significance for each compound treatment compared to DMSO control was determined by one-way ANOVA with Dunnett's post hoc test for multiple comparisons and is denoted by asterisks: * $P < 0.05$; ** $P < 0.01$; *** $P < 0.001$; **** $P < 0.0001$.

were nucleoside-dependent. I have demonstrated in previous chapters that the antiviral activity of remdesivir and NHC were not due to toxicity at the concentrations tested here. This holds true for 2'-C-MeA: the CC₅₀ of this compound was > 100 μM (Table 3). Together, these results demonstrate the inhibition of WT MHV by the panel of nucleoside analogues in this study at nontoxic concentrations.

Nucleoside analogue inhibition in WT MHV is MOI-dependent

To begin probing the antiviral activity of this nucleoside analogue panel, I tested the effect of viral load on WT MHV inhibition by these compounds. Previous reports have proposed that mutagenic nucleoside analogues may be more effective upon multiple rounds of infection as more mutations accumulate in the viral population (Moreno et al., 2012; Smith et al., 2013). However, these studies have not investigated this effect in depth with compounds proposed to act by other mechanisms. Thus, I infected cells with WT MHV at either a high (1) or low (0.01) multiplicity of infection (MOI) and treated with a dose-range of each of the nucleoside analogues. Each compound in this panel decreased WT MHV titer significantly more at low MOI than high MOI (Fig. 26A-C), especially at higher concentrations tested. These results demonstrate that increased rounds of replication increase inhibition by these nucleoside analogues in CoVs, regardless of proposed mechanism of action.

Effect of exogenous ribonucleoside addition on nucleoside analogue inhibition

Several nucleoside analogues inhibit viruses through multiple mechanisms. For example, the broad-spectrum antiviral activity of ribavirin (RBV) has been attributed to both mutagenesis

Table 3. Cytotoxicity of the nucleoside analogue panel.

Compound	CC ₅₀ (μ M)
remdesivir	39
NHC	>200
2'-C-MeA	>100

(Crotty et al., 2000; 2014) and depletion of cellular GTP pools attributed to inosine monophosphate dehydrogenase (IMPDH) inhibition (Leyssen et al., 2005; Streeter et al., 1973). As such, addition of exogenous guanosine (G) can restore nucleoside pools and viral titer in the presence of RBV. Thus, I sought to address whether exogenous ribonucleosides could compete with any of the nucleoside analogues in this panel to prevent inhibition. To investigate this proposition, I determined viral titer after I treated cells with fixed, inhibitory concentrations of each of the nucleoside analogues in the panel and added back individual exogenous ribonucleosides. Treatment with exogenous ribonucleosides itself did not alter viral titer (Fig. 27A). However, treatment with adenosine (A) significantly increased viral titer in the presence of 2'-C-MeA, suggesting that 2'-C-MeA competes with A prior to inhibiting WT MHV (Fig. 27B). After treatment with NHC, both cytidine (C) and uridine (U) significantly restored viral titer compared with NHC treated controls (Fig. 27C), suggesting that NHC competes with both C and U before inhibiting CoVs. However, viral titer was not restored in the presence of any tested exogenous nucleosides after treatment with the parent nucleoside of remdesivir, GS-441524 (Fig. 27D), suggesting that remdesivir metabolism and viral inhibition do not rely on similar pathways as these particular nucleosides. Overall, each nucleoside showed different patterns of titer restoration after exogenous nucleoside addition indicating potential differences in the mechanisms, uptake, and metabolism of these nucleoside analogues (Furuta et al., 2005).

Nucleoside analogues can decrease CoV specific infectivity

To further probe the mechanisms of inhibition of these nucleoside analogue inhibitors, I next tested the ratio of infectious virus per viral RNA, or specific infectivity, after treatment with this panel of compounds. Some previous studies have reported that treatment with mutagens decrease

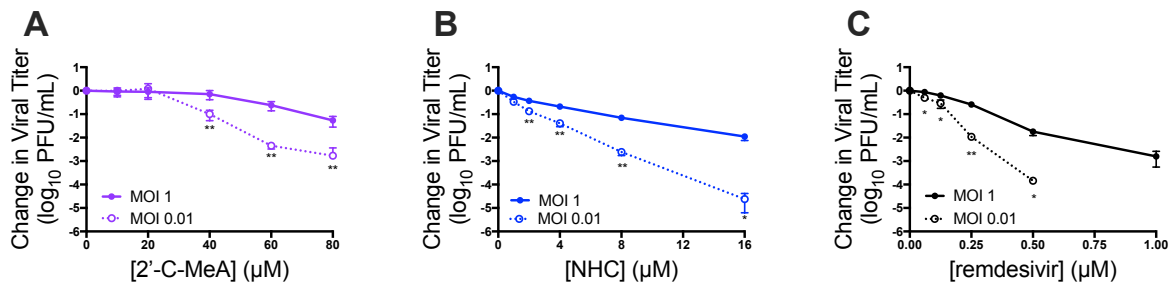


Figure 26. Nucleoside analogues more potently inhibit WT MHV at lower MOI regardless of proposed mechanism of action.

(A) Change in viral titer relative to vehicle control after infection with WT MHV at a high (1) or low (0.01) MOI and treatment with 2'-C-MeA, (B) NHC, or (C) remdesivir. Viral titer was significantly reduced at a low MOI (0.01) compared with a high (1) MOI after treatment with each of these compounds. All data in this figure represent the results of two independent experiments, each with 3 replicates. Error bars represent SEM. Statistical significance compared to higher MOI at each concentration was determined by unpaired *t* test using the Holm-Sidak method to correct for multiple comparisons and is denoted by asterisks: *, $P < 0.05$; **, $P < 0.01$.

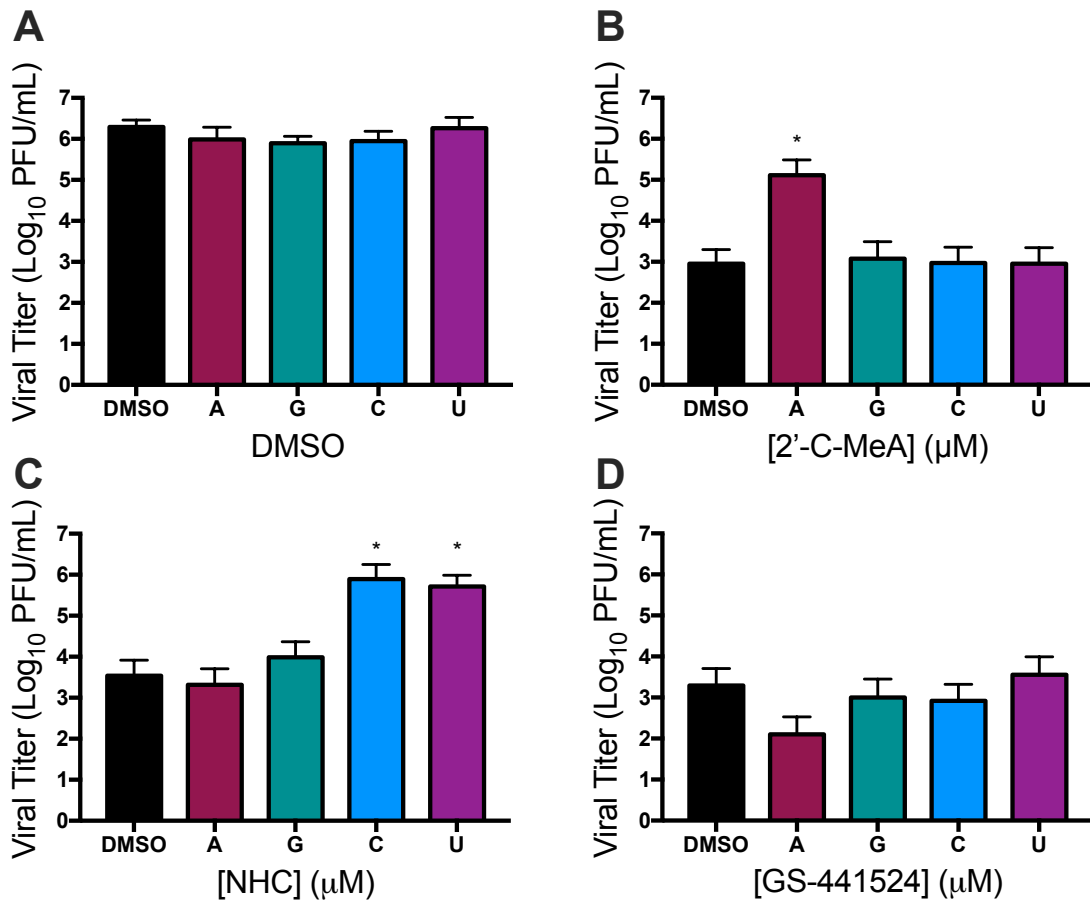


Figure 27. Addition of exogenous ribonucleosides can restore viral titer after treatment with 2'-C-MeA and NHC but not remdesivir.

(A) Addition of exogenous ribonucleosides in the presence of DMSO do not alter viral titer compared to DMSO controls. (B) Addition of exogenous Adenosine (A) significantly increases viral titer in the presence of 40 μ M 2'-C-MeA. (C) Addition of exogenous cytidine (C) and uridine (U) significantly increased titer after treatment with 4 μ M NHC. (D) None of the ribonucleosides tested here could restore viral titer after treatment with GS-441524 when added exogenously. All data in this figure represent the results of two independent experiments, each with 3 replicates. Error bars represent SEM. Statistical significance compared to the respective compound's DMSO control was determined using the Kruskal-Wallis test with Dunn's post hoc test to correct for multiple comparisons and is denoted by asterisks: *, $P < 0.05$.

specific infectivity (Crotty et al., 2001) and others have hypothesized that specific infectivity would not be altered by non-mutagenic nucleoside analogues. However, very few studies have directly addressed whether other mechanisms of action of nucleoside analogues alter viral specific infectivity, particularly in CoVs (Delang et al., 2014). Thus, I used my panel composed of nucleoside analogues with multiple proposed mechanisms of action to determine their effect on specific infectivity in CoVs. Using the concentration range established in Fig. 20 that similarly reduced viral titer for each nucleoside analogue, I demonstrate that specific infectivity is not significantly decreased by 2'-C-MeA (Fig. 28A). As expected from its mutagenic mechanism of action, NHC significantly decreased specific infectivity of WT MHV (Fig. 28B). However, remdesivir, a proposed chain terminator, also significantly decreased specific infectivity (Fig. 28C). Together, these results suggest that nucleoside analogues may decrease specific infectivity of WT MHV regardless of proposed mechanism of action.

NHC is the only nucleoside analogue in the panel that induces mutagenesis

Because decreases in specific infectivity have been associated with mutagenesis, I directly investigated whether this nucleoside analogue panel induced mutagenesis by performing full-genome next-generation sequencing (NGS) on released MHV RNA after compound treatment. Neither 2'-C-MeA (Fig. 29B) or remdesivir (Fig. 29D) treatment resulted in an increase in low-frequency mutations compared to vehicle control (Fig. 29A). However, as has been previously reported, NHC increased the number of low-frequency transition mutations after a single infection (Fig. 29C) compared with WT MHV. Together, these results indicate that NHC is the only mutagenic nucleoside analogue in this panel and that the decrease in specific infectivity observed after nucleoside analogue treatment is not solely associated with mutagenesis in CoVs.

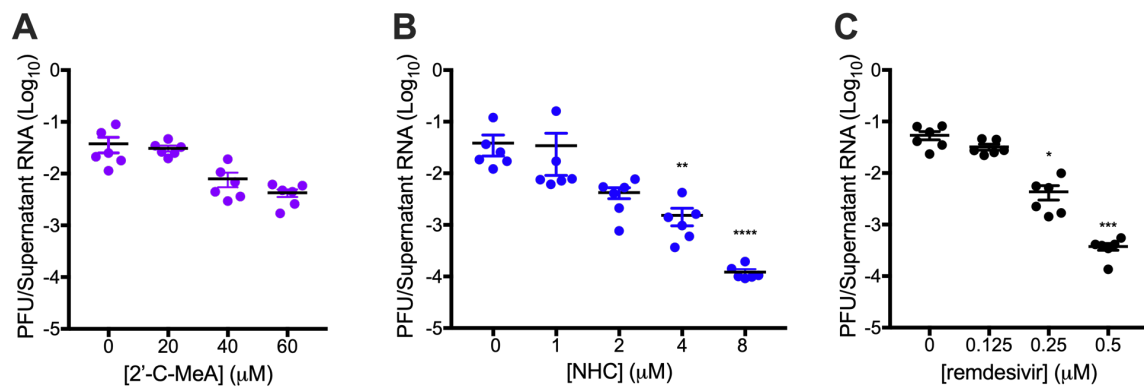


Figure 28. Treatment with NHC and remdesivir significantly decreases specific infectivity.

(A) The ratio of infectious WT MHV to genomic MHV RNA present in supernatant, or specific infectivity, after treatment with $2'$ -C-MeA, (B) NHC, or (C) remdesivir. The specific infectivity of WT MHV is significantly decreased by NHC and remdesivir. All data in this figure represent the results of two independent experiments, each with 3 replicates. Error bars represent SEM. Statistical significance compared to DMSO control was determined using the Kruskal-Wallis test with Dunn's post hoc test to correct for multiple comparisons and is denoted by asterisks: *, $P < 0.05$; **, $P < 0.01$; ***, $P < 0.001$; ****, $P < 0.0001$.

A qPCR-based approach to detect truncated RNAs after nucleoside analogue treatment

Only NHC increased low-frequency mutations across the genome, suggesting that decreases in CoV specific infectivity represent mechanisms beyond mutagenesis. To begin to determine whether a chain termination mechanism of action could decrease specific infectivity of WT MHV, I designed a qPCR assay to detect the ends of ORF1 in genomic RNA released after viral infection. Specifically, I designed primers with similar efficiencies to detect nsp1 and nsp16 of positive-sense MHV RNA in an effort to identify truncated RNA species. Using this approach, I detected a significant decrease in the amount of nsp16 relative to nsp1 in supernatant RNA after treatment with higher concentrations of 2'-C-MeA (Fig. 30A), indicating potential truncations. I did not detect a significant difference in the amount of nsp16 and nsp1 after treatment with NHC (Fig. 30B). Treatment with remdesivir may have decreased the amount of nsp16 relative to nsp1 present, but this result was also associated with an increase in this ratio over vehicle control (Fig. 30C). Overall, this qPCR-based approach to detect truncated RNAs in viral supernatants proved to be highly variable, suggesting this method may require further refinement or that it may lack the capability to reliably detect small changes in these targets when low levels of viral RNA are available after treatment with highly inhibitory nucleoside analogue concentrations.

RNA species released after infection are altered after treatment with nucleoside analogues

To better address the viral RNA species released after treatment with nucleoside analogues, I used NGS approaches. First, I collected RNA released from WT-infected cells after treatment with each of the nucleosides in this panel. I subjected RNA from the same biological samples to library preparation with and without selecting for polyadenylated [poly(A)] RNAs. Poly(A) library selection should detect only RNAs with a poly(A) tail and may include viral genomic

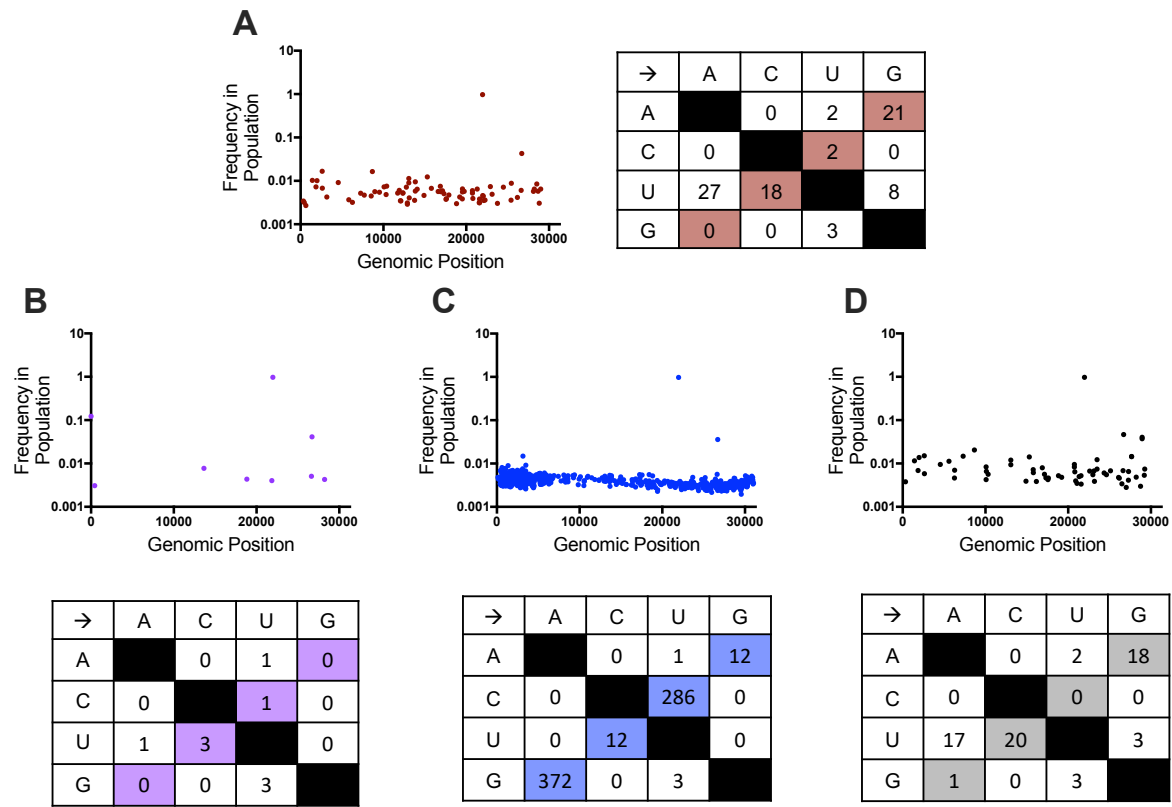


Figure 29. NHC is the only nucleoside analogue in the panel that increases low-frequency mutations spread across the WT MHV genome compared with the vehicle control.

(A) Frequency in the population, distribution across the genome, and mutation type for variants detected by NGS after treatment with vehicle (DMSO), (B) 40 μ M 2'-C-MeA, (C) 4 μ M NHC, or (D) 0.25 μ M remdesivir. Transition mutations in the table are shown in shaded boxes.

RNA, sgmRNAs, or cellular mRNAs. However, lack of poly(A) selection will also detect RNAs without a poly(A) tail, which may include but is not limited to, truncated, degraded, or unprocessed RNAs. We first determined sequencing coverage across the genome with poly(A) library selection using Bowtie2 for alignment to the MHV genome. I found that coverage is similar and relatively uniform across the MHV genome after treatment with DMSO (Fig. 31A), 2'-C-MeA (Fig. 31B), NHC (Fig. 31C), and remdesivir (Fig. 31D). In addition, coverage in the absence of poly(A) selection was minimally altered for the vehicle control compared with the poly(A) selected libraries (Fig. 31E). However, coverage across the genome after nucleoside analogue treatment in the absence of poly(A) selection was much more variable for 2'-C-MeA (Fig. 31F), NHC (Fig. 31G), and remdesivir (Fig. 31H), and this change in coverage was dose-dependent for remdesivir (Fig. 32A-C). Together, these results serve as additional evidence that nucleoside analogue treatment may alter the released viral RNA species.

Lack of cross-resistance across the nucleoside analogue panel

To continue to address the similarities and differences in CoV inhibition across this nucleoside analogue panel, I utilized the viruses with altered susceptibility to remdesivir and NHC that I identified in the previous chapters to test loosely for cross-resistance. I first assessed the sensitivity of remdesivir resistant MHV to NHC. I found that remdesivir resistance mutations, either individually or in combination, did not confer resistance to NHC and may actually increase sensitivity to NHC, though this difference did not reach statistical significance (Fig. 33A). Further, remdesivir resistance also did not confer resistance to 2'-C-MeA, despite both being adenosine analogues proposed to act by chain termination (Fig. 33B). Given this lack of cross-resistance, I also assessed the sensitivity of NHC MHV p19 and p30 viruses to remdesivir.

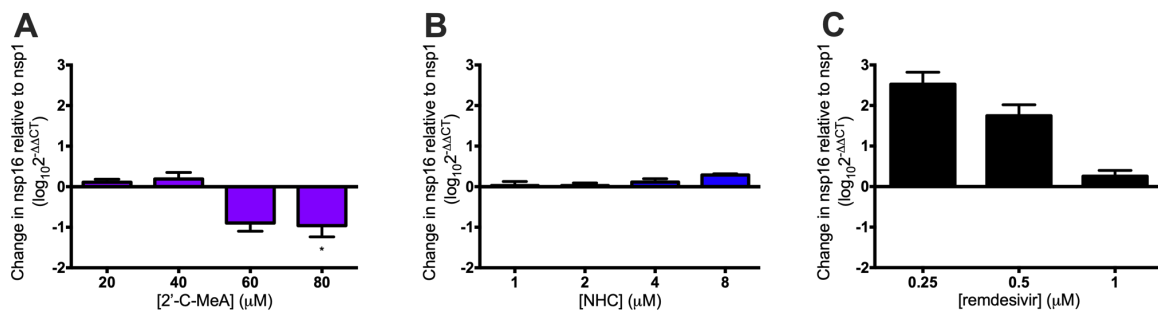


Figure 30. Change in levels of nsp16 relative to nsp1 after nucleoside analogue treatment.

(A) Levels of nsp16 relative to nsp1 of MHV RNA after treatment with 2'-C-MeA. Treatment with the highest concentration of 2'-C-MeA results in a significant decrease in the amount of nsp16 relative to nsp1. (B) Levels of nsp16 relative to nsp1 of MHV RNA after treatment with NHC. NHC treatment does not significantly alter the level of nsp16 relative to nsp1. (C) Levels of nsp16 relative to nsp1 of MHV RNA after treatment with remdesivir. The ratio of nsp16 relative to nsp1 decreases with increasing concentrations of remdesivir, but not compared with the DMSO control. All data in this figure represent the results of two independent experiments, each with 3 replicates. Statistical significance compared to DMSO control was determined by Kruskal-Wallis test using the Dunn's post hoc test to correct for multiple comparisons and is denoted by asterisks: *, $P < 0.05$.

I found that neither lineage of NHC passaged viruses decreased sensitivity to remdesivir inhibition compared to WT MHV (Fig. 33C). Together, these results demonstrate the lack of cross-resistance across this nucleoside panel and support their compatibility in resistance mitigation.

Discussion

In this chapter, I present data that probes the details of CoV inhibition by a panel of nucleoside analogues that are proposed to act by distinct mechanisms. I demonstrate that, regardless of proposed mechanism of action, nucleoside analogues more potently inhibit CoVs during infection with low viral loads. Further, MHV specific infectivity can be decreased by nucleoside analogues even if they do not induce mutagenesis. I also show preliminary data that suggests nucleoside analogue treatment alters viral RNA released after infection. However, regardless of proposed mechanism, no cross-resistance was detected across this panel of nucleoside analogues, suggesting their utility in controlling antiviral resistance. Together, these results contribute to a better understanding of the mechanisms of action of these compounds in CoVs.

Lower viral load enhances CoV inhibition by nucleoside analogues regardless of proposed mechanism. Each of the nucleoside analogues investigated here had a proposed mechanism of action in other viral systems, but specific inhibitory details may vary from virus to virus. While specific differences in multiple phenotypes emerged after treatment with this nucleoside analogue panel, I observed that they all inhibited MHV more potently after multiple rounds of replication within a single infection, regardless of proposed mechanism of action. This result suggests that nucleoside analogue impacts on viral replication are compounded over time.

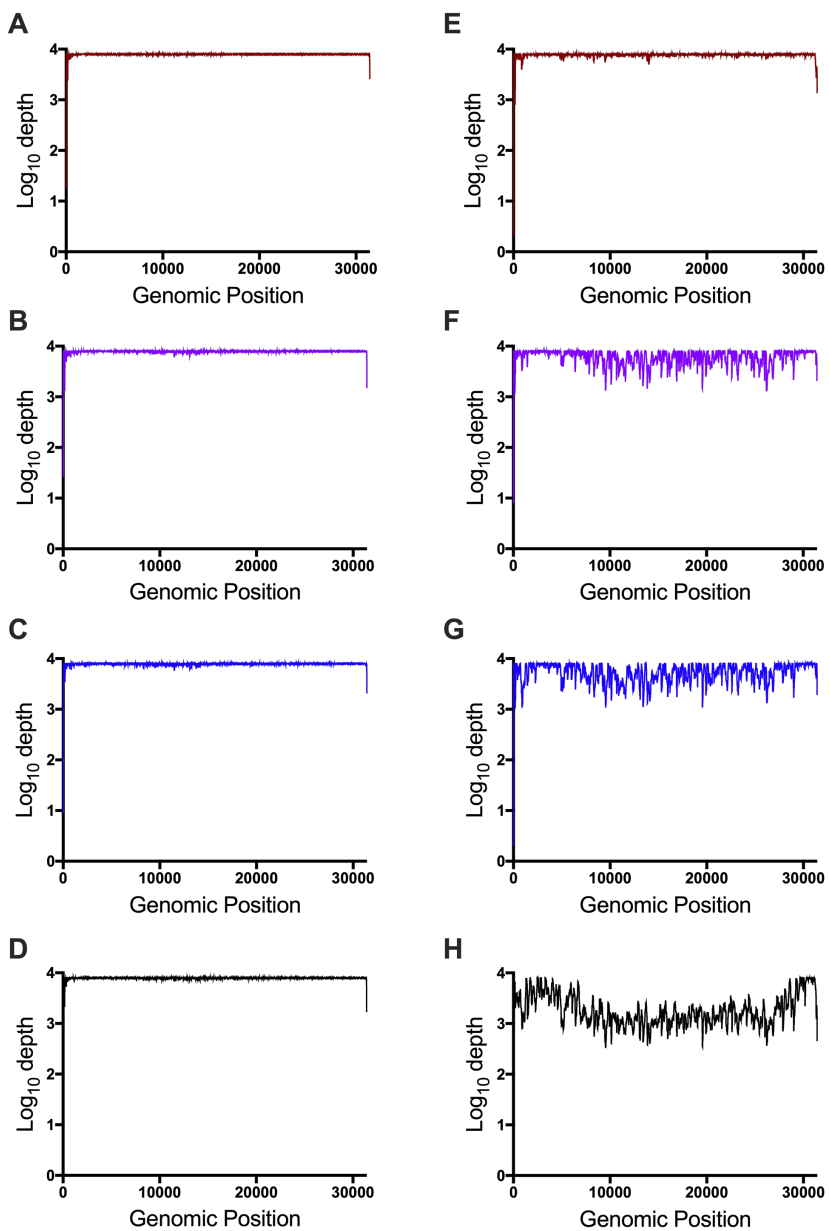


Figure 31. Sequencing coverage is more variable in the absence of poly(A) library selection after nucleoside analogue treatment.

(A) Number of NGS reads aligned to the genome at each nucleotide position after poly(A) library selection of MHV-infected samples treated with vehicle (DMSO), (B) 40 μ M 2'-C-MeA, (C) 4 μ M NHC, or (D) 0.25 μ M remdesivir. (E) Number of NGS reads aligned to the genome at each nucleotide position without poly(A) library selection of MHV-infected samples treated with vehicle (DMSO), (F) 40 μ M 2'-C-MeA, (G) 4 μ M NHC, or (H) 0.25 μ M remdesivir.

Further, it also suggests that some aspects of inhibition may not be indicative of a particular mechanism of action and may be shared across nucleoside analogues. This is particularly interesting because few studies have investigated the impact of viral load on nucleoside analogue efficacy, especially with nucleoside analogues that do not act by a mutagenic mechanism (Moreno et al., 2012; Perales et al., 2011; Sierra et al., 2000). In addition, this result could be clinically relevant. For example, nucleoside analogue treatment may be more effective earlier in infection, when the viral load of a patient is lower. This is consistent with the increased efficacy of remdesivir when given prophylactically vs therapeutically, but future studies are warranted to more deeply investigate this proposition. Future studies may also address whether these findings are consistent across different types of inhibitors beyond nucleoside analogues in CoVs, as a protease inhibitor of chikungunya virus also showed a similar effect of viral load-dependent inhibition (Das et al., 2016).

Nucleoside analogue treatment may alter viral RNA released after infection. In this chapter, I demonstrate that non-mutagenic compounds, such as remdesivir, can significantly decrease MHV specific infectivity. Since remdesivir treatment did not increase low-frequency mutations present across the genome, these data indicate that changes in specific infectivity can represent more than mutagenesis. But what, beyond mutagenesis, may damage infectivity of viral RNA after nucleoside analogue treatment? Because remdesivir is proposed to be a chain terminator, one potential explanation is that CoVs package truncated or defective RNAs after remdesivir treatment. While truncated RNAs may result from chain termination, they could also represent loss of polymerase processivity in the presence of remdesivir. However, loss of polymerase processivity may also lead to template switching and the generation of defective recombinants

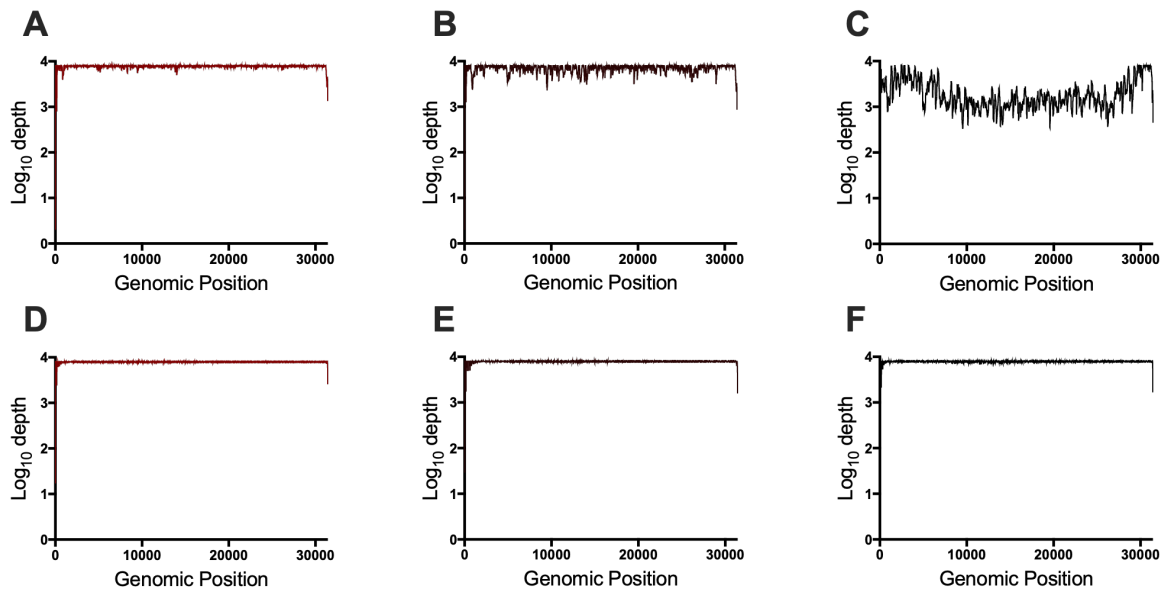


Figure 32. Dose-dependent change in sequencing coverage variability without poly(A) library selection after remdesivir treatment.

(A) Number of NGS reads aligned to the genome at each nucleotide position without poly(A) library selection of MHV-infected samples treated with vehicle (DMSO), (B) 0.125 μ M remdesivir, or (C) 0.25 μ M remdesivir. Sequencing coverage variability increases with increasing concentrations of remdesivir. (D) Number of NGS reads aligned to the genome at each nucleotide position with poly(A) library selection of MHV-infected samples treated with vehicle (DMSO), (E) 0.125 μ M remdesivir, or (F) 0.25 μ M remdesivir. Sequencing coverage in the presence of poly(A) library selection at the same concentrations of remdesivir shows less variability.

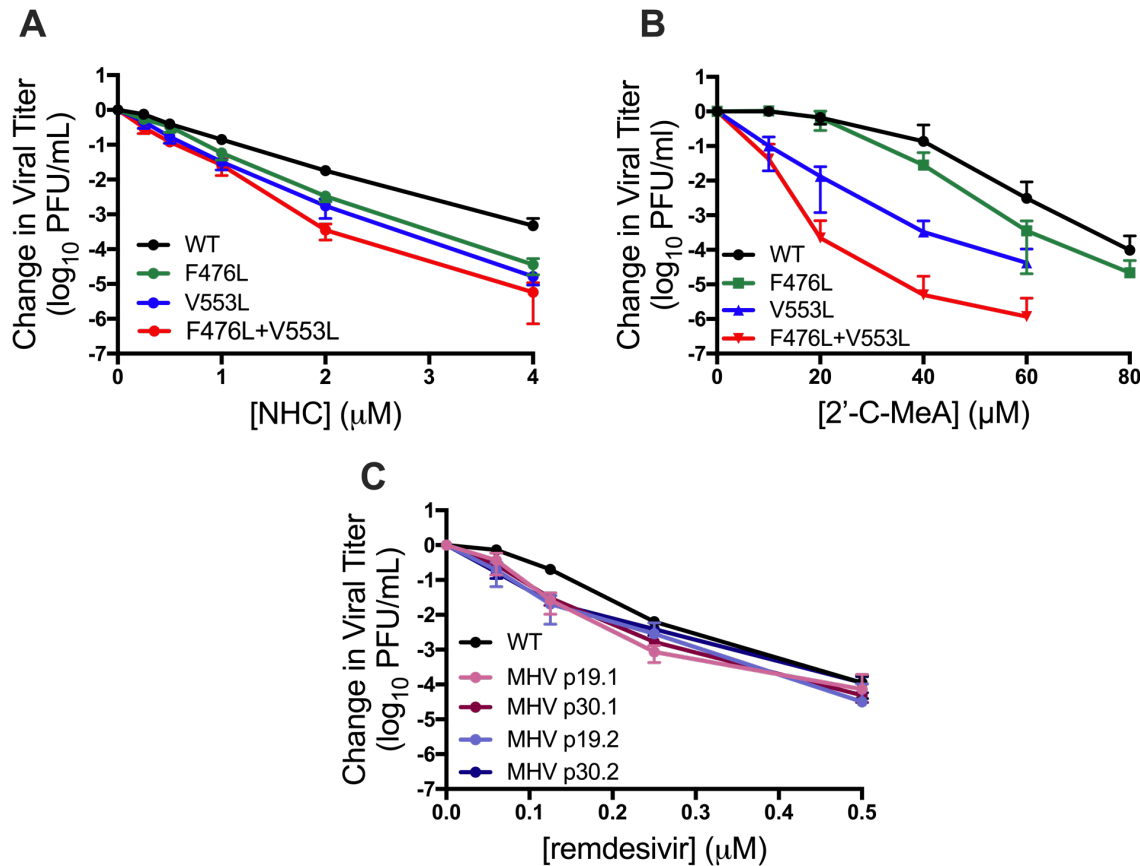


Figure 33. Resistance to a single nucleoside analogue does not confer broad cross-resistance.

(A) Change in viral titer for WT MHV and remdesivir resistant MHV relative to vehicle control after treatment with NHC or (B) 2'-C-MeA. Remdesivir resistant mutants are not less sensitive to NHC or 2'-C-MeA inhibition. (C) Change in viral titer for WT MHV and NHC passage 19 and passage 30 virus lineages relative to vehicle control after treatment with remdesivir. NHC passage lineages are not less sensitive to remdesivir inhibition. All data in this figure represent the results of two independent experiments, each with 3 replicates. No statistical significance compared to WT was detected by the Kruskal-Wallis test using the Dunn's post hoc test to correct for multiple comparisons.

(Kim and Kao, 2001). Since nucleoside analogues in this panel also made coverage across the genome by Bowtie2 more variable, as is seen during generation of defective RNA genomes (Jaworski and Routh, 2017), it will be important to further investigate truncation and recombination events in the presence of these nucleoside analogues. Beyond truncation and recombination, CoVs could lead to nonspecific packaging, especially of sgmRNAs or negative-sense RNA based on less genomic RNA being present. However, another possibility remains that chain termination occurs when the nucleoside is incorporated in the template strand (Deval, 2009), decreasing infectivity and altering the coverage of this template RNA. Overall, the data presented here raise many unanswered questions about the precise effects of nucleoside analogue treatment on released viral RNA that warrant further exploration.

Lack of cross-resistance between nucleoside analogues indicates their potential to control antiviral resistance. Multiple therapeutic regimens have employed combinations of antivirals to combat infection and control resistance (De Clercq and Li, 2016a; Hofmann et al., 2009). Previous reports in HIV have studied the effect of M184V, a lamivudine (3TC) resistance mutation that increases sensitivity to other nucleoside inhibitors such as AZT (Larder et al., 1989), and this relationship may be important for the efficacy of some drug combinations (Larder et al., 1995). Thus, with the increasing number of nucleoside analogues that inhibit CoVs, I sought to understand the compatibility between these compounds. Here, I demonstrate no evidence of cross-resistance between a panel of nucleosides with different proposed mechanisms of action. Interestingly, both remdesivir and 2'-C-MeA are adenosine analogues proposed to act by non-obligate chain termination, but I found differences in their inhibition profiles of CoVs, including the lack of cross-resistance between these two nucleosides. This

suggests that residues involved in resistance may recognize distinct features of these nucleosides (Deval et al., 2016a). Overall, these results support the potential of nucleoside analogues to be used in conjunction to mitigate CoV antiviral drug resistance. Future studies will be important to probe the mechanisms of resistance to these compounds and to better understand the utility of nucleoside analogue combinations in combating CoV antiviral resistance.

Conclusion

The data presented in this chapter highlight some of the similarities and differences of CoV inhibition by three distinct nucleoside analogues. Specifically, this chapter begins to probe the ability of this nucleoside analogue panel to cause CoV inhibition by the two most common mechanisms of action: chain termination and mutagenesis. Collectively, these results expand our knowledge of nucleoside analogue inhibition of CoVs and provide insights into CoV replication. Finally, these results indicate the potential of these nucleoside analogues to be used in combination to control antiviral resistance.

CHAPTER V

MATERIALS AND METHODS

Cell culture

Murine astrocytoma delayed brain tumor (DBT) cells (Chen and Baric, 1996), Vero cells (ATCC CCL-81), and baby hamster kidney 21 cells expressing the MHV receptor (BHK-R) (Yount et al., 2002) were maintained at 37°C in Dulbecco's modified Eagle medium (DMEM; Gibco) containing 10% fetal bovine serum (FBS; Invitrogen), penicillin and streptomycin (Gibco), HEPES (Gibco), and amphotericin B (Corning). BHK-R cells were further supplemented with 0.8 mg/ml of G418 (Mediatech). The human lung epithelial cell line Calu-3 (clone 2B4) was kindly donated by C. T. Tseng (University of Texas Medical Branch) (Sims et al., 2013) and maintained in DMEM (Gibco), 20% fetal bovine serum (HyClone), and 1× Gibco antibiotic-antimycotic solution. Human tracheobronchial epithelial cells were obtained from airway specimens resected from patients undergoing surgery under University of North Carolina Institutional Review Board-approved protocols by the Cystic Fibrosis Center Tissue Culture Core (UNC Tissue Core). Primary cells were expanded to generate passage 1 cells, and passage 2 cells were plated at a density of 250,000 cells per well on Transwell-COL (12-mm diameter) supports. Human airway epithelium cultures were generated by provision of an air-liquid interface (ALI) for 6 to 8 weeks to form well-differentiated, polarized cultures that resembled *in vivo* pseudostratified mucociliary epithelium (Leslie Fulcher et al., 2004; Scobey et al., 2013; Sims et al., 2005).

Viruses

All work with MHV was performed using the recombinant WT strain MHV-A59 (GenBank accession number AY9108610 (Yount et al., 2002)). SARS-CoV expressing green fluorescent protein (SARS-GFP) and MERS-CoV expressing red fluorescent protein (MERS-RFP) used in the remdesivir work were created from molecular cDNA clones according to protocols described previously (Scobey et al., 2013; Sims et al., 2005). MERS-CoV stocks used in the NHC work were generated from cDNA clones (GenBank accession number JX869059 (Almazán et al., 2015)).

Compounds and cell viability studies

GS-441524 and remdesivir (GS-5734) were synthesized at Gilead Sciences and prepared as 50 mM and 20 mM stock solutions in dimethyl sulfoxide (DMSO), respectively. NHC was synthesized at the Emory Institute for Drug Development and prepared as a 20 mM stock solution in DMSO. Cell viability was assessed using CellTiter-Glo (Promega) in 96-well plates according to the manufacturer's instructions. DBT cells were incubated with indicated concentration of compound at 37°C for 24 h. Vero cells were incubated with indicated concentration of compound at 37°C for 48 hours. DBT cell viability was determined using a Veritas microplate luminometer (Promega) and Vero cell viability was determined using the GloMax (Promega) with values normalized to those of untreated cells.

Compound sensitivity studies and generation of EC₅₀ curves

Subconfluent monolayers of DBT cells were infected with the indicated virus at a multiplicity of infection (MOI) of 0.01 PFU per cell for 1 h at 37°C. The inoculum was removed and replaced

with medium containing the indicated compound concentration. Cell supernatants were harvested 24 h post-infection. Titers were determined by plaque assay (Eckerle et al., 2007). MOI effect experiments were performed as described above except that cells infected at a high MOI (1 PFU/cell) were collected 12 h post-infection. Subconfluent monolayers of Vero cells were infected with an MOI of 0.01 PFU/cell of MERS-CoV. After virus adsorption for 30 minutes at 37°C, the inoculum was removed. Cells were washed with PBS and incubated with medium containing the indicated concentrations of NHC or DMSO (vehicle control). After 48 h, supernatant was collected and titers were determined by plaque assay as described previously (Coleman and Frieman, 2015). EC₅₀ curves as well as EC₅₀ and/or EC₉₀ values were generated with the nonlinear regression curve fit in GraphPad Prism software (La Jolla, CA).

***In vitro* efficacy in human airway epithelial cells**

Fully mature HAE cultures were obtained from the UNC Tissue Core. At 48 h prior to infection the apical surface of the culture was washed with 500 µl 1× phosphate-buffered saline (PBS) for 1.5 h at 37°C, and the cultures were moved into wells containing fresh air-liquid interface (ALI) medium (Leslie Fulcher et al., 2004). Immediately prior to infection, 500 µl of PBS was added to the apical surface of the HAE cultures for 30 min at 37°C, the first wash was removed, and a second wash was added prior to moving the HAE cultures into ALI medium containing remdesivir concentrations ranging from 0.0016 to 10 µM, as indicated for each experiment. The second wash was removed, and 200 µl of viral inoculum (MOI of 0.5 PFU/cell for MERS-RFP and SARS-GFP) was added to the apical surface of the cultures for 3 h at 37°C. The viral inoculum was then removed, and the apical surface of the cultures was washed three times with 500 µl 1× PBS, the final wash was removed, and the cultures were incubated at 37°C for a total

of 48 h post-infection. For all cultures, apical washes were performed (100 µl 1× PBS) to assess viral replication titers, and then total RNA was collected in 500 µl TRIzol (Life Technologies/ ThermoFisher) and frozen at -80°C prior to extraction for real-time PCR analysis. The data that are shown are representative of duplicate sample sets performed with a minimum of three different patient isolates. For the therapeutic HAE experiments, cultures were washed as described above, and HAE cells remained in drug-free ALI medium for the first day of infection. At 24 h post-infection, cultures were moved to ALI medium containing remdesivir concentrations ranging from 1 to 10 µM as indicated. Cultures were harvested at 48 h post-drug treatment, which was 72 h post-infection.

Time-of-drug addition assay

Subconfluent monolayers of DBT cells were treated with media containing DMSO, 2 µM remdesivir, or 16 µM NHC at the indicated time pre- or post-infection. Cells were infected with WT MHV at an MOI of 1 PFU/cell for 1 hour at 37°C. Virus inoculum was removed and medium was replaced. Culture supernatant was harvested 12 hours post-infection, and viral titer was determined by plaque assay.

Quantification of viral genomic RNA

Subconfluent DBT cells were infected with WT MHV at an MOI of 0.01 PFU/cell. Inoculum was removed after 1 h incubation at 37°C and medium containing indicated compound concentration was added. Total RNA from cells and supernatant RNA was harvested using the TRIzol reagent (Invitrogen) after 20 hours. Both total RNA and supernatant RNA were extracted by phase separation. Total RNA was purified by ethanol precipitation and supernatant RNA was

purified using the PureLink RNA mini kit (Invitrogen) according to manufacturer's protocol. Total RNA was reverse transcribed using SuperScript III (Invitrogen) to generate cDNA that was quantified by polymerase chain reaction (qPCR) as previously described (Smith et al., 2013). Data are presented as $2^{-\Delta\Delta CT}$, where $\Delta\Delta CT$ denotes the change in the threshold cycle for the viral target (nsp10) normalized to the control Glyceraldehyde 3-phosphate dehydrogenase (GAPDH) before and after drug treatment. Supernatant RNA was quantified using one-step reverse transcriptase-quantitative PCR (qRT-PCR) as previously described (Sexton et al., 2016). Data are presented as the fold change in genome RNA copies normalized to vehicle control.

Determination of specific infectivity

Subconfluent DBT cells were infected with WT MHV at an MOI of 0.01 PFU/cell. Inoculum was removed after 1 h incubation at 37°C and medium containing indicated concentrations of NHC was added. Supernatant RNA was harvested using the TRIzol reagent (Invitrogen) after 20 hours, followed by extraction and quantification as described above. Viral titer was determined by plaque assay. Specific infectivity was calculated as PFU per supernatant genome RNA copy.

NGS studies

Subconfluent DBT cells were infected with WT MHV at an MOI of 0.01 PFU/cell and treated with the indicated concentrations of NHC. Supernatant was collected 24 hours post-infection. Purified viral RNA was submitted to GENEWIZ for library preparation and sequencing. Briefly, after performing quality controls, viral RNAs were randomly fragmented using heat. Libraries were prepared and sequenced on the Illumina HiSeq platform. GENEWIZ performed base-calling and read demultiplexing. Trimmomatic was used to trim adapter contaminants and reads

shorter than 36 basepairs as well as filter low quality bases (Q-score <30) (Bolger et al., 2014). The paired-end fastq reads were then aligned to the MHV genome using Bowtie2 to generate a SAM file (Langmead et al., 2019). SAMtools was used to process the resultant alignment file and calculate coverage depth at each nucleotide, generating a sorted and indexed BAM file. LoFreq was used to call substitution variants, including low- frequency variants, and generate a variant file (Wilm et al., 2012). The Bash shell and Excel were used to further process and analyze the resultant vcf file. A frequency of 0.001 was used as a cutoff for variants, consistent with previous reports (Nakamura et al., 2011). Absolute numbers of mutations are reported for each NHC treatment. The percentage of the total mutations for each specific mutation type was calculated using these numbers. The difference in percentage for each class of mutation after treatment as compared with vehicle control is referred to as the relative proportion of these mutations.

Selection of remdesivir resistance mutations

WT MHV was passaged in triplicate in increasing concentrations of GS-441524, ranging from 1 to 12 µM. Infection was initiated for passage 1 at an MOI of 0.1 PFU/cell. Supernatant was harvested and frozen when the cell monolayer demonstrated 80% cytopathic effect (CPE) or after 24 h. A constant volume of 16 µl was used to initiate subsequent passages. All lineages were maintained until passage 17 (p17). Lineages 2 and 3 were lost after p17 and p20, respectively, when virus CPE did not reach above 50% upon multiple efforts and at various concentrations of GS-441524. Lineage 1 demonstrated an increase in visible CPE, and thus lineage 1 was carried to passage 23. After each passage, total RNA was harvested from infected cell monolayers using the TRIzol reagent to be used for viral population sequencing. After

passage 23, RNA was extracted and reverse transcribed using SuperScript III, followed by generation of amplicons for all three lineages covering nsp12 and nsp14 at passage 16 and 12 PCR amplicons to cover the whole genome after 23 passages of lineage 1. Dideoxy amplicon sequencing was performed by GenHunter (Nashville, TN) and analyzed to identify mutations using MacVector.

MHV population passage in the presence of NHC

WT MHV was passaged in triplicate in increasing concentrations of NHC, ranging from 1 μ M to 5 μ M. Infection was initiated for passage 1 at an MOI = 0.1 PFU/cell. Viral supernatants were harvested and frozen when the cell monolayer demonstrated 80% cytopathic effect (CPE) or after 24 hrs. A constant volume of 16 μ l was used to initiate subsequent passages. All three lineages were maintained until passage 16 when lineage 3 demonstrated no visible CPE upon multiple attempts at varying concentrations. Lineage 1 and 2 were maintained until passage 30. After each passage, total RNA was harvested from infected cell monolayers using the TRIzol reagent. Viral RNA was extracted from passage 19 and passage 30 samples and reverse transcribed using SuperScript III, followed by generation of 12 PCR amplicons to cover the whole genome. Dideoxy amplicon sequencing was performed by GENEWIZ and analyzed to identify mutations present at greater than 50% of total using MacVector. Viral mutation maps depicting the identified mutations were generated using MacVector.

MERS-CoV population passage in the presence of NHC

Three parallel, independent passage series of WT MERS-CoV were performed on Vero cells in the presence of escalating concentrations of NHC up to a maximum of 6.5 μ M to select for drug-

resistant mutant viruses. Virus adaptation to replication in the presence of NHC-supplemented complete culture medium was assessed by monitoring progression of characteristic MERS-CoV CPE. Volumes of transferred culture supernatants were adjusted empirically to balance continuous selective pressure against culture extinction. Each of triplicate lineages in the MERS-CoV passage experiment was sustained through passage 30. However, the third lineage was severely impaired in replication and was excluded from further analysis. Total infected-cell MERS-CoV RNA purified from monolayers infected with terminal-passage (p30) culture supernatant was used to generate RT-PCR products for consensus Sanger sequencing of the complete viral genome (GENEWIZ). Changes in passaged virus nucleotide and deduced amino acid sequences were identified via alignment with the WT parental virus genomic sequence using MacVector.

Modeling and conservation of resistance mutations in the CoV MHV nsp12 RdRp

The F476 and V553 residues were located on the previously described MHV RdRp model (Sexton et al., 2016) using the Pymol Molecular Graphics System (Schrödinger, LLC). A model of the MHV RdRp was also generated using Phyre² (Kelley et al., 2015) based on the solved structure of SARS-CoV, and mutations were modeled on this polymerase model (Kirchdoerfer and Ward, 2019). Multiple sequence alignments were generated using MacVector.

Cloning, recovery, and verification of mutant viruses

QuikChange mutagenesis was performed according to the manufacturer's protocol to generate mutations in MHV individual genome cDNA fragment plasmids using the previously described infectious clone reverse-genetics system (Yount et al., 2002). Mutants were recovered in BHK-R

cells following electroporation of *in vitro*-transcribed genomic RNA. All fragments containing mutations as well as virus stocks were sequenced to ensure mutations were present before use in further studies (GenHunter). To generate SARS-CoV encoding nsp12 resistance substitutions, a 1,450-bp cassette encoding the substitutions (F480L and V557L) was synthesized by BioBasic. The synthesized cassette was then cloned into the SARS-CoV D infectious cDNA plasmid at unique MluI and MstI sites, and the subsequent selected clone was sequence verified across the cassette. SARS-CoV expressing the resistance substitutions along with the nanoluciferase (NanoLuc) reporter in place of ORF7 was produced as described previously (Yount et al., 2011).

SARS-CoV remdesivir resistance assessment

Calu-3 2B4 cells were seeded in 96-well plates at a density of 5×10^5 cells/well 48 h prior to infection. The medium was replaced with fresh medium 24 h prior to infection to encourage optimal cell growth. Cells were then infected with SARS-CoV F480L + V557L-NanoLuc or SARS-CoV-WT-NanoLuc at an MOI of ~5 PFU/cell in the presence or absence of remdesivir at 1:3 dilutions, with DMSO (diluent) as an untreated control and UV-inactivated virus as a NanoLuc reporter background control. Cells were lysed after incubation at 37°C for 72 h using a Promega NanoGlo assay kit and assayed on a luminescence plate reader (SpectraMax M3; Molecular Devices). EC₅₀ values and curves were generated with the nonlinear regression curve fit feature in GraphPad Prism software (La Jolla, CA).

Virus replication assays

For MHV, Subconfluent monolayers of DBT cells were infected with the indicated virus at an MOI of 0.01 PFU/cell for 1 h. For MERS-CoV, subconfluent monolayers of Vero cells were

infected with MERS-CoV at an MOI of 0.01 PFU/cell for 30 min. Inocula were removed, and cells were washed with PBS before addition of prewarmed medium. Supernatants were harvested at indicated times post-infection, and titers were determined by plaque assay.

Competitive fitness of mutant viruses

Subconfluent DBT cells were coinfecte^d with F476L + V553L and WT MHV at input ratios of 1:9, 1:1, or 9:1 at an MOI of 0.01 PFU/cell for 1 h at 37°C. The virus inoculum was removed, and fresh medium was added. At 20 h post-infection, virus supernatants were collected, and infected cell monolayers were harvested using the TRIzol reagent. Samples were frozen, and cell supernatant was passaged onto fresh DBT cells for a total of four passages. Supernatants and cell monolayers in TRIzol were collected from each passage when nearly all of the monolayer was involved in CPE—approximately 16 h post-infection. RNA was extracted and reverse transcribed using SuperScript III, and PCR amplicons covering the region of the mutations were sequenced (GenHunter). Results represent the combined frequency of F476L and V553L mutations as determined by chromatographic traces and analyzed using MacVector.

Assessment of resistant virus virulence *in vivo*

Groups of 10 to 12 10-week old female BALB/c (Charles River, Inc.) mice were anesthetized with ketamine-xylazine and intranasally infected with either 10^4 or 10^3 PFU/50 µl wild-type mouse-adapted SARS-CoV expressing NanoLuc (WT SARS-CoV) or SARS-MA15 NanoLuc engineered to harbor resistance mutations in nsp12 (F480L + V557L SARS-CoV). Animals were weighed daily to monitor virus-associated weight loss. On days 2 and 4 post-infection, 5 to 6 animals per group were sacrificed by isoflurane overdose and the inferior right lobe was

harvested and frozen at -80°C until the titer was determined by plaque assay as described previously (Gralinski et al., 2013). A 5- to 6-animal cohort was monitored out to 7 days post-infection in order to compare the kinetics of recovery, after which lung samples were harvested and the titer determined as described for previous samples.

Relative quantification of viral nsp1 and nsp16 RNA

Subconfluent monolayers of DBT cells were infected with the indicated virus at a multiplicity of infection (MOI) of 0.01 PFU per cell for 1 h at 37°C. The inoculum was removed and replaced with medium containing the indicated compound concentration. Cell supernatants were harvested 24 h post-infection. Supernatant RNA was extracted by phase separation and purified using the PureLink RNA mini kit (Invitrogen) according to manufacturer's protocol. Supernatant RNA was quantified using the Power SYBR Green RNA-to-Ct 1-step kit (ThermoFisher) using primers designed to detect nsp1 or nsp16. Primer sequences are listed below as nsp1B and nsp16A. Briefly, dilution of viral RNA from were made from 10³ to 10⁸ genome equivalents to generate standard curves and determine primer efficiencies. Reaction mixtures were set up on ice, with enzyme added last. The final volume for individual reaction mixtures was 20 µl, with 200 nM each primer, 1 µl sample RNA, 0.16 µl 125× RT Enzyme Mix and 10 µl 2× Power SYBR Green RT-PCR Mix. Samples were plated in duplicate and run on the StepOnePlus real-time PCR system (ThermoFisher) with the following conditions according to manufacturer protocol: 48°C for 30 min, 95°C for 10 min, 95°C for 15 s, and 60°C for 1 min, with the last two steps repeated 40 times. Data are presented as 2^{-ΔΔCT}, where ΔΔCT denotes the change in the threshold cycle for the viral target (nsp16) relative to the control (nsp1) normalized the vehicle (DMSO) control after drug treatment.

Exogenous nucleoside addition assays

Subconfluent monolayers of DBT cells were infected with WT MHV at a multiplicity of infection (MOI) of 0.01 PFU per cell for 1 h at 37°C. The inoculum was removed. Medium containing DMSO, 60 µM 2'-C-MeA, 3 µM NHC, 5 µM GS-441524 together with 100 µM of the indicated nucleoside (A, G, C, or U) or equivalent volume of DMSO vehicle was added to infected cells. Cell supernatants were harvested 24 h post-infection. Viral titers were determined by plaque assay.

Statistics

Statistical tests were performed using GraphPad Prism 7 software (La Jolla, CA) as described in the respective figure legends.

Primers generated for this dissertation research

Table 4. Primers generated for this dissertation research^a

Primer name	Sequence 5'-3'
QuikChange primers for generation of viruses containing replicase mutations after remdesivir passage	
V553L_S_F	CTAAGAACGGGCCGCACCC <ins>T</ins> TGCTGGTGTCTATTCTATTTC
V553L_S_R	GAATAGAGACACCAGCAA <ins>G</ins> GGTGCGGGCCCTATTCTTAG
V553L_D_F	CTAAGAACGGGCCGCACCC <ins>T</ins> C <ins>G</ins> GCTGGTGTCTATTTC
V553L_D_R	GAATAGAGACACCAGC <ins>G</ins> A <ins>G</ins> GGTGCGGGCCCTATTCTTAG

F476L_S_F	GAAGTTGTTAATAAGTATTAAGATCTATGAGGGTGGG
F476L_S_R	CCCACCCTCATAGATCTCTAGATACTTATTAACAACTTC
F476L_D_F	GAAGTTGTTAATAAGTATCTAGAGATCTATGAGGGTGGG
F476L_D_R	CCCACCCTCATAGATCTCTAGATACTTATTAACAACTTC
13A335V_F	GCACGCGTATTGTTCCCTGTCAGGTGCGTAGATTGTTATG
13A335V_R	CATAACAATCTACACGCACCTTGA CAGGAACAATACGCGTGC
qPCR primers	
nsp1A_F	AACACCAGGGAGTGCTCTTG
nsp1A_R	ATGGCTGTGACTGGAACGAA
nsp16A_F	CGGTAAAACCATGCATGCCA
nsp16A_R	TAACAACAGCCGTACCAGCC
nsp1B_F	CTGCCATGGGGTTGTTCAAG
nsp1B_R	GGCCATTACCCAGGCATACA
nsp16B_F	TCTGGAATTATGGCAAGCCGA
nsp16B_R	CGCATATTAGCCGGAACTGC

^aPrimers were generated by IDT.

CHAPTER VI

SUMMARY AND FUTURE DIRECTIONS

Introduction

New viral infections will continue to emerge into human populations to cause disease.

Throughout the course of this dissertation, several emerging virus outbreaks have been reported: Ebola virus has caused large outbreaks in two different regions of Africa, MERS has caused an outbreak in Korea and continues to infect humans in the Middle East, and Zika virus has emerged as a disease culprit particularly throughout the tropics. This dissertation work focuses on CoVs, a set of viruses with a demonstrated ability to emerge into humans from animal reservoirs. While all human CoVs are proposed to have animal origins, two CoVs are of particular importance. Both SARS-CoV and MERS-CoV have crossed into humans to cause severe disease within the last 20 years, and many related CoVs still circulate in bats (Menachery et al., 2015; Woo et al., 2018). Thus, CoVs will likely continue to emerge into human populations, emphasizing the importance of developing antivirals that can broadly inhibit them. While several antiviral targets exist, the conserved and essential role of the viral polymerase in replication makes it a particularly enticing antiviral target. The importance of polymerase inhibitors is only reinforced by the clinical success of these compounds in combating other viral diseases. Compounds that target viral polymerases primarily come in two flavors: nucleoside and non-nucleoside inhibitors. Nucleoside inhibitors share the structure of naturally occurring nucleosides and contain modifications along this backbone, whereas non-nucleoside inhibitors target sites distinct from the active site that may be specific to a particular polymerase (Heck et

al., 2008; Siberry and Hazra, 2012). Given that all viral polymerases must utilize nucleotides for genome synthesis, nucleoside analogues serve as an enticing strategy to combat a wide range of emerging infections.

At the beginning of this dissertation research, the primary nucleoside analogues that had been tested in CoVs were broad-spectrum agents, such as RBV, that did not potently inhibit WT CoVs (Smith et al., 2013). Throughout the course of this dissertation research, multiple broad-spectrum antiviral nucleoside analogues have been identified and investigated as inhibitors for several viral infections (Delang et al., 2014; Deval et al., 2015; Kulkarni et al., 2016; Warren et al., 2015). The main goals of this dissertation research were to identify nucleoside analogues that could broadly inhibit across CoVs, to understand their mechanism of action, and to identify impacts of resistance to these compounds as they relate to CoV biology. In this chapter, I summarize the findings of this dissertation work and highlight important areas for future study.

Nucleoside analogues with broad antiviral spectrum potently inhibit CoVs

The continued threat for zoonotic viral infections emphasizes the need for broad-spectrum antivirals that can inhibit any emerging virus. In this dissertation work, I demonstrated that two broad-spectrum nucleoside analogues, remdesivir and NHC, potently inhibit CoVs. Interestingly, remdesivir inhibits positive-sense RNA viruses such as CoVs, but the many of the viruses most potently inhibited by this compound are negative-sense RNA viruses such as filo-, pneumo- and paramyxoviruses (Lo et al., 2017b). Notably, NHC potently inhibits alphaviruses, a positive-sense RNA virus family absent from the antiviral spectrum of remdesivir (Cho et al., 2012; Urakova et al., 2017). Thus, the antiviral spectrum of these compounds that potently inhibit

CoVs overlap but are not identical. Further, nucleoside analogues, such as favipiravir and sofosbuvir, are active against multiple viruses that remdesivir and NHC inhibit, but they do not appear to inhibit WT MHV (unpublished observations). Understanding antiviral spectrum may help illuminate particular features of a compound or virus that promote robust inhibition. Ultimately, these discoveries may also guide rational design of single broad-spectrum antivirals or combination regimens that could combat any emerging infection of the future.

Specific determinants must underlie viral susceptibility patterns to antiviral compounds. Much of the focus for identifying viral susceptibility determinants, especially for remdesivir and NHC, will remain on viral polymerases, as they are the central target of these compounds for every virus they inhibit. Viral RdRps have seven conserved motifs. Motifs A and C make up the active site and are assisted by motifs B and D. Motif G interacts with incoming template; motif E specifically interacts with the 3' end of that template; and motif F interacts with the incoming NTPs. All of these motifs are relatively closely clustered around the active site in the SARS-CoV RdRp , making them all potentially important in resistance to nucleoside analogues (Kirchdoerfer and Ward, 2019). For remdesivir, as was previously reported, antiviral spectrum may be predicated on sequence similarities between motifs A and B of the viral polymerase across viruses potently inhibited by this compound (Lo et al., 2017b). However, direct assessment of the involvement of these motifs in remdesivir susceptibility across viruses by mutagenesis would strengthen this conclusion. In addition, investigating resistance mutations across viral families may contribute to a more complete understanding of antiviral spectrum. The studies described in this dissertation work, along with structural data of the CoV RdRp, demonstrate that remdesivir resistance mutations in CoVs may impact critical viral motifs.

Specifically, F476 and V553 are located outside of motif B and motif F, respectively (Kirchdoerfer and Ward, 2019), further supporting the importance of motif B in determining susceptibility to remdesivir and implicating a potential role for motif F. However, some CoVs naturally contain the resistant mutation at the F476 residue and this does not prevent remdesivir inhibition, suggesting this is not the sole susceptibility determinant (Brown et al., 2019). Future studies may investigate the role of the identified CoV resistance mutations on remdesivir susceptibility in other viral families through homology, but this may be challenging due to the low sequence conservation of polymerases outside the motifs, where these mutations lie (Choi, 2012). Since this dissertation work describes the only reported remdesivir resistance mutations, studies are also warranted to address regions of the polymerase where remdesivir resistance mutations arise in different viruses. Testing the portability of remdesivir resistance mutations identified in other viruses into CoVs may also contribute to a better understanding of the antiviral spectrum of remdesivir. For NHC, approaches that focus on resistance portability may be challenging since even low-level NHC resistance is remarkably difficult to obtain in multiple viral systems (Stuyver et al., 2003). The mutations that have been identified in Venezuelan equine encephalitis virus (VEEV) lie in the fingers domain (Urakova et al., 2017). Thus, the role of homologous mutations in CoVs and other viruses should be assessed for their susceptibility to NHC. However, identifying and analyzing specific variations in polymerase motifs that coincide with susceptibility may provide the best insight into determinants of NHC's antiviral spectrum. Overall, when taken together, identifying determinants of susceptibility to these compounds across viruses will likely enhance our understanding of interactions between polymerase determinants and specific features of nucleoside analogues. This knowledge will strengthen our ability to rationally design and develop potent broad-spectrum antivirals. And designing broad-

spectrum antiviral regimens that could inhibit across virus families to combat whatever virus emerges next could potentially keep the world a step ahead of the next viral pandemic.

Nucleoside analogues can potently inhibit CoVs by multiple mechanisms of action

Remdesivir and NHC are among the first nucleoside analogues demonstrated to potently inhibit CoV replication. However, there are distinct differences between these compounds; remdesivir likely inhibits through a chain termination mechanism of action and NHC likely acts by mutagenizing viral RNA. Since some nucleoside analogues that have the same proposed mechanisms have not potently inhibited CoVs, it is possible that specific features of these particular nucleoside analogues encourage potent inhibition of CoVs. Approaches to probe these differences are discussed below.

NHC is the first mutagenic nucleoside analogue reported to potently inhibit WT CoVs. Mutagenic nucleoside analogues, such as ribavirin (RBV) and 5-fluorouracil (5-FU), have been incapable of inhibiting WT CoVs, raising the question of what in particular sets NHC apart from these mutagenic nucleoside analogues. One potential explanation is that the mutagenic signature of NHC is different than the other tested nucleoside analogues. While NHC introduces G:A and C:U transitions, 5-FU introduces A:G and C:U transitions in MHV (Smith et al., 2013). However, both RBV and favipiravir increase G:A and C:U transitions in viruses (Galli et al., 2018; Goldhill et al., 2019), the same types as NHC, but do not potently inhibit WT MHV (Smith et al., 2013). Thus, the inhibition of WT CoVs by NHC is not purely due to the types of mutations that it introduces. How is NHC able to potently inhibit CoVs when other previously identified mutagens could not? A combination of factors could be involved. For example, NHC

may be more efficiently incorporated by the polymerase than the nucleoside analogues that have been tested previously. NHC may also be more stably incorporated into the RNA or less susceptible to removal, and this hypothesis is consistent with the results I observed in ExoN(-) MHV. Another possibility is that NHC could inhibit by additional mechanisms beyond mutagenesis. Previous studies have suggested NHC may interfere with RNA secondary structure or interfere with release of productive virions (Stuyver et al., 2003; Urakova et al., 2017). Other nucleoside analogues also have multiple proposed mechanisms of action that may occur either independently or together in a specific virus (Furuta et al., 2017). While the multiple mechanisms of RBV do not encourage CoV inhibition, this relationship may be distinct for specific nucleoside analogues and may not hold true for NHC. Future studies of CoV inhibition by NHC will be important to better address these possibilities.

Both 2'-C-MeA and remdesivir are adenosine analogues that are proposed to act by chain termination mechanisms. Though precise differences in these chain termination mechanisms have been proposed biochemically, the differences I observed here demonstrate that remdesivir does not inhibit CoVs in precisely the same way as 2'-C-MeA during viral replication. Even further, remdesivir resistance mutations did not confer cross-resistance to 2'-C-MeA. This result suggests that the different modifications on these compounds may interact with the polymerase differently, even if they are both proposed to result in chain termination. These differences in resistance could indicate a difference between immediate and delayed chain termination in CoV replication, but future studies are warranted to examine this prospect further. However, given that 2'-C-MeA does not inhibit CoVs as potently as remdesivir, the differences between these

compounds may represent an interesting avenue to determine specific factors that contribute to the potent inhibition of CoVs by remdesivir.

Nucleoside analogues are important tools for investigating CoV replication

Nucleoside analogues have been important tools to better understand replication in several systems (Kuchta, 2010). Thus, since CoVs are the only RNA viruses with demonstrated proofreading activity, nucleoside analogues may serve as essential tools to understand the role of proofreading in RNA virus replication. During this dissertation work, other groups have investigated the ability of the CoV ExoN to remove incorrect nucleosides biochemically, and these studies suggest that the CoV ExoN can remove RBV to prevent potent inhibition by this compound (Ferron et al., 2017). But the presence of proofreading does not prevent potent inhibition by all nucleoside analogues, raising questions of the role of proofreading when the nucleoside analogues can potently inhibit CoVs. Since remdesivir and NHC act by different mechanisms of action, they may provide insight into the differing roles of proofreading depending on specific nucleoside analogue characteristics. For instance, a proofreading-deficient MHV mutant [ExoN(-)] was approximately 4-fold more susceptible to remdesivir inhibition than WT MHV, suggesting that proofreading does still have an effect on inhibition by remdesivir. However, this does not prevent inhibition by this compound, perhaps because ExoN does not efficiently and consistently recognize remdesivir or because the compound is stably incorporated into viral RNA by the polymerase (Feng, 2018). In contrast, ExoN seems to play even less of a role in NHC inhibition. While ExoN(-) MHV is more sensitive to NHC inhibition, this difference is only approximately 2-fold. As more mutagenic compounds that potently inhibit CoVs are discovered, it will be interesting to investigate if strong recognition of a mutagenic nucleoside by

ExoN always prevents potent inhibition of CoVs. Though the CoV ExoN does not appear to have a preference for removal of specific 3'-end mismatches (Bouvet et al., 2012), future studies may investigate whether the CoV ExoN may more efficiently remove nucleosides with specific modifications as well as the role of the other replicase proteins in this process.

The mutations uncovered after passage in the presence of NHC will likely aid in our understanding of CoV replication. Specific mutations that underlie the low-level resistance phenotype of NHC have yet to be identified and characterized in MHV or MERS-CoV. Because nearly none of the mutations overlap between the MHV or MERS-CoV passage series, there are likely several pathways to resistance that can be explored further. After particular mutations have been identified, determining their role in viral replication may provide interesting insights into the CoV replication machinery. For example, HIV resistance to AZT may be because its excision is enhanced in the presence of resistance mutations (Boyer et al., 2002). In the case of NHC inhibition of CoVs, the large number of potentially neutral or deleterious mutations could provide insight into regions that are capable of tolerating change within the CoV genome. Since the mutations were spread across the genome, determinants in other replicase proteins outside the polymerase may be involved and may give us a better idea of interactions between CoV these replicase proteins. In addition, several studies have identified replication fidelity determinants from mutations that confer resistance to mutagenic nucleoside analogues (Coffey et al., 2011; Pfeiffer and Kirkegaard, 2003a; Zeng et al., 2013). Further investigation of the mutations present after NHC passage might identify determinants of replication fidelity, nucleotide selectivity, replicase processivity, or phenotypes that have yet to be linked to nucleoside analogue inhibition, emphasizing the importance of this avenue of investigation.

While this dissertation research identified the importance of F476L and V553L in remdesivir resistance as well as their attenuation in combination, the precise role they play in viral replication was not thoroughly investigated. While these mutations did not confer cross-resistance to NHC or 2'-C-MeA, assessing cross-resistance to other related and unrelated nucleosides will undoubtedly lead to a better understanding of specific modifications that resistance mutations recognize to prevent inhibition (Deval et al., 2016b). Specifically, GS-441285 has been reported to inhibit HCV and combines the modifications of remdesivir and 2'-C-MeA; given the lack of cross-resistance between these compounds, it makes an interesting candidate to investigate (Feng et al., 2014). In addition, the V553 residue has been identified by homology modeling as a potential fidelity determinant in CoVs (Sexton et al., 2016), further emphasizing the role of nucleoside analogue resistance in replication fidelity. Interestingly, the V553L mutation in MHV was identified after remdesivir passage and the mutation in MERS was identified in the NHC passage series. However, the residue was changed to an isoleucine (I) after NHC passage and leucine (L) after remdesivir passage. Given that the V553L virus was not more resistant to NHC in MHV and the V553I mutation was implicated in replication fidelity, the particular change at this residue may be important in the specific response to the nucleoside. This differential effect based on the specific amino acid change has been observed previously for replication fidelity in chikungunya virus (Rozen-Gagnon et al., 2014), making exhaustive mutagenesis at the MHV V553 residue an enticing prospect for investigating its role in CoV replication.

In addition, one of the six mutations that emerged after 23 passages in the presence of GS-

441524 was in nsp13 (Agostini et al., 2018), which encodes the helicase and NTPase. Previous studies have identified nucleoside analogues that target the viral helicase and NTPase (Borowski et al., 2002; 2003). The CoV NTPase hydrolyzes nucleoside triphosphates (NTPs), with a particular preference among ribonucleosides for adenosine, and facilitates nucleic acid unwinding (Tanner et al., 2003). Thus, it is not improbable that nsp13 may play a role in the inhibition by the adenosine analogue remdesivir. Specifically, the mutation that emerged after passage was the A335V mutation in the helicase core (Hao et al., 2017) that has previously been reported to decrease viral fitness (Zhang et al., 2015). Given the small differences in sensitivity between F476L+V553L MHV and p23 MHV to remdesivir, it may be difficult to discern the role of this mutation during viral replication in remdesivir resistance. However, this mutation may still play an important role in viral replication. Helicases have also been shown to contribute to replication fidelity (Stapleford et al., 2015), and it is possible that this resistance mutation could play a role in replication fidelity. While other studies in CoVs have suggested the importance of other replicase proteins outside of nsp10, nsp12, and nsp14 in replication fidelity (Graepel et al., 2017), this has not been explicitly demonstrated and warrants further investigation.

Interestingly, treatment with nucleoside analogue antivirals may also help elucidate questions related to CoV packaging. The significant decrease in specific infectivity I observed after NHC and remdesivir treatment suggests that viral RNA produced under these conditions is less infectious. Given that decreases in specific infectivity have traditionally been linked with mutagenic mechanisms of action, this result is seemingly clear for NHC. However, these results are likely much more complex for remdesivir, which did not increase mutations to levels above WT MHV. One explanation for the decreased infectivity of viral RNA after remdesivir treatment

is that truncated viral nucleic acid resulting from chain termination is packaged, raising interesting questions about what is necessary to package and release CoV RNA. While a packaging signal in nsp15 of MHV has been reported, it appears that it aids in correct packaging but is not absolutely required (Kuo and Masters, 2013). The loss of this packaging signal is associated with aberrant packaging, especially as it relates to sgmRNAs. Thus, it is possible that increased concentrations of remdesivir would result in more truncated nucleic acid that would not contain this packaging signal. Further, a nucleoside analogue, such as remdesivir, could also interrupt secondary structure of this packaging signal. Either of these possibilities would likely lead to more aberrant packaging of CoVs. Additional avenues of investigation may include examining recombination and defective genomes after nucleoside analogue treatment using NGS approaches since these species may also be generated and are more likely to be packaged in the absence of a functioning packaging signal. One way these defective genomes could be generated is alteration of polymerase processivity by a nucleoside analogue. If a polymerase falls off and reanneals more readily, this may increase recombination (Simon-Loriere and Holmes, 2011). This would likely occur through increased template switching. NTP availability, which could be altered in the presence of these compounds, has been shown to affect template switching that occurs to generate recombinants (Kim and Kao, 2001). In addition, previous studies in HIV have demonstrated increased template-switching in the presence of the nucleoside inhibitor AZT (Nikolenko et al., 2005), and initial NGS studies described here have revealed a change in genome coverage in the absence of poly(A) selection, which may further support this hypothesis. Interestingly, previous studies with CoVs have identified defective genomes that contain the 5' and 3' genomic ends that are necessary for their replication (Yang and Leibowitz, 2015). However, coverage by Bowtie2 is increasingly variable only without poly(A) selection,

suggesting that defective RNAs that do not contain the poly(A) tail may be generated in the presence of these nucleoside analogues. Together, future studies to address these questions may elucidate necessary elements for CoV packaging and the importance of genomic ends in CoV recombination, among other aspects of CoV replication.

Nucleoside analogue combination treatments to prevent and control resistance emergence

Traditionally, antiviral combination therapies have been designed to inhibit multiple independent targets. However, if resistance to these targets is independent, it seems that, given enough evolutionary time, a multi-drug resistant virus would emerge. But if resistance is not independent, for instance when compounds inhibit the same target differently, resistance to multiple compounds would be more difficult to achieve (Deval et al., 2016; Mangel et al., 2001). Given the lack of cross-resistance between the nucleoside analogues I have tested here, resistance to both of these compounds simultaneously could be difficult to achieve. However, passaging virus in both compounds simultaneously or passaging virus resistant to one compound in the other may provide more direct insight on this possibility. In addition, I demonstrate that mutations that arise in the presence of NHC and remdesivir treatment are not more fit than WT, suggesting that combining them may result in a virus that is even less fit. Thus, these results suggest that combining these compounds could form an enticing antiviral strategy. Additionally, one of the NHC resistance mutations identified in VEEV may increase sensitivity to RBV, suggesting that different combination regimens may be successful against multiple viruses due to lack of cross-resistance (Urakova et al., 2017). However, more work is necessary to further investigate cross-resistance and nucleoside analogue combinations before this approach could become reality. Assessing cross-resistance to related and unrelated nucleoside analogues will

lead to a better understanding of specific nucleoside analogue modifications that the RdRp recognizes and will inform nucleoside analogue compatibility in combinations. Because this work did not address the stability of any of the resistance phenotypes in the absence of compound, future studies may focus on resistance emergence and stability in the presence of single or combination regimens to WT virus. Overall, these studies will advance our understanding of whether combinations of compounds may prove useful in treating CoVs or other emerging infections.

Concluding remarks

Within approximately 24 hours, an increasingly global travel network could transport an unknown emerging disease anywhere in the world. This idea will continue to alarm humans for as long as there are limited countermeasures to address these events. Thus far, the most promising strategy to prevent this prospect from continuing to become reality is to have broad-spectrum antiviral cocktails on hand to inhibit a wide range of viruses. This approach could help circumvent the necessity of determining the precise identity of the viral culprit and may be refined as we advance our knowledge of viral biology. This dissertation work describes my contributions toward these efforts. I begin to define the antiviral activity of two broad-spectrum compounds in CoVs, a group of viruses that has continually been among the emerging viral threats. I also begin to address antiviral complementarity of these compounds to further the discussion on combination treatments. Given the distinct spectrum of these compounds, combining these drugs could expand the range of emerging viral infections we could combat with a single antiviral regimen. While the studies described here have contributed to our knowledge about these broad-spectrum antivirals, I hope they also provide insights into CoV

replication that can clarify our approach to treat and prevent CoV disease. We have been ill-equipped to address emerging infections of the past. There is still much work to be done, but I hope that this work will bring us one step closer to effectively combating the emerging viruses, especially CoVs, of the future.

**APPENDIX A: CORONAVIRUS SUSCEPTIBILITY TO THE ANTIVIRAL
REMDESIVIR (GS-5734) IS MEDIATED BY THE VIRAL POLYMERASE AND THE
PROOFREADING EXORIBONUCLEASE**



Coronavirus Susceptibility to the Antiviral Remdesivir (GS-5734) Is Mediated by the Viral Polymerase and the Proofreading Exoribonuclease

Maria L. Agostini,^a Erica L. Andres,^b Amy C. Sims,^c Rachel L. Graham,^c Timothy P. Sheahan,^c Xiaotao Lu,^b Everett Clinton Smith,^{b,d} James Brett Case,^a Joy Y. Feng,^e Robert Jordan,^e Adrian S. Ray,^e Tomas Cihlar,^e Dustin Siegel,^e Richard L. Mackman,^e Michael O. Clarke,^e Ralph S. Baric,^c Mark R. Denison^{a,b}

^aDepartment of Pathology, Microbiology, and Immunology, Vanderbilt University Medical Center, Nashville, Tennessee, USA

^bDepartment of Pediatrics, Vanderbilt University Medical Center, Nashville, Tennessee, USA

^cDepartment of Epidemiology, University of North Carolina at Chapel Hill, Chapel Hill, North Carolina, USA

^dDepartment of Biology, the University of the South, Sewanee, Tennessee, USA

^eGilead Sciences, Inc., Foster City, California, USA

ABSTRACT Emerging coronaviruses (CoVs) cause severe disease in humans, but no approved therapeutics are available. The CoV nsp14 exoribonuclease (ExoN) has complicated development of antiviral nucleosides due to its proofreading activity. We recently reported that the nucleoside analogue GS-5734 (remdesivir) potently inhibits human and zoonotic CoVs *in vitro* and in a severe acute respiratory syndrome coronavirus (SARS-CoV) mouse model. However, studies with GS-5734 have not reported resistance associated with GS-5734, nor do we understand the action of GS-5734 in wild-type (WT) proofreading CoVs. Here, we show that GS-5734 inhibits murine hepatitis virus (MHV) with similar 50% effective concentration values (EC_{50}) as SARS-CoV and Middle East respiratory syndrome coronavirus (MERS-CoV). Passage of WT MHV in the presence of the GS-5734 parent nucleoside selected two mutations in the nsp12 polymerase at residues conserved across all CoVs that conferred up to 5.6-fold resistance to GS-5734, as determined by EC_{50} . The resistant viruses were unable to compete with WT in direct coinfection passage in the absence of GS-5734. Introduction of the MHV resistance mutations into SARS-CoV resulted in the same *in vitro* resistance phenotype and attenuated SARS-CoV pathogenesis in a mouse model. Finally, we demonstrate that an MHV mutant lacking ExoN proofreading was significantly more sensitive to GS-5734. Combined, the results indicate that GS-5734 interferes with the nsp12 polymerase even in the setting of intact ExoN proofreading activity and that resistance can be overcome with increased, nontoxic concentrations of GS-5734, further supporting the development of GS-5734 as a broad-spectrum therapeutic to protect against contemporary and emerging CoVs.

IMPORTANCE Coronaviruses (CoVs) cause severe human infections, but there are no approved antivirals to treat these infections. Development of nucleoside-based therapeutics for CoV infections has been hampered by the presence of a proofreading exoribonuclease. Here, we expand the known efficacy of the nucleotide prodrug remdesivir (GS-5734) to include a group β-2a CoV. Further, GS-5734 potently inhibits CoVs with intact proofreading. Following selection with the GS-5734 parent nucleoside, 2 amino acid substitutions in the nsp12 polymerase at residues that are identical across CoVs provide low-level resistance to GS-5734. The resistance mutations decrease viral fitness of MHV *in vitro* and attenuate pathogenesis in a SARS-CoV animal model of infection. Together, these studies define the target of GS-5734 activity and demonstrate that resistance is difficult to select, only partial, and impairs fitness

Received 29 January 2018 Accepted 1 February 2018 Published 6 March 2018
Citation Agostini ML, Andres EL, Sims AC, Graham RL, Sheahan TP, Lu X, Smith EC, Case JB, Feng JY, Jordan R, Ray AS, Cihlar T, Siegel D, Mackman RL, Clarke MO, Baric RS, Denison MR. 2018. Coronavirus susceptibility to the antiviral remdesivir (GS-5734) is mediated by the viral polymerase and the proofreading exoribonuclease. *mBio* 9:e00221-18. <https://doi.org/10.1128/mBio.00221-18>.

Editor Kanta Subbarao, NIAID, NIH

Copyright © 2018 Agostini et al. This is an open-access article distributed under the terms of the Creative Commons Attribution 4.0 International license.

Address correspondence to Ralph S. Baric, rbaric@email.unc.edu, or Mark R. Denison, mark.denison@vanderbilt.edu.

M.L.A. and E.L.A. contributed equally to this article.

This article is a direct contribution from a Fellow of the American Academy of Microbiology. Solicited external reviewers: Tom Gallagher, Loyola University Medical Center; Luis Enjuanes, Centro Nacional de Biotecnología, CNB-CSIC.

and virulence of MHV and SARS-CoV, supporting further development of GS-5734 as a potential effective pan-CoV antiviral.

KEYWORDS RNA polymerases, SARS-CoV, antiviral agents, antiviral resistance, coronavirus, nucleoside analogs, pandemic

Coronaviruses (CoVs) are positive-sense, single-stranded RNA viruses that infect a wide range of animal hosts. In humans, CoVs were recognized as typically causing colds and pneumonia until the emergence of severe acute respiratory syndrome coronavirus (SARS-CoV) in 2002 and Middle East respiratory syndrome coronavirus (MERS-CoV) in 2012 from zoonotic sources (1, 2). Although the SARS epidemic was controlled by public health measures within a year of its emergence, the virus spread to over 30 countries and was associated with a 10% mortality rate (3). Efforts to treat SARS patients with existing antivirals did not conclusively provide a clinical benefit and may have even worsened disease (4–7). MERS-CoV continues to circulate in the Middle East, with a case fatality rate approaching 40% (<http://www.who.int/emergencies/mers-cov/en/>). Currently, there are no FDA-approved antivirals or vaccines for the treatment and prevention of MERS-CoV infection. Supportive care and prevention of complications constitute the current standard of treatment for patients, emphasizing the need for direct-acting antivirals (8, 9). Furthermore, SARS- and MERS-like bat CoVs circulate in nature, can replicate efficiently in primary human airway cells, and use the same cellular receptors for entry as human CoVs (10–13). The imminent threat of human emergence underscores the need for broadly active antivirals to combat any CoV that may emerge.

Nucleoside analogues commonly target viral replication, particularly the viral DNA or RNA polymerase (14), and have succeeded clinically in treating multiple viral infections (15). However, identification and development of antiviral nucleosides against coronaviruses have been hampered by the presence of the unique CoV proofreading 3'-5' exoribonuclease (ExoN) (16–18). While nucleoside analogues such as BCX4430 inhibit CoVs (19), several previously tested nucleoside analogues have been incapable of potently inhibiting CoV replication, and others have demonstrated poor selectivity indexes (20, 21). We have shown that CoV resistance to the mutagens 5-fluorouracil (5-FU) and ribavirin (RBV) *in vitro* is attributed to their removal by the proofreading ExoN (22), supporting the hypothesis that an effective nucleoside analogue must evade proofreading to successfully interfere with CoV RNA synthesis.

We recently reported that GS-5734, the monophosphoramidate prodrug of the C-adenosine nucleoside analogue GS-441524 (Fig. 1A), inhibits SARS-CoV, MERS-CoV, and bat CoV strains that are capable of replicating in primary human airway epithelial cells and mediate entry using human CoV receptors (23–25). GS-5734 also demonstrates both prophylactic and therapeutic efficacy against SARS-CoV disease in a mouse model (23). However, the study was not designed to define, nor did it report, potential pathways and implications of resistance for virus fitness and virulence. Further, studies demonstrating the efficacy of GS-5734 against CoVs and other viruses, including Ebolavirus, have not described resistance mutations. Using the model β-coronavirus murine hepatitis virus (MHV), we here demonstrate that GS-5734 dramatically inhibits viral replication and viral RNA synthesis in wild-type (WT) virus, while an nsp14 ExoN(–) mutant lacking proofreading demonstrates increased susceptibility to GS-5734. Passage of WT MHV with the GS-5734 parent nucleoside GS-441524 resulted in phenotypic resistance associated with two nonsynonymous mutations in the predicted fingers domain of the nsp12 RNA-dependent RNA polymerase (F476L and V553L). The engineered mutations in the MHV cloned background closely recapitulated the partial resistance phenotype and restored RNA levels in the presence of GS-5734. However, resistant viruses could not compete with WT MHV during *in vitro* coinfection passage in the absence of GS-5734. Introduction of homologous substitutions in mouse-adapted SARS-CoV conferred resistance to GS-5734 similar to that seen in MHV but also attenuated *in vivo* pathogenesis of SARS-CoV in a mouse model. Overall, our results are consistent with an RNA-dependent RNA polymerase (RdRp)-mediated mechanism of

Downloaded from <http://mbio.asm.org/> on July 25, 2019 by guest

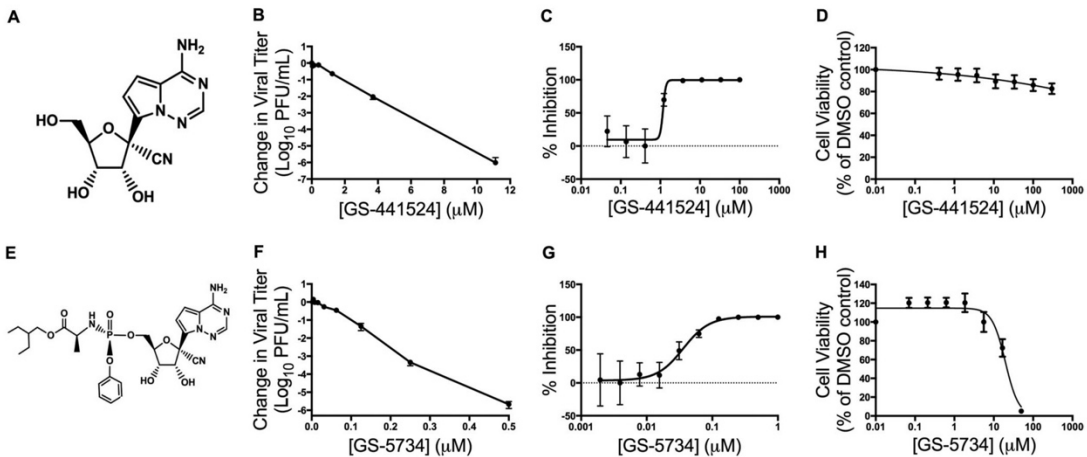


FIG 1 GS-441524 and GS-5734 inhibit MHV with minimal cytotoxicity. (A) GS-441524 is a 1'-cyano 4-aza-7,9-dideazaadenosine C-adenosine nucleoside analogue. (B) Change in viral titer of MHV compared to vehicle control after treatment with GS-441524. The data represent the results from 2 independent experiments, each with 3 replicates. Error bars represent standard error of the mean (SEM). (C) Viral titer data from panel B presented as the percentage of uninhibited control. The EC₅₀ of GS-441524 was calculated to be 1.1 μM. (D) Cell viability normalized to the vehicle control after treatment with GS-441524. The data represent the results from 3 independent experiments, each with 3 replicates. Error bars represent SEM. (E) GS-5734 is a monophosphoramidate prodrug of GS-441524. (F) Change in viral titer of MHV compared to vehicle control after treatment with GS-5734. The data represent the results from 4 independent experiments, each with 3 replicates. Error bars represent SEM. (G) Viral titer data from panel F presented as the percentage of uninhibited control. The EC₅₀ of GS-5734 was calculated to be 0.03 μM. (H) Cell viability normalized to vehicle control after treatment with GS-5734. The data represent the results from 3 independent experiments, each with 3 replicates. Error bars represent SEM.

potent CoV inhibition by GS-5734, even in the setting of intact ExoN-mediated proofreading.

RESULTS

GS-441524 and GS-5734 inhibit MHV replication. GS-441524, a 1'-cyano 4-aza-7,9-dideazaadenosine C-nucleoside (Fig. 1A), has been shown to inhibit multiple virus families *in vitro* (24, 26). To determine if GS-441524 inhibited the model β-2a CoV, murine hepatitis virus (MHV), we infected delayed brain tumor (DBT) cells with MHV and treated them with increasing concentrations of drug. We observed a dose-dependent reduction in viral titer with up to a 6-log₁₀ decrease at 11.1 μM GS-441524 (Fig. 1B). The half-maximum effective concentration (EC₅₀) value resulting from GS-441524 treatment was 1.1 μM (Fig. 1C). We observed minimal detectable cytotoxicity within the tested range, with the concentration resulting in 50% cytotoxicity (CC₅₀) >300 μM (Fig. 1D). This resulted in a selectivity index (CC₅₀/EC₅₀) of >250. Having demonstrated the inhibition of MHV by GS-441524, we next tested its monophosphoramidate prodrug GS-5734 (Fig. 1E). Treatment with increasing concentrations of GS-5734 resulted in up to a 6-log₁₀ decrease in viral titer, and virus was undetectable by plaque assay at concentrations above 0.5 μM GS-5734 (Fig. 1F). GS-5734 inhibited MHV more potently than GS-441524, with a GS-5734 EC₅₀ of 0.03 μM (Fig. 1G), consistent with higher cellular permeability and more efficient metabolism of the prodrug into the active nucleoside triphosphate by bypassing the rate-limiting first phosphorylation step (27, 28). We also observed minimal cytotoxicity at concentrations required for antiviral activity of GS-5734, in line with previously reported extensive cytotoxicity studies in relevant human cell types (27), with a CC₅₀ value of 39 μM (Fig. 1H), resulting in a selectivity index of >1,000. These results expand the breadth of GS-441524 and GS-5734 inhibition of CoVs to include the β-2a model CoV MHV.

GS-441524 and GS-5734 potently inhibit SARS-CoV and MERS-CoV in HAE cells. Primary human airway epithelial cell (HAE) cultures are among the most clinically relevant *in vitro* models of the lung, recapitulating the cellular complexity and physi-

Downloaded from <http://mbio.asm.org/> on July 25, 2019 by guest

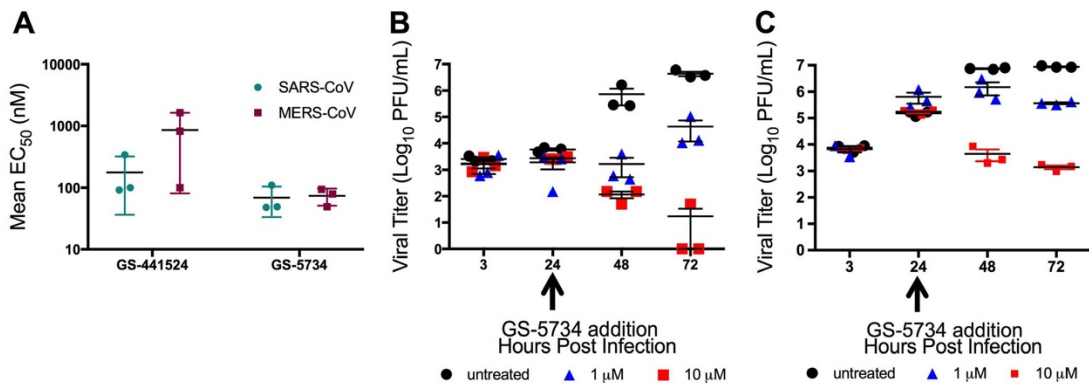


FIG 2 Antiviral activity of GS-441524 and GS-5734 and modeled therapeutic efficacy of GS-5734 against SARS-CoV and MERS-CoV in HAE cultures. (A) Mean EC_{50} values of SARS-CoV and MERS-CoV-infected HAE cultures from three different patient isolates treated with GS-441524 or GS-5734. (B) Viral titers of SARS-CoV-infected HAE cultures when treated with various doses of GS-5734 24 h postinfection. (C) Viral titers of MERS-CoV-infected HAE cultures when treated with various doses of GS-5734 24 h postinfection.

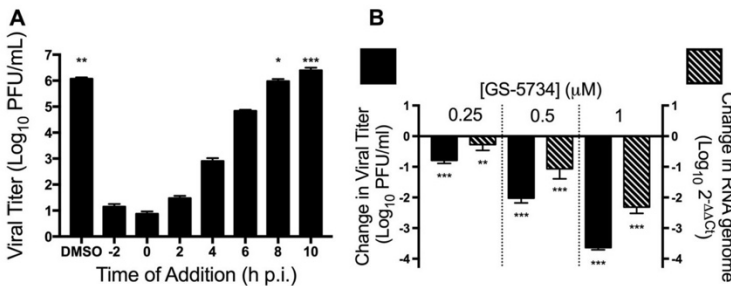
ology of the epithelium in the human conducting airway (29). Previous results have demonstrated that GS-5734 inhibits the viral titer of multiple CoVs in this model, but did not assess the potency or the effect of delaying treatment with the compound. Thus, we determined the EC_{50} values after treatment with GS-441524 and GS-5734 in SARS-CoV- and MERS-CoV-infected HAE cultures. Mean EC_{50} values for both viruses were approximately 0.86 μ M for GS-441524 and 0.074 μ M for GS-5734 (Fig. 2A). Further, delaying addition of GS-5734 until 24 hours (h) postinfection resulted in decreased viral titer in HAE cultures for both SARS-CoV (Fig. 2B) and MERS-CoV (Fig. 2C) at 48 and 72 h postinfection. No measurable cellular toxicity was observed in HAE cultures for either compound (Table 1). These results demonstrate a similar high potency of GS-5734 across divergent CoVs, supporting the utility of the model MHV system to study GS-5734 inhibition and resistance.

GS-5734 acts at early times postinfection to decrease viral RNA levels. The predicted mechanism of action of GS-5734 is through incorporation of the active triphosphate into viral RNA (27). We therefore tested the hypothesis that GS-5734 would inhibit CoVs at early steps in replication by inhibiting viral RNA synthesis. To determine which stage in the viral replication cycle GS-5734 inhibited CoVs, we infected cells with MHV at a multiplicity of infection (MOI) of 1 PFU/cell, which with MHV results in a single-cycle infection, and treated them with 2 μ M GS-5734 at 2-h intervals from 2 h preinfection to 10 h postinfection. We observed maximal inhibition when GS-5734 was added between 2 h preinfection and 2 h postinfection. Less inhibition was detected when GS-5734 was added between 4 and 6 h postinfection, and no inhibition was observed when GS-5734 was added after 8 h postinfection (Fig. 3A). These results demonstrate that GS-5734 inhibits CoVs at early steps during infection. Because viral RNA is synthesized early in infection and GS-5734 is implicated in inhibiting viral RNA synthesis (25, 30, 31), we next determined the cellular level of viral RNA by real-time quantitative PCR (qPCR) after treatment with GS-5734. Treatment with increasing

TABLE 1 EC_{50} and CC_{50} values of GS-441524 or GS-5734 in MERS-CoV- or SARS-CoV-infected HAE cultures^a

Virus	GS-441524		GS-5734	
	EC_{50} (μ M)	CC_{50} (μ M)	EC_{50} (μ M)	CC_{50} (μ M)
MERS	0.86 ± 0.78	>100	0.074 ± 0.023	>10
SARS	0.18 ± 0.14	>100	0.069 ± 0.036	>10

^aValues represent the average (mean ± SD) from HAE cultures from at least three donors.



concentrations of GS-5734 resulted in decreased viral RNA levels that correlated with the decrease in titer we observed (Fig. 3B). These results suggest that GS-5734 inhibits CoVs early after infection by interfering with viral RNA replication.

Viruses lacking ExoN-mediated proofreading are more sensitive to treatment with GS-5734. We have shown that the profound resistance of CoVs to the nucleoside and base analogues RBV and 5-FU is due to the proofreading ExoN in nsp14, as engineered ExoN(−) mutant MHV and SARS-CoV are profoundly more sensitive to these compounds (22). We therefore compared the sensitivity of WT and ExoN(−) MHV to GS-5734. ExoN(−) MHV demonstrated up to a 100-fold greater reduction in viral titer at 0.25 μ M GS-5734 compared to WT virus (Fig. 4A), and the calculated EC₅₀ for ExoN(−) virus in this experiment was 0.019 μ M, a 4.5-fold decrease compared to the WT EC₅₀ of 0.087 μ M (Fig. 4B). This increased sensitivity of ExoN(−) virus to GS-5734 is similar to that of other nucleoside analogues and suggests that GS-5734 is incorporated into viral RNA and can be removed by ExoN. However, the results also suggest there is a fundamentally different relationship of GS-5734 with the CoV replicase and/or template RNA compared with other nucleosides such as ribavirin or 5-fluorouracil, since GS-5734 potently inhibits CoVs with intact proofreading (22).

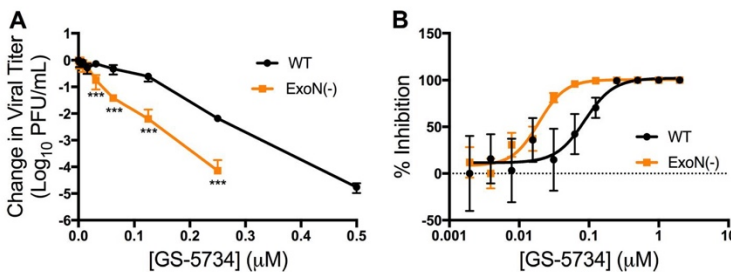


FIG 4 Viruses lacking ExoN-mediated proofreading are more sensitive to GS-5734 inhibition. (A) Change in viral titer of WT and ExoN(−) viruses normalized to vehicle control after treatment with GS-5734. The data represent the results from 2 independent experiments, each with 3 replicates. Error bars represent SEM. Statistical significance compared to WT at each concentration was determined by *t* test using the Holm-Sidak method to correct for multiple comparisons and is denoted by asterisks: ***, $P < 0.001$. (B) Viral titer reduction from panel A represented as percentage of vehicle control, resulting in a WT EC₅₀ value of 0.087 μ M and an ExoN(−) EC₅₀ of 0.019 μ M.

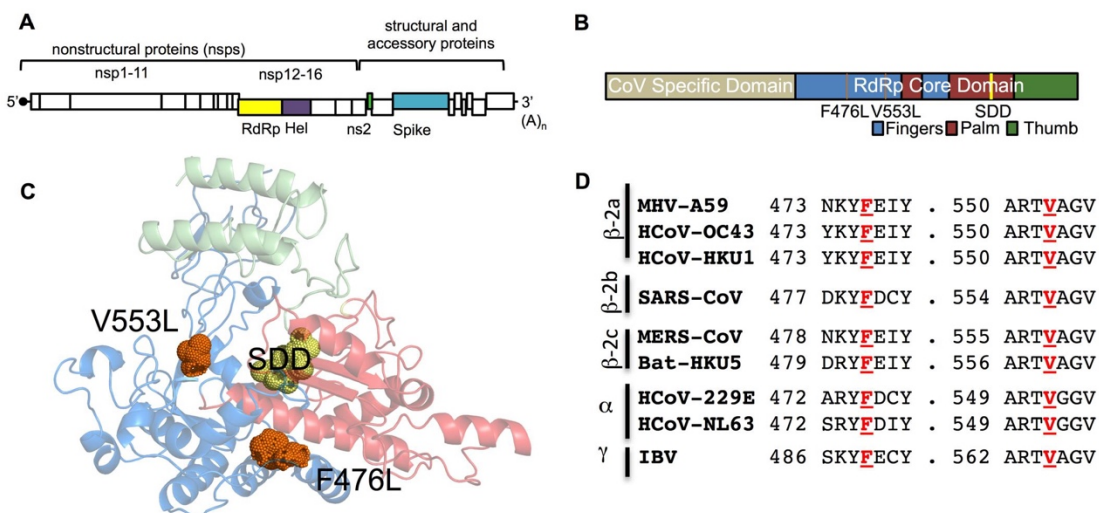


FIG 5 Two mutations in the predicted fingers domain of the nsp12 RdRp, F476L and V553L, arose after 23 passages in the presence of GS-441524, and these residues are completely conserved across CoVs. (A) Schematic of the MHV genome displaying proteins with mutations identified after passage with GS-441524. The nsp12 RdRp is shown in yellow, nsp13-helicase in purple, ns2 in green, and spike in blue. (B) Linear schematic of nsp12 showing the locations of F476L and V553L within the predicted fingers of the RdRp core domain. (C) The previously described (32) Phyre2 model of the MHV RdRp core domain was used to map the predicted locations of the F476L and V553L residues, shown here in orange. The SDD active site residues are shown in yellow, the palm in red, the fingers in blue, and the thumb in green. (D) Amino acid conservation of F476 and V553 residues across CoVs demonstrating that both of these residues are completely conserved.

Two mutations in the RdRp mediate partial resistance and restoration of RNA levels in the presence of GS-5734. We next sought to identify the target(s) of GS-5734 inhibition. Three lineages of WT MHV were serially passaged in the presence of increasing concentrations of GS-441524. GS-441524 was chosen for passage selection because GS-5734 and GS-441524 are both metabolized to the same active triphosphate metabolite (27), but GS-441524 provided a larger working range of concentrations. Two lineages did not demonstrate an increase in viral cytopathic effect (CPE) over passage and were lost after passages 17 (p17) and p20. After 23 passages, we observed an increased ability of one passage lineage to replicate in the presence of GS-441524 as determined by increased viral CPE. Full-genome sequencing of p23 viral RNA revealed 6 nonsynonymous mutations in four viral protein-coding regions (Fig. 5A): the nsp13 helicase (A335V), the ns2 2',5' phosphodiesterase (Q67H), the spike glycoprotein (A34V and I924T), and the nsp12 RdRp (F476L and V553L) (Fig. 5B). Molecular modeling of the MHV RdRp predicts that both the F476 and V553 residues reside within the predicted fingers domain of the conserved right-hand structure of the RdRp (Fig. 5C) (32, 33). In addition, both the F476 and V553 residues are identical across sequenced α , β , and γ -CoVs (Fig. 5D). Based on the known role of polymerase mutations in resistance to nucleoside analogues for other viruses (34–37) and the previous work describing inhibition of the respiratory syncytial virus (RSV) polymerase by GS-5734 (27), we first engineered and recovered recombinant MHV containing the F476L and V553L RdRp mutations to determine if they were necessary and sufficient for the observed resistance phenotype of the p23 virus population. Recombinant MHV containing either F476L or V553L individually was less sensitive to GS-5734 than WT MHV, but still more sensitive than the p23 virus population across a broad range of concentrations. In contrast, MHV encoding both F476L and V553L demonstrated a resistance pattern comparable to p23 (Fig. 6A). Neither the p23 virus population nor any of the recombinant viruses were completely resistant to GS-5734; all viruses remained sensitive to higher but nontoxic concentrations of GS-5734. Compared to WT MHV, the F476L virus

Downloaded from <http://mbio.asm.org/> on July 25, 2019 by guest

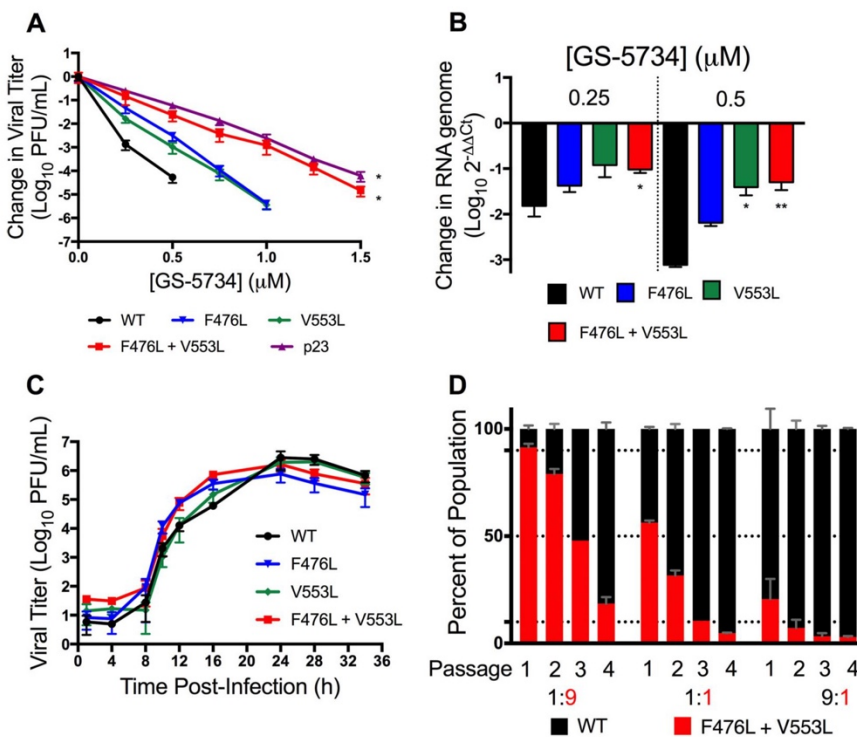


FIG 6 The F476L and V553L mutations mediate resistance to GS-5734 and are associated with a fitness defect. (A) Change in viral titer of WT, F476L, V553L, F476L + V553L, and p23 viruses normalized to the vehicle control after treatment with GS-5734. The data represent 2 independent experiments, each with 3 replicates. Error bars represent SEM. Statistical significance compared to WT was determined by Kolmogorov-Smirnov test and is denoted by asterisks: *, $P < 0.05$. (B) The change in genomic RNA levels of WT, F476L, V553L, and F476L + V553L MHV normalized to vehicle control after treatment with GS-5734. The data represent the results from 2 independent experiments, each with 3 replicates. Error bars represent SEM. Statistical significance compared to WT at each concentration was determined by one-way ANOVA with Dunnett's *post hoc* test for multiple comparisons and is denoted by asterisks: *, $P < 0.05$; **, $P < 0.01$. (C) Multi-cycle replication kinetics of WT, F476L, V553L, or F476L + V553L MHV. The data represent the results from 2 independent experiments, each with 3 replicates. Error bars represent SEM. (D) Coinfection competition assay of WT and F476L V553L MHV at the indicated ratios. The percentage of the population of each mutation was assessed after four successive passages. The data are representative of 2 independent experiments each with 2 replicates. Error bars represent standard deviation (SD).

showed 2.4-fold resistance to GS-5734, and V553L virus demonstrated 5-fold resistance to GS-5734, while combined mutations mediated 5.6-fold resistance to GS-5734 based on EC₅₀ values (Table 2). Because GS-5734 decreases viral RNA levels, we next tested if resistance mutations restored RNA synthesis. We observed that RdRp resistance mutations partially restored RNA levels in the presence of GS-5734 and that the degree of

Downloaded from <http://mbio.asm.org/> on July 25, 2019 by guest

TABLE 2 F476L and V553L mutations confer up to 5.6-fold resistance to GS-5734 in MHV^a

Virus	EC ₅₀ (μM)	Fold resistance
WT	0.024 ± 0.011	1
F476L	0.057 ± 0.040	2.4
V553L	0.12 ± 0.06	5.0
F476L + V553L	0.13 ± 0.06	5.6

^aMean EC₅₀ values ± SD and fold resistance of GS-5734-resistant viruses were calculated using viral titer data following infection of DBT cells with the indicated virus at an MOI of 0.01 PFU/cell and treatment with increasing concentrations of GS-5734. Fold resistance was calculated as EC₅₀ of mutant/EC₅₀ of WT. The data represent the results from 3 independent experiments, each with 3 replicates.

restoration of RNA levels correlated with their fold resistance to GS-5734 (Fig. 6B). Together, these results are consistent with a mechanism of action of GS-5734 primarily targeting RdRp-mediated RNA synthesis.

GS-5734 resistance mutations impair competitive fitness of MHV. To assess the effect of GS-5734 resistance on viral fitness, we first determined the replication capacity of recombinant MHV carrying the F476L, V553L, and F476L + V553L mutations. Each of these viruses replicated similarly to WT MHV, both in replication kinetics and in observed peak titer (Fig. 6C). We next tested the competitive fitness of F476L + V553L MHV compared to WT MHV during coinfection over multiple passages. Murine DBT cells were coinfecting with WT MHV and F476L + V553L MHV at WT/mutant ratios of 1:1, 1:9, or 9:1 in the absence of GS-5734, and infected culture supernatants were serially passaged 3 times to fresh cell monolayers. By passage 2, F476L + V553L MHV was outcompeted by WT MHV in the population at every input ratio (Fig. 6D), demonstrating a competitive fitness cost of the F476L + V553L mutations in the absence of GS-5734. This competitive fitness cost further suggests that GS-5734 resistance mutations will not persist in the absence of treatment.

Mutations identified in GS-5734-resistant MHV also confer resistance in SARS-CoV. Given the complete conservation of the F476 and V553 residues across CoVs, we next tested whether substitutions at the homologous SARS-CoV residues (F480L and V557L) could confer resistance to GS-5734. We recovered SARS-CoV carrying the homologous F480L and V557L substitutions and tested recovered mutant viruses for resistance to GS-5734 in Calu-3 2B4 cells. WT SARS-CoV demonstrated dose-dependent inhibition by GS-5734, with an EC₅₀ of 0.01 μM (Fig. 7A). The F480L + V557L recombinant virus was inhibited by GS-5734, with an EC₅₀ value of 0.06 μM, representing a 6-fold resistance to GS-5734 (Fig. 7B), nearly identical to the fold resistance of F476L + V553L MHV. These results support the conclusion that the conserved residues across divergent CoVs reflect conserved functions impaired by GS-5734, potentially implying common pathways to resistance across CoVs.

GS-5734-resistant SARS-CoV is attenuated *in vivo*. To gain insight into the pathogenic potential of GS-5734-resistant viruses, we directly compared WT SARS-CoV and F480L V557L SARS-CoV following non-lethal high-dose (10⁴ PFU) and low-dose (10³ PFU) inoculation in a well-characterized mouse model of SARS-CoV pathogenesis with disease reminiscent of that observed in humans (38). Mice infected with a high dose of F480L V557L SARS-CoV lost significantly less weight ($P < 0.05$) than WT SARS-CoV-infected mice (Fig. 7C). At 2 days postinfection, mouse lung viral titers were similar between WT and F480L + V557L SARS-CoV, but by 4 days postinfection, lung viral titers were significantly reduced ($P < 0.05$) in mice infected with F480L + V557L SARS-CoV (Fig. 7D). Together, these data demonstrate that GS-5734-resistant SARS-CoV is attenuated in its ability to cause disease and replicates less efficiently than WT virus in robust mouse models of human SARS-CoV disease.

DISCUSSION

Broadly active antivirals are needed to treat contemporary human CoV infections, including endemic MERS-CoV in the Middle East and potential future zoonotic CoV epidemics. We recently demonstrated the prophylactic and therapeutic efficacy of GS-5734 (remdesivir) in a mouse model of SARS-CoV infection, as well as *in vitro* activity against multiple other human and zoonotic CoVs (23). In this study, we have defined the ability of GS-5734 to inhibit CoVs—expanded to include group 2a β-CoVs—in the setting of intact nsp14 proofreading activities. While ExoN(−) MHV is 4.5-fold more sensitive to GS-5734 treatment than WT MHV, the potent inhibition of WT CoVs suggests a unique mechanism of inhibition of CoV RNA synthesis that is able to circumvent ExoN surveillance and activity. Further, we report for the first time for any virus inhibited by GS-5734 that selection for partial resistance to GS-5734 required prolonged passage. Surprisingly, no resistance mutations were selected within ExoN, but rather two mutations of highly conserved residues in the RdRp reduced the sensitivity to GS-5734 to a level comparable to that of the passaged virus. Introduction

Downloaded from <http://mbio.asm.org/> on July 25, 2019 by guest

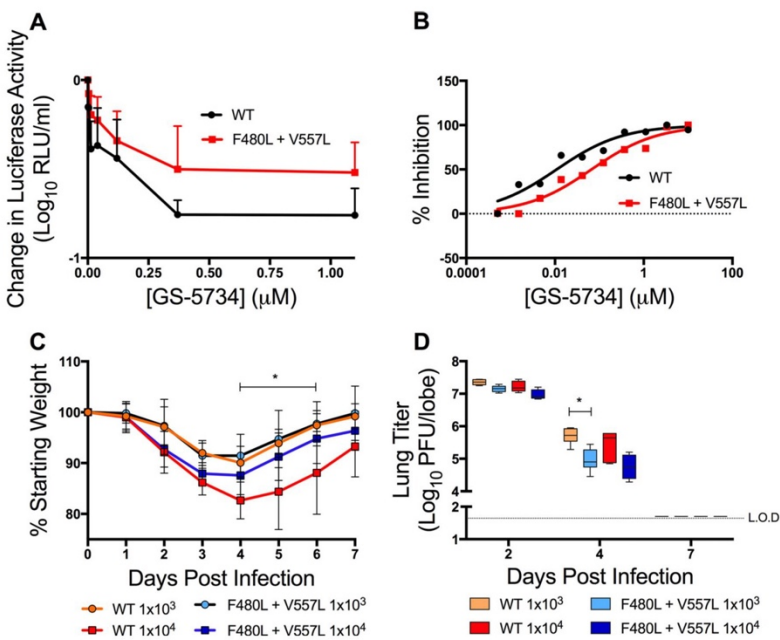


FIG 7 MHV resistance mutations confer resistance and are attenuated in SARS-CoV. (A) Change in luciferase activity normalized to vehicle control of WT or F480L + V557L SARS-CoV containing the NanoLUC reporter. The data are representative of the results from 2 independent experiments, each with 3 replicates. Error bars represent SEM. (B) Viral titer data from panel A presented as the percentage of vehicle control. This EC₅₀ value was calculated as 0.01 μ M for WT and 0.06 μ M for F480L + V557L virus, which represents a 6-fold increase in resistance. (C) Percent starting weight of BALB/c mice inoculated with WT or F480L + V557L SARS-CoV containing the NanoLUC reporter at 10³ or 10⁴ PFU. The data are representative of the results from 2 independent experiments, each with 10 to 12 animals per group. Error bars represent SEM. Statistical significance was determined by 2-way ANOVA and is denoted by asterisks: *, P < 0.05. (D) Lung titers from animals in panel C 2, 4, and 7 days postinfection. The data are representative of the results from 2 independent experiments, each with 3 animals per group. Error bars represent SEM. Statistical significance was determined by Wilcoxon test and is denoted by asterisks: *, P < 0.05.

of the homologous substitutions in SARS-CoV reproduced the fold resistance to GS-5734 observed in MHV, demonstrating the potential for common, family-wide drug resistance pathways in the RdRp.

Potential GS-5734 mechanism of action. Nucleoside analogues can have multiple mechanisms of action, including lethal mutagenesis, obligate or nonobligate chain termination, and perturbation of natural nucleotide triphosphate pools via inhibition of nucleotide biosynthesis (14, 39–44). GS-5734 has been reported to cause premature termination of nascent RNA transcripts by the purified RSV polymerase, but the mechanism of inhibition of other viral polymerases has not been fully explored (27). Our data demonstrate that GS-5734 acts early in infection and decreases RNA levels in a dose-dependent manner that parallels impairment of viral titer. Further, while GS-5734 is highly active against WT CoVs, it is 4.5-fold more active in MHV lacking the proof-reading activity of ExoN. Finally, GS-5734 is 3 to 30 times more active than GS-441524 in all of the CoVs we have tested (23). The result is consistent with the report that GS-5734 is metabolized more efficiently than GS-441524 into the triphosphate metabolite (27). All of the above findings support a mechanism involving incorporation of GS-5734 into nascent CoV RNA, but do not discriminate between chain termination and incorporation mutagenesis. In fact, other nucleoside analogues have multiple proposed mechanisms of virus inhibition, including favipiravir in influenza virus and RBV in HCV (41–43). Future studies using deep sequencing and biochemical approaches will allow us to precisely define the GS-5734 mechanism(s) of action against CoVs.

Downloaded from <http://mbio.asm.org/> on July 25, 2019 by guest

**APPENDIX B: THE SMALL MOLECULE ANTIVIRAL β -D- N^4 -HYDROXYCYTIDINE
INHIBITS A PROOFREADING-INTACT CORONAVIRUS WITH A HIGH GENETIC
BARRIER TO RESISTANCE**

- 1 Small molecule antiviral β -D- N^4 -hydroxycytidine inhibits a proofreading-intact
2 coronavirus with a high genetic barrier to resistance
3 Maria L. Agostini¹, Andrea J. Pruijssers², James D. Chappell², Jennifer Gribble¹, Xiaotao Lu²,
4 Erica L. Andres², Gregory R. Bluemling³, Mark A. Lockwood³, Timothy P. Sheahan⁴, Amy C.
5 Sims⁴, Michael G. Natchus³, Manohar Saindane³, Alexander A. Kolykhalov³, George R.
6 Painter^{3,5}, Ralph S. Baric⁴, Mark R. Denison^{1,2}
- 7
- 8 ¹Department of Pathology, Microbiology, and Immunology , Vanderbilt University School of
9 Medicine, Nashville, TN, ² Department of Pediatrics, Vanderbilt University School of Medicine,
10 Nashville, TN, ³Emory Institute for Drug Development, Emory University, Atlanta, GA,
11 ⁴Department of Epidemiology, University of North Carolina at Chapel Hill, Chapel Hill, NC
12 ⁵Department of Pharmacology and Chemical Biology, Emory University School of Medicine,
13 Atlanta, GA
- 14
- 15 *Corresponding author: Mark R. Denison
- 16 E-mail: mark.denison@vumc.org
- 17
- 18
- 19 Running title: Coronavirus inhibition by NHC
- 20 Keywords: coronavirus, nucleoside analogue, RdRp, RNA-dependent RNA polymerase, SARS-
21 CoV, MERS-CoV, pandemic, antiviral resistance

ABSTRACT

Coronaviruses (CoVs) have emerged from animal reservoirs to cause severe and lethal disease in humans, but there are currently no FDA approved antivirals to treat these infections. One class of antiviral compounds, nucleoside analogues, mimics naturally occurring nucleosides to inhibit viral replication. While these compounds have been successful therapeutics for several viral infections, mutagenic nucleoside analogues, such as ribavirin and 5-fluorouracil, have been ineffective at inhibiting CoVs. This has been attributed to the proofreading activity of the viral 3'-5' exoribonuclease (ExoN). β -D- N^4 -hydroxycytidine (NHC, EIDD-1931; Emory Institute for Drug Development) has recently been reported to inhibit multiple viruses. Here, we demonstrate that NHC inhibits both murine hepatitis virus (MHV) ($EC_{50}=0.17 \mu M$) and Middle East respiratory syndrome CoV (MERS-CoV) ($EC_{50}=0.56 \mu M$) with minimal cytotoxicity. NHC inhibited MHV lacking ExoN-proofreading activity similarly to WT MHV, suggesting an ability to evade or overcome ExoN activity. NHC inhibited MHV only when added early during infection, decreased viral specific infectivity, and increased the number and proportion of G:A and C:U transition mutations present after a single infection. Low-level NHC resistance was difficult to achieve and was associated with multiple transition mutations across the genome in both MHV and MERS-CoV. These results point toward a virus-mutagenic mechanism of NHC inhibition in CoVs and indicate a high genetic barrier to NHC resistance. Together, these data support further development of NHC for treatment of CoVs and suggest a novel mechanism of NHC interaction with the CoV replication complex that may shed light on critical aspects of replication.

43 **IMPORTANCE**

44 The emergence of coronaviruses (CoVs) into human populations from animal reservoirs has
45 demonstrated their epidemic capability, pandemic potential, and ability to cause severe disease.
46 However, no antivirals have been approved to treat these infections. Here, we demonstrate the
47 potent antiviral activity of a broad-spectrum ribonucleoside analogue, β -D- N^4 -hydroxycytidine
48 (NHC), against two divergent CoVs. Viral proofreading activity does not markedly impact
49 sensitivity to NHC inhibition, suggesting a novel interaction between a nucleoside analogue
50 inhibitor and the CoV replicase. Further, passage in the presence of NHC generates only low-
51 level resistance, likely due to the accumulation of multiple, potentially deleterious, transition
52 mutations. Together, these data support a mutagenic mechanism of inhibition by NHC and
53 further support the development of NHC for treatment of CoV infections.

54 INTRODUCTION

55 The emergence of severe acute respiratory syndrome (SARS) in 2002 and Middle East
56 respiratory syndrome (MERS) in 2012 has underscored the ability of coronaviruses (CoVs) to
57 cause lethal disease in humans (1, 2). MERS-CoV continues to infect humans in the Middle East
58 and four additional human CoVs (HCoVs), HCoV-229E, HCoV-NL63, HCoV-OC43, and
59 HCoV-HKU1, continue to circulate globally and cause respiratory disease (3-6). The continued
60 circulation of SARS- and MERS- like CoVs that can replicate efficiently in primary human
61 airway cells in bat populations further demonstrates the potential for CoVs to emerge and cause
62 severe disease in the future (7-10). While SARS-CoV and MERS-CoV outbreaks have been
63 controlled largely through public health measures (11-13), the potential for future outbreaks
64 highlights the need for safe and effective therapeutics to combat CoV infections. There are
65 currently no approved therapeutics or vaccines for any human CoV infection. Previous efforts to
66 treat CoV infections with existing antivirals did not conclusively benefit clinical outcome; thus,
67 the current standard of care remains mostly supportive (14-16) .

68 Several targets for direct-acting antivirals are being investigated to treat CoV infections
69 (17-19). Because the viral replication machinery performs an essential role in genome
70 replication, therapeutics approved to treat multiple different viral infections are aimed at this
71 target (20). Many approved antivirals are classified as nucleoside analogues, compounds that
72 mimic natural nucleosides to inhibit viral replication (21). Inhibition by nucleoside analogues
73 can be accomplished through a variety of mechanisms. Common mechanisms of action include
74 incorporation of the analogue by the viral polymerase to induce premature termination of strand

75 synthesis or loss of essential genetic information through mutagenesis (22-25). A previous study
76 reported that the nucleoside analogues ribavirin (RBV) and 5-fluorouracil (5-FU) did not
77 potently inhibit CoVs, and this finding was attributed to the proofreading capabilities of the viral
78 3'-5' exoribonuclease (ExoN) (26). Recent reports have demonstrated the inhibition of WT
79 CoVs by nucleoside analogues such as galidesivir (BCX4430) and remdesivir (GS-5734) (27-
80 29). While these compounds have shown efficacy against CoVs, administration of multiple
81 compounds simultaneously may be required to effectively treat CoV infections and control the
82 emergence of drug resistance, as has been demonstrated for other viral infections (30).

83 β -D- N^4 -hydroxycytidine (NHC) (EIDD-1931, Emory Institute for Drug Development), a
84 cytidine analogue, has recently been shown to inhibit multiple viruses, including chikungunya
85 virus, Venezuelan equine encephalitis virus, respiratory syncytial virus, hepatitis C virus,
86 norovirus, influenza A and B viruses, and Ebola virus (31-36). Previous reports have
87 demonstrated an increased introduction of transition mutations in viral genomes after treatment
88 as well as a high genetic barrier to resistance (31, 36). Antiviral activity of NHC has also been
89 reported against the human α -CoV HCoV-NL63, as well as the β -CoV SARS-CoV (38-40).
90 Neither NHC mechanism of action nor NHC resistance have been described for any CoVs to
91 date.

92 In this study, we investigated NHC inhibition and resistance in two divergent β -CoVs,
93 murine hepatitis virus (MHV) and MERS-CoV. We show that NHC potently inhibits WT MHV
94 and MERS-CoV with minimal cytotoxicity. We also demonstrate that MHV ExoN proofreading
95 activity has a limited but measurable effect on sensitivity to NHC. We observe an NHC
96 inhibition profile consistent with a mutagenic mechanism of action featuring an accumulation of
97 transition mutations, indicative of a high genetic barrier to resistance.

98 **RESULTS**

99 **NHC inhibits MHV and MERS-CoV replication with minimal cytotoxicity.**

100 NHC (Fig. 1) has potent broad-spectrum antiviral activity against many RNA viral families (31-
101 36). We first determined if NHC also inhibits CoV replication using a dose-response experiment
102 with two divergent β -CoVs: the model CoV, MHV, and the epidemically circulating zoonotic
103 CoV, MERS-CoV. NHC treatment resulted in a dose-dependent reduction in viral titer for MHV
104 (Fig. 2A) and MERS-CoV (Fig. 2B). This inhibition resulted in a 50% effective concentration
105 (EC_{50}) of 0.17 μ M for MHV (Fig. 2C) and 0.56 μ M for MERS-CoV (Fig. 2D). We detected
106 negligible changes in DBT-9 cell viability out to 200 μ M (Fig. 2E) and CC_{50} values above 10
107 μ M in Vero cells (Fig. 2F). The antiviral activity was not due to cytotoxicity, as the selectivity
108 index was >1000 for MHV and >20 for MERS-CoV. Together, these results confirm potent
109 inhibition of β -CoVs by NHC.

110

111 **NHC inhibition profile in CoVs is consistent with mutagenesis.**

112 To better understand the mechanism through which NHC inhibits CoV replication, we performed
113 a time-of-drug addition assay to determine at what point in the viral replication cycle NHC acts
114 (37). We added 16 μ M (~100x EC_{50} concentration) NHC at the indicated times pre- or post-
115 infection of cells with WT MHV at a MOI of 1 PFU/cell and quantified viral replication after a
116 single infectious cycle. Compared to the vehicle (DMSO) control, NHC significantly inhibited
117 MHV replication when added at or before six hours post-infection (Fig. 3A), suggesting that
118 NHC acts at early stages of the viral replication cycle. We next determined the effect of NHC on
119 MHV RNA levels and compared to effect on infectious viral titer. RNA levels were reduced by

120 approximately 10-fold at the highest tested concentration of NHC in both MHV-infected cell
121 monolayers (Fig. 3B) and supernatants (Fig. 3C). In contrast, viral titer was reduced up to 5,000-
122 fold at this concentration. We therefore calculated the ratio of infectious virus per viral RNA
123 genome copy number normalized to the untreated control (specific infectivity) after NHC
124 treatment and found that the specific infectivity of WT MHV was reduced in a dose-dependent
125 manner after treatment with increasing concentrations of NHC (Fig. 3D). Together, these data
126 are consistent with a mutagenic mechanism of NHC anti-CoV activity.

127

128 **NHC treatment increases transition mutations present across the MHV genome.**

129 To directly test the effect of NHC treatment on mutational burden, we treated WT MHV with
130 increasing concentrations of NHC and performed full-genome next-generation sequencing
131 (NGS) on viral populations released after a single round of infection. Our data demonstrate a
132 dose-dependent increase in mutations present at low frequencies (<5 % of viral population)
133 across the genome after treatment with increasing concentrations of NHC (Fig. 4A-C). Further
134 analysis of the types of mutations introduced by NHC revealed an increase in the total number of
135 transition mutations with increasing NHC concentrations (Fig. 4D-F). The relative proportion of
136 G:A and C:U transitions among all observed mutations was increased by 13-15% in the presence
137 of 2 μ M NHC and 36-40% in the presence of 4 μ M NHC compared to the vehicle control (Fig.
138 4G, H). Conversely, the relative proportion of A:G and U:C transitions was decreased with
139 increasing NHC concentrations compared to the vehicle control (Fig. 4G, H). Together, these
140 results demonstrate that NHC treatment during a single round of WT MHV infection causes
141 predominantly G:A and C:U transition mutations that are detectable at low frequencies across the
142 genome. These data further support a mutagenic mechanism of action for NHC inhibition of WT

143 MHV.

144

145 **NHC inhibition is modestly enhanced in the absence of ExoN proofreading.**

146 Mutagenic nucleoside analogues, such as RBV and 5-fluorouracil (5-FU), have been ineffective
147 at potently inhibiting WT CoVs due to the ExoN proofreading activity (26). A proofreading-
148 deficient MHV mutant, ExoN(-), displays increased sensitivity to previously tested nucleoside
149 analogues, indicating that proofreading dampens inhibition by these compounds (26, 38, 39).
150 Thus, we tested the sensitivity of ExoN(-) MHV to NHC inhibition. Our results indicate that
151 NHC decreases viral titer of both WT and ExoN(-) MHV in a dose-dependent manner, but that
152 ExoN(-) MHV demonstrates a statistically significant increase in sensitivity to NHC inhibition
153 compared to WT MHV (Fig. 5A). However, this difference is reflected in only a modest decrease
154 in EC₉₀ concentration by approximately 2-fold for ExoN(-) (0.72 μM) compared to WT MHV
155 (1.59 μM) (Fig. 5B). The minimal change in sensitivity to NHC observed for ExoN(-) MHV
156 indicates that NHC potency is only marginally affected by ExoN proofreading activity.

157

158 **Passage in the presence of NHC yields low-level resistance associated with multiple
159 transition mutations.**

160 To better understand the development and impact of NHC resistance in CoVs, we passaged two
161 lineages of WT MHV in thirty times in the presence of increasing concentrations of NHC and
162 tested the sensitivity of passage 30 (p30) MHV populations to NHC inhibition. We found that the
163 lineage 1 (MHV p30.1) viral population showed no change in sensitivity to NHC compared to
164 WT MHV (Fig. 6A). However, lineage 2 (MHV p30.2) showed a decrease in sensitivity to NHC
165 inhibition in a titer-reduction assay, especially at higher concentrations of compound. We

166 observed a modest, approximately 2-fold, increase in EC₉₀ values for MHV NHC passage
167 viruses (MHV p30.1 EC₉₀ = 2.61 μM; MHV p30.2 EC₉₀ = 2.41 μM; WT MHV EC₉₀ = 1.53 μM)
168 (Fig. 6B). This suggests that MHV passage resulted in minimal resistance to NHC. We next
169 sought to determine if passaging WT MHV in the presence of NHC altered the replication
170 capacity of these viruses. We found that both lineages showed a delay in replication but
171 ultimately reached similar peak titers as WT MHV (Fig. 6C). This delay in replication suggests
172 that MHV p30 viruses are less fit than WT MHV.

173 To identify mutations associated with these phenotypes after passage, we sequenced
174 complete genomes of MHV p30.1 and MHV p30.2. Both lineages passaged in the presence NHC
175 had accumulated over 100 consensus mutations distributed across the genome (Fig. 6D, E; Table
176 S1). By comparison, a previous study reported that WT MHV accumulated only 23 total
177 mutations after 250 passages in the absence of drug (39). Further analysis of the p30 MHV
178 mutational profile demonstrated that slightly more of the total mutations in both lineages were
179 synonymous changes that did not result in an amino acid change as opposed to nonsynonymous
180 changes that did alter amino acid sequence (Fig. 6F; Table S1). Additionally, the vast majority of
181 mutations in both lineages were transition mutations resulting in a purine-to-purine or
182 pyrimidine-to-pyrimidine change (Fig. 6G). Both lineages contained only two transversion
183 mutations resulting in a purine-to-pyrimidine or pyrimidine-to-purine change. Though all
184 possible transition mutation types were detected in both viral lineage populations, the majority in
185 both passage lineages were G:A transitions (Fig. 6H), which is consistent with the MHV NGS
186 data (Fig. 4). To determine if the mutational profile at p30 was consistent with an earlier passage,
187 we analyzed the whole genome of both lineage 1 and 2 at passage 19 (p19). Both lineages
188 demonstrated fewer mutations at p19 than at p30, but the profiles of synonymous vs.

189 nonsynonymous changes and the transition mutations were similar (Fig. S1; Table S2).
190 To determine whether the lack of robust resistance to NHC was broadly applicable across
191 β -CoVs, we assessed the capacity of MERS-CoV to evolve resistance to NHC. Like MHV, we
192 passaged two lineages of MERS-CoV 30 times in the presence of increasing concentrations of
193 NHC and tested the sensitivity of these lineages to inhibition by NHC. Compared to WT MERS-
194 CoV passaged in the absence of drug, both MERS-CoV NHC p30.1 and p30.2 exhibited
195 decreased sensitivity to NHC inhibition (Fig. 7A). This correlated with modestly increased EC₉₀
196 values for the passage lineages (WT MERS-CoV EC₉₀ = 1.31 μ M; MERS-CoV p30.1 EC₉₀ =
197 3.04 μ M; MERS-CoV p30.2 EC₉₀ = 2.12 μ M) (Fig. 7B), corresponding to approximately 2-fold
198 resistance. Similar to MHV, we observed no substantial shift in dose response curve for MERS-
199 CoV, indicating minimal acquired resistance. NHC p30 viruses replicated similarly to WT p30
200 MERS-CoV (Fig. 7C). We sequenced both lineages of MERS-CoV p30 population virus and
201 detected 27 consensus mutations in MERS-CoV NHC p30.1 (Fig. 7D; Table S3) and 41
202 consensus mutations in MERS-CoV NHC p30.2 (Fig. 7E; Table S3) that were randomly
203 distributed across the genome. Both MERS-CoV NHC p30.1 and MERS-CoV NHC p30.2
204 accumulated nonsynonymous and synonymous mutations in roughly equal proportions (Fig. 7F).
205 Like in MHV, the mutations detected in MERS-CoV p30 lineages were predominantly transition
206 mutations (Fig. 7G). Further analysis of these mutations revealed that the predominant type of
207 transition was lineage-dependent. The majority of transition mutations in MERS-CoV NHC
208 p30.1 were G:A transitions, as was observed in both p30 MHV lineages, whereas MERS-CoV
209 NHC p30.2 contained a similar number of each type (Fig. 7H). These results indicate that
210 MERS-CoV can achieve low-level resistance to NHC and that development of resistance is
211 associated with the accumulation of multiple transition mutations. Together, our data suggest

212 NHC acts as a mutagen and that it poses a high genetic barrier to resistance for β -CoVs.

213 **DISCUSSION**

214 In this study, we demonstrate that NHC potently inhibits the divergent β -CoVs MHV and
215 MERS-CoV. Our data are consistent with a virus mutagenic mechanism of action as evidenced
216 by a decrease in specific infectivity and an increase in G:A and C:U transition mutations present
217 at low frequencies across the genome after treatment with NHC. We also demonstrate that robust
218 resistance to NHC is difficult to achieve in both MHV and MERS-CoV. Both WT MHV and
219 ExoN(-) MHV are sensitive to NHC inhibition, suggesting that NHC is able to overcome ExoN-
220 mediated proofreading to inhibit WT CoVs and that it interacts with CoVs differently than other
221 previously tested nucleoside analogues.

222

223 **Utility of the broad spectrum antiviral NHC as a pan-CoV therapeutic.**

224 Early work with NHC focused on the mutagenic effects of this compound in multiple bacterial
225 systems (40-42). More recently, the antiviral properties of this compound have been reported for
226 multiple RNA viruses, including chikungunya virus, Venezuelan equine encephalitis virus,
227 respiratory syncytial virus, hepatitis C virus, norovirus, influenza A and B viruses, and Ebola
228 virus (31-36). NHC has also been shown potently inhibited SARS-CoV and HCoV-NL63 (43,
229 44), suggesting potential utility in treating CoV infections (17). Based on previous studies, NHC
230 appears to primarily inhibit viral replication by mutagenesis (31, 34). Serial passaging in the
231 presence of NHC led to low-level resistance for VEEV, but no detectable resistance for RSV,
232 IAV, or bovine viral diarrhea virus, indicating a high barrier to resistance (31, 34, 36). Consistent
233 with these previous studies, we demonstrate that NHC is mutagenic in CoVs and that serial

234 passaging yields low-level, approximately 2-fold resistance. Low-level resistance has also been
235 observed for remdesivir, another nucleoside analogue that potently inhibits CoVs.

236 Approximately 6-fold resistance to remdesivir is conferred by two mutations in the CoV RdRp
237 (38). This study further expands the known antiviral spectrum of NHC to include MHV and
238 MERS-CoV, two genetically divergent β-CoVs and supports NHC development as a broad-
239 spectrum CoV antiviral.

240

241 **NHC inhibition may circumvent ExoN-mediated proofreading.**

242 NHC is the first mutagenic nucleoside analogue demonstrated to potently inhibit proofreading-
243 intact CoVs. Previous studies have demonstrated that viruses lacking ExoN proofreading
244 activity, or ExoN(-) viruses, are more sensitive to inhibition by nucleoside analogues, especially
245 RBV and 5-FU (26, 38, 39, 45). This increased sensitivity has been attributed to an inability of
246 ExoN(-) to efficiently remove incorrect nucleosides (46). However, we observed a minimal
247 change in NHC sensitivity between WT MHV and ExoN(-) MHV, especially by EC₉₀. This
248 suggests that NHC interacts with the CoV replicase differently than other previously tested
249 nucleoside analogues. One explanation is that NHC may evade removal by the proofreading
250 ExoN. Studies investigating nucleosides that inhibit DNA viruses have suggested an inability of
251 the viral exonuclease to efficiently excise some nucleoside analogues (47, 48). Further, a
252 previous study suggested that the T4 DNA exonuclease activity was incapable of removing NHC
253 (49). While the SARS-CoV ExoN efficiently removes 3' terminal mismatches regardless of type
254 (46, 50), the effect of NHC on this activity has not been investigated. Interestingly, mismatches
255 readily observed during single nucleotide elongation by the SARS-CoV polymerase in the
256 absence of drugs correspond to mismatches that would lead to the G:A and C:U transitions

257 observed after NHC treatment (46). This suggests that the CoV polymerase could be naturally
258 more prone to make these types of errors, which are then magnified by NHC. This could lead to
259 a scenario where ExoN cannot prevent dipping below the error threshold, ultimately resulting in
260 lethal mutagenesis and similar inhibition of both WT MHV and ExoN(-) MHV (51).

261 Several nucleosides including the mutagenic RBV have multiple demonstrated
262 mechanisms other than direct incorporation into the genome (52, 53). Thus, another explanation
263 for the unique potency of NHC in the presence of an active proofreading ExoN is that it may
264 inhibit viral replication by additional mechanisms beyond mutagenesis. Indeed, previous reports
265 have suggested that NHC may also interfere with the RNA secondary structure or virion release
266 to cause inhibition (31, 36). Further, exogenous C or U in the presence of NHC could rescue
267 viral replication in HCV, Chikungunya virus, RSV, and Influenza A virus (32, 34, 36),
268 indicating that NHC competes with exogenous nucleosides at some stage prior to viral inhibition.
269 These results raise the possibility that NHC could inhibit a process that results in similar
270 inhibition of these viruses by a mechanism unrelated to ExoN. Thus, future studies will be
271 important to investigate the role of proofreading in NHC inhibition of CoVs to shed light on
272 intricacies of NHC inhibition of the CoV replication complex.

273

274 **NHC mutagenesis may hinder emergence of robust resistance to NHC.**

275 The decrease in specific infectivity along with the accumulation of transitions across the CoV
276 genome support a mutagenic mechanism of action for NHC in CoVs. NHC resistance in CoVs
277 was modest and difficult to achieve, as we obtained approximately 2-fold resistance after 30
278 passages. Resistance was associated with multiple mutations. Interestingly, MERS-CoV
279 accumulated less mutations over 30 passages than MHV. While differences in viral mutation

280 rates could be the driver of this difference, previous studies have suggested that MHV does not
281 have a higher mutation rate than MERS-CoV (54-56). The differences in mutation accumulation
282 between MHV and MERS-CoV may be a product of different passage conditions. While MHV
283 was passaged with a consistent transfer volume, MERS-CoV passage volumes were adjusted
284 over time to sustain viral replication under escalating selection for drug resistance. The constant
285 volume passaging conditions may have more severely bottlenecked MHV populations and fixed
286 more mutations in the genome than the variable volume passaging conditions applied to MERS-
287 CoV (57). Alternatively, this difference could also reflect a difference in mutational robustness
288 of the MHV and MERS-CoV genomes, though this proposition would need to be investigated
289 further (58, 59). While a portion of the mutations that accumulated over passage likely contribute
290 to NHC resistance, other mutations, such as those in ns2 or nsp2, which encode proteins
291 dispensable for viral replication in cell culture, may be merely tolerated because of their limited
292 effect on viral fitness in the context of our passage conditions (60-62). Few common mutations
293 arose in both MHV and MERS-CoV passage series, (Supp. Table 1-3), suggesting that multiple
294 pathways to low-level NHC resistance exist in CoVs. Interestingly, for both MHV and MERS-
295 CoV, the p30 lineage that demonstrated a greater change in sensitivity to NHC was the lineage
296 that had fewer overall mutations (Fig. 6, 7). Both MHV passage lineages replicated less well than
297 WT MHV, suggesting that the accumulation of mutations during passage may negatively impact
298 viral fitness and the ability of MHV to evolve robust resistance to NHC. Further, the MHV
299 lineage that did not result in changed sensitivity to NHC by p30 (MHV p30.1) had fewer
300 mutations present at consensus by p19 than the other lineage (Fig. S1). Thus, it is possible that
301 the accumulation of deleterious mutations counteracts potential benefits of resistance mutations
302 (63). If this is the case, mutations promoting NHC resistance would need to arise early during

303 passage to help mitigate the accumulation of excess deleterious mutations. Alternatively, the
304 inability to evade inhibition by NHC may lead to the accumulation of a greater number of NHC-
305 associated transitions and ultimately a higher mutational burden that may impact viral fitness
306 (64, 65). Together, our results support the hypothesis that establishment of resistance to NHC in
307 CoVs requires a delicate balance of resistance-promoting mutations, viral fitness, and
308 accumulation of deleterious mutations. Thus, defining the roles of individual NHC resistance-
309 associated mutations will be an important goal for future studies. Overall, our results support
310 further development of NHC as a broad-spectrum antiviral for treatment of CoV infections and
311 contribute new insights into important aspects of CoV replication.

312 **MATERIALS AND METHODS**

313 **Cell culture.** Murine astrocytoma delayed brain tumor (DBT) (66) and Vero cells (ATCC CCL-
314 81) were maintained at 37°C in Dulbecco's modified Eagle medium (DMEM, Gibco)
315 supplemented with 10% fetal bovine serum (FBS, Invitrogen), 1% penicillin and streptomycin
316 (Gibco), and 0.1% amphotericin B (Corning).

317 **Viruses.** All work with MHV was performed using the recombinant WT strain MHV-A59
318 (GenBank accession number AY910861 (67)). MERS-CoV stocks were generated from cDNA
319 clones (GenBank accession number JX869059(68)).

320 **Compounds and cell viability studies.** NHC was synthesized at the Emory Institute for Drug
321 Development and prepared as a 20 mM stock solution in dimethyl sulfoxide (DMSO). Cell
322 viability was assessed using CellTiter-Glo (Promega) in 96-well plates according to the
323 manufacturer's instructions. DBT and Vero cells were incubated with indicated concentration of
324 compound at 37°C for 24 hours (DBT) or 48 hours (Vero). Cell viability was determined using a
325 Veritas Microplate Luminometer (Promega) or GloMax (Promega) with values normalized to
326 those of vehicle-treated cells.

327 **Nucleoside analogue sensitivity studies and generation of EC₅₀ curves.** Subconfluent
328 monolayers of DBT cells were infected with MHV at a multiplicity of infection (MOI) of 0.01
329 PFU per cell for 1 hour at 37°C. The inoculum was removed and replaced with media containing
330 the indicated compound concentration. Cell supernatants were harvested 24 hours post-infection.
331 Titers were determined by plaque assay as described previously (69). Subconfluent monolayers
332 of Vero cells were infected with an MOI of 0.01 PFU/cell of MERS-CoV. After virus adsorption
333 for 30 minutes at 37°C, the inoculum was removed. Cells were washed with PBS and incubated
334 with medium containing the indicated concentrations of NHC or DMSO (vehicle control). After

335 48 h, supernatant was collected and titers were determined by plaque assay as described
336 previously (70). EC₅₀ and EC₉₀ values and curves were generated using the nonlinear regression
337 curve fit in GraphPad Prism software (La Jolla, CA).

338 **Time-of-drug addition assay.** Subconfluent monolayers of DBT cells were treated with media
339 containing DMSO or 16 µM NHC (~100x EC₅₀) at the indicated time pre- or post-infection.
340 Cells were infected with WT MHV at an MOI of 1 PFU/cell for 1 hour at 37°C. Virus inoculum
341 was removed and fresh medium was replaced. Culture supernatant was harvested 12 hours post-
342 infection, and viral titer was determined by plaque assay.

343 **Quantification of viral genomic RNA.** Subconfluent DBT cells were infected with WT MHV at
344 an MOI of 0.01 PFU/cell. Inoculum was removed after 1 h incubation at 37°C and medium
345 containing indicated concentrations of NHC was added. Total RNA from cells and supernatant
346 RNA was harvested using TRIzol reagent (Invitrogen) after 20 hours. Both total RNA and
347 supernatant RNA were extracted by phase separation. Total RNA was purified by ethanol
348 precipitation and supernatant RNA was purified using the PureLink RNA mini kit (Invitrogen)
349 according to manufacturer's protocol. Total RNA was reverse transcribed using SuperScript III
350 (Invitrogen) to generate cDNA that was quantified by quantitative polymerase chain reaction
351 (qPCR) as previously described (26). Data are presented as 2^{-ΔΔCT}, where ΔΔCT denotes the
352 change in the threshold cycle for the viral target (nsp10) normalized to the control (GAPDH)
353 before and after drug treatment. Supernatant RNA was quantified using one-step reverse
354 transcriptase quantitative PCR (qRT-PCR) as previously described (45). Data are presented as
355 the fold change in genome RNA copies normalized to vehicle control.

356 **Determination of specific infectivity.** Subconfluent DBT cells were infected with WT MHV at
357 a MOI of 0.01 PFU/cell. Inoculum was removed after 1 h incubation at 37°C and medium

358 containing indicated concentrations of NHC was added. Supernatant RNA was harvested using
359 the TRIzol reagent (Invitrogen) after 20 hours, followed by extraction and quantification as
360 described above. Viral titer was determined by plaque assay. The specific infectivity was
361 calculated as PFU divided by supernatant genome RNA copy number. This ratio was then
362 normalized to the vehicle control.

363 **NGS studies.** Subconfluent DBT cells were infected with WT MHV at an MOI of 0.01 PFU/cell
364 and treated with the indicated concentrations of NHC. Supernatant was collected 24 hours post-
365 infection. Purified viral RNA was submitted to GENEWIZ for library preparation and
366 sequencing. Briefly, after quality controls, viral RNAs were randomly fragmented using heat.
367 Libraries were prepared and sequenced on the Illumina HiSeq platform.
368 GENEWIZ performed base-calling and read demultiplexing. Trimmomatic was used to trim
369 adapter contaminants and reads shorter than 36 basepairs and filter low quality bases (Q-score
370 <30) (71). The paired-end fastq reads were then aligned to the MHV genome using Bowtie2 to
371 generate a SAM file (72). SAMtools was used to process the resultant alignment file and
372 calculate coverage depth at each nucleotide, generating a sorted and indexed BAM file. LoFreq
373 was used to call substitution variants, including low-frequency variants, and generate a variant
374 file (73). The Bash shell and Excel were used to further process and analyze the resultant vcf file.
375 A frequency of 0.001 was used as a cutoff for variants, consistent with previous reports (74).
376 Absolute numbers of mutations are reported for each NHC treatment. The percentage of the total
377 mutations for each specific mutation type was calculated using these numbers. The difference in
378 percentage for each class of mutation after treatment as compared with vehicle control is referred
379 to as the relative proportion of these mutations.

380 **MHV population passage in the presence of NHC.** WT MHV was passaged in triplicate in

381 increasing concentrations of NHC, from 1 μ M to a maximum of 5 μ M. Infection was initiated
382 for passage 1 at MOI = 0.1 PFU/cell. Viral supernatants were harvested from each viral lineage
383 and frozen when the cell monolayer demonstrated 80% cytopathic effect (CPE) or after 24 hrs. A
384 constant volume of 16 μ L was used to initiate subsequent passages. All three lineages were
385 maintained until passage 16 when lineage 3 demonstrated no visible CPE upon multiple attempts
386 at varying concentrations. Lineage 1 and 2 were maintained until passage 30. After each passage,
387 total RNA was harvested from infected cell monolayers using the TRIzol reagent. Viral RNA
388 was extracted from passage 19 and passage 30 samples and reverse transcribed using SuperScript
389 III, followed by generation of 12 PCR amplicons to cover the whole genome. Dideoxy amplicon
390 sequencing was performed by GENEWIZ and analyzed to identify mutations present at greater
391 than 50% of total using MacVector. Viral mutation maps depicting the identified mutations were
392 generated using MacVector.

393 **MERS-CoV population passage in the presence of NHC.** Three parallel, independent passage
394 series of WT MERS-CoV were performed on Vero cells in the presence of gradually increasing
395 concentrations of NHC up to a maximum concentration of 6.5 μ M to select for drug-resistant
396 mutant viruses. Virus adaptation to NHC-supplemented complete culture medium was assessed
397 by monitoring progression of characteristic MERS-CoV CPE. Volumes of transferred culture
398 supernatants were adjusted empirically to balance continuous selective pressure against culture
399 extinction. Each of triplicate lineages in the MERS-CoV passage experiment was sustained
400 through passage 30. However, the third lineage was severely impaired in replication and was
401 excluded from further analysis. Total infected-cell MERS-CoV RNA purified from monolayers
402 infected with terminal-passage (p30) culture supernatant was used to generate RT-PCR products
403 for consensus Sanger sequencing of the complete viral genome (Genewiz). Changes in passaged

404 virus nucleotide and deduced amino acid sequences were identified via alignment with the WT
405 parental virus genomic sequence using MacVector.
406 **Virus replication assays.** Subconfluent monolayers of DBT (MHV) or Vero (MERS-CoV) cells
407 were infected with WT or NHC-passaged viral populations at an MOI of 0.01 PFU/cell for 1
408 hour (MHV) or 30 minutes (MERS-CoV). Inocula were removed and cells were washed with
409 PBS before addition of pre-warmed media. Supernatants were harvested at indicated times post-
410 infection, and titers were determined by plaque assay.
411 **Statistics.** Statistical tests were performed using GraphPad Prism 7 software (La Jolla, CA) as
412 described in the respective figure legends.
413

414 ACKNOWLEDGEMENTS

415 We thank members of the Denison lab for thoughtful discussions regarding this work.

416

417 FUNDING INFORMATION

418 This work was supported by the Antiviral Drug Discovery and Development Center

419 U19AI109680 (MRD, RSB), National Institutes of Health HHSN272201500008C (GRP), and

420 National Institutes of Health grants T32AI089554 (MLA), F31AI133952 (MLA),

421 T32GM065086 (JG).

422 REFERENCES

- 423 1. Ksiazek TG, Erdman D, Goldsmith CS, Zaki SR, Peret T, Emery S, Tong S,
424 Urbani C, Comer JA, Lim W, Rollin PE, Dowell SF, Ling A-E, Humphrey CD,
425 Shieh W-J, Guarner J, Paddock CD, Rota P, Fields B, DeRisi J, Yang J-Y, Cox N,
426 Hughes JM, DeLuc JW, Bellini WJ, Anderson LJ. 2003. A Novel Coronavirus
427 Associated with Severe Acute Respiratory Syndrome. *New England Journal of
428 Medicine* 1–14.
- 429 2. Zaki AM, van Boheemen S, Bestebroer TM, Osterhaus ADME, Fouchier RAM.
430 2012. Isolation of a Novel Coronavirus from a Man with Pneumonia in Saudi Arabia.
431 *New England Journal of Medicine* 367:1814–1820.
- 432 3. Nassar MS, Bakrebah MA, Meo SA, Alsuaibeyl MS, Zaher WA. 2018. Global
433 seasonal occurrence of middle east respiratory syndrome coronavirus (MERS-CoV)
434 infection. *European Review for Medical and Pharmacological Sciences* 1–6.
- 435 4. McIntosh K, Kapikian AZ, Turner HC, Hartley JW, Parrott RH, Chanock RM.
436 1970. Seroepidemiologic Studies of Coronavirus Infection in Adults and Children.
437 *American Journal of Epidemiology* 91:585–592.
- 438 5. Gaunt ER, Hardie A, Claas ECJ, Simmonds P, Templeton KE. 2010.
439 Epidemiology and Clinical Presentations of the Four Human Coronaviruses 229E,
440 HKU1, NL63, and OC43 Detected over 3 Years Using a Novel Multiplex Real-Time
441 PCR Method. *Journal of Clinical Microbiology* 48:2940–2947.
- 442 6. Walsh EE, Shin JH, Falsey AR. 2013. Clinical Impact of Human Coronaviruses
443 229E and OC43 Infection in Diverse Adult Populations. *J Infect Dis* 208:1634–1642.
- 444 7. Menachery VD, Yount BL, Debbink K, Agnihothram S, Gralinski LE, Plante JA,
445 Graham RL, Scobey T, Ge X-Y, Donaldson EF, Randell SH, Lanzavecchia A,
446 Marasco WA, Shi Z-L, Baric RS. 2015. A SARS-like cluster of circulating bat
447 coronaviruses shows potential for human emergence. *Nature Medicine* 21:1508–1513.
- 448 8. Menachery VD, Yount BL Jr., Sims AC, Debbink K, Agnihothram SS, Gralinski
449 LE, Graham RL, Scobey T, Plante JA, Royal SR, Swanstrom J, Sheahan TP,
450 Pickles RJ, Corti D, Randell SH, Lanzavecchia A, Marasco WA, Baric RS. 2016.
451 SARS-like WIV1-CoV poised for human emergence. *Proc Natl Acad Sci USA*
452 113:3048–3053.
- 453 9. Anthony SJ, Gilardi K, Menachery VD, Goldstein T, Ssebide B, Mbabazi R,
454 Navarrete-Macias I, Liang E, Wells H, Hicks A, Petrosov A, Byarugaba DK,
455 Debbink K, Dinnon KH, Scobey T, Randell SH, Yount BL, Cranfield M, Johnson
456 CK, Baric RS, Lipkin WI, Mazet JAK. 2017. Further Evidence for Bats as the
457 Evolutionary Source of Middle East Respiratory Syndrome Coronavirus. *mBio*
458 8:e00373–17.

- 459 10. **Yang Y, Du L, Liu C, Wang L, Ma C, Tang J, Baric RS, Jiang S, Li F.** 2014. Receptor usage and cell entry of bat coronavirus HKU4 provide insight into bat-to-human transmission of MERS coronavirus. *Proc Natl Acad Sci USA* **111**:12516–12521.
- 463 11. **Twu S-J, Chen T-J, Chen C-J, Olsen SJ, Lee L-T, Fisk T, Hsu K-H, Chang S-C, Chen K-T, Chiang I-H, Wu Y-C, Wu J-S, Dowell SF.** 2003. Control Measures for Severe Acute Respiratory Syndrome (SARS) in Taiwan. *Emerging Infectious Diseases* 1–3.
- 467 12. **Balkhy HH, Alenazi TH, Alshamrani MM, Baffoe-Bonnie H, Arabi Y, Hijazi R, Al-Abdely HM, El-Saied A, Johani Al S, Assiri AM, bin Saeed A.** 2016. Description of a Hospital Outbreak of Middle East Respiratory Syndrome in a Large Tertiary Care Hospital in Saudi Arabia. *Infection Control & Hospital Epidemiology* **37**:1147–1155.
- 471 13. **Park GE, Ko J-H, Peck KR, Lee JY, Lee JY, Cho SY, Ha YE, Kang C-I, Kang J-M, Kim Y-J, Huh HJ, Ki C-S, Lee NY, Lee JH, Jo IJ, Jeong B-H, Suh GY, Park J, Chung CR, Song J-H, Chung DR.** 2016. Control of an Outbreak of Middle East Respiratory Syndrome in a Tertiary Hospital in Korea. *Ann Intern Med* **165**:87–8.
- 475 14. **Cheng VCC, Chan JFW, To KK, Yuen KY.** 2013. Clinical management and infection control of SARS: Lessons learned. *Antiviral Research* **100**:407–419.
- 477 15. **Stockman LJ, Bellamy R, Garner P.** 2006. SARS: Systematic Review of Treatment Effects. *PLoS Medicine* **3**:e343.
- 479 16. **Arabi Y, Shalhoub S, Mandourah Y, Al-Hameed F, Al-Omari A, Qasim Al E, Jose J, Alraddadi B, Almotairi A, Khatib Al K, Abdulmomen A, Qushmaq I, Sindi AA, Mady A, Solaiman O, Al-Raddadi R, Maghrabi K, Ragab A, Mekhlafi Al GA, Balkhy HH, Harthy Al A, Kharaba A, Gramish JA, Al-Aithan AM, Al-Dawood A, Merson L, Hayden FG, Fowler R, Group SCCT.** 2019. Ribavirin and Interferon Therapy for Critically Ill Patients with the Middle East Respiratory Syndrome: A multicenter observational study. *Clinical Infectious Diseases* 1–23.
- 486 17. **De Clercq E.** 2014. Potential antivirals and antiviral strategies against SARS coronavirus infections. *Expert Review of Anti-infective Therapy* **4**:291–302.
- 488 18. **Zumla A, Chan JFW, Azhar EI, Hui DSC, Yuen K-Y.** 2016. Coronaviruses - drug discovery and therapeutic options. *Nature Reviews Drug Discovery* **15**:327–347.
- 490 19. **Adedeji AO, Sarafianos SG.** 2014. Antiviral drugs specific for coronaviruses in preclinical development. *Current Opinion in Virology* **8**:45–53.
- 492 20. **Clercq ED.** 2004. Antivirals and antiviral strategies. *Nat Rev Micro* **2**:704–720.
- 493 21. **De Clercq E, Li G.** 2016. Approved Antiviral Drugs over the Past 50 Years. *Clin Microbiol Rev* **29**:695–747.

- 495 22. Jordheim LP, Durantel D, Zoulim F, Dumontet C. 2013. Advances in the
496 development of nucleoside and nucleotide analogues for cancer and viral diseases.
497 Nature Publishing Group **12**:447–464.
- 498 23. Deval J. 2009. Antimicrobial Strategies. Drugs **69**:151–166.
- 499 24. Mahmoud S, Hasabelnaby S, Hammad S, Sakr T. 2018. Antiviral Nucleoside and
500 Nucleotide Analogs: A Review. Journal of Advanced Pharmacy Research **2**:73–88.
- 501 25. Eltahla A, Luciani F, White P, Lloyd A, Bull R. 2015. Inhibitors of the Hepatitis C
502 Virus Polymerase; Mode of Action and Resistance. Viruses **7**:5206–5224.
- 503 26. Smith EC, Blanc H, Vignuzzi M, Denison MR. 2013. Coronaviruses Lacking
504 Exoribonuclease Activity Are Susceptible to Lethal Mutagenesis: Evidence for
505 Proofreading and Potential Therapeutics. PLoS Pathog **9**:e1003565–11.
- 506 27. Warren TK, Wells J, Panchal RG, Stuthman KS, Garza NL, Van Tongeren SA,
507 Dong L, Retterer CJ, Eaton BP, Pegoraro G, Honnold S, Bantia S, Kotian P,
508 Chen X, Taubenheim BR, Welch LS, Minning DM, Babu YS, Sheridan WP,
509 Bavari S. 2015. Protection against filovirus diseases by a novel broad-spectrum
510 nucleoside analogue BCX4430. Nature **508**:402–405.
- 511 28. Warren TK, Jordan R, Lo MK, Ray AS, Mackman RL, Soloveva V, Siegel D,
512 Perron M, Bannister R, Hui HC, Larson N, Strickley R, Wells J, Stuthman KS,
513 Van Tongeren SA, Garza NL, Donnelly G, Shurtliff AC, Retterer CJ, Gharaibeh
514 D, Zamani R, Kenny T, Eaton BP, Grimes E, Welch LS, Gomba L, Wilhelmsen
515 CL, Nichols DK, Nuss JE, Nagle ER, Kugelman JR, Palacios G, Doerffler E,
516 Neville S, Carra E, Clarke MO, Zhang L, Lew W, Ross B, Wang Q, Chun K,
517 Wolfe L, Babusis D, Park Y, Stray KM, Trancheva I, Feng JY, Barauskas O, Xu
518 Y, Wong P, Braun MR, Flint M, McMullan LK, Chen S-S, Fearns R,
519 Swaminathan S, Mayers DL, Spiropoulou CF, Lee WA, Nichol ST, Cihlar T,
520 Bavari S. 2016. Therapeutic efficacy of the small molecule GS-5734 against Ebola
521 virus in rhesus monkeys. Nature **531**:381–385.
- 522 29. Sheahan TP, Sims AC, Graham RL, Menachery VD, Gralinski LE, Case JB, Leist
523 SR, Pyre K, Feng JY, Trantcheva I, Bannister R, Park Y, Babusis D, Clarke MO,
524 Mackman RL, Spahn JE, Palmiotti CA, Siegel D, Ray AS, Cihlar T, Jordan R,
525 Denison MR, Baric RS. 2017. Broad-spectrum antiviral GS-5734 inhibits both
526 epidemic and zoonotic coronaviruses. Science Translational Medicine 1–11.
- 527 30. Hofmann WP, Soriano V, Zeuzem S. 2009. Antiviral Combination Therapy for
528 Treatment of Chronic Hepatitis B, Hepatitis C, and Human Immunodeficiency Virus
529 Infection, pp. 321–346. In Antiviral Strategies. Springer Berlin Heidelberg, Berlin,
530 Heidelberg.
- 531 31. Urakova N, Kuznetsova V, Crossman DK, Sokratian A, Guthrie DB, Kolykhalov
532 AA, Lockwood MA, Natchus MG, Crowley MR, Painter GR, Frolova EI, Frolov

- 533 32. I. 2017. β -D-N(4)-hydroxycytidine is a potent anti-alphavirus compound that induces
534 high level of mutations in viral genome. *J Virol* **92**:491.
- 535 32. Ehteshami M, Tao S, Zandi K, Hsiao H-M, Jiang Y, Hammond E, Amblard F,
536 Russell OO, Merits A, Schinazi RF. 2017. Characterization of β -d-N4-
537 Hydroxycytidine as a Novel Inhibitor of Chikungunya Virus. *Antimicrob Agents
538 Chemother* **61**:270.
- 539 33. Costantini VP, Whitaker T, Barclay L, Lee D, McBrayer TR, Schinazi RF, Vinjé
540 J. 2012. Antiviral activity of nucleoside analogues against norovirus. *Antivir Ther
541 (Lond)* **17**:981–991.
- 542 34. Yoon J-J, Toots M, Lee S, Lee M-E, Ludeke B, Luczo JM, Ganti K, Cox RM,
543 Sticher ZM, Edpuganti V, Mitchell DG, Lockwood MA, Kolykhalov AA,
544 Greninger AL, Moore ML, Painter GR, Lowen AC, Tompkins SM, Fearn R,
545 Natchus MG, Plemper RK. 2018. Orally Efficacious Broad-Spectrum
546 Ribonucleoside Analog Inhibitor of Influenza and Respiratory Syncytial Viruses.
547 *Antimicrob Agents Chemother* **62**:1427.
- 548 35. Reynard O, Nguyen X-N, Alazard-Dany N, Barateau V, Cimarelli A, Volchkov
549 VE. 2015. Identification of a New Ribonucleoside Inhibitor of Ebola Virus
550 Replication. *Viruses* **7**:6233–6240.
- 551 36. Stuyver LJ, Whitaker T, McBrayer TR, Hernandez-Santiago BI, Lostia S,
552 Tharnish PM, Ramesh M, Chu CK, Jordan R, Shi J, Rachakonda S, Watanabe
553 KA, Otto MJ, Schinazi RF. 2003. Ribonucleoside Analogue That Blocks Replication
554 of Bovine Viral Diarrhea and Hepatitis C Viruses in Culture. *Antimicrob Agents
555 Chemother* **47**:244–254.
- 556 37. Daelemans D, Pauwels R, De Clercq E, Panneccouque C. 2011. A time-of-drug
557 addition approach to target identification of antiviral compounds. *Nature Protocols*
558 **6**:925–933.
- 559 38. Agostini ML, Andres EL, Sims AC, Graham RL, Sheahan TP, Lu X, Smith EC,
560 Case JB, Feng JY, Jordan R, Ray AS, Cihlar T, Siegel D, Mackman RL, Clarke
561 MO, Baric RS, Denison MR. 2018. Coronavirus Susceptibility to the Antiviral
562 Remdesivir (GS-5734) Is Mediated by the Viral Polymerase and the Proofreading
563 Exoribonuclease. *mBio* **9**:1953.
- 564 39. Graepel KW, Lu X, Case JB, Sexton NR, Smith EC, Denison MR. 2017.
565 Proofreading-Deficient Coronaviruses Adapt for Increased Fitness over Long-Term
566 Passage without Reversion of Exoribonuclease-Inactivating Mutations. *mBio*, 1st ed.
567 **8**:281.
- 568 40. Popowska E, Janion C. 1974. N4-hydroxycytidine — A new mutagen of a base
569 analogue type. *Biochemical and Biophysical Research Communications* **56**:459–466.

- 570 41. Salganik RI, Vasjunina EA, Poslovina AS, Andreeva IS. 1973. Mutagenic action of
571 N4-hydroxycytidine on Escherichia coli B cyt⁻. Mutation Research/Fundamental and
572 Molecular Mechanisms of Mutagenesis **20**:1–5.
- 573 42. Popowska E, research CJNA, 1975. The metabolism of N4-hydroxycytidine – a
574 mutagen for Salmonella typhimurium. academicoupcom
575 .
- 576 43. Pyrc K, Bosch BJ, Ben Berkhout, Jebbink MF, Dijkman R, Rottier P, van der
577 Hoek L. 2006. Inhibition of Human Coronavirus NL63 Infection at Early Stages of the
578 Replication Cycle. Antimicrob Agents Chemother **50**:2000–2008.
- 579 44. Barnard DL, Hubbard VD, Burton J, Smee DF, Morrey JD, Otto MJ, Sidwell
580 RW. 2004. Inhibition of Severe Acute Respiratory Syndrome-Associated Coronavirus
581 (SARS-CoV) by Calpain Inhibitors and β-D-N4-Hydroxycytidine. Antiviral Chemistry
582 and Chemotherapy **15**:15–22.
- 583 45. Sexton NR, Smith EC, Blanc H, Vignuzzi M, Peersen OB, Denison MR. 2016.
584 Homology-Based Identification of a Mutation in the Coronavirus RNA-Dependent
585 RNA Polymerase That Confers Resistance to Multiple Mutagens. J Virol **90**:7415–
586 7428.
- 587 46. Ferron F, Subissi L, Silveira De Moraes AT, Le NTT, Sevajol M, Gluais L,
588 Decroly E, Vonrhein C, Bricogne G, Canard B, Imbert I. 2017. Structural and
589 molecular basis of mismatch correction and ribavirin excision from coronavirus RNA.
590 Proc Natl Acad Sci USA **15**:201718806–10.
- 591 47. Derse D, Cheng Y-C, Furman PA, Clair MHS, Elion GB. 1981. Inhibition of
592 Purified Human and Herpes Simplex Virus-induced DNA Polymerases by 9-(2-
593 Hydroxyethoxymethyl)guanine Triphosphate. Journal of Biological Chemistry **1**:5.
- 594 48. Chamberlain JM, Sortino K, Sethna P, Bae A, Lanier R, Bambara RA, Dewhurst
595 S. 2019. Cidofovir Diphosphate Inhibits Adenovirus 5 DNA Polymerase via both
596 Nonobligate Chain Termination and Direct Inhibition, and Polymerase Mutations
597 Confer Cidofovir Resistance on Intact Virus. Antimicrob Agents Chemother **63**:331.
- 598 49. Śledziewska-Gójska E, Janion C. 1982. Effect of proofreading and<Emphasis
599 Type="Italic">dam</Emphasis>-instructed mismatch repair systems on
600 N<Superscript>4</Superscript>-hydroxycytidine-induced mutagenesis. Molec Gen
601 Genet **186**:411–418.
- 602 50. Bouvet M, Imbert I, Subissi L, Gluais L, Canard B, Decroly E. 2012. RNA 3'-end
603 mismatch excision by the severe acute respiratory syndrome coronavirus nonstructural
604 protein nsp10/nsp14 exoribonuclease complex. Proc Natl Acad Sci USA **109**:9372–
605 9377.

- 606 51. **Tejero H, Montero F, Nuño JC.** 2016. Theories of Lethal Mutagenesis: From Error
607 Catastrophe to Lethal Defection. *Curr Top Microbiol Immunol* **392**:161–179.
- 608 52. **Biktasova A, Hajek M, Sewell A, Gary C, Bellinger G, Deshpande HA, Bhatia A,**
609 **Burtness B, Judson B, Mehra S, Yarbrough WG, Isaeva N.** 2017. Demethylation
610 Therapy as a Targeted Treatment for Human Papillomavirus-Associated Head and
611 Neck Cancer. *Clin Cancer Res* **23**:7276–7287.
- 612 53. **Leyssen P, Balzarini J, De Clercq E, Neyts J.** 2005. The Predominant Mechanism by
613 Which Ribavirin Exerts Its Antiviral Activity In Vitro against Flaviviruses and
614 Paramyxoviruses Is Mediated by Inhibition of IMP Dehydrogenase. *J Virol* **79**:1943–
615 1947.
- 616 54. **Sanjuan R, Nebot MR, Chirico N, Mansky LM, Belshaw R.** 2010. Viral Mutation
617 Rates. *J Virol* **84**:9733–9748.
- 618 55. **Hemida MG, Chu DKW, Poon LLM, Perera RAPM, Alhammadi MA, Ng H-Y,**
619 **Siu LY, Guan Y, Alnaem A, Peiris M.** 2014. MERS coronavirus in dromedary
620 camel herd, Saudi Arabia. *Emerging Infectious Diseases* **20**:1231–1234.
- 621 56. **Cotten M, Watson SJ, Zumla AI, Makhdoom HQ, Palser AL, Ong SH, Rabieeah**
622 **Al AA, Alhakeem RF, Assiri A, Al-Tawfiq JA, Albarakat A, Barry M, Shibli A,**
623 **Alrabiah FA, Hajjar S, Balkhy HH, Flemban H, Rambaut A, Kellam P, Memish**
624 **Z A.** 2014. Spread, circulation, and evolution of the Middle East respiratory syndrome
625 coronavirus. *mBio* **5**:1814.
- 626 57. **Domingo E, Sheldon J, Perales C.** 2012. Viral Quasispecies Evolution. *Microbiol*
627 *Mol Biol Rev*, 2nd ed. **76**:159–216.
- 628 58. **Bloom JD, Lu Z, Chen D, Raval A, Venturelli OS, Arnold FH.** 2007. Evolution
629 favors protein mutational robustness in sufficiently large populations. *BMC Biol* **5**:29–
630 21.
- 631 59. **Fares MA.** 2015. The origins of mutational robustness. *Trends Genet* **31**:373–381.
- 632 60. **Schwarz B, Routledge E, Siddell SG.** 1990. Murine coronavirus nonstructural protein
633 ns2 is not essential for virus replication in transformed cells. *J Virol* **64**:4784–4791.
- 634 61. **Zhao L, Rose KM, Elliott R, Van Rooijen N, Weiss SR.** 2011. Cell-type-specific
635 type I interferon antagonism influences organ tropism of murine coronavirus. *J Virol*
636 **85**:10058–10068.
- 637 62. **Graham RL, Sims AC, Brockway SM, Baric RS, Denison MR.** 2005. The nsp2
638 replicase proteins of murine hepatitis virus and severe acute respiratory syndrome
639 coronavirus are dispensable for viral replication. *J Virol* **79**:13399–13411.
- 640 63. **Manrubia Cuevas S, Domingo E, Lázaro E.** 2010. Pathways to extinction: Beyond
641 the error threshold.

- 642 64. Sanjuán R, Moya A, Elena SF. 2004. The contribution of epistasis to the architecture
643 of fitness in an RNA virus. Proc Natl Acad Sci USA **101**:15376–15379.
- 644 65. Lyons D, Lauring A. 2018. Mutation and Epistasis in Influenza Virus Evolution.
645 Viruses **10**:407.
- 646 66. Chen W, Baric RS. 1996. Molecular anatomy of mouse hepatitis virus persistence:
647 coevolution of increased host cell resistance and virus virulence. J Virol **70**:3947–
648 3960.
- 649 67. Yount B, Denison MR, Weiss SR, Baric RS. 2002. Systematic Assembly of a Full-
650 Length Infectious cDNA of Mouse Hepatitis Virus Strain A59. J Virol **76**:11065–
651 11078.
- 652 68. Almazán F, Márquez-Jurado S, Nogales A, Enjuanes L. 2015. Engineering
653 infectious cDNAs of coronavirus as bacterial artificial chromosomes. Methods Mol
654 Biol **1282**:135–152.
- 655 69. Eckerle LD, Lu X, Sperry SM, Choi L, Denison MR. 2007. High Fidelity of Murine
656 Hepatitis Virus Replication Is Decreased in nsp14 Exoribonuclease Mutants. J Virol
657 **81**:12135–12144.
- 658 70. Coleman CM, Frieman MB. 2015. Growth and Quantification of MERS-CoV
659 Infection. Curr Protoc Microbiol **37**:15E.2.1–9.
- 660 71. Bolger AM, Lohse M, Usadel B. 2014. Trimmomatic: a flexible trimmer for Illumina
661 sequence data. Bioinformatics **30**:2114–2120.
- 662 72. Langmead B, Wilks C, Antonescu V, Charles R. 2019. Scaling read aligners to
663 hundreds of threads on general-purpose processors. Bioinformatics **35**:421–432.
- 664 73. Wilm A, Aw PPK, Bertrand D, Yeo GHT, Ong SH, Wong CH, Khor CC, Petric
665 R, Hibberd ML, Nagarajan N. 2012. LoFreq: a sequence-quality aware, ultra-
666 sensitive variant caller for uncovering cell-population heterogeneity from high-
667 throughput sequencing datasets. Nucleic Acids Research **40**:11189–11201.
- 668 74. Nakamura K, Oshima T, Morimoto T, Ikeda S, Yoshikawa H, Shiwa Y, Ishikawa
669 S, Linak MC, Hirai A, Takahashi H, Altaf-Ul-Amin M, Ogasawara N, Kanaya S.
670 2011. Sequence-specific error profile of Illumina sequencers. Nucleic Acids Research
671 **39**:e90–e90.
- 672
- 673

674 **Fig. 1.** Chemical structure of EIDD-1931, β -D- N^4 -hydroxycytidine (NHC).

675

676 **Fig. 2. NHC inhibits MHV and MERS-CoV with minimal cytotoxicity.** (A) Change in MHV
677 and (B) MERS-CoV titer relative to vehicle control after treatment with increasing
678 concentrations of NHC. The data represent the results of 6 independent experiments, each with 3
679 replicates. Error bars represent standard error of the mean (SEM). (C) Change in titer data from
680 (A) represented as percent of vehicle control. WT MHV EC₅₀ = 0.17 μ M. (D) Change in titer
681 data from (B) represented as percent of vehicle control. WT MERS-CoV EC₅₀ = 0.56 μ M. (E)
682 DBT-9 cell viability as a percent of DMSO control across NHC concentrations. No cytotoxicity
683 was detected up to 200 μ M. The data represent the results of 2 independent experiments, each
684 with 2 replicates (MHV). Error bars represent standard error of the mean (SEM). (F) Vero cell
685 viability as a percent of DMSO control across NHC concentrations. Less than 50% cytotoxicity
686 was detected up to 10 μ M. The data represent the results of 2 independent experiments, each
687 with 3 replicates. Error bars represent standard error of the mean (SEM).

688

689 **Fig. 3. NHC inhibition profile of MHV is consistent with mutagenesis.** (A) Treatment with
690 16 μ M NHC (~100X EC₅₀) significantly inhibits MHV replication during a single infection when
691 added before 6 h p.i. (B) Both MHV titer and monolayer RNA copies decrease after treatment
692 with increasing concentrations of NHC. (C) NHC treatment results in a decrease in supernatant
693 MHV RNA. (D) Data from (C) represented as the ratio of infectious WT MHV to genomic MHV
694 RNA present in supernatant, or specific infectivity, normalized to vehicle control. NHC
695 treatment results in a decrease in specific infectivity of MHV. All data in this figure represent the
696 results of 2 independent experiments, each with 3 replicates. Error bars represent standard error
697 of the mean (SEM). Statistical significance compared to DMSO control was determined by one-

698 way analysis of variance (ANOVA) with Dunnett's *post-hoc* test for multiple comparisons and is
699 denoted *, $P < 0.05$; **, $P < 0.01$; ***, $P < 0.001$; ****, $P < 0.0001$.

700

701 **Fig. 4. NHC treatment drives increase in low-frequency G:A and C:U transition mutations**
702 **in WT MHV during a single infection.** (A) Distribution and frequency of variants across the
703 genome detected by NGS after vehicle treatment, (B) 2 μ M NHC treatment, or (C) 4 μ M NHC
704 treatment. \log_{10} depth of coverage at each genomic position is depicted by the line; frequency of
705 individual mutations spread across the genome are represented by dots. (D) Number of mutations
706 in WT MHV after infection in the presence of (D) vehicle, (E) 2 μ M NHC, or (F) 4 μ M NHC
707 presented by type. Transition mutations are shown in grey and transversion mutations are shown
708 in white. (G) Change in relative proportion of each mutation type after treatment with (G) 2 μ M
709 NHC, or (H) 4 μ M NHC compared to vehicle control. The relative proportions of G:A and C:U
710 transitions increase with increasing concentrations of NHC treatment and are denoted by green
711 shading.

712

713 **Fig. 5. Sensitivity of ExoN(-) MHV to inhibition by NHC.** (A) Change in viral titer for WT
714 MHV and ExoN(-) MHV relative to vehicle control after treatment with NHC. ExoN(-) is more
715 sensitive to NHC than WT. The data represent the results of 3 independent experiments, each
716 with 3 replicates. Error bars represent SEM. Statistical significance compared to WT MHV was
717 determined by Wilcoxon test and is denoted **, $P < 0.01$. (B) Change in viral titer data from (A)
718 represented as percent of vehicle control. WT EC₉₀ = 1.59 μ M, ExoN(-) EC₉₀ = 0.72 μ M. ExoN(-)
719) MHV is approximately 2-fold more sensitive to NHC than WT MHV.

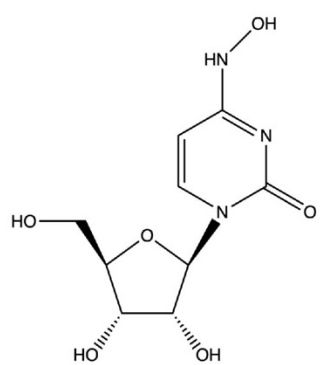
720

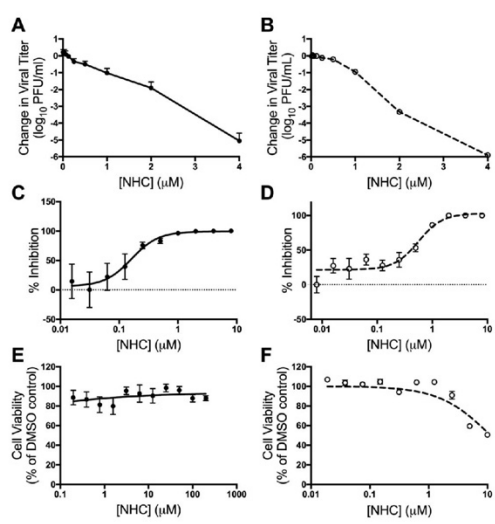
721

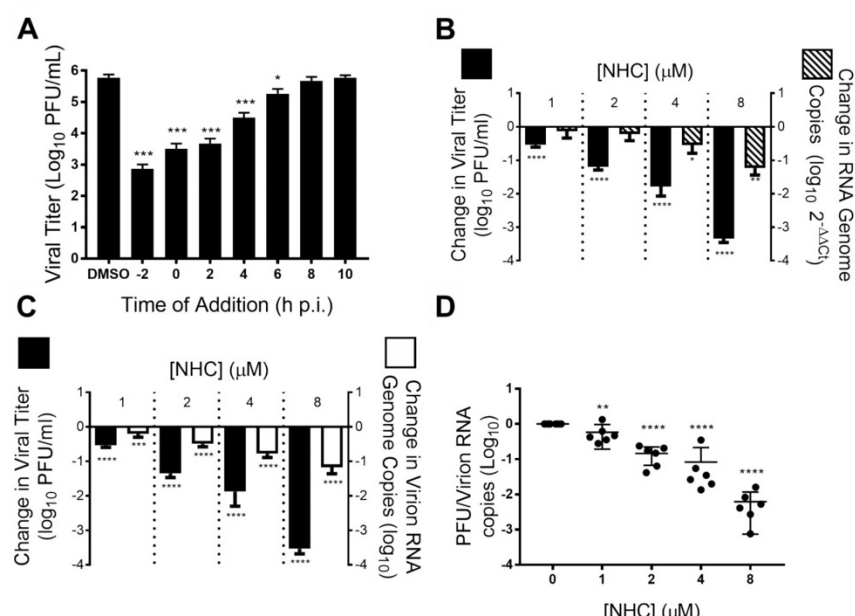
722 **Fig. 6. Resistance and mutational profile of MHV after 30 passages in the presence of NHC.**
723 (A) Change in viral titer for WT MHV, MHV NHC passage 30 (p30) lineage 1 (MHV p30.1),
724 and MHV NHC p30 lineage 2 (MHV p30.2) relative to vehicle controls after treatment with
725 NHC. MHV NHC p30.2 is less sensitive to NHC than WT MHV while MHV p30.1 shows no
726 change in sensitivity. The data represent the results of 2 independent experiments, each with 3
727 replicates. Error bars represent SEM. Statistical significance compared to WT MHV was
728 determined by ratio paired *t* test and is denoted *, $P < 0.05$. (B) Change in viral titer data from
729 (A) represented as percent of vehicle control. WT MHV EC₉₀ = 1.53 μ M; MHV p30.1 EC₉₀ =
730 2.61 μ M, MHV p30.2 EC₉₀ = 2.41 μ M. (C) Replication kinetics of NHC passage viruses. MHV
731 p30.1 and p30.2 are delayed in replication compared to WT MHV but ultimately reach similar
732 peak titers. The data represent the results of 2 independent experiments, each with 3 replicates.
733 Error bars represent standard deviation (SD). (D) MHV p30.1 accumulated a total of 162
734 consensus mutations across the genome detectable by Sanger sequencing. Of these mutations, 81
735 were synonymous, 64 were nonsynonymous, and 17 were noncoding. (E) MHV p30.2
736 accumulated 102 total mutations across the genome. Of these mutations, 54 were synonymous,
737 42 were nonsynonymous, and 7 were noncoding. (F) Each lineage accumulated more
738 synonymous changes than nonsynonymous or noncoding changes over passage. (G) Breakdown
739 of transition and transversion mutations present in each lineage after passage. MHV p30.1 and
740 p30.2 mutations were predominantly transitions. (H) Breakdown of the types of transition
741 mutations present in each lineage across passage. G:A transitions were the most abundant for
742 both MHV p30.1 and p30.2.

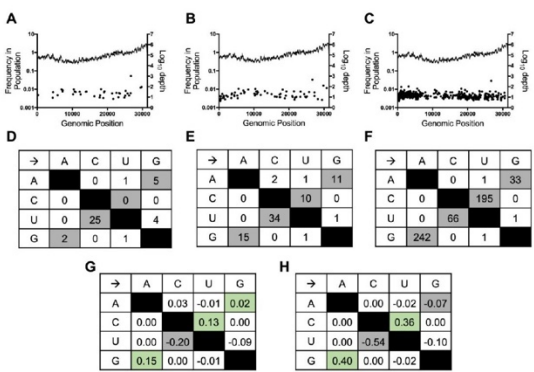
743

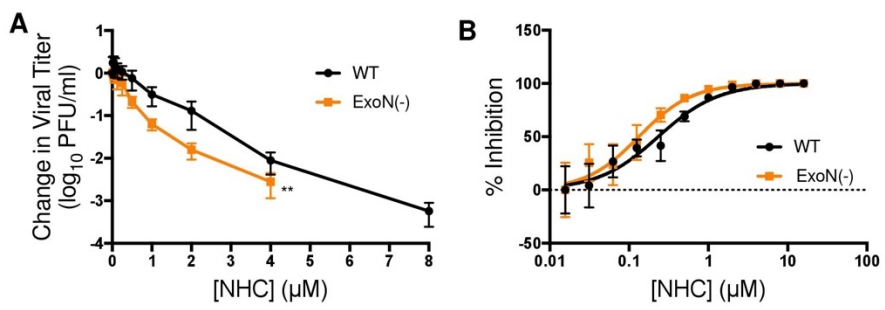
744 **Fig. 7. Resistance and mutational profile of MERS-CoV after 30 passages in the presence of**
745 **NHC.** (A) Change in viral titer relative to vehicle controls after treatment with NHC for WT
746 MERS-CoV passaged 30 times in the absence of drug, MERS-CoV NHC passage 30 lineage 1
747 (MERS-CoV p30.1), and MERS-CoV NHC passage 30 lineage 2 (MERS-CoV p30.2) relative to
748 vehicle controls after treatment with NHC. Both MERS-CoV p30.1 and p30.2 are less sensitive
749 to NHC than WT MERS-CoV. The data represent the results of 2 independent experiments, each
750 with 3 replicates. Error bars represent SEM. (B) Change in viral titer data from (A) represented
751 as percent of vehicle control. WT MERS-CoV EC₉₀ = 1.31 μM, MERS-CoV p30.1 EC₉₀ = 3.04
752 μM, MERS-CoV p30.2 EC₉₀ = 2.12 μM. (C) Replication kinetics of NHC passage viruses. WT
753 MERS-CoV, MERS-CoV p30.1, and MERS-CoV p30.2 replicate with similar kinetics and reach
754 similar peak titers. The data represent the results of 2 independent experiments, each with 3
755 replicates. Error bars represent SEM. (D) MERS-CoV p30.1 accumulated 27 total mutations
756 across the genome. Of these mutations, 14 were synonymous and 13 were nonsynonymous. (E)
757 MERS-CoV p30.2 accumulated 41 total mutations. Of these mutations, 17 were synonymous,
758 and 24 were nonsynonymous. (F) Both MERS-CoV p30.1 and p30.2 accumulated a similar
759 numbers of nonsynonymous and synonymous changes during passage. (G) MERS-CoV p30.1
760 and p30.2 acquired predominantly transitions. (H) The types of transition mutations present in
761 each lineage across passage. MERS-CoV p30.1 acquired relatively more G:A transitions,
762 whereas MERS-CoV p30.2 acquired similar numbers of each transition type.
763
764
765
766

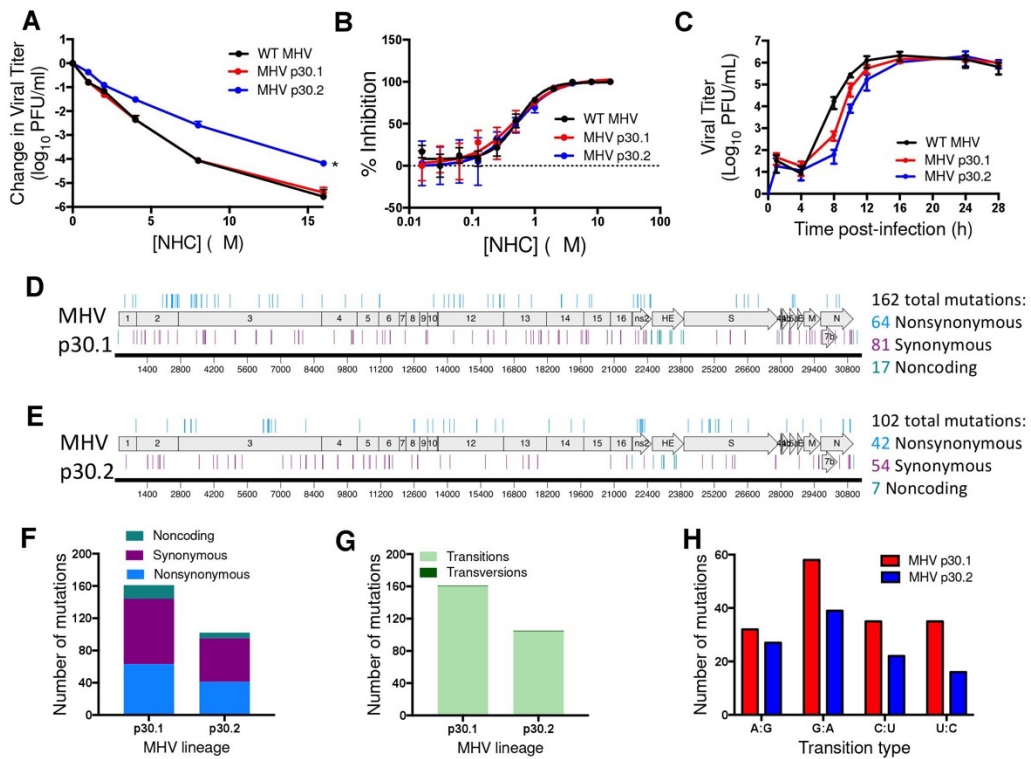


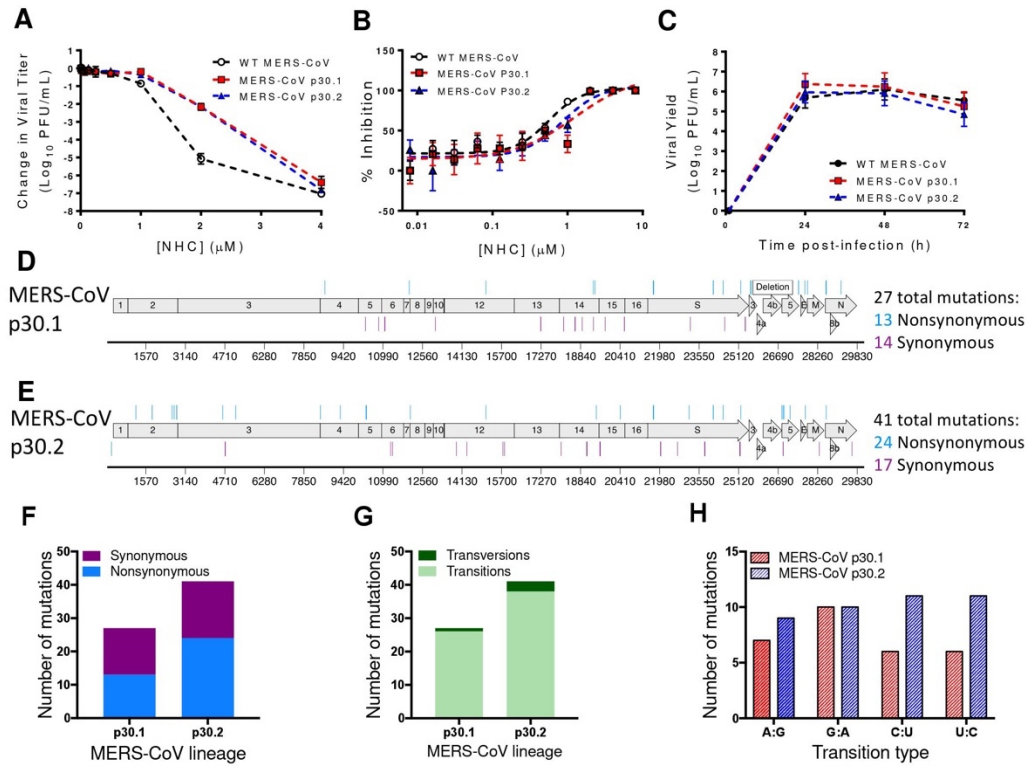












APPENDIX C: MUTATIONS IN PASSAGED VIRUSES

C.1 MHV p30.1 mutations^a

ORF	Gene	Residue	SNP	Change	Gene AA
UTR	UTR	181		n/a	
ORF1ab	nsp1	456	GAT->AAT	Asp83Asn	
		792	GGT->AGT	Gly195Ser	G195S
		830	CGC->CGT	Arg207	
		915	TGC->CGC	Cys236Arg	C236R
	nsp2	965	CTG->CTA	Leu252	
		1160	GTA->GTG	Val317	
		1307	TCC->TCT	Ser366	
		1703	ATT->ATC	Ile498	
		1898	TGC->TGT	Cys563	
		1952	GTG->GTA	Val581	
		2043	ATG->GTG	Met612Val	M365V
		2214	TAC->CAC	Tyr669His	Y422H
		2276	GTG->GTA	Val689	
		2422	GAA->GGA	Glu738Gly	E491G
		2448	TAT->CAT	Tyr747His	Y500H
		2470	AGC->AAC	Ser754Asn	S507N
		2581	TCT->TTT	Ser791Phe	S544F
		2663	GAC->GAT	Asp818	
		2665	ACT->ATT	Thr819Ile	T572I
	nsp3	2730	AAG->GAG	Lys841Glu	K9E
		3237	GGA->AGA	Gly1010Arg	G178R
		3270	ACC->GCC	Thr1021Ala	T189A
		3363	GAG->AAG	Glu1052Lys	E220K
		3433	GCG->GTG	Ala1075Val	A243V
		3470	GCC->GCT	Ala1087	
		3474	TGC->CGC	Cys1089Arg	C257R
		3676	TGC->TAC	Cys1156Tyr	C324Y
		3681	GTG->ATG	Val1158Met	V326M
		3743	GCA->GCG	Ala1178	
		3776	AGC->AGT	Ser1189	
		3815	GAC->GAT	Asp1202	
		3839	TTG->TTA	Leu1210	
		3901	ACC->ATC	Thr1231Ile	T399I
		4236	ATT->GTT	Ile1343Val	I511V
		4247	CCT->CCC	Pro1346	

ORF1ab	nsp3	4383	GCC->ACC	Ala1392Thr	A560T
		4878	GTT->ATT	Val1557Ile	V725I
		5090	GTA->GTG	Val1627	
		5972	TTT->TTC	Phe1921	
		6099	GTC->ATC	Val1964Ile	V1132I
		6525	GAT->AAT	Asp2106Asn	D1274N
		6611	CCT->CCC	Pro2134	
		6658	ACC->ATC	Thr2150Ile	T1318I
		6870	GTC->ATC	Val2221Ile	V1389I
		7589	ATC->ATT	Ile2460	
ORF1ab	nsp4	7757	GGC->GGT	Gly2516	
		7909	ACA->ATA	Thr2567Ile	T1735I
		7925	GTT->GTC	Val2572	
	nsp5	8738	ATG->ATA	Met2843Ile	
		9245	CAC->CAT	His3012	M2011I
	nsp6	9717	GTT->ATT	Val3170Ile	V29I
		9971	TTT->TTC	Phe3254	
		10040	TTG->TTA	Leu3277	
	nsp7	10408	TGT->TAT	Cys3400Tyr	C67Y
		10430	AGC->AGT	Ser3407	
		11043	TTA->CTA	Leu3612	
ORF1ab	nsp6	11152	TGC->TAC	Cys3648Tyr	C12Y
		11273	GTA->GTG	Val3688	
		11375	TAC->TAT	Tyr3722	
		11585	GCC->GCT	Ala3792	
		11604	CTA->TTA	Leu3799	
	nsp9	12224	GTT->GTC	Val4005	
		13100	GTG->GTA	Val4297	
		13106	GGG->GGA	Gly4299	
	nsp10	13163	TTG->TTA	Leu4318	
		13422	GTT->ATT	Val4405Ile	V86I
ORF1ab	nsp12	13862	GTG->ATG	Val4552Met	V96M
		14054	AAG->GAG	Lys4616Glu	K160E
		14263	TGT->TGC	Cys4685	
		14276	GCA->ACA	Ala4690Thr	A234T
		14522	GTC->ATC	Val4772Ile	V316I
		14663	TCT->CCT	Ser4819Pro	S363P
		15049	GTT->GTC	Val4947	
		15701	CAC->TAC	His5165Tyr	H709Y
		15703	CAC->CAT	His5165	
		15915	CAG->CGG	Gln5236Arg	Q780R

	nsp12	15943 16200	TTT->TTC AAT->AGT	Phe5245 Asn5331Ser	N875S
ORF1ab	nsp13	16379	GTC->ATC	Val5391Ile	V7I
		16459	CAT->CAC	His5417	
		16995	CGC->CAC	Arg5596His	R212H
		17305	GCG->GCA	Ala5699	
		17509	CTG->CTA	Leu5767	
		17528	GTT->ATT	Val5774Ile	V390I
		17608	CTA->CTG	Leu5800	
		17840	TTA->CTA	Leu5878	
		17926	AAG->AAA	Lys5906	
	nsp14	18247 18643 18688 18789 19024 19442 19609 19666	GAC->GAT GTT->GTC TTG->TTA ACC->ATC TCT->TCC GCT->ACT GAG->GAA TTT->TTC	Asp6013 Val6145 Leu6160 Thr6194Ile Ser6272 Ala6412Thr Glu6467 Phe6486	T210I A428T
	nsp15	19822 19855 19924 19959 20054 20710	GCC->GCT AAA->AAG CCC->CCT GTG->GCG GAA->AAA GAT->GAC	Ala6538 Lys6549 Pro6572 Val6584Ala Glu6616Lys Asp6834	V79A E111K
	nsp16	20905 21274	TCG->TCA AAC->AAT	Ser6899 Asn7022	
2a	ns2	21810 21896 21971 21999 22019 22125 22223 22264 22283 22346 22497 22531	CCC->TCC CAG->CAA CAA->CAT GAG->AAG GAC->GAT CAA->TAA CTC->CTT GTG->GCG AAA->AAG CCT->CCC GTG->ATG TGT->TAT	Pro14Ser Gln42 Gln67His Glu77Lys Asp83 Gln119STOP Leu151 Val165Ala Lys171 Pro192 Val243Met Cys254Tyr	P14S Q67H E77K V165A V243M C254Y

	HE	HE	22565 22818 22894 22895 22930 22972 23332 23382 23427 23818 23902 23909			
S		Spike	25308 25872 26130 26458 26493 26499 26630 27048 27846	AAA->AAG GAA->GAG ATG->ATA AAT->GAT ACA->ACG GCT->GCC CGT->CCT AAA->AAG GAG->GAA	Lys460 Glu648 Met734Ile Asn844Asp Thr855 Ala857 Arg901Pro Lys1040 Glu1306	M734I N844D R901P
4	noncoding		27917			
	4a		28049	TTG->TTA	Leu19	
	noncoding		28054			
	4b		28354 28360	CTT->CTC AGG->AGA	Leu99 Arg101	
5		5a	28422 28477 28519 28586	TTA->TTG AAT->GAT AAG->GAG GGT->GAT	Leu16 Asn35Asp Lys49Glu Gly71Asp	N35D K49E G71D
E	E		28768	GCA->GCG	Ala21	
M		M	29067 29213 29306 29426	CTA->TTA GTG->GTA GGT->GGC GGC->GGT	Leu34 Val82 Gly113 Gly153	
N		N	29677 29939 29992 30283 30323	TTT->TTC ATT->GTT AAC->AAT TCG->TCA AGT->GGT	Phe3 Ile91Val Asn108 Ser205 Ser219Gly	I91V S219G

N	N	30450 30661 30901 30971	AAA>AGA GAA>GAG AGC>AGT TTG>CTG	Lys261Arg Glu331 Ser411 Leu435	K261R
UTR	noncoding	31047 31203			

^aMutations in orange represent residues that are conserved across human CoVs. Mutations in green represent residues where mutations arose in both MHV passage lineages.

C.2 MHV p30.2 mutations^a

ORF	Gene	Residue	SNP	Change	Gene AA
ORF1ab	nsp1	512	AGT->AGC	Ser101	
		928	GCT->GTT	Ala240Val	A240V
	nsp2	1418	GGC->GGT	Gly403	
		1634	CCA->CCG	Pro475	
		1853	CTT->CTC	Leu548	
		1925	CTT->CTC	Leu572	
		2099	GTT->GTC	Val630	
		2239	GCA->GTA	Ala677Val	A430V
	nsp3	2973	GTC->ATC	Val922Ile	V90I
		3238	GGA->GAA	Gly1010Glu	G178E
		3442	ACC->ATC	Thr1078Ile	T246I
		3578	CTG->CTA	Leu1123	
		4175	CCA->CCG	Pro1322	
		4340	GTG->GTA	Val1377	
		4793	GCG->GCA	Ala1528	
		5090	GTA->GTG	Val1627	
		5382	CTG->TTG	Leu1725	
		6277	ATT->ACT	Ile2023Thr	I1191T
		6463	GAT->GGT	Asp2085Gly	D1253G
		6480	GGT->AGT	Gly2091Ser	G1259S
		6513	GCT->ACT	Ala2102Thr	A1270T
		6612	GTT->ATT	Val2135Ile	V1303I
		6786	AAG->GAG	Lys2193Glu	K1361E
		7088	TTT->TTC	Phe2293	
		7451	CTG->CTA	Leu2414	
		7835	CAT->CAC	His2542	
		8055	GTG->ATG	Val2616Met	V1784M
		8066	GAG->GAA	Glu2619	
		8444	AAT->AAC	Asn2745	
		8765	TTG->TTA	Leu2852	
		9390	TTA->CTA	Leu3061	
		9398	GAG->GAA	Glu3063	
	nsp4	10037	TAC->TAT	Tyr3276	
	nsp5	10312	AAA->AGA	Lys3368Arg	K35R
		10485	CTG->TTG	Leu3426	
		10715	ACT->ACC	Thr3502	
		10760	CCC->CCT	Pro3517	

	nsp5	11009	AAG->AAA	Lys3600	
	nsp6	11369 11558 11696	GTT->GTC AGC->AGT GTG->GTA	Val3720 Ser3783 Val3829	
	nsp8	12509 12604 12752	TTG->TTA GCA->GTA CAA->CAG	Leu4100 Ala4132Val Gln4181	A117V
	nsp10	13176 13383	GCA->ACA GTT->ATT	Ala4323Thr Val4392Ile	A4T V73I
ORF1ab	nsp12	13702 13848 14096 14107 14277 15231 15595 16016 16329	CGA->CGG AAA->AGA GTG->ATG AAG->AAA GCA->GTA ACC->ATC CCA->CCG ATG->GTG AAG->AGG	Arg4498 Lys4547Arg Val4630Met Lys4633 Ala4690Val Thr5008Ile Pro5129 Met5270Val Lys5374Arg	K91R V174M A234V T552I M814V K918R
		16480 17176 17416 17788	AAA->AAG GGA->GGG CGC->CGT AAG->AAA	Lys5424 Gly5656 Arg5736 Lys5860	
		18266 19197	GAT->AAT AAG->AGG	Asp6020Asn Lys6330Arg	D36N K346R
	nsp15	19733	AAT->GAT	Asn6509Asp	N4D
	nsp16	20854 21532	GCT->GCC CTG->CTA	Ala6882 Leu7108	
	noncoding region	21752			
	2a	ns2	21971 22087 22134 22194 22259 22281	CAA->CAT ATT->ACT CAC->TAC CAA->TAA GAG->GAA AAA->GAA	Gln67His Ile106Thr His122Tyr Gln142STOP Glu163 Lys171Glu
					Q67H I106T H122Y Q142*
HE	HE	22646 22995 23082 23526 23601			
S	Spike	24109 24691	GCC->ACC GCT->ACT	Ala61Thr Ala255Thr	A61T A255T

S	Spike	24708 24978 25028 25125 25250 25384 25701 25924 25968 26067 26630 27780	GTT->GTC ACT->ACC GCT->GTT AGG->AGA CAT->CGT ATA->GTA CAA->CAG ATT->GTT TTG->TTA CGC->CGT CGT->CCT TTC->TTT	Val260 Thr350 Ala367Val Arg399 His441Arg Ile486Val Gln591 Ile666Val Leu680 Arg713 Arg901Pro Phe1284	A367V H441R I486V I666V R901P
4	4b	28242	ACA->ATA	Thr62Ile	T62I
E	E	28768 28923	GCA->GCG ATG->ACG	Ala21 Met73Thr	M73T
M	M	29369 29591	GTG->GTA GTC->GTT	Val134 Val208	
N	N	29678 30460 30615 30841 30874 30898 30905	GTT->ATT AGG->AGA GAG->GGG AAG->AAA GAA->GAG GTA->GTG GCA->ACA	Val4Ile Arg264 Glu316Gly Lys391 Glu402 Val410 Ala413Thr	E316G A413T
UTR	noncoding region	31055			

^aMutations in orange represent residues that are conserved across human CoVs. Mutations in green represent residues where mutations arose in both MHV passage lineages.

C.3 MHV p19.1 mutations^a

ORF	Gene	Residue	SNP	Change	Gene AA
ORF1ab	nsp2	965	CTG->CTA	Leu252	
		1160	GTA->GTG	Val317	
		2581	TCT->TTT	Ser791Phe	S544F
	nsp3	3237	GGA->AGA	Gly1010Arg	G178R
		3363	GAG->AAG	Glu1052Lys	E220K
		4383	GCC->ACC	Ala1392Thr	A560T
		5090	GTA->GTG	Val1627	
		6611		Pro2134	
		6870	GGC->GGT	Gly2516	
	nsp5	10430	AGC->AGT	Ser3407	
	nsp6	11273	GTA->GTG	Val3688	
	nsp12	15703	CAC->CAT	His5165	
		15915	CAG->CGG	Gln5236Arg	Q780R
2a	ns2	21971	CAA->CAT	Gln67His	Q67H
S	Spike	25716	GAG->GAA	Glu596	
		26630	CGT->CCT	Arg901Pro	R901P
UTR	noncoding	31047			

^a. Mutations in green represent residues where mutations arose in both MHV passage lineages.

C.4 MHV p19.2 mutations^a

ORF	Gene	Residue	SNP	Change	Gene AA
ORF1ab	nsp1	512	AGT->AGC	Ser101	
	nsp2	1634	CCA->CCG	Pro475	
		1853	CTT->CTC	Leu548	
		2099	GTT->GTC	Val630	
	nsp3	2973	GTC->ATC	Val922Ile	V90I
		3442	ACC->ATC	Thr1078Ile	T246I
		3578	CTG->CTA	Leu1123	
		4793	GCG->GCA	Ala1528	
		5382	CTG->TTG	Leu1725	
		6480	GGT->AGT	Gly2091Ser	G1259S
		6513	GCT->ACT	Ala2102Thr	A1270T
		6786	AAG->GAG	Lys2193Glu	K1361E
		7451	CTG->CTA	Leu2414	
		7835	CAT->CAC	His2542	
		8444	AAT->AAC	Asn2745	
		8765	TTG->TTA	Leu2852	
	nsp5	9390	TTA->CTA	Leu3061	
		9398	GAG->GAA	Glu3063	
	nsp8	10485	CTG->TTG	Leu3426	
		10715	ACT->ACC	Thr3502	
		10760	CCC->CCT	Pro3517	
		11009	AAG->AAA	Lys3600	
	nsp10	12509	TTG->TTA	Leu4100	
		12604	GCA->GTA	Ala4132Val	A117V
	nsp10	13383	GTT->ATT	Val4392Ile	V73I
	nsp12	14096	GTG->ATG	Val4630Met	V174M
		15231	ACC->ATC	Thr5008Ile	T552I
		16329	AAG->AGG	Lys5374Arg	K918R
	nsp13	16480	AAA->AAG	Lys5424	
		17788	AAG->AAA	Lys5860	
	nsp14	18266	GAT->AAT	Asp6020Asn	D36N
		19197	AAG->AGG	Lys6330Arg	K346R
	nsp15	21532	CTG->CTA	Leu7108	
	Noncoding	21752			
2a	ns2	21971	CAA->CAT	Gln67His	Q67H
		22087	ATT->ACT	Ile106Thr	I106T
HE	HE	23082			

HE	HE	23601			
S	Spike	24691	GCT->ACT	Ala255Thr	A255T
		24708	GTT->GTC	Val260	
		25125	AGG->AGA	Arg399	
		25250	CAT->CGT	His441Arg	H441R
		25701	CAA->CAG	Gln591	
		25924	ATT->GTT	Ile666Val	I666V
		25968	TTG->TTA	Leu680	
		26067	CGC->CGT	Arg713	
		26630	CGT->CCT	Arg901Pro	R901P
		27780	TTC->TTT	Phe1284	
E	E	28768	GCA->GCG	Ala21	
		28923	ATG->ACG	Met73Thr	M73T
M	M	29369	GTG->GTA	Val134	
N	N	29678	GTT->ATT	Val4Ile	V4I
		30460	AGG->AGA	Arg264	
		30615	GAG->GGG	Glu316Gly	E316G
		30841	AAG->AAA	Lys391	
		30874	GAA->GAG	Glu402	
		30898	GTA->GTG	Val410	
		30905	GCA->ACA	Ala413Thr	A413T

^aMutations in orange represent residues that are conserved across human CoVs. Mutations in green represent residues where mutations arose in both MHV passage lineages.

C.5 MERS-CoV p30.1 mutations^a

ORF	Gene	Residue	SNP	Change	Gene AA
ORF1ab	nsp4	8685	GTA -> ATA	Val2803Ile	V63I
	nsp5	10295	TTG -> TTA	Leu3339	
		10823	GCG -> GCA	Ala3515	
	nsp6	11066	ACA -> ACG	Thr3596	
	nsp 7	12033	GAT -> AAT	Asp3919Asn	D74N
	nsp10	13073	CTC -> CTT	Leu4265	
	nsp12	15080	GTT -> ATT	Val4935Ile	V558I
	nsp13	17260	ACA -> ACG	Thr5661	
		18169	TCC -> TCT	Ser5964	
		18622	TGT -> TGC	Cys6115	
	nsp14	18907	GAA -> GAG GAA -> GGA	Glu6210	
		19347	CAT -> CAC	Glu6357Gly	E449G
		19354	GCT -> ACT	His6359	
		19418		Ala6381Thr	A473T
		19816	TAC -> TAT	Tyr6513	
	nsp15	20581	CAA -> CAG	Gln6768	
S	Spike	21735	GGC -> CGC	Gly94Arg	G94R
		23201	AAT -> AAC	Asn582	
		23201	AAT -> AAC	Asn582	
		24112	GCA -> GTA	Ala886Val	A886V
		24504	GAA -> AAA	Glu1017Lys	E1017L
		24569	AGC -> AGT	Ser1038	
		25207	TCC -> TTC	Ser1251Phe	S1251F
		25383	TTA -> CTA	Leu1310	
		25601	AAA -> GAA	Lys24Glu	K24D
Deletion: 25685-27263; Part of ORFs 3 and 5, and all of ORFs 4a and 4b were deleted.					
5	ORF5	27500	TCG -> CCG	Ser221Pro	S221P
E	Envelope	27752	GCA -> ACA	Ala55Thr	A55T
M	Membrane	27859	AAT -> GAT	Asn3Asp	N3D
N	Nucleocapsid	28593	GTT -> ATT	Val10Ile	V10I
		29187	GCA -> ACA	Ala208Thr	A208T

^aMutations in green represent residues where mutations arose in both MHV passage lineages.

C.6 MERS-CoV p30.2 mutations^a

ORF	Gene	Residue	SNP	Change	Gene AA
ORF1ab	nsp2	1173	CGC -> TGC	Arg299Cys	R105C
		1822	AAA -> AGA	Lys515Arg	K322R
		2611	ACT -> ATT	Thr778Ile	T585I
		2693	ATG -> ATA	Met805Ile	M612I
		2797	AAT -> AGT	Asn840Ser	N647S
	nsp3	4626	AAG -> GAG	Lys1450Glu	K596E
		4724	CAG -> CAA	Gln1482	
		5139	CAT -> TAT	His1621Tyr	H767Y
	nsp4	8506	ACA -> ATA	Thr2743Ile	T3I
		9294	GAT -> AAT	Asp3006Asn	D266N
	nsp5	10326	GCC -> ACC	Ala3350Thr	A103T
	nsp6	11297	ATT -> ATC	Ile3673	
		11372	TTG -> TTA	Leu3698	
	nsp8	12076	GAG -> GGG	Glu3933Gly	E5G
	nsp12	13906	TTT -> TTC	Phe4543	
		14323	GAC -> GAT	Asp4682	
		15080	GTT -> ATT	Val4935Ile	V558I
		15754	AAT -> AAC	Asn5159	
		15820	ACC -> ACT	Thr5181	
	nsp13	18067	TAT -> TAC	Tyr5930	
	nsp14	19090	CTT -> CTC	Leu6271	
		19466	AGA -> GGA	Arg6397Gly	R489G?
	nsp15	19615	CAT -> CAC	His6446	
		20423	GCT -> ACT	Ala6716Thr	A284T
	S	21735	GGC -> CGC	Gly94Arg	G94R
		22022	CCT -> CCC	Pro189	
		22691	ACC -> ACT	Thr412	
		23152	CAA -> CGA	Gln566Arg	Q566R
		23777	AAT -> AAC	Asn774	
		24112	GCA -> GTA	Ala886Val	A886V
		24504	GAA -> AAA	Glu1017Lys	E1017L
		25175	AAA -> AAG	Lys1240	
		25207	TCC -> TTC	Ser1251Phe	S1251F
5	ORF5	26841	ATG -> ACG	Met1Thr	M1T
		26886	GTT -> GCT	Val16Ala	V16A
		26888	TCT -> ACT	Ser17	
		26889	TCT -> TGT	Ser17	
	5	ORF5	26922	TCT -> TTT	Ser28Phe

		27163	TGG -> TGA	Trp108Stop	Y108*
E	Envelope	27768	AAT -> AGT	Asn60Ser	N60S
M	Membrane	28323	GCT -> GCC	Ala157	
N	Nucleocapsid	28597 29624	TCC -> TTC CAA -> CAG	Ser11Phe Gln353	S11F

^aMutations in green represent residues where mutations arose in both MHV passage lineages.

APPENDIX D: COPYRIGHT PERMISSIONS

D.1. Ferrer-Orta et al., 2006, reproduced in Figure 5.

ELSEVIER LICENSE TERMS AND CONDITIONS

Aug 21, 2019

This Agreement between Ms. Maria Agostini ("You") and Elsevier ("Elsevier") consists of your license details and the terms and conditions provided by Elsevier and Copyright Clearance Center.

License Number	4653900435565
License date	Aug 21, 2019
Licensed Content Publisher	Elsevier
Licensed Content Publication	Current Opinion in Structural Biology
Licensed Content Title	A comparison of viral RNA-dependent RNA polymerases
Licensed Content Author	Cristina Ferrer-Orta,Armando Arias,Cristina Escarmís,Nuria Verdaguer
Licensed Content Date	Feb 1, 2006
Licensed Content Volume	16
Licensed Content Issue	1
Licensed Content Pages	8
Start Page	27
End Page	34
Type of Use	reuse in a thesis/dissertation
Portion	figures/tables/illustrations
Number of figures/tables/illustrations	1
Format	both print and electronic
Are you the author of this Elsevier article?	No
Will you be translating?	No
Original figure numbers	Figure 1
Title of your thesis/dissertation	Investigating Nucleoside Analogue Inhibition of Coronavirus Replication

Expected completion date	Oct 2019
Estimated size (number of pages)	200
Requestor Location	Ms. Maria Agostini Vanderbilt University Medical Center MCN D-6221 1161 21st Ave S NASHVILLE, TN 37232 United States Attn: Maria Agostini
Publisher Tax ID	98-0397604
Total	0.00 USD

[Terms and Conditions](#)

INTRODUCTION

1. The publisher for this copyrighted material is Elsevier. By clicking "accept" in connection with completing this licensing transaction, you agree that the following terms and conditions apply to this transaction (along with the Billing and Payment terms and conditions established by Copyright Clearance Center, Inc. ("CCC"), at the time that you opened your Rightslink account and that are available at any time at <http://myaccount.copyright.com>).

GENERAL TERMS

2. Elsevier hereby grants you permission to reproduce the aforementioned material subject to the terms and conditions indicated.

3. Acknowledgement: If any part of the material to be used (for example, figures) has appeared in our publication with credit or acknowledgement to another source, permission must also be sought from that source. If such permission is not obtained then that material may not be included in your publication/copies. Suitable acknowledgement to the source must be made, either as a footnote or in a reference list at the end of your publication, as follows:

"Reprinted from Publication title, Vol /edition number, Author(s), Title of article / title of chapter, Pages No., Copyright (Year), with permission from Elsevier [OR APPLICABLE SOCIETY COPYRIGHT OWNER]." Also Lancet special credit - "Reprinted from The Lancet, Vol. number, Author(s), Title of article, Pages No., Copyright (Year), with permission from Elsevier."

4. Reproduction of this material is confined to the purpose and/or media for which permission is hereby given.

5. Altering/Modifying Material: Not Permitted. However figures and illustrations may be altered/adapted minimally to serve your work. Any other abbreviations, additions, deletions and/or any other alterations shall be made only with prior written authorization of Elsevier Ltd. (Please contact Elsevier at permissions@elsevier.com). No modifications can be made to any Lancet figures/tables and they must be reproduced in full.

6. If the permission fee for the requested use of our material is waived in this instance, please be advised that your future requests for Elsevier materials may attract a fee.

7. Reservation of Rights: Publisher reserves all rights not specifically granted in the combination of (i) the license details provided by you and accepted in the course of this

licensing transaction, (ii) these terms and conditions and (iii) CCC's Billing and Payment terms and conditions.

8. License Contingent Upon Payment: While you may exercise the rights licensed immediately upon issuance of the license at the end of the licensing process for the transaction, provided that you have disclosed complete and accurate details of your proposed use, no license is finally effective unless and until full payment is received from you (either by publisher or by CCC) as provided in CCC's Billing and Payment terms and conditions. If full payment is not received on a timely basis, then any license preliminarily granted shall be deemed automatically revoked and shall be void as if never granted. Further, in the event that you breach any of these terms and conditions or any of CCC's Billing and Payment terms and conditions, the license is automatically revoked and shall be void as if never granted. Use of materials as described in a revoked license, as well as any use of the materials beyond the scope of an unrevoked license, may constitute copyright infringement and publisher reserves the right to take any and all action to protect its copyright in the materials.

9. Warranties: Publisher makes no representations or warranties with respect to the licensed material.

10. Indemnity: You hereby indemnify and agree to hold harmless publisher and CCC, and their respective officers, directors, employees and agents, from and against any and all claims arising out of your use of the licensed material other than as specifically authorized pursuant to this license.

11. No Transfer of License: This license is personal to you and may not be sublicensed, assigned, or transferred by you to any other person without publisher's written permission.

12. No Amendment Except in Writing: This license may not be amended except in a writing signed by both parties (or, in the case of publisher, by CCC on publisher's behalf).

13. Objection to Contrary Terms: Publisher hereby objects to any terms contained in any purchase order, acknowledgment, check endorsement or other writing prepared by you, which terms are inconsistent with these terms and conditions or CCC's Billing and Payment terms and conditions. These terms and conditions, together with CCC's Billing and Payment terms and conditions (which are incorporated herein), comprise the entire agreement between you and publisher (and CCC) concerning this licensing transaction. In the event of any conflict between your obligations established by these terms and conditions and those established by CCC's Billing and Payment terms and conditions, these terms and conditions shall control.

14. Revocation: Elsevier or Copyright Clearance Center may deny the permissions described in this License at their sole discretion, for any reason or no reason, with a full refund payable to you. Notice of such denial will be made using the contact information provided by you. Failure to receive such notice will not alter or invalidate the denial. In no event will Elsevier or Copyright Clearance Center be responsible or liable for any costs, expenses or damage incurred by you as a result of a denial of your permission request, other than a refund of the amount(s) paid by you to Elsevier and/or Copyright Clearance Center for denied permissions.

LIMITED LICENSE

The following terms and conditions apply only to specific license types:

15. Translation: This permission is granted for non-exclusive world **English** rights only unless your license was granted for translation rights. If you licensed translation rights you may only translate this content into the languages you requested. A professional translator must perform all translations and reproduce the content word for word preserving the integrity of the article.

16. Posting licensed content on any Website: The following terms and conditions apply as follows: Licensing material from an Elsevier journal: All content posted to the web site must maintain the copyright information line on the bottom of each image; A hyper-text must be included to the Homepage of the journal from which you are licensing at <http://www.sciencedirect.com/science/journal/xxxxx> or the Elsevier homepage for books at <http://www.elsevier.com>; Central Storage: This license does not include permission for a scanned version of the material to be stored in a central repository such as that provided by Heron/XanEdu.

Licensing material from an Elsevier book: A hyper-text link must be included to the Elsevier homepage at <http://www.elsevier.com>. All content posted to the web site must maintain the copyright information line on the bottom of each image.

Posting licensed content on Electronic reserve: In addition to the above the following clauses are applicable: The web site must be password-protected and made available only to bona fide students registered on a relevant course. This permission is granted for 1 year only. You may obtain a new license for future website posting.

17. For journal authors: the following clauses are applicable in addition to the above:

Preprints:

A preprint is an author's own write-up of research results and analysis, it has not been peer-reviewed, nor has it had any other value added to it by a publisher (such as formatting, copyright, technical enhancement etc.).

Authors can share their preprints anywhere at any time. Preprints should not be added to or enhanced in any way in order to appear more like, or to substitute for, the final versions of articles however authors can update their preprints on arXiv or RePEc with their Accepted Author Manuscript (see below).

If accepted for publication, we encourage authors to link from the preprint to their formal publication via its DOI. Millions of researchers have access to the formal publications on ScienceDirect, and so links will help users to find, access, cite and use the best available version. Please note that Cell Press, The Lancet and some society-owned have different preprint policies. Information on these policies is available on the journal homepage.

Accepted Author Manuscripts: An accepted author manuscript is the manuscript of an article that has been accepted for publication and which typically includes author-incorporated changes suggested during submission, peer review and editor-author communications.

Authors can share their accepted author manuscript:

- immediately
 - via their non-commercial person homepage or blog
 - by updating a preprint in arXiv or RePEc with the accepted manuscript

- via their research institute or institutional repository for internal institutional uses or as part of an invitation-only research collaboration work-group
 - directly by providing copies to their students or to research collaborators for their personal use
 - for private scholarly sharing as part of an invitation-only work group on commercial sites with which Elsevier has an agreement
- After the embargo period
 - via non-commercial hosting platforms such as their institutional repository
 - via commercial sites with which Elsevier has an agreement

In all cases accepted manuscripts should:

- link to the formal publication via its DOI
- bear a CC-BY-NC-ND license - this is easy to do
- if aggregated with other manuscripts, for example in a repository or other site, be shared in alignment with our hosting policy not be added to or enhanced in any way to appear more like, or to substitute for, the published journal article.

Published journal article (JPA): A published journal article (PJA) is the definitive final record of published research that appears or will appear in the journal and embodies all value-adding publishing activities including peer review co-ordination, copy-editing, formatting, (if relevant) pagination and online enrichment.

Policies for sharing publishing journal articles differ for subscription and gold open access articles:

Subscription Articles: If you are an author, please share a link to your article rather than the full-text. Millions of researchers have access to the formal publications on ScienceDirect, and so links will help your users to find, access, cite, and use the best available version.

Theses and dissertations which contain embedded PJAs as part of the formal submission can be posted publicly by the awarding institution with DOI links back to the formal publications on ScienceDirect.

If you are affiliated with a library that subscribes to ScienceDirect you have additional private sharing rights for others' research accessed under that agreement. This includes use for classroom teaching and internal training at the institution (including use in course packs and courseware programs), and inclusion of the article for grant funding purposes.

Gold Open Access Articles: May be shared according to the author-selected end-user license and should contain a [CrossMark logo](#), the end user license, and a DOI link to the formal publication on ScienceDirect.

Please refer to Elsevier's [posting policy](#) for further information.

18. For book authors the following clauses are applicable in addition to the above: Authors are permitted to place a brief summary of their work online only. You are not allowed to download and post the published electronic version of your chapter, nor may you scan the printed edition to create an electronic version. **Posting to a**

repository: Authors are permitted to post a summary of their chapter only in their institution's repository.

19. Thesis/Dissertation: If your license is for use in a thesis/dissertation your thesis may be submitted to your institution in either print or electronic form. Should your thesis be published commercially, please reapply for permission. These requirements include permission for the Library and Archives of Canada to supply single copies, on demand, of the complete thesis and include permission for Proquest/UMI to supply single copies, on demand, of the complete thesis. Should your thesis be published commercially, please reapply for permission. Theses and dissertations which contain embedded PJsAs as part of the formal submission can be posted publicly by the awarding institution with DOI links back to the formal publications on ScienceDirect.

Elsevier Open Access Terms and Conditions

You can publish open access with Elsevier in hundreds of open access journals or in nearly 2000 established subscription journals that support open access publishing.

Permitted third party re-use of these open access articles is defined by the author's choice of Creative Commons user license. See our [open access license policy](#) for more information.

Terms & Conditions applicable to all Open Access articles published with Elsevier:

Any reuse of the article must not represent the author as endorsing the adaptation of the article nor should the article be modified in such a way as to damage the author's honour or reputation. If any changes have been made, such changes must be clearly indicated. The author(s) must be appropriately credited and we ask that you include the end user license and a DOI link to the formal publication on ScienceDirect.

If any part of the material to be used (for example, figures) has appeared in our publication with credit or acknowledgement to another source it is the responsibility of the user to ensure their reuse complies with the terms and conditions determined by the rights holder.

Additional Terms & Conditions applicable to each Creative Commons user license:

CC BY: The CC-BY license allows users to copy, to create extracts, abstracts and new works from the Article, to alter and revise the Article and to make commercial use of the Article (including reuse and/or resale of the Article by commercial entities), provided the user gives appropriate credit (with a link to the formal publication through the relevant DOI), provides a link to the license, indicates if changes were made and the licensor is not represented as endorsing the use made of the work. The full details of the license are available at <http://creativecommons.org/licenses/by/4.0>.

CC BY NC SA: The CC BY-NC-SA license allows users to copy, to create extracts, abstracts and new works from the Article, to alter and revise the Article, provided this is not done for commercial purposes, and that the user gives appropriate credit (with a link to the formal publication through the relevant DOI), provides a link to the license, indicates if changes were made and the licensor is not represented as endorsing the use made of the work. Further, any new works must be made available on the same conditions. The full details of the license are available at <http://creativecommons.org/licenses/by-nc-sa/4.0>.

CC BY NC ND: The CC BY-NC-ND license allows users to copy and distribute the Article, provided this is not done for commercial purposes and further does not permit distribution of the Article if it is changed or edited in any way, and provided the user gives appropriate credit (with a link to the formal publication through the relevant DOI), provides a link to the license, and that the licensor is not represented as endorsing the use made of the work. The full details of the license are available at <http://creativecommons.org/licenses/by-nc-nd/4.0>. Any commercial reuse of Open Access articles published with a CC BY NC SA or CC BY NC ND license requires permission from Elsevier and will be subject to a fee.

Commercial reuse includes:

- Associating advertising with the full text of the Article
- Charging fees for document delivery or access
- Article aggregation
- Systematic distribution via e-mail lists or share buttons

Posting or linking by commercial companies for use by customers of those companies.

20. Other Conditions:

v1.9

Questions? customercare@copyright.com or +1-855-239-3415 (toll free in the US) or +1-978-646-2777.

D.2. de Wit et al., 2016, reproduced in Figure 6.

**SPRINGER NATURE LICENSE
TERMS AND CONDITIONS**

Aug 21, 2019

This Agreement between Ms. Maria Agostini ("You") and Springer Nature ("Springer Nature") consists of your license details and the terms and conditions provided by Springer Nature and Copyright Clearance Center.

License Number	4653900544322
License date	Aug 21, 2019
Licensed Content Publisher	Springer Nature
Licensed Content Publication	Nature Reviews Microbiology
Licensed Content Title	SARS and MERS: recent insights into emerging coronaviruses
Licensed Content Author	Emmie de Wit, Neeltje van Doremalen, Darryl Falzarano, Vincent J. Munster
Licensed Content Date	Jun 27, 2016
Licensed Content Volume	14
Licensed Content Issue	8
Type of Use	Thesis/Dissertation
Requestor type	academic/university or research institute
Format	print and electronic
Portion	figures/tables/illustrations
Number of figures/tables/illustrations	1
High-res required	no
Will you be translating?	no
Circulation/distribution	<501
Author of this Springer Nature content	no
Title	Investigating Nucleoside Analogue Inhibition of Coronavirus Replication
Institution name	n/a
Expected presentation date	Oct 2019
Portions	Figure 1b
Requestor Location	Ms. Maria Agostini Vanderbilt University Medical Center

MCN D-6221
1161 21st Ave S
NASHVILLE, TN 37232
United States
Attn: Maria Agostini

Total 0.00 USD

Terms and Conditions

Springer Nature Customer Service Centre GmbH

Terms and Conditions

This agreement sets out the terms and conditions of the licence (the **Licence**) between you and **Springer Nature Customer Service Centre GmbH** (the **Licensor**). By clicking 'accept' and completing the transaction for the material (**Licensed Material**), you also confirm your acceptance of these terms and conditions.

1. Grant of License

1. The Licensor grants you a personal, non-exclusive, non-transferable, world-wide licence to reproduce the Licensed Material for the purpose specified in your order only. Licences are granted for the specific use requested in the order and for no other use, subject to the conditions below.
2. The Licensor warrants that it has, to the best of its knowledge, the rights to license reuse of the Licensed Material. However, you should ensure that the material you are requesting is original to the Licensor and does not carry the copyright of another entity (as credited in the published version).
3. If the credit line on any part of the material you have requested indicates that it was reprinted or adapted with permission from another source, then you should also seek permission from that source to reuse the material.

2. Scope of Licence

1. You may only use the Licensed Content in the manner and to the extent permitted by these Ts&Cs and any applicable laws.
2. A separate licence may be required for any additional use of the Licensed Material, e.g. where a licence has been purchased for print only use, separate permission must be obtained for electronic re-use. Similarly, a licence is only valid in the language selected and does not apply for editions in other languages unless additional translation rights have been granted separately in the licence. Any content owned by third parties are expressly excluded from the licence.
3. Similarly, rights for additional components such as custom editions and derivatives require additional permission and may be subject to an additional fee. Please apply to Journalpermissions@springernature.com/bookpermissions@springernature.com for these rights.
4. Where permission has been granted **free of charge** for material in print, permission may also be granted for any electronic version of that work, provided that the

material is incidental to your work as a whole and that the electronic version is essentially equivalent to, or substitutes for, the print version.

5. An alternative scope of licence may apply to signatories of the [STM Permissions Guidelines](#), as amended from time to time.

- **Duration of Licence**

1. A licence for is valid from the date of purchase ('Licence Date') at the end of the relevant period in the below table:

Scope of Licence	Duration of Licence
Post on a website	12 months
Presentations	12 months
Books and journals	Lifetime of the edition in the language purchased

- **Acknowledgement**

1. The Licensor's permission must be acknowledged next to the Licensed Material in print. In electronic form, this acknowledgement must be visible at the same time as the figures/tables/illustrations or abstract, and must be hyperlinked to the journal/book's homepage. Our required acknowledgement format is in the Appendix below.

- **Restrictions on use**

1. Use of the Licensed Material may be permitted for incidental promotional use and minor editing privileges e.g. minor adaptations of single figures, changes of format, colour and/or style where the adaptation is credited as set out in Appendix 1 below. Any other changes including but not limited to, cropping, adapting, omitting material that affect the meaning, intention or moral rights of the author are strictly prohibited.
2. You must not use any Licensed Material as part of any design or trademark.
3. Licensed Material may be used in Open Access Publications (OAP) before publication by Springer Nature, but any Licensed Material must be removed from OAP sites prior to final publication.

- **Ownership of Rights**

1. Licensed Material remains the property of either Licensor or the relevant third party and any rights not explicitly granted herein are expressly reserved.

- **Warranty**

IN NO EVENT SHALL LICENSOR BE LIABLE TO YOU OR ANY OTHER PARTY OR ANY OTHER PERSON OR FOR ANY SPECIAL, CONSEQUENTIAL, INCIDENTAL OR INDIRECT DAMAGES, HOWEVER CAUSED, ARISING OUT OF OR IN CONNECTION WITH THE DOWNLOADING, VIEWING OR USE OF THE MATERIALS REGARDLESS OF THE FORM OF ACTION, WHETHER FOR BREACH OF CONTRACT, BREACH OF WARRANTY, TORT, NEGLIGENCE, INFRINGEMENT OR OTHERWISE (INCLUDING, WITHOUT LIMITATION, DAMAGES BASED ON LOSS OF PROFITS, DATA, FILES,

USE, BUSINESS OPPORTUNITY OR CLAIMS OF THIRD PARTIES), AND WHETHER OR NOT THE PARTY HAS BEEN ADVISED OF THE POSSIBILITY OF SUCH DAMAGES. THIS LIMITATION SHALL APPLY NOTWITHSTANDING ANY FAILURE OF ESSENTIAL PURPOSE OF ANY LIMITED REMEDY PROVIDED HEREIN.

- **Limitations**

1. **BOOKS ONLY:** Where '**reuse in a dissertation/thesis**' has been selected the following terms apply: Print rights of the final author's accepted manuscript (for clarity, NOT the published version) for up to 100 copies, electronic rights for use only on a personal website or institutional repository as defined by the Sherpa guideline (www.sherpa.ac.uk/romeo/).

- **Termination and Cancellation**

1. Licences will expire after the period shown in Clause 3 (above).
2. Licensee reserves the right to terminate the Licence in the event that payment is not received in full or if there has been a breach of this agreement by you.

Appendix 1 — Acknowledgements:

For Journal Content:

Reprinted by permission from [the Licensor]: [Journal Publisher (e.g. Nature/Springer/Palgrave)] [JOURNAL NAME] [REFERENCE CITATION](Article name, Author(s) Name), [COPYRIGHT] (year of publication)

For Advance Online Publication papers:

Reprinted by permission from [the Licensor]: [Journal Publisher (e.g. Nature/Springer/Palgrave)] [JOURNAL NAME] [REFERENCE CITATION](Article name, Author(s) Name), [COPYRIGHT] (year of publication), advance online publication, day month year (doi: 10.1038/sj.[JOURNAL ACRONYM].)

For Adaptations/Translations:

Adapted/Translated by permission from [the Licensor]: [Journal Publisher (e.g. Nature/Springer/Palgrave)] [JOURNAL NAME] [REFERENCE CITATION](Article name, Author(s) Name), [COPYRIGHT] (year of publication)

Note: For any republication from the British Journal of Cancer, the following credit line style applies:

Reprinted/adapted/translated by permission from [the Licensor]: on behalf of Cancer Research UK: : [Journal Publisher (e.g. Nature/Springer/Palgrave)] [JOURNAL NAME] [REFERENCE CITATION] (Article name, Author(s) Name), [COPYRIGHT] (year of publication)

For Advance Online Publication papers:

Reprinted by permission from The [the Licensor]: on behalf of Cancer Research UK: [Journal Publisher (e.g. Nature/Springer/Palgrave)] [JOURNAL NAME] [REFERENCE CITATION] (Article name, Author(s) Name), [COPYRIGHT] (year of publication), advance online publication, day month year (doi: 10.1038/sj.[JOURNAL ACRONYM])

For Book content:

Reprinted/adapted by permission from [the Licensor]: [Book Publisher] (e.g. Palgrave Macmillan, Springer etc) [Book Title] by [Book author(s)] [COPYRIGHT] (year of publication)

Other Conditions:

Version 1.2

Questions? customercare@copyright.com or +1-855-239-3415 (toll free in the US) or +1-978-646-2777.

REFERENCES

- Adedeji, A.O., Singh, K., Calcaterra, N.E., DeDiego, M.L., Enjuanes, L., Weiss, S., and Sarafianos, S.G. (2012). Severe acute respiratory syndrome coronavirus replication inhibitor that interferes with the nucleic acid unwinding of the viral helicase. *Antimicrob. Agents Chemother.* *56*, 4718–4728.
- Adedeji, A.O., and Lazarus, H. (2016). Biochemical characterization of Middle East respiratory syndrome coronavirus helicase. *mSphere* *1*, 4894.
- Adedeji, A.O., and Sarafianos, S.G. (2014). Antiviral drugs specific for coronaviruses in preclinical development. *Curr Opin Virol.* *8*, 45–53.
- Adedeji, A.O., Singh, K., Kassim, A., Coleman, C.M., Elliott, R., Weiss, S.R., Frieman, M.B., and Sarafianos, S.G. (2014). Evaluation of SSYA10-001 as a replication inhibitor of severe acute respiratory syndrome, mouse hepatitis, and Middle East respiratory syndrome coronaviruses. *Antimicrob. Agents Chemother.* *58*, 4894–4898.
- Agnihothram, S., Gopal, R., Yount, B.L., Donaldson, E.F., Menachery, V.D., Graham, R.L., Scobey, T.D., Gralinski, L.E., Denison, M.R., Zambon, M., et al. (2014). Evaluation of serologic and antigenic relationships between middle eastern respiratory syndrome coronavirus and other coronaviruses to develop vaccine platforms for the rapid response to emerging coronaviruses. *J Infect Dis.* *209*, 995–1006.
- Agostini, M.L., Andres, E.L., Sims, A.C., Graham, R.L., Sheahan, T.P., Lu, X., Smith, E.C., Case, J.B., Feng, J.Y., Jordan, R., et al. (2018). Coronavirus susceptibility to the antiviral remdesivir (GS-5734) is mediated by the viral polymerase and the proofreading exoribonuclease. *mBio* *9*, 1953.
- Ahn, D.-G., Choi, J.-K., Taylor, D.R., and Oh, J.-W. (2012). Biochemical characterization of a recombinant SARS coronavirus nsp12 RNA-dependent RNA polymerase capable of copying viral RNA templates. *Arch Virol* *157*, 2095–2104.
- Almazán, F., Márquez-Jurado, S., Nogales, A., and Enjuanes, L. (2015). Engineering infectious cDNAs of coronavirus as bacterial artificial chromosomes. *Methods Mol. Biol.* *1282*, 135–152.
- Alqahtani, F.Y., Aleanizy, F.S., Hadi Mohamed, El, R.A., Alanazi, M.S., Mohamed, N., Alrasheed, M.M., Abanmy, N., and Alhawassi, T. (2019). Prevalence of comorbidities in cases of Middle East respiratory syndrome coronavirus: a retrospective study. *Epidemiology and Infection* *147*, 1–5.
- Alshukairi, A.N., Zheng, J., Zhao, J., Nehdi, A., Baharoon, S.A., Layqah, L., Bokhari, A., Johani, Al, S.M., Samman, N., Boudjelal, M., et al. (2018). High prevalence of MERS-CoV infection in camel workers in Saudi Arabia. *mBio* *9*, e01985–18.

Antaki, N., Craxi, A., Kamal, S., Moucari, R., Van der Merwe, S., Haffar, S., Gadano, A., Zein, N., Lai, C.L., Pawlotsky, J.-M., et al. (2010). The neglected hepatitis C virus genotypes 4, 5 and 6: an international consensus report. *Liver Int.* *30*, 342–355.

Anthony, S.J., Gilardi, K., Menachery, V.D., Goldstein, T., Ssebide, B., Mbabazi, R., Navarrete-Macias, I., Liang, E., Wells, H., Hicks, A., et al. (2017). Further evidence for bats as the evolutionary source of Middle East respiratory syndrome coronavirus. *mBio* *8*, e00373–17.

Aouadi, W., Eydoux, C., Coutard, B., Martin, B., Debart, F., Vasseur, J.J., Contreras, J.M., Morice, C., Quérat, G., Jung, M.-L., et al. (2017). Toward the identification of viral cap-methyltransferase inhibitors by fluorescence screening assay. *Antiviral Res.* *144*, 330–339.

Arabi, Y.M., Alothman, A., Balkhy, H.H., Al-Dawood, A., AlJohani, S., Harbi, Al, S., Kojan, S., Jeraisy, Al, M., Deeb, A.M., Assiri, A.M., et al. (2018). Treatment of Middle East respiratory syndrome with a combination of lopinavir-ritonavir and interferon- β 1b (MIRACLE trial): study protocol for a randomized controlled trial. *Trials* *19*.

Arabi, Y., Shalhoub, S., Mandourah, Y., Al-Hameed, F., Al-Omari, A., Qasim, Al, E., Jose, J., Alraddadi, B., Almotairi, A., Khatib, Al, K., et al. (2019). Ribavirin and Interferon Therapy for Critically Ill Patients with the Middle East Respiratory Syndrome: A multicenter observational study. *Clinical Infectious Diseases* *1*–23.

Arnold, J.J., Ghosh, S.K.B., and Cameron, C.E. (1999). Poliovirus RNA-dependent RNA polymerase (3Dpol). *J. Biol. Chem.* *274*, 37060–37069.

Azhar, E.I., El-Kafrawy, S.A., Farraj, S.A., Hassan, A.M., Al-Saeed, M.S., Hashem, A.M., and Madani, T.A. (2014). Evidence for camel-to-human transmission of MERS coronavirus. *N. Engl. J. Med.* *370*, 2499–2505.

Balkhy, H.H., Alenazi, T.H., Alshamrani, M.M., Baffoe-Bonnie, H., Arabi, Y., Hijazi, R., Al-Abdely, H.M., El-Saied, A., Johani, Al, S., Assiri, A.M., et al. (2016). Description of a hospital outbreak of Middle East respiratory syndrome in a large tertiary care hospital in Saudi Arabia. *Infection Control & Hospital Epidemiology* *37*, 1147–1155.

Baranov, P.V., Henderson, C.M., Anderson, C.B., Gesteland, R.F., Atkins, J.F., and Howard, M.T. (2005). Programmed ribosomal frameshifting in decoding the SARS-CoV genome. *Virology* *332*, 498–510.

Baranovich, T., Wong, S.S., Armstrong, J., Marjuki, H., Webby, R.J., Webster, R.G., and Govorkova, E.A. (2013). T-705 (Favipiravir) induces lethal mutagenesis in Influenza A H1N1 viruses in vitro. *J. Virol.* *87*, 3741–3751.

Barnard, D.L., Hubbard, V.D., Burton, J., Smee, D.F., Morrey, J.D., Otto, M.J., and Sidwell, R.W. (2004). Inhibition of severe acute respiratory syndrome-associated coronavirus (SARSCoV) by calpain inhibitors and β -D-N4-Hydroxycytidine. *Antiviral Chem. and Chemo.* *15*, 15–22.

- Baron, S., and Cloyd, M.W. (1996). Human Retroviruses. In *Medical Microbiology*, (Galveston (TX): University of Texas Medical Branch at Galveston).
- Baron, S., and Whitley, R.J. (1996). Herpesviruses. In *Medical Microbiology*, (Galveston (TX): University of Texas Medical Branch at Galveston).
- Bartosch, B. (2010). Hepatitis B and C viruses and hepatocellular carcinoma. *Viruses* *2*, 1504–1509.
- Bárcena, M., Oostergetel, G.T., Bartelink, W., Faas, F.G.A., Verkleij, A., Rottier, P.J.M., Koster, A.J., and Bosch, B.J. (2009). Cryo-electron tomography of mouse hepatitis virus: Insights into the structure of the coronavirion. *Proc Natl Acad Sci USA* *106*, 582–587.
- Belouzard, S., Millet, J.K., Licitra, B.N., and Whittaker, G.R. (2012). Mechanisms of coronavirus cell entry mediated by the viral spike protein. *Viruses* *4*, 1011–1033.
- Biktasova, A., Hajek, M., Sewell, A., Gary, C., Bellinger, G., Deshpande, H.A., Bhatia, A., Burtness, B., Judson, B., Mehra, S., et al. (2017). Demethylation therapy as a targeted treatment for human papillomavirus-associated head and neck cancer. *Clin. Cancer Res.* *23*, 7276–7287.
- Bloom, J.D., Lu, Z., Chen, D., Raval, A., Venturelli, O.S., and Arnold, F.H. (2007). Evolution favors protein mutational robustness in sufficiently large populations. *BMC Biol.* *5*, 29–21.
- Blumberg, B.S. (1997). Hepatitis B virus, the vaccine, and the control of primary cancer of the liver. *Proc Natl Acad Sci USA* *94*, 7121–7125.
- Bolger, A.M., Lohse, M., and Usadel, B. (2014). Trimmomatic: a flexible trimmer for Illumina sequence data. *Bioinformatics* *30*, 2114–2120.
- Borowski, P., Deinert, J., Schalinski, S., Bretner, M., Ginalski, K., Kulikowski, T., and Shugar, D. (2003). Halogenated benzimidazoles and benzotriazoles as inhibitors of the NTPase/helicase activities of hepatitis C and related viruses. *European Journal of Biochemistry* *270*, 1645–1653.
- Borowski, P., Lang, M., Haag, A., Schmitz, H., Choe, J., Chen, H.-M., and Hosmane, R.S. (2002). Characterization of imidazo[4,5-d]pyridazine nucleosides as modulators of unwinding reaction mediated by West Nile virus nucleoside triphosphatase/helicase: evidence for activity on the level of substrate and/or enzyme. *Antimicrob. Agents Chemother.* *46*, 1231–1239.
- Boutureira, O., Matheu, M.I., Nucleoside, Y.D.O., 2013 Synthesis of C-Nucleosides. Wiley Online Library
- Bouvet, M., Imbert, I., Subissi, L., Gluais, L., Canard, B., and Decroly, E. (2012). RNA 3'-end mismatch excision by the severe acute respiratory syndrome coronavirus nonstructural protein nsp10/nsp14 exoribonuclease complex. *Proc Natl Acad Sci USA* *109*, 9372–9377.

- Boyer, P.L., Sarafianos, S.G., Arnold, E., and Hughes, S.H. (2002). The M184V mutation reduces the selective excision of zidovudine 5'-monophosphate (AZTMP) by the reverse transcriptase of human immunodeficiency virus type 1. *J. Virol.* *76*, 3248–3256.
- Böttcher, T., and Sieber, S.A. (2010). Showdomycin as a versatile chemical tool for the detection of pathogenesis-associated enzymes in bacteria. *J. Am. Chem. Soc.* *132*, 6964–6972.
- Brierley, I., Digard, P., and Inglis, S.C. (1989). Characterization of an efficient coronavirus ribosomal frameshifting signal: Requirement for an RNA pseudoknot. *Cell* *57*, 537–547.
- Brown, A.J., Won, J.J., Graham, R.L., Dinnon, K.H., III, Sims, A.C., Feng, J.Y., Cihlar, T., Denison, M.R., Baric, R.S., and Sheahan, T.P. (2019). Broad spectrum antiviral remdesivir inhibits human endemic and zoonotic deltacoronaviruses with a highly divergent RNA dependent RNA polymerase. *Antiviral Research* *169*, 104541.
- Brown, D.M., and Hewlins, M.J.E. (1968). The reaction between hydroxylamine and cytosine derivatives. *Journal of the Chemical Society C: Organic* *0*, 1922–1924.
- Brown, D.M., and Schell, P. (1965) 32. Nucleotides. Part XLVIII. The reaction of hydroxylamine with cytosine and related compounds. *Journal of the Chemical Society*. 208-215.
- Bruenn, J.A. (2003). A structural and primary sequence comparison of the viral RNA-dependent RNA polymerases. *Nucleic Acids Res.* *31*, 1821–1829.
- Brunn, von, A., Teepe, C., Simpson, J.C., Pepperkok, R., Friedel, C.C., Zimmer, R., Roberts, R., Baric, R., and Haas, J. (2007). Analysis of intraviral protein-protein interactions of the SARS coronavirus ORFeome. *PLoS ONE* *2*, e459.
- Burstow, N.J., Mohamed, Z., Gomaa, A.I., Sonderup, M.W., Cook, N.A., Waked, I., Spearman, C.W., and Taylor-Robinson, S.D. (2017). Hepatitis C treatment: where are we now? *Int J Gen Med* *10*, 39–52.
- Cady, S.D., Luo, W., Hu, F., and Hong, M. (2009). Structure and function of the influenza A M2 proton channel. *Biochemistry* *48*, 7356–7364.
- Campagnola, G., McDonald, S., Beaucourt, S., Vignuzzi, M., Peersen, O.B., and Kirkegaard, K. (2015). Structure-function relationships underlying the replication fidelity of viral RNA-dependent RNA polymerases. *J. Virol.* *89*, 275–286.
- Carroll, S.S., Tomassini, J.E., Bosserman, M., Getty, K., Stahlhut, M.W., Eldrup, A.B., Bhat, B., Hall, D., Simcoe, A.L., LaFemina, R., et al. (2003). Inhibition of hepatitis C virus RNA replication by 2'-modified nucleoside analogs. *J. Biol. Chem.* *278*, 11979–11984.
- Case, J.B., Ashbrook, A.W., Dermody, T.S., and Denison, M.R. (2016). Mutagenesis of S-adenosyl-L-methionine-binding residues in coronavirus nsp14 N7-methyltransferase demonstrates differing requirements for genome translation and resistance to innate immunity. *J. Virol.* *90*, JVI.00542–16–7256.

Cavanagh, D. (2007). Coronaviruses in poultry and other birds. *Avian Pathology* 34, 439–448.

Centers for Disease Control and Prevention (CDC) (2003). Severe acute respiratory syndrome (SARS) and coronavirus testing--United States, 2003. *MMWR Morb. Mortal. Wkly. Rep.* 52, 297–302.

Centers for Disease Control and Prevention (CDC) (2019). Inuenza Antiviral Medications: Summary for Clinicians. Center for Disease Control and Prevention CDC 1–11.

Chamberlain, J.M., Sortino, K., Sethna, P., Bae, A., Lanier, R., Bambara, R.A., and Dewhurst, S. (2019). Cidofovir diphosphate inhibits adenovirus 5 DNA polymerase via both nonobligate chain termination and direct inhibition, and polymerase mutations confer cidofovir resistance on intact virus. *Antimicrob. Agents Chemother.* 63, 331.

Chan, K.S., Zheng, J.P., Mok, Y.W., Li, Y.M., LIU, Y.N., CHU, C.M., and Ip, M.S. (2003). SARS: prognosis, outcome and sequelae. *Respirology* 8, S36–S40.

Channappanavar, R., and Perlman, S. (2017). Pathogenic human coronavirus infections: causes and consequences of cytokine storm and immunopathology. *Semin Immunopathol* 39, 529–539.

Channappanavar, R., Fehr, A.R., Vijay, R., Mack, M., Zhao, J., Meyerholz, D.K., and Perlman, S. (2016). Dysregulated type I interferon and inflammatory monocyte-macrophage responses cause lethal pneumonia in SARS-CoV-infected mice. *Cell Host & Microbe* 19, 181–193.

Charette, M., and Gray, M.W. (2000). Pseudouridine in RNA: what, where, how, and why. *IUBMB Life* 49, 341–351.

Chen, W., and Baric, R.S. (1996). Molecular anatomy of mouse hepatitis virus persistence: coevolution of increased host cell resistance and virus virulence. *J. Virol.* 70, 3947–3960.

Chen, Y., and Guo, D. (2016). Molecular mechanisms of coronavirus RNA capping and methylation. *Virol Sin* 31, 3–11.

Cheng, A., Zhang, W., Xie, Y., Jiang, W., Arnold, E., Sarafianos, S.G., and Ding, J. (2005). Expression, purification, and characterization of SARS coronavirus RNA polymerase. *Virology* 335, 165–176.

Cheng, V.C.C., Chan, J.F.W., To, K.K.W., and Yuen, K.Y. (2013). Clinical management and infection control of SARS: Lessons learned. *Antiviral Res.* 100, 407–419.

Chevaliez, S., and, J.P.H.C.V.G., 2006 HCV genome and life cycle. Books.Google.com

Cho, A., Saunders, O.L., Butler, T., Zhang, L., Xu, J., Vela, J.E., Feng, J.Y., Ray, A.S., and Kim, C.U. (2012). Synthesis and antiviral activity of a series of 1'-substituted 4-aza-7,9-dideazaadenosine C-nucleosides. *Bioorganic & Medicinal Chemistry Letters* 22, 2705–2707.

- Choi, K.H. (2012). Viral Polymerases. In *Viral Molecular Machines*, (Boston, MA: Springer, Boston, MA), pp. 267–304.
- Choo, Q.L., Kuo, G., Weiner, A.J., Overby, L.R., Bradley, D.W., and Houghton, M. (1989). Isolation of a cDNA clone derived from a blood-borne non-A, non-B viral hepatitis genome. *Science* *244*, 359–362.
- Cihlar, T., and Ray, A.S. (2010). Nucleoside and nucleotide HIV reverse transcriptase inhibitors: 25 years after zidovudine. *Antiviral Research* *85*, 39–58.
- Cinatl, J., Morgenstern, B., Bauer, G., Chandra, P., Rabenau, H., and Doerr, H.W. (2003). Treatment of SARS with human interferons. *Lancet* *362*, 293–294.
- Clercq, E.D. (2004). Antivirals and antiviral strategies. *Nat Rev Micro* *2*, 704–720.
- Coffey, L.L., Beeharry, Y., Borderia, A.V., Blanc, H., and Vignuzzi, M. (2011). Arbovirus high fidelity variant loses fitness in mosquitoes and mice. *Proc Natl Acad Sci USA* *108*, 16038–16043.
- Coleman, C.M., and Frieman, M.B. (2015). Growth and quantification of MERS-CoV infection. *Curr Protoc Microbiol* *37*, 15E.2.1–E.2.9.
- Coleman, C.M., Sisk, J.M., Mingo, R.M., Nelson, E.A., White, J.M., and Frieman, M.B. (2016). ABL kinase inhibitors are potent inhibitors of SARS-CoV and MERS-CoV fusion. *J. Virol.* *JVI.01429–16*.
- Collins, P.L., Farnes, R., and Graham, B.S. (2013). Respiratory syncytial virus: virology, reverse genetics, and pathogenesis of disease. In *Challenges and Opportunities for Respiratory Syncytial Virus Vaccines*, (Berlin, Heidelberg: Springer, Berlin, Heidelberg), pp. 3–38.
- Costantini, V.P., Whitaker, T., Barclay, L., Lee, D., McBrayer, T.R., Schinazi, R.F., and Vinjé, J. (2012). Antiviral activity of nucleoside analogues against norovirus. *Antivir. Ther. (Lond.)* *17*, 981–991.
- Cotten, M., Watson, S.J., Zumla, A.I., Makhdoom, H.Q., Palser, A.L., Ong, S.H., Rabieeah Al, A.A., Alhakeem, R.F., Assiri, A., Al-Tawfiq, J.A., et al. (2014). Spread, circulation, and evolution of the Middle East respiratory syndrome coronavirus. *mBio* *5*, 1814.
- Crotty, S., Cameron, C.E., and Andino, R. (2001). RNA virus error catastrophe: Direct molecular test by using ribavirin. *Proc Natl Acad Sci USA* *1–6*.
- Crotty, S., Cameron, C., and Andino, R. (2014). Ribavirin's antiviral mechanism of action: lethal mutagenesis? *J Mol Med* *80*, 86–95.
- Crotty, S., Maag, D., Arnold, J.J., zhong, W., Lau, J.Y.N., Hong, Z., Andino, R., and Cameron, C.E. (2000). The broad-spectrum antiviral ribonucleoside ribavirin is an RNA virus mutagen. *Nature Medicine* *1–5*.

- Crowe, J.E. (2017). Principles of broad and potent antiviral human antibodies: Insights for vaccine design. *Cell Host & Microbe* 22, 193–206.
- Daelemans, D., Pauwels, R., De Clercq, E., and Pannecouque, C. (2011). A time-of-drug addition approach to target identification of antiviral compounds. *Nature Protocols* 6, 925–933.
- Dahiya, M., Hussaini, T., Journal, E.Y.B.C.M., 2019 The revolutionary changes in hepatitis C treatment: A concise review. *British Columbia Medical Journal*.
- Das, P.K., Puusepp, L., Varghese, F.S., Utt, A., Ahola, T., Kananovich, D.G., Lopp, M., Merits, A., and Karelson, M. (2016). Design and validation of novel chikungunya virus protease inhibitors. *Antimicrob. Agents Chemother.* 60, 7382–7395.
- de Béthune, M.-P. (2010). Non-nucleoside reverse transcriptase inhibitors (NNRTIs), their discovery, development, and use in the treatment of HIV-1 infection: a review of the last 20 years (1989–2009). *Antiviral Res.* 85, 75–90.
- De Clercq, E., and Neyts, J. (2009). Antiviral agents acting as DNA or RNA chain terminators. In *Antiviral Strategies*, (Berlin, Heidelberg: Springer, Berlin, Heidelberg), pp. 53–84.
- De Clercq, E. (2007). The design of drugs for HIV and HCV. *Nat Rev* 6, 1001–1018.
- De Clercq, E. (2014). Potential antivirals and antiviral strategies against SARS coronavirus infections. *Expert Review of Anti-Infective Therapy* 4, 291–302.
- De Clercq, E., and Li, G. (2016a). Approved antiviral drugs over the past 50 years. *Clin. Microbiol. Rev.* 29, 695–747.
- De Clercq, E., and Li, G. (2016b). Approved antiviral drugs over the past 50 years. *Clin. Microbiol. Rev.* 29, 695–747.
- De Clercq, E., Férid, G., Kaptein, S., and Neyts, J. (2010). Antiviral treatment of chronic hepatitis B virus (HBV) infections. *Viruses* 2, 1279–1305.
- de Groot, R.J., Baker, S.C., Baric, R.S., Brown, C.S., Drosten, C., Enjuanes, L., Fouchier, R.A.M., Galiano, M., Gobalena, A.E., Memish, Z.A., et al. (2013). Commentary: Middle East respiratory syndrome coronavirus (MERS-CoV): Announcement of the coronavirus study group. *J. Virol.* 87, 7790–7792.
- de Haan, C.A.M., and Rottier, P.J.M. (2005). Molecular interactions in the assembly of coronaviruses. *Advances in Virus Research* 64, 165–230.
- de Wilde, A.H., Jochmans, D., Posthuma, C.C., Zevenhoven-Dobbe, J.C., van Nieuwkoop, S., Bestebroer, T.M., van den Hoogen, B.G., Neyts, J., and Snijder, E.J. (2014). Screening of an FDA-approved compound library identifies four small-molecule inhibitors of Middle East respiratory syndrome coronavirus replication in cell culture. *Antimicrob. Agents Chemother.* 58, 4875–4884.

- de Wilde, A.H., Snijder, E.J., Kikkert, M., and van Hemert, M.J. (2017). Host factors in coronavirus replication. In Roles of Host Gene and Non-Coding RNA Expression in Virus Infection, (Cham: Springer, Cham), pp. 1–42.
- de Wilde, A.H., Zevenhoven-Dobbe, J.C., van der Meer, Y., Thiel, V., Narayanan, K., Makino, S., Snijder, E.J., and van Hemert, M.J. (2011). Cyclosporin A inhibits the replication of diverse coronaviruses. *J. Gen. Virol.* *92*, 2542–2548.
- de Wit, E., van Doremalen, N., Falzarano, D., and Munster, V.J. (2016). SARS and MERS: recent insights into emerging coronaviruses. *Nature Reviews Microbiology* *2016* *14*, 523–534.
- Deeks, S.G., Lewin, S.R., and Havlir, D.V. (2013). The end of AIDS: HIV infection as a chronic disease. *Lancet* *382*, 1525–1533.
- Delamou, A., Delvaux, T., Ayadi, El, A.M., Beavogui, A.H., Okumura, J., Van Damme, W., and De Brouwere, V. (2017). Public health impact of the 2014-2015 Ebola outbreak in West Africa: seizing opportunities for the future. *BMJ Glob Health* *2*, e000202.
- Delang, L., Segura Guerrero, N., Tas, A., Querat, G., Pastorino, B., Froeyen, M., Dallmeier, K., Jochmans, D., Herdewijn, P., Bello, F., et al. (2014). Mutations in the chikungunya virus non-structural proteins cause resistance to favipiravir (T-705), a broad-spectrum antiviral. *Journal of Antimicrobial Chemotherapy* *69*, 2770–2784.
- Deng, X., and Baker, S.C. (2018). An “Old” protein with a new story: Coronavirus endoribonuclease is important for evading host antiviral defenses. *Virology* *517*, 157–163.
- Deng, X., Hackbart, M., Mettelman, R.C., O'Brien, A., Mielech, A.M., Yi, G., Kao, C.C., and Baker, S.C. (2017). Coronavirus nonstructural protein 15 mediates evasion of dsRNA sensors and limits apoptosis in macrophages. *Proc Natl Acad Sci USA* *114*, E4251–E4260.
- Derse, D., Cheng, Y.-C., Furman, P.A., Clair, M.H.S., and Elion, G.B. (1981). Inhibition of purified human and herpes simplex virus-induced DNA polymerases by 9-(2-hydroxyethoxymethyl)guanine triphosphate. *J. Biol. Chem.* *1*–5.
- Detels, R., Muñoz, A., McFarlane, G., Kingsley, L.A., Margolick, J.B., Giorgi, J., Schrager, L.K., and Phair, J.P. (1998). Effectiveness of potent antiretroviral therapy on time to AIDS and death in men with known HIV infection duration. Multicenter AIDS Cohort Study Investigators. *Jama* *280*, 1497–1503.
- Deval, J. (2009). Antimicrobial strategies. *Drugs* *69*, 151–166.
- Deval, J., Fung, A., Stevens, S.K., Jordan, P.C., Gromova, T., Taylor, J.S., Hong, J., Meng, J., Wang, G., Dyatkina, N., et al. (2016a). Biochemical effect of resistance mutations against synergistic inhibitors of RSV RNA polymerase. *PLoS ONE* *11*, e0154097.

Deval, J., Fung, A., Stevens, S.K., Jordan, P.C., Gromova, T., Taylor, J.S., Hong, J., Meng, J., Wang, G., Dyatkina, N., et al. (2016b). Biochemical Effect of Resistance Mutations against Synergistic Inhibitors of RSV RNA Polymerase. *PLoS ONE* *11*, e0154097–19.

Deval, J., Hong, J., Wang, G., Taylor, J., Smith, L.K., Fung, A., Stevens, S.K., Liu, H., Jin, Z., Dyatkina, N., et al. (2015). Molecular basis for the selective inhibition of respiratory syncytial virus RNA polymerase by 2“-fluoro-4-”chloromethyl-cytidine triphosphate. *PLoS Pathog* *11*, e1004995–24.

Domingo, E., Sheldon, J., and Perales, C. (2012). Viral quasispecies evolution. *Microbiol. Mol. Biol. Rev.* *76*, 159–216.

Dörnemann, J., Burzio, C., Ronsse, A., Sprecher, A., De Clerck, H., Van Herp, M., Kolié, M.-C., Yosifiva, V., Caluwaerts, S., McElroy, A.K., et al. (2017). First newborn baby to receive experimental therapies survives Ebola virus disease. *J Infect Dis.* *215*, 171–174.

Dudas, G., Carvalho, L.M., Rambaut, A., Elife, T.B., 2018 MERS-CoV spillover at the camel-human interface. Cdn.Elfesciences.org

Dulin, D., Arnold, J.J., van Laar, T., Oh, H.-S., Lee, C., Perkins, A.L., Harki, D.A., Depken, M., Cameron, C.E., and Dekker, N.H. (2017). Signatures of nucleotide analog incorporation by an RNA-dependent RNA polymerase revealed using high-throughput magnetic tweezers. *Cell Reports* *21*, 1063–1076.

Dyall, J., Coleman, C.M., Hart, B.J., Venkataraman, T., Holbrook, M.R., Kindrachuk, J., Johnson, R.F., Olinger, G.G., Jahrling, P.B., Laidlaw, M., et al. (2014). Repurposing of clinically developed drugs for treatment of Middle East respiratory syndrome coronavirus infection. *Antimicrob. Agents Chemother.* *58*, 4885–4893.

Dybul, M., Fauci, A.S., Bartlett, J.G., Kaplan, J.E., Pau, A.K., Panel on Clinical Practices for the Treatment of HIV (2002). Guidelines for using antiretroviral agents among HIV-infected adults and adolescents. Recommendations of the Panel on Clinical Practices for Treatment of HIV. *MMWR Recomm Rep* *51*, 1–55.

Dziewiatkowski, N.A., Osmon, E.N., Chahine, E.B., and Thornby, K.-A. (2019). Baloxavir: A novel single-dose oral antiviral for the treatment of influenza. *Sr Care Pharm* *34*, 243–252.

Eckerle, L.D., Lu, X., Sperry, S.M., Choi, L., and Denison, M.R. (2007). High fidelity of murine hepatitis virus replication is decreased in nsp14 exoribonuclease mutants. *J. Virol.* *81*, 12135–12144.

Egloff, M.P., Ferron, F., Campanacci, V., Longhi, S., Rancurel, C., Dutartre, H., Snijder, E.J., Gorbalenya, A.E., Cambillau, C., and Canard, B. (2004). The severe acute respiratory syndrome-coronavirus replicative protein nsp9 is a single-stranded RNA-binding subunit unique in the RNA virus world. *Proc Natl Acad Sci USA* *101*, 3792–3796.

- Ehteshami, M., Tao, S., Zandi, K., Hsiao, H.-M., Jiang, Y., Hammond, E., Amblard, F., Russell, O.O., Merits, A., and Schinazi, R.F. (2017). Characterization of β -D-N4-Hydroxycytidine as a novel inhibitor of chikungunya virus. *Antimicrob. Agents Chemother.* *61*, 270.
- Elion, G.B. (1982). Mechanism of action and selectivity of acyclovir. *The American Journal of Medicine* *73*, 7–13.
- Eltaala, A., Luciani, F., White, P., Lloyd, A., and Bull, R. (2015). Inhibitors of the hepatitis C virus polymerase; Mode of action and resistance. *Viruses* *7*, 5206–5224.
- Eyer, L., Nencka, R., De Clercq, E., Seley-Radtke, K., and Růžek, D. (2018). Nucleoside analogs as a rich source of antiviral agents active against arthropod-borne flaviviruses:. *Antiviral Chem. and Chemo.* *26*, 204020661876129.
- Eyer, L., Zouharová, D., Širmarová, J., Fojtíková, M., Štefánik, M., Havíerník, J., Nencka, R., De Clercq, E., and Růžek, D. (2017). Antiviral activity of the adenosine analogue BCX4430 against West Nile virus and tick-borne flaviviruses. *Antiviral Res.* *142*, 63–67.
- Falzarano, D., de Wit, E., Rasmussen, A.L., Feldmann, F., Okumura, A., Scott, D.P., Brining, D., Bushmaker, T., Martellaro, C., Baseler, L., et al. (2013). Treatment with interferon- α 2b and ribavirin improves outcome in MERS-CoV–infected rhesus macaques. *Nature Medicine* *19*, 1313–1317.
- Fares, M.A. (2015). The origins of mutational robustness. *Trends Genet.* *31*, 373–381.
- Fehr, A.R., and Perlman, S. (2015). Coronaviruses: An overview of their replication and pathogenesis. In *Cancer Cell Culture*, (New York, NY: Springer New York), pp. 1–23.
- Feng, J.Y. (2018). Addressing the selectivity and toxicity of antiviral nucleosides. *Antiviral Chem. and Chemo.* *26*, 204020661875852.
- Feng, J.Y., Cheng, G., Perry, J., Barauskas, O., Xu, Y., Fenaux, M., Eng, S., Tirunagari, N., Peng, B., Yu, M., et al. (2014). Inhibition of hepatitis C virus replication by GS-6620, a potent C-nucleoside monophosphate prodrug. *Antimicrob. Agents Chemother.* *58*, 1930–1942.
- Fensterl, V., and Sen, G.C. (2009). Interferons and viral infections. *BioFactors* *35*, 14–20.
- Ferrer-Orta, C., Arias, A., Escarmis, C., and Verdaguér, N. (2006). A comparison of viral RNA-dependent RNA polymerases. *Current Opinion in Structural Biology* *16*, 27–34.
- Ferrer-Orta, C., Arias, A., Pérez-Luque, R., Escarmis, C., Domingo, E., and Verdaguér, N. (2007). Sequential structures provide insights into the fidelity of RNA replication. *Proc Natl Acad Sci USA* 1–6.
- Ferron, F., Decroly, E., Selisko, B., and Canard, B. (2012). The viral RNA capping machinery as a target for antiviral drugs. *Antiviral Res.* *96*, 21–31.

- Ferron, F., Subissi, L., Silveira De Moraes, A.T., Le, N.T.T., Sevajol, M., Gluais, L., Decroly, E., Vonrhein, C., Bricogne, G., Canard, B., et al. (2017). Structural and molecular basis of mismatch correction and ribavirin excision from coronavirus RNA. *Proc Natl Acad Sci USA* *15*, 201718806–201718810.
- Finkelman, B.S., Viboud, C., Koelle, K., Ferrari, M.J., Bharti, N., and Grenfell, B.T. (2007). Global patterns in seasonal activity of influenza A/H3N2, A/H1N1, and B from 1997 to 2005: viral coexistence and latitudinal gradients. *PLoS ONE* *2*, e1296.
- Fischl, M.A., Richman, D.D., Grieco, M.H., Gottlieb, M.S., Volberding, P.A., Laskin, O.L., Leedom, J.M., Groopman, J.E., Mildvan, D., and Schooley, R.T. (1987). The efficacy of azidothymidine (AZT) in the treatment of patients with AIDS and AIDS-related complex. A double-blind, placebo-controlled trial. *N England J Med* *317*, 185–191.
- Fried, M.W., Schiffman, M.L., Reddy, K.R., Smith, C., Marinos, G., Gonçales, F.L., Häussinger, D., Diago, M., Carosi, G., Dhumeaux, D., et al. (2002). Peginterferon alfa-2a plus ribavirin for chronic hepatitis C virus infection. *N. Engl. J. Med.* *347*, 975–982.
- Frieman, M., Basu, D., Matthews, K., Taylor, J., Jones, G., Pickles, R., Baric, R., and Engel, D.A. (2011). Yeast based small molecule screen for inhibitors of SARS-CoV. *PLoS ONE* *6*, e28479.
- Frobert, E., Ooka, T., Cortay, J.C., Lina, B., Thouvenot, D., and Morfin, F. (2005). Herpes simplex virus thymidine kinase mutations associated with resistance to acyclovir: a site-directed mutagenesis study. *Antimicrob. Agents Chemother.* *49*, 1055–1059.
- Furuta, Y., Takahashi, K., Kuno-Maekawa, M., Sangawa, H., Uehara, S., Kozaki, K., Nomura, N., Egawa, H., and Shiraki, K. (2005). Mechanism of action of T-705 against influenza virus. *Antimicrob. Agents Chemother.* *49*, 981–986.
- Furuta, Y., Komeno, T., and Nakamura, T. (2017). Favipiravir (T-705), a broad spectrum inhibitor of viral RNA polymerase. *Proc. Jpn. Acad., Ser. B, Phys. Biol. Sci.* *93*, 449–463.
- Galli, A., Mens, H., Gottwein, J.M., Gerstoft, J., and Bukh, J. (2018). Antiviral effect of ribavirin against HCV associated with increased frequency of G-to-A and C-to-U transitions in infectious cell culture model. *Scientific Reports* *8*, 4619.
- Gallo, R.C., and Montagnier, L. (2003). The discovery of HIV as the cause of AIDS. *N. Engl. J. Med.* *349*, 2283–2285.
- Galmarini, C.M., Mackey, J.R., and Dumontet, C. (2002). Nucleoside analogues and nucleobases in cancer treatment. *Lancet Oncol.* *3*, 415–424.
- Gao, J., Lu, G., Qi, J., Li, Y., Wu, Y., Deng, Y., Geng, H., Li, H., Wang, Q., Xiao, H., et al. (2013). Structure of the fusion core and inhibition of fusion by a heptad repeat peptide derived from the S protein of Middle East respiratory syndrome coronavirus. *J. Virol.* *87*, 13134–13140.

Garriga, D., Ferrer-Orta, C., Querol-Audí, J., Oliva, B., and Verdaguer, N. (2013). Role of motif B loop in allosteric regulation of RNA-dependent RNA polymerization activity. *Journal of Molecular Biology* *425*, 2279–2287.

Gaunt, E.R., Hardie, A., Claas, E.C.J., Simmonds, P., and Templeton, K.E. (2010). Epidemiology and clinical presentations of the four human coronaviruses 229E, HKU1, NL63, and OC43 detected over 3 years using a novel multiplex real-time PCR method. *Journal of Clinical Microbiology* *48*, 2940–2947.

Ge, X.-Y., Li, J.-L., Yang, X.-L., Chmura, A.A., Zhu, G., Epstein, J.H., Mazet, J.K., Hu, B., Zhang, W., Peng, C., et al. (2013). Isolation and characterization of a bat SARS-like coronavirus that uses the ACE2 receptor. *Nature* *503*, 535–538.

Goldhill, D.H., Langat, P., Xie, H., Galiano, M., Miah, S., Kellam, P., Zambon, M., Lackenby, A., Barclay, W.S., and García-Sastre, A. (2019). Determining the mutation bias of favipiravir in influenza virus using next-generation sequencing. *J. Virol.* *93*, e01217–e01218.

Gorbalenya, A.E., Pringle, F.M., Zeddam, J.-L., Luke, B.T., Cameron, C.E., Kalmakoff, J., Hanzlik, T.N., Gordon, K.H.J., and Ward, V.K. (2002). The Palm Subdomain-based Active Site is Internally Permuted in Viral RNA-dependent RNA Polymerases of an Ancient Lineage. *Journal of Molecular Biology* *324*, 47–62.

Gorbalenya, A.E., Snijder, E.J., and Ziebuhr, J. (2000). Virus-encoded proteinases and proteolytic processing in the Nidovirales. *Journal of General Virology* *81*, 853–879.

Graci, J.D., Gnadig, N.F., Galarraga, J.E., Castro, C., Vignuzzi, M., and Cameron, C.E. (2012). Mutational robustness of an RNA virus influences sensitivity to lethal mutagenesis. *J. Virol.* *86*, 2869–2873.

Graepel, K.W., Lu, X., Case, J.B., Sexton, N.R., Smith, E.C., and Denison, M.R. (2017). Proofreading-deficient coronaviruses adapt for increased fitness over long-term passage without reversion of exoribonuclease-inactivating mutations. *mBio* *8*, 281.

Graham, R.L., Sims, A.C., Brockway, S.M., Baric, R.S., and Denison, M.R. (2005). The nsp2 replicase proteins of murine hepatitis virus and severe acute respiratory syndrome coronavirus are dispensable for viral replication. *J. Virol.* *79*, 13399–13411.

Gralinski, L.E., Bankhead, A., Jeng, S., Menachery, V.D., Proll, S., Belisle, S.E., Matzke, M., Webb-Robertson, B.J.M., Luna, M.L., Shukla, A.K., et al. (2013). Mechanisms of severe acute respiratory syndrome coronavirus-induced acute lung injury. *mBio* *4*, e00271–13–e00271–13.

Gralinski, L.E., and Baric, R.S. (2015). Molecular pathology of emerging coronavirus infections. *The Journal of Pathology* *235*, 185–195.

Grinde, B. (2013). Herpesviruses: latency and reactivation - viral strategies and host response. *J Oral Microbiol* *5*, 22766.

Haagmans, B.L., Kuiken, T., Martina, B.E., and Med, R.F.N. , KH Chan, M. Tashiro, and 18 AD Osterhaus. 2004. Pegylated interferon-alpha protects type 1 pneumocytes against 19 SARS coronavirus infection in

Han, H.-J., Yu, H., and Yu, X.-J. (2016). Evidence for zoonotic origins of Middle East respiratory syndrome coronavirus. *J. Gen. Virol.* *97*, 274–280.

Hao, W., Wojdyla, J.A., Zhao, R., Han, R., Das, R., Zlatev, I., Manoharan, M., Wang, M., and Cui, S. (2017). Crystal structure of Middle East respiratory syndrome coronavirus helicase. *PLoS Pathog* *13*, e1006474.

Hart, B.J., Dyall, J., Postnikova, E., Zhou, H., Kindrachuk, J., Johnson, R.F., Olinger, G.G., Jr, Frieman, M.B., Holbrook, M.R., et al. (2014). Interferon- β and mycophenolic acid are potent inhibitors of Middle East respiratory syndrome coronavirus in cell-based assays. *J. Gen. Virol.* *95*, 571–577.

Hayden, F.G., Sugaya, N., Hirotsu, N., Lee, N., de Jong, M.D., Hurt, A.C., Ishida, T., Sekino, H., Yamada, K., Portsmouth, S., et al. (2018). Baloxavir marboxil for uncomplicated influenza in adults and adolescents. *N. Engl. J. Med.* *379*, 913–923.

Hazuda, D.J., Felock, P., Witmer, M., Wolfe, A., Stillmock, K., Grobler, J.A., Espeseth, A., Gabryelski, L., Schleif, W., Blau, C., et al. (2000). Inhibitors of strand transfer that prevent integration and inhibit HIV-1 replication in cells. *Science* *287*, 646–650.

Hecker, S.J., and Erion, M.D. (2008). Prodrugs of phosphates and phosphonates. *J. Med. Chem.* *51*, 2328–2345.

Hemida, M.G., Chu, D.K.W., Poon, L.L.M., Perera, R.A.P.M., Alhammadi, M.A., Ng, H-Y, Siu, L.Y., Guan, Y., Alnaeem, A., Peiris, M. (2014). MERS coronavirus in dromedary camel herd, Saudi Arabia. *Emerging Infectious Diseases* *20*, 1231–1234.

Hirai, A., Ohtsuka, N., Ikeda, T., Taniguchi, R., Blau, D., Nakagaki, K., Miura, H.S., Ami, Y., Yamada, Y.K., Itohara, S., et al. (2010). Role of mouse hepatitis virus (MHV) receptor murine CEACAM1 in the resistance of mice to MHV infection: Studies of mice with chimeric mCEACAM1a and mCEACAM1b. *J. Virol.* *84*, 6654–6666.

Hirsch, A. (1883). Handbook of geographical and historical pathology.

Hofmann, W.P., Soriano, V., and Zeuzem, S. (2009). Antiviral combination therapy for treatment of chronic hepatitis B, hepatitis C, and human immunodeficiency virus infection. In *Antiviral Strategies*, (Berlin, Heidelberg: Springer Berlin Heidelberg), pp. 321–346.

Holland, J., Spindler, K., Horodyski, F., Grabau, E., Nichol, S., and VandePol, S. (1982). Rapid evolution of RNA genomes. *Science* *215*, 1577–1585.

Holmes, K.V. (2003). SARS coronavirus: a new challenge for prevention and therapy. *J Clin Invest* *111*, 1605–1609.

Houser, K.V., Gretebeck, L., Ying, T., Wang, Y., Vogel, L., Lamirande, E.W., Bock, K.W., Moore, I.N., Dimitrov, D.S., and Subbarao, K. (2016). Prophylaxis with a Middle East respiratory syndrome coronavirus (MERS-CoV)-specific human monoclonal antibody protects rabbits from MERS-CoV infection. *J Infect Dis.* *213*, 1557–1561.

Hsu, M. (1997). Higher fidelity of RNA-dependent DNA mispair extension by M184V drug-resistant than wild-type reverse transcriptase of human immunodeficiency virus type 1. *Nucleic Acids Research* *25*, 4532–4536.

Huang, K.-W., Hsu, K.-C., Chu, L.-Y., Yang, J.-M., Yuan, H.S., and Hsiao, Y.-Y. (2016). Identification of inhibitors for the DEDDh family of exonucleases and a unique inhibition mechanism by crystal structure analysis of CRN-4 bound with 2-morpholin-4-ylethanesulfonate (MES). *J. Med. Chem.* *59*, 8019–8029.

Iuliano, A.D., Roguski, K.M., Chang, H.H., Muscatello, D.J., Palekar, R., Tempia, S., Cohen, C., Gran, J.M., Schanzer, D., Cowling, B.J., et al. (2018). Estimates of global seasonal influenza-associated respiratory mortality: a modelling study. *Lancet* *391*, 1285–1300.

Ivanov, K.A., Hertzig, T., Rozanov, M., Bayer, S., Thiel, V., Gorbatenya, A.E., and Ziebuhr, J. (2004a). Major genetic marker of nidoviruses encodes a replicative endoribonuclease. *Proc Natl Acad Sci USA* *101*, 12694–12699.

Ivanov, K.A., Thiel, V., Dobbe, J.C., van der Meer, Y., Snijder, E.J., and Ziebuhr, J. (2004b). Multiple enzymatic activities associated with severe acute respiratory syndrome coronavirus helicase. *J. Virol.* *78*, 5619–5632.

Jablonski, S.A., and Morrow, C.D. (1995). Mutation of the aspartic acid residues of the GDD sequence motif of poliovirus RNA-dependent RNA polymerase results in enzymes with altered metal ion requirements for activity. *J. Virol.* *69*, 1532–1539.

Jacobs, M., Rodger, A., Bell, D.J., Bhagani, S., Cropley, I., Filipe, A., Gifford, R.J., Hopkins, S., Hughes, J., Jabeen, F., et al. (2016). Late Ebola virus relapse causing meningoencephalitis: a case report. *Lancet* *388*, 498–503.

James, L., Shindo, N., Cutter, J., Ma, S., and Chew, S.K. (2006). Public health measures implemented during the SARS outbreak in Singapore, 2003. *Public Health* *120*, 20–26.

Jaworski, E., and Routh, A. (2017). Parallel ClickSeq and Nanopore sequencing elucidates the rapid evolution of defective-interfering RNAs in Flock House virus. *PLoS Pathog* *13*, e1006365.

Jácome, R., Becerra, A., de León, S.P., and Lazcano, A. (2015). Structural analysis of monomeric RNA-dependent polymerases: evolutionary and therapeutic implications. *PLoS ONE* *10*, e0139001.

Johnson, N.P.A.S., and Mueller, J. (2002). Updating the accounts: global mortality of the 1918–1920 “Spanish” influenza pandemic. *Bull Hist Med* *76*, 105–115.

Johnson, R.F., Bagci, U., Keith, L., Tang, X., Mollura, D.J., Zeitlin, L., Qin, J., Huzella, L., Bartos, C.J., Bohorova, N., et al. (2016). 3B11-N, a monoclonal antibody against MERS-CoV, reduces lung pathology in rhesus monkeys following intratracheal inoculation of MERS-CoV Jordan-n3/2012. *Virology* *490*, 49–58.

Jones, J.C., Marathe, B.M., Lerner, C., Kreis, L., Gasser, R., Pascua, P.N.Q., Nájera, I., and Govorkova, E.A. (2016). A novel endonuclease inhibitor exhibits broad-spectrum anti-influenza virus activity in vitro. *Antimicrob. Agents Chemother.* *60*, 5504–5514.

Jordan, P.C., Liu, C., Raynaud, P., Lo, M.K., Spiropoulou, C.F., Symons, J.A., Beigelman, L., and Deval, J. (2018). Initiation, extension, and termination of RNA synthesis by a paramyxovirus polymerase. *PLoS Pathog* *14*, e1006889.

Jordheim, L.P., Durantel, D., Zoulim, F., and Dumontet, C. (2013). Advances in the development of nucleoside and nucleotide analogues for cancer and viral diseases. *Nat Rev* *12*, 447–464.

Julander, J.G., Siddharthan, V., Evans, J., Taylor, R., Tolbert, K., Apuli, C., Stewart, J., Collins, P., Gebre, M., Neilson, S., et al. (2017). Efficacy of the broad-spectrum antiviral compound BCX4430 against Zika virus in cell culture and in a mouse model. *Antiviral Res.* *137*, 14–22.

Kelley, L.A., Mezulis, S., Yates, C.M., Wass, M.N., and Sternberg, M.J.E. (2015). The Phyre2 web portal for protein modeling, prediction and analysis. *Nature Protocols* *10*, 845–858.

Kilby, J.M., Hopkins, S., Venetta, T.M., DiMassimo, B., Cloud, G.A., Lee, J.Y., Alldredge, L., Hunter, E., Lambert, D., Bolognesi, D., et al. (1998). Potent suppression of HIV-1 replication in humans by T-20, a peptide inhibitor of gp41-mediated virus entry. *Nature Medicine* *4*, 1302–1307.

Kim, M.J., and Kao, C. (2001). Factors regulating template switch in vitro by viral RNA-dependent RNA polymerases: Implications for RNA–RNA recombination. *Proc Natl Acad Sci USA* *98*, 4972–4977.

Kim, M.K., Yu, M.-S., Park, H.R., Kim, K.B., Lee, C., Cho, S.Y., Kang, J., Yoon, H., Kim, D.-E., Choo, H., et al. (2011). 2,6-Bis-arylmethoxy-5-hydroxychromones with antiviral activity against both hepatitis C virus (HCV) and SARS-associated coronavirus (SCV). *Eur J Med Chem* *46*, 5698–5704.

Kim, Y., Liu, H., Galasiti Kankanamalage, A.C., Weerasekara, S., Hua, D.H., Groutas, W.C., Chang, K.-O., and Pedersen, N.C. (2016). Reversal of the progression of fatal coronavirus infection in cats by a broad-spectrum coronavirus protease inhibitor. *PLoS Pathog* *12*, e1005531.

Kim, Y., Lovell, S., Tiew, K.-C., Mandadapu, S.R., Alliston, K.R., Battaile, K.P., Groutas, W.C., and Chang, K.-O. (2012). Broad-spectrum antivirals against 3C or 3C-like proteases of picornaviruses, noroviruses, and coronaviruses. *J. Virol.* *86*, 11754–11762.

Kirchdoerfer, R.N., and Ward, A.B. (2019). Structure of the SARS-CoV nsp12 polymerase bound to nsp7 and nsp8 co-factors. *Nature Communications* *2019* *10*:1 10, 2342.

Klinkenberg, D., Fraser, C., and Heesterbeek, H. (2006). The effectiveness of contact tracing in emerging epidemics. *PLoS ONE* 1, e12.

Koops, K., Kikkert, M., van den Worm, S.H.E., Zevenhoven-Dobbe, J.C., van der Meer, Y., Koster, A.J., Mommaas, A.M., and Snijder, E.J. (2008). SARS-coronavirus replication is supported by a reticulovesicular network of modified endoplasmic reticulum. *PLoS Biol.* 6, e226.

Ksiazek, T.G., Erdman, D., Goldsmith, C.S., Zaki, S.R., Peret, T., Emery, S., Tong, S., Urbani, C., Comer, J.A., Lim, W., et al. (2003). A novel coronavirus associated with severe acute respiratory syndrome. *N England J Med* 1–14.

Kuchta, R.D. (2010). Nucleotide analogues as probes for DNA and RNA polymerases. *Current Protocols in Chemical Biology* 2, 111–124.

Kulkarni, A.S., Damha, M.J., Schinazi, R.F., Mo, H., Doeble, B., Sagan, S.M., and Götte, M. (2016). A complex network of interactions between S282 and G283 of HCV NS5B and the template strand affect susceptibility to Sofosbuvir and Ribavirin. *Antimicrob. Agents Chemother.* AAC.02436–15–28.

Kumar, V., Shin, J.S., Shie, J.-J., Ku, K.B., Kim, C., Go, Y.Y., Huang, K.-F., Kim, M., and Liang, P.-H. (2017). Identification and evaluation of potent Middle East respiratory syndrome coronavirus (MERS-CoV) 3CLPro inhibitors. *Antiviral Res.* 141, 101–106.

Kumar, V., Tan, K.-P., Wang, Y.-M., Lin, S.-W., and Liang, P.-H. (2016). Identification, synthesis and evaluation of SARS-CoV and MERS-CoV 3C-like protease inhibitors. *Bioorg. Med. Chem.* 24, 3035–3042.

Kuo, L., and Masters, P.S. (2013). Functional analysis of the murine coronavirus genomic RNA packaging signal. *J. Virol.* 87, 5182–5192.

Lai, M.M., and Stohlman, S.A. (1978). RNA of mouse hepatitis virus. *J. Virol.* 26, 236–242.

Lai, M.M., and Stohlman, S.A. (1981). Comparative analysis of RNA genomes of mouse hepatitis viruses. *J. Virol.* 38, 661–670.

Lai, M.M., Patton, C.D., and Stohlman, S.A. (1982). Further characterization of mRNA's of mouse hepatitis virus: presence of common 5'-end nucleotides. *J. Virol.* 41, 557–565.

Lai, M.M.C. (2005). RNA replication without RNA-dependent RNA polymerase: Surprises from hepatitis delta virus. *J. Virol.* 79, 7951–7958.

Langmead, B., Wilks, C., Antonescu, V., and Charles, R. (2019). Scaling read aligners to hundreds of threads on general-purpose processors. *Bioinformatics* 35, 421–432.

Larder, B.A., Darby, G., and Richman, D.D. (1989). HIV with reduced sensitivity to zidovudine (AZT) isolated during prolonged therapy. *Science* 243, 1731–1734.

Larder, B., Kemp, S., and Harrigan, P. (1995). Potential mechanism for sustained antiretroviral efficacy of AZT-3TC combination therapy. *Science* *269*, 696–699.

Lau, S.K.P., Li, K.S.M., Tsang, A.K.L., Lam, C.S.F., Ahmed, S., Chen, H., Chan, K.-H., Woo, P.C.Y., and Yuen, K.-Y. (2013). Genetic characterization of Betacoronavirus lineage C Viruses in bats reveals marked sequence divergence in the spike protein of pipistrellus bat coronavirus HKU5 in Japanese pipistrelle: Implications for the origin of the novel Middle East respiratory syndrome coronavirus. *J. Virol.* *87*, 8638–8650.

Lauring, A.S., and Andino, R. (2010). Quasispecies theory and the behavior of RNA viruses. *PLoS Pathog* *6*, e1001005–e1001008.

Lavi, E., Suzumura, A., Hirayama, M., Highkin, M.K., Dambach, D.M., Silberberg, D.H., and Weiss, S.R. (1987). Coronavirus mouse hepatitis virus (MHV)-A59 causes a persistent, productive infection in primary glial cell cultures. *Microbial Pathogenesis* *3*, 79–86.

Lee, C., Lee, J.M., Lee, N.-R., Jin, B.-S., Jang, K.J., Kim, D.-E., Jeong, Y.-J., and Chong, Y. (2009). Aryl diketoacids (ADK) selectively inhibit duplex DNA-unwinding activity of SARS coronavirus NTPase/helicase. *Bioorganic & Medicinal Chemistry Letters* *19*, 1636–1638.

Lehmann, K.C., Gulyaeva, A., Zevenhoven-Dobbe, J.C., Janssen, G.M.C., Ruben, M., Overkleef, H.S., van Veelen, P.A., Samborskiy, D.V., Kravchenko, A.A., Leontovich, A.M., et al. (2015). Discovery of an essential nucleotidylating activity associated with a newly delineated conserved domain in the RNA polymerase-containing protein of all nidoviruses. *Nucleic Acids Res.* *43*, 8416-8434.

Leslie Fulcher, M., Gabriel, S., Burns, K.A., Yankaskas, J.R., and Randell, S.H. (2004). Well-differentiated human airway epithelial cell cultures. In *Human Cell Culture Protocols*, (New Jersey: Humana Press), pp. 183–206.

Leyssen, P., Balzarini, J., De Clercq, E., and Neyts, J. (2005). The predominant mechanism by which ribavirin exerts its antiviral activity in vitro against flaviviruses and paramyxoviruses is mediated by inhibition of IMP dehydrogenase. *J. Virol.* *79*, 1943–1947.

Li, H.S., Kuok, D.I.T., Cheung, M.C., Ng, M.M.T., Ng, K.C., Hui, K.P.Y., Peiris, J.S.M., Chan, M.C.W., and Nicholls, J.M. (2018). Effect of interferon alpha and cyclosporine treatment separately and in combination on Middle East respiratory syndrome coronavirus (MERS-CoV) replication in a human in-vitro and ex-vivo culture model. *Antiviral Res.* *155*, 89–96.

Li, W., Moore, M.J., Vasilieva, N., Sui, J., Wong, S.-K., Berne, M.A., Somasundaran, M., Sullivan, J.L., Luzuriaga, K., Greenough, T.C., et al. (2003). Angiotensin-converting enzyme 2 is a functional receptor for the SARS coronavirus. *Nature* *426*, 450–454.

Li, W., Wong, S.-K., Li, F., Kuhn, J.H., Huang, I.-C., Choe, H., and Farzan, M. (2006). Animal origins of the severe acute respiratory syndrome coronavirus: insight from ACE2-S-protein interactions. *J. Virol.* *80*, 4211–4219.

Liang, R., Wang, L., Zhang, N., Deng, X., Su, M., Su, Y., Hu, L., He, C., Ying, T., Jiang, S., et al. (2018). Development of small-molecule MERS-CoV inhibitors. *Viruses* *10*, 721.

Licitra, B.N., Duhamel, G.E., and Whittaker, G.R. (2014). Canine enteric coronaviruses: emerging viral pathogens with distinct recombinant spike proteins. *Viruses* *6*, 3363–3376.

Lim, Y.X., Ng, Y.L., Tam, J.P., and Liu, D.X. (2016). Human coronaviruses: A review of virus–host interactions. *Diseases* *2016*, Vol. 4, Page 26 4, 26.

Lin, F.-C., and Young, H.A. (2014). Interferons: Success in anti-viral immunotherapy. *Cytokine Growth Factor Rev.* *25*, 369–376.

Lin, M.-H., Moses, D.C., Hsieh, C.-H., Cheng, S.-C., Chen, Y.-H., Sun, C.-Y., and Chou, C.-Y. (2018). Disulfiram can inhibit MERS and SARS coronavirus papain-like proteases via different modes. *Antiviral Res.* *150*, 155–163.

Lo, M.K., Feldmann, F., Gary, J.M., Jordan, R., Bannister, R., Cronin, J., Patel, N.R., Klena, J.D., Nichol, S.T., Cihlar, T., et al. (2019). Remdesivir (GS-5734) protects African green monkeys from Nipah virus challenge. *Science Translational Medicine* *11*, eaau9242.

Lo, M.K., Jordan, R., Arvey, A., Sudhamsu, J., Shrivastava-Ranjan, P., Hotard, A.L., Flint, M., McMullan, L.K., Siegel, D., Clarke, M.O., et al. (2017a). GS-5734 and its parent nucleoside analog inhibit Filo-, Pneumo-, and Paramyxoviruses. *Scientific Reports* *7*, 43395.

Lo, M.K., Jordan, R., Arvey, A., Sudhamsu, J., Shrivastava-Ranjan, P., Hotard, A.L., Flint, M., McMullan, L.K., Siegel, D., Clarke, M.O., et al. (2017b). GS-5734 and its parent nucleoside analog inhibit Filo-, Pneumo-, and Paramyxoviruses. *Scientific Reports* *7*, 43395.

Lomniczi, B. (1977). Biological properties of avian coronavirus RNA. *J. Gen. Virol.* *36*, 531–533.

Lu, L., Liu, Q., Zhu, Y., Chan, K.-H., Qin, L., Li, Y., Wang, Q., Chan, J.F.-W., Du, L., Yu, F., et al. (2014). Structure-based discovery of Middle East respiratory syndrome coronavirus fusion inhibitor. *Nature Communications* *2019* *10*:1 5, 3067.

Lundin, A., Dijkman, R., Bergström, T., Kann, N., Adamiak, B., Hannoun, C., Kindler, E., Jónsdóttir, H.R., Muth, D., Kint, J., et al. (2014). Targeting membrane-bound viral RNA synthesis reveals potent inhibition of diverse coronaviruses including the Middle East respiratory syndrome virus. *PLoS Pathog* *10*, e1004166.

Lv, Z., Chu, Y., and Wang, Y. (2015). HIV protease inhibitors: a review of molecular selectivity and toxicity. *HIV AIDS (Auckl)* *7*, 95–104.

Lyons, D., and Lauring, A. (2018). Mutation and epistasis in influenza virus evolution. *Viruses* *10*, 407.

Macnaughton, M.R., and Madge, M.H. (1978). The genome of human coronavirus strain 229E. *J. Gen. Virol.* *39*, 497–504.

Mahmoud, S., Hasabelnaby, S., Hammad, S., and Sakr, T. (2018). Antiviral nucleoside and nucleotide analogs: A review. *Journal of Advanced Pharmacy Research* *2*, 73–88.

Manrubia Cuevas, S., Domingo, E., and Lázaro, E. (2010). Pathways to extinction: Beyond the error threshold.

Masters, P.S. (2006). The molecular biology of coronaviruses. *Advances in Virus Research* *66*, 193–292.

McBride, R., Van Zyl, M., and Fielding, B.C. (2014). The coronavirus nucleocapsid is a multifunctional protein. *Viruses* *6*, 2991–3018.

McIntosh, K., Kapikian, A.Z., Turner, H.C., Hartley, J.W., Parrott, R.H., and Chanock, R.M. (1970). Seroepidemiologic studies of coronavirus infection in adults and children. *American Journal of Epidemiology* *91*, 585–592.

Mehellou, Y., Balzarini, J., and McGuigan, C. (2009). Aryloxy phosphoramidate triesters: A technology for delivering monophosphorylated nucleosides and sugars into cells. *ChemMedChem* *4*, 1779–1791.

Menachery, V.D., Yount, B.L., Debbink, K., Agnihothram, S., Gralinski, L.E., Plante, J.A., Graham, R.L., Scobey, T., Ge, X.-Y., Donaldson, E.F., et al. (2015). A SARS-like cluster of circulating bat coronaviruses shows potential for human emergence. *Nature Medicine* *21*, 1508–1513.

Menachery, V.D., Yount, B.L., Jr., Sims, A.C., Debbink, K., Agnihothram, S.S., Gralinski, L.E., Graham, R.L., Scobey, T., Plante, J.A., Royal, S.R., et al. (2016). SARS-like WIV1-CoV poised for human emergence. *Proc Natl Acad Sci USA* *113*, 3048–3053.

Messina, J.P., Humphreys, I., Flaxman, A., Brown, A., Cooke, G.S., Pybus, O.G., and Barnes, E. (2015). Global distribution and prevalence of hepatitis C virus genotypes. *Hepatology* *61*, 77–87.

Migliaccio, G., Tomassini, J.E., Carroll, S.S., Tomei, L., Altamura, S., Bhat, B., Bartholomew, L., Bosserman, M.R., Ceccacci, A., Colwell, L.F., et al. (2003). Characterization of resistance to non-obligate chain-terminating ribonucleoside analogs that inhibit hepatitis C virus replication in vitro. *J. Biol. Chem.* *278*, 49164–49170.

Miller, V., Stürmer, M., Staszewski, S., Gröschel, B., Hertogs, K., de Béthune, M.-P., Pauwels, R., Harrigan, P.R., Bloor, S., Kemp, S.D., et al. (1998). The M184 V mutation in HIV-1 reverse transcriptase (RT) conferring lamivudine resistance does not result in broad cross-resistance to nucleoside analogue RT inhibitors. *Aids* *12*, 705–712.

Minskaia, E., Hertzig, T., Gorbatenya, A.E., Campanacci, V., Cambillau, C., Canard, B., and Ziebuhr, J. (2006). Discovery of an RNA virus 3“-5” exoribonuclease that is critically involved in coronavirus RNA synthesis. *Proc Natl Acad Sci USA* 1–6.

Moghadami, M. (2017). A narrative review of influenza: A seasonal and pandemic disease. *Iranian Journal of Medical Sciences* 42, 2–588.

Monchatre-Leroy, E., Boué, F., Boucher, J.-M., Renault, C., Moutou, F., Gouilh, M.A., and Umhang, G. (2017). Identification of Alpha and Beta coronavirus in wildlife species in France: Bats, rodents, rabbits, and hedgehogs. *Viruses* 9, 364.

Moni, M.A., and Pietro Liò (2014). Network-based analysis of comorbidities risk during an infection: SARS and HIV case studies. *BMC Bioinformatics* 2014 15:1 15, 333.

Moreno, H., Tejero, H., la Torre, de, J.C., Domingo, E., and Martín, V. (2012). Mutagenesis-mediated virus extinction: Virus-dependent effect of viral load on sensitivity to lethal defection. *PLoS ONE* 7, e32550–18.

Moscona, A. (2005). Neuraminidase inhibitors for influenza. *N. Engl. J. Med.* 353, 1363–1373.

Murakami, E., Niu, C., Bao, H., Micolochick Steuer, H.M., Whitaker, T., Nachman, T., Sofia, M.A., Wang, P., Otto, M.J., and Furman, P.A. (2008). The mechanism of action of β-D-2'-deoxy-2'-fluoro-2'-C-methylcytidine involves a second metabolic pathway leading to β-D-2'-deoxy-2"-fluoro-2-¹⁴C-methyluridine 5'-triphosphate, a potent inhibitor of the hepatitis C virus RNA-dependent RNA polymerase. *Antimicrob. Agents Chemother.* 52, 458–464.

Müller, C., Schulte, F.W., Lange-Grünweller, K., Obermann, W., Madhugiri, R., Pleschka, S., Ziebuhr, J., Hartmann, R.K., and Grünweller, A. (2018). Broad-spectrum antiviral activity of the eIF4A inhibitor silvestrol against corona- and picornaviruses. *Antiviral Res.* 150, 123–129.

Myrrha, L.W., Silva, F.M.F., Peternelly, E.F. de O., Junior, A.S., Resende, M., and de Almeida, M.R. (2011). The paradox of feline coronavirus pathogenesis: a review. *Adv Virol* 2011, 109849–8.

Nakagawa, K., Lokugamage, K.G., and Makino, S. (2016). Viral and cellular mRNA translation in coronavirus-infected cells. *Advances in Virus Research* 96, 165–192.

Nakamura, K., Oshima, T., Morimoto, T., Ikeda, S., Yoshikawa, H., Shiwa, Y., Ishikawa, S., Linak, M.C., Hirai, A., Takahashi, H., et al. (2011). Sequence-specific error profile of Illumina sequencers. *Nucleic Acids Research* 39, e90–e90.

Nakkazi, E. (2018). Randomised controlled trial begins for Ebola therapeutics. *Lancet* 392, 2338.

Nassar, M.S., Bakrebah, M.A., Meo, S.A., Alsabeyl, M.S., and Zaher, W.A. (2018). Global seasonal occurrence of Middle East respiratory syndrome coronavirus (MERS-CoV) infection. *European Review for Medical and Pharmacological Sciences* 1–6.

Ng, K.K.S., Arnold, J.J., and Cameron, C.E. (2008). Structure-function relationships among RNA-dependent RNA polymerases. In *RNA Interference*, (Berlin, Heidelberg: Springer Berlin Heidelberg), pp. 137–156.

Nikolenko, G.N., Palmer, S., Maldarelli, F., Mellors, J.W., Coffin, J.M., and Pathak, V.K. (2005). Mechanism for nucleoside analog-mediated abrogation of HIV-1 replication: Balance between RNase H activity and nucleotide excision. *Proc Natl Acad Sci USA* *102*, 2093–2098.

Nishimura, H., Mayama, M., Komatsu, Y., Kato, H., Shimaoka, N., and Tanaka, Y. (1964). Showdomycin, a new antibiotic from a *Streptomyces* Sp. *J. Antibiot.* *17*, 148–155.

Oh, M.-D., Park, W.B., Choe, P.G., Choi, S.-J., Kim, J.-I., Chae, J., Park, S.S., Kim, E.-C., Oh, H.S., Kim, E.J., et al. (2016). Viral load kinetics of MERS coronavirus infection. *N Engl J Med* *375*, 1303–1305.

Oma, V.S., Tråvén, M., Alenius, S., Myrmel, M., and Stokstad, M. (2016). Bovine coronavirus in naturally and experimentally exposed calves; viral shedding and the potential for transmission. *Virology Journal* *13*, 100.

Ortiz-Alcantara, J., Bhrdwaj, K., Palaninathan, S., Frieman, M., Baric, R.S., and Kao, C.C. Small molecule inhibitors of the SARS-CoV nsp15 endoribonuclease. *Virus Adaptation and Treatment* *2010*:2, 125–133.

Paarlberg, P. (2014). Updated estimated economic welfare impacts of porcine epidemic diarrhea virus (PEDV).

Paredes, R., Sagar, M., Marconi, V.C., Hoh, R., Martin, J.N., Parkin, N.T., Petropoulos, C.J., Deeks, S.G., and Kuritzkes, D.R. (2009). In vivo fitness cost of the M184V mutation in multidrug-resistant human immunodeficiency virus type 1 in the absence of lamivudine. *J. Virol.* *83*, 2038–2043.

Park, G.E., Ko, J.-H., Peck, K.R., Lee, J.Y., Lee, J.Y., Cho, S.Y., Ha, Y.E., Kang, C.-I., Kang, J.-M., Kim, Y.-J., et al. (2016). Control of an outbreak of Middle East respiratory syndrome in a tertiary hospital in Korea. *Ann Intern Med* *165*, 87–88.

Park, J.-Y., Yuk, H.J., Ryu, H.W., Lim, S.H., Kim, K.S., Park, K.H., Ryu, Y.B., and Lee, W.S. (2017). Evaluation of polyphenols from *Broussonetia papyrifera* as coronavirus protease inhibitors. *J Enzyme Inhib Med Chem* *32*, 504–515.

Pascal, K.E., Coleman, C.M., Mujica, A.O., Kamat, V., Badithe, A., Fairhurst, J., Hunt, C., Strein, J., Berrebi, A., Sisk, J.M., et al. (2015). Pre- and postexposure efficacy of fully human antibodies against spike protein in a novel humanized mouse model of MERS-CoV infection. *Proceedings of the National Academy of Sciences of the United States of America* *112*, 8738–8743.

Pau, A.K., and George, J.M. (2014). Antiretroviral therapy: current drugs. *Infect. Dis. Clin. North Am.* *28*, 371–402.

Peck, K.M., Burch, C.L., Heise, M.T., and Baric, R.S. (2015). Coronavirus host range expansion and Middle East respiratory syndrome coronavirus emergence: Biochemical mechanisms and evolutionary perspectives. [Http://Dx.Doi.org/10.1146/Annurev-Virology-100114-055029](http://Dx.Doi.org/10.1146/Annurev-Virology-100114-055029) 2, 95–117.

Peiris, J., CHU, C.M., Cheng, V., Chan, K.S., Hung, I., Poon, L., Law, K.I., Tang, B., Hon, T., Chan, C.S., et al. (2003). Clinical progression and viral load in a community outbreak of coronavirus-associated SARS pneumonia: a prospective study. *Lancet* 361, 1767–1772.

Perales, C., Agudo, R., Manrubia, S.C., and Domingo, E. (2011). Influence of mutagenesis and viral load on the sustained low-level replication of an RNA virus. *Journal of Molecular Biology* 407, 60–78.

Perlman, S., and Netland, J. (2009). Coronaviruses post-SARS: update on replication and pathogenesis. *Nat Rev Micro* 7, 439–450.

Peters, H.L., Jochmans, D., de Wilde, A.H., Posthuma, C.C., Snijder, E.J., Neyts, J., and Seley-Radtke, K.L. (2015). Design, synthesis and evaluation of a series of acyclic fleximer nucleoside analogues with anti-coronavirus activity. *Bioorganic & Medicinal Chemistry Letters* 25, 2923–2926.

Pfeiffer, J.K., and Kirkegaard, K. (2003a). A single mutation in poliovirus RNA-dependent RNA polymerase confers resistance to mutagenic nucleotide analogs via increased fidelity. *Proc Natl Acad Sci USA* 100, 7289–7294.

Pfeiffer, J.K., and Kirkegaard, K. (2003b). A single mutation in poliovirus RNA-dependent RNA polymerase confers resistance to mutagenic nucleotide analogs via increased fidelity. *Proc Natl Acad Sci USA* 1–6.

Pfeiffer, J.K., and Kirkegaard, K. (2005). Increased Fidelity Reduces Poliovirus Fitness and Virulence under Selective Pressure in Mice. *PLoS Pathog* 1, e11–e19.

Piret, J., and Boivin, G. (2011). Resistance of herpes simplex viruses to nucleoside analogues: Mechanisms, prevalence, and management. *Antimicrob. Agents Chemother.* 55, 459–472.

Pirrone, V., Thakkar, N., Jacobson, J.M., Wigdahl, B., and Krebs, F.C. (2011). Combinatorial approaches to the prevention and treatment of HIV-1 infection. *Antimicrob. Agents Chemother.* 55, 1831–1842.

Poch, O., Sauvaget, I., Delarue, M., and Tordo, N. (1989). Identification of four conserved motifs among the RNA-dependent polymerase encoding elements. *Embo* 8, 3867–3874.

Popowska, E., and Janion, C. (1974). N4-hydroxycytidine — A new mutagen of a base analogue type. *Biochemical and Biophysical Research Communications* 56, 459–466.

Popowska, E., and Janion, C. The metabolism of N4-hydroxycytidine – a mutagen for *Salmonella typhimurium*. *Nucleic Acids Research* 2, 1143–1152.

- Pradere, U., Garnier-Amblard, E.C., Coats, S.J., Amblard, F., and Schinazi, R.F. (2014). Synthesis of nucleoside phosphate and phosphonate prodrugs. *Chem. Rev.* *114*, 9154–9218.
- Principi, N., Camilloni, B., Alunno, A., Polinori, I., Argentiero, A., and Esposito, S. (2019). Drugs for Influenza Treatment: Is There Significant News? *Frontiers in Medicine* *6*, 697.
- Pruijssers, A.J., and Denison, M.R. (2019). Nucleoside analogues for the treatment of coronavirus infections. *Curr Opin Virol.* *35*, 57–62.
- Pyrc, K., Berkhout, B., and van der Hoek, L. (2007). The novel human coronaviruses NL63 and HKU1. *J. Virol.* *81*, 3051–3057.
- Pyrc, K., Bosch, B.J., Ben Berkhout, Jebbink, M.F., Dijkman, R., Rottier, P., and van der Hoek, L. (2006). Inhibition of human coronavirus NL63 infection at early stages of the replication cycle. *Antimicrob. Agents Chemother.* *50*, 2000–2008.
- Qi, X., Lan, S., Wang, W., Schelde, L.M., Dong, H., Wallat, G.D., Ly, H., Liang, Y., and Dong, C. (2010). Cap binding and immune evasion revealed by Lassa nucleoprotein structure. *Nature* *468*, 779–783.
- Ragno, R., Gioia, U., Pietro Laneve, Bozzoni, I., Mai, A., and Caffarelli, E. (2011). Identification of small-molecule inhibitors of the XendoU endoribonucleases family. *ChemMedChem* *6*, 1797–1805.
- Raj, V.S., Mou, H., Smits, S.L., Dekkers, D.H.W., Müller, M.A., Dijkman, R., Muth, D., Demmers, J.A.A., Zaki, A., Fouchier, R.A.M., et al. (2013). Dipeptidyl peptidase 4 is a functional receptor for the emerging human coronavirus-EMC. *Nature* *495*, 251–254.
- Ramanathan, A., Robb, G.B., and Chan, S.-H. (2016). mRNA capping: biological functions and applications. *Nucleic Acids Research* *44*, 7511–7526.
- Ravi, S.J., Snyder, M.R., and Rivers, C. (2019). Review of international efforts to strengthen the global outbreak response system since the 2014–16 West Africa Ebola Epidemic. *Health Policy and Planning* *34*, 47–54.
- Reynard, O., Nguyen, X.-N., Alazard-Dany, N., Barateau, V., Cimarelli, A., and Volchkov, V.E. (2015). Identification of a new ribonucleoside inhibitor of Ebola virus replication. *Viruses* *7*, 6233–6240.
- Robertson, K.D., Hayward, S.D., Ling, P.D., Samid, D., and Ambinder, R.F. (1995). Transcriptional activation of the Epstein-Barr virus latency C promoter after 5-azacytidine treatment: evidence that demethylation at a single CpG site is crucial. *Mol. Cell. Biol.* *15*, 6150–6159.
- Rooke, R., Tremblay, M., Soudeyns, H., DeStephano, L., Yao, X.J., Fanning, M., Montaner, J.S., O'Shaughnessy, M., Gelmon, K., and Tsoukas, C. (1989). Isolation of drug-resistant variants of

HIV-1 from patients on long-term zidovudine therapy. Canadian Zidovudine Multi-Centre Study Group. *Aids* 3, 411–415.

Rozen-Gagnon, K., Stapleford, K.A., Mongelli, V., Blanc, H., Failloux, A.-B., Saleh, M.-C., and Vignuzzi, M. (2014). Alphavirus mutator variants present host-specific defects and attenuation in mammalian and insect models. *PLoS Pathog* 10, e1003877.

Saberi, A., Gulyaeva, A.A., Brubacher, J.L., Newmark, P.A., and Gorbalenya, A.E. (2018). A planarian nidovirus expands the limits of RNA genome size. *PLoS Pathog* 14, e1007314.

Saijo, M., Morikawa, S., Fukushi, S., MIZUTANI, T., HASEGAWA, H., NAGATA, N., IWATA, N., and KURANE, I. (2005). Inhibitory effect of mizoribine and ribavirin on the replication of severe acute respiratory syndrome (SARS)-associated coronavirus. *Antiviral Research* 66, 159–163.

Salganik, R.I., Vasjunina, E.A., Poslovina, A.S., and Andreeva, I.S. (1973). Mutagenic action of N4-Hydroxycytidine on *Escherichia coli* B *cyt-*. *Mutation Research/Fundamental and Molecular Mechanisms of Mutagenesis* 20, 1–5.

Sangawa, H., Komeno, T., Nishikawa, H., Yoshida, A., Takahashi, K., Nomura, N., and Furuta, Y. (2013). Mechanism of action of T-705 ribosyl triphosphate against influenza virus RNA polymerase. *Antimicrob. Agents Chemother.* 57, 5202–5208.

Sanjuán, R., Moya, A., and Elena, S.F. (2004). The contribution of epistasis to the architecture of fitness in an RNA virus. *Proc Natl Acad Sci USA* 101, 15376–15379.

Sanjuan, R., Nebot, M.R., Chirico, N., Mansky, L.M., Belshaw, R. (2010). Viral mutation rates. *J Virol* 84, 9733–9748.

Sankaranantham, M. (2019). HIV - Is a cure possible? *Indian J Sex Transm Dis AIDS* 40, 1–5.

Sawicki, S.G., and Sawicki, D.L. (1998). A new model for coronavirus transcription. In *Coronaviruses and Arteriviruses*, (New York, NY: Springer, Boston, MA), pp. 215–219.

Sawicki, S.G., Sawicki, D.L., and Siddell, S.G. (2007). A contemporary view of coronavirus transcription. *J. Virol.* 81, 20–29.

Schwarz, B., Routledge, E., and Siddell, S.G. (1990). Murine coronavirus nonstructural protein ns2 is not essential for virus replication in transformed cells. *J. Virol.* 64, 4784–4791.

Scobey, T., Yount, B.L., Sims, A.C., Donaldson, E.F., Agnihothram, S.S., Menachery, V.D., Graham, R.L., Swanstrom, J., Bove, P.F., Kim, J.D., et al. (2013). Reverse genetics with a full-length infectious cDNA of the Middle East respiratory syndrome coronavirus. *Proc Natl Acad Sci USA* 110, 16157–16162.

- Seley-Radtke, K.L., and Yates, M.K. (2018). The evolution of nucleoside analogue antivirals: A review for chemists and non-chemists. Part 1: Early structural modifications to the nucleoside scaffold. *Antiviral Research* *154*, 66–86.
- Sexton, N.R., Smith, E.C., Blanc, H., Vignuzzi, M., Peersen, O.B., and Denison, M.R. (2016). Homology-based identification of a mutation in the coronavirus RNA-dependent RNA polymerase that confers resistance to multiple mutagens. *J. Virol.* *90*, 7415–7428.
- Sheahan, T.P., Sims, A.C., Graham, R.L., Menachery, V.D., Gralinski, L.E., Case, J.B., Leist, S.R., Pyrc, K., Feng, J.Y., Trantcheva, I., et al. (2017). Broad-spectrum antiviral GS-5734 inhibits both epidemic and zoonotic coronaviruses. *Science Translational Medicine* 1–11.
- Shi, T., McAllister, D.A., O'Brien, K.L., Simoes, E.A.F., Madhi, S.A., Gessner, B.D., Polack, F.P., Balsells, E., Acacio, S., Aguayo, C., et al. (2017). Global, regional, and national disease burden estimates of acute lower respiratory infections due to respiratory syncytial virus in young children in 2015: a systematic review and modelling study. *Lancet* *390*, 946–958.
- Shu, B., and Gong, P. (2016). Structural basis of viral RNA-dependent RNA polymerase catalysis and translocation. *Proc Natl Acad Sci USA* *113*, E4005–E4014.
- Sierra, S., Dávila, M., Lowenstein, P.R., and Domingo, E. (2000). Response of foot-and-mouth disease virus to increased mutagenesis: Influence of viral load and fitness in loss of infectivity. *J. Virol.* *74*, 8316–8323.
- Simmons, G., Gosalia, D.N., Rennekamp, A.J., Reeves, J.D., Diamond, S.L., and Bates, P. (2005). Inhibitors of cathepsin L prevent severe acute respiratory syndrome coronavirus entry. *Proc Natl Acad Sci USA* *102*, 11876–11881.
- Simon-Loriere, E., and Holmes, E.C. (2011). Why do RNA viruses recombine? *Nature Reviews Microbiology* *2016* *14:8* 9, 617–626.
- Sims, A.C., Baric, R.S., Yount, B., Burkett, S.E., Collins, P.L., and Pickles, R.J. (2005). Severe acute respiratory syndrome coronavirus infection of human ciliated airway epithelia: Role of ciliated cells in viral spread in the conducting airways of the lungs. *J. Virol.* *79*, 15511–15524.
- Sims, A.C., Tilton, S.C., Menachery, V.D., Gralinski, L.E., Schäfer, A., Matzke, M.M., Webb-Robertson, B.-J.M., Chang, J., Luna, M.L., Long, C.E., et al. (2013). Release of severe acute respiratory syndrome coronavirus nuclear import block enhances host transcription in human lung cells. *J. Virol.* *87*, 3885–3902.
- Singh, S., Tank, N.K., Dwiwedi, P., Charan, J., Kaur, R., Sidhu, P., and Chugh, V.K. (2018). Monoclonal antibodies: A review. *Curr Clin Pharm* *13*, 85–99.
- Sinokrot, H., Smerat, T., Najjar, A., and Karaman, R. (2017). Advanced prodrug strategies in nucleoside and non-nucleoside antiviral agents: A review of the recent five years. *Molecules* *22*, 1736.

Siu, Y.L., Teoh, K.T., Lo, J., Chan, C.M., Kien, F., Escriou, N., Tsao, S.W., Nicholls, J.M., Altmeyer, R., Peiris, J.S.M., et al. (2008). The M, E, and N structural proteins of the severe acute respiratory syndrome coronavirus are required for efficient assembly, trafficking, and release of virus-like particles. *J. Virol.* *82*, 11318–11330.

Slusarczyk, M., Serpi, M., and Pertusati, F. (2018). Phosphoramidates and phosphonamidates (ProTides) with antiviral activity. *Antiviral Chem. and Chemo.* *26*, 204020661877524.

Smith, E.C., Blanc, H., Vignuzzi, M., and Denison, M.R. (2013). Coronaviruses lacking exoribonuclease activity are susceptible to lethal mutagenesis: Evidence for proofreading and potential therapeutics. *PLoS Pathog* *9*, e1003565–11.

Smith, E.C., Case, J.B., Blanc, H., Isakov, O., Shomron, N., Vignuzzi, M., and Denison, M.R. (2015). Mutations in coronavirus nonstructural protein 10 decrease virus replication fidelity. *J. Virol.* *89*, 6418–6426.

Smith, E.C., Sexton, N.R., and Denison, M.R. (2014). Thinking outside the triangle: Replication fidelity of the largest RNA viruses. *Annual Review of Virology* *1*, 111–132.

Snijder, E.J., Bredenbeek, P.J., Dobbe, J.C., Thiel, V., Ziebuhr, J., Poon, L.L.M., Guan, Y., Rozanov, M., Spaan, W.J.M., and Gorbalenya, A.E. (2003). Unique and conserved features of genome and proteome of SARS-coronavirus, an early split-off from the coronavirus group 2 lineage. *Journal of Molecular Biology* *331*, 991–1004.

Sofia, M.J., Chang, W., Furman, P.A., Mosley, R.T., and Ross, B.S. (2012). Nucleoside, nucleotide, and non-nucleoside inhibitors of hepatitis C virus NS5B RNA-dependent RNA-polymerase. *J. Med. Chem.* *55*, 2481–2531.

Soriano, V., Vispo, E., Labarga, P., Medrano, J., and Barreiro, P. (2010). Viral hepatitis and HIV co-infection. *Antiviral Research* *85*, 303–315.

Stadler, K., Massignani, V., Eickmann, M., Becker, S., Abrignani, S., Klenk, H.-D., and Rappuoli, R. (2003). SARS--beginning to understand a new virus. *Nat Rev Micro* *1*, 209–218.

Stapleford, K.A., Rozen-Gagnon, K., Das, P.K., Saul, S., Poirier, E.Z., Blanc, H., Vidalain, P.-O., Merits, A., and Vignuzzi, M. (2015). Viral polymerase-helicase complexes regulate replication fidelity to overcome intracellular nucleotide depletion. *J. Virol.* *89*, 11233–11244.

Stark, G.R., Kerr, I.M., Williams, B.R., Silverman, R.H., and Schreiber, R.D. (1998). How cells respond to interferons. *Annu. Rev. Biochem.* *67*, 227–264.

Stockman, L.J., Bellamy, R., and Garner, P. (2006). SARS: Systematic review of treatment effects. *PLoS Medicine* *3*, e343.

Streeter, D.G., Witkowski, J.T., Khare, G.P., Sidwell, R.W., Bauer, R.J., Robins, R.K., and Simon, L.N. (1973). Mechanism of action of 1-β-D-ribofuranosyl-1,2,4-triazole-3-carboxamide (Virazole), a new broad-spectrum antiviral agent. *Proc Natl Acad Sci USA* *70*, 1174–1178.

Ströher, U., DiCaro, A., Li, Y., Strong, J.E., Aoki, F., Plummer, F., Jones, S.M., and Feldmann, H. (2004). Severe acute respiratory syndrome-related coronavirus is inhibited by interferon-alpha. *J Infect Dis.* *189*, 1164–1167.

Stuyver, L.J., Whitaker, T., McBrayer, T.R., Hernandez-Santiago, B.I., Lostia, S., Tharnish, P.M., Ramesh, M., Chu, C.K., Jordan, R., Shi, J., et al. (2003). Ribonucleoside analogue that blocks replication of bovine viral diarrhea and hepatitis C viruses in culture. *Antimicrob. Agents Chemother.* *47*, 244–254.

Subissi, L., Posthuma, C.C., Collet, A., Zevenhoven-Dobbe, J.C., Gorbatenya, A.E., Decroly, E., Snijder, E.J., Canard, B., and Imbert, I. (2014). One severe acute respiratory syndrome coronavirus protein complex integrates processive RNA polymerase and exonuclease activities. *Proc Natl Acad Sci USA* *111*, E3900–E3909.

Sun, Y., Wang, Z., Tao, J., Wang, Y., Wu, A., Yang, Z., Wang, K., Shi, L., Chen, Y., and Guo, D. (2014). Yeast-based assays for the high-throughput screening of inhibitors of coronavirus RNA cap guanine-N7-methyltransferase. *Antiviral Res.* *104*, 156–164.

Svarovskaia, E.S., Gane, E., Dvory-Sobol, H., Martin, R., Doehle, B., Hedskog, C., Jacobson, I.M., Nelson, D.R., Lawitz, E., Brainard, D.M., et al. (2016). L159F and V321A sofosbuvir-associated hepatitis C virus NS5B substitutions. *J Infect Dis.* *213*, 1240–1247.

Svoboda, T., Henry, B., Shulman, L., Kennedy, E., Rea, E., Ng, W., Wallington, T., Yaffe, B., Gournis, E., Vicencio, E., et al. (2004). Public health measures to control the spread of the severe acute respiratory syndrome during the outbreak in Toronto. *N. Engl. J. Med.* *350*, 2352–2361.

Śledziewska-Gójska, E., and Janion, C. (1982). Effect of proofreading and *dam*-instructed mismatch repair systems on N4-Hydroxycytidine-induced mutagenesis. *Molec. Gen. Genet.* *186*, 411–418.

Tan, E.L.C., Ooi, E.E., Lin, C.-Y., Tan, H.C., Ling, A.-E., Lim, B., and Stanton, L.W. (2004). Inhibition of SARS coronavirus infection in vitro with clinically approved antiviral drugs. *Emerging Infectious Diseases* *10*, 581–586.

Tang, C.-M., Yau, T.O., and Yu, J. (2014). Management of chronic hepatitis B infection: Current treatment guidelines, challenges, and new developments. *World J. Gastroenterol.* *20*, 6262–6278.

Tanner, J.A., Watt, R.M., Chai, Y.-B., Lu, L.-Y., Lin, M.C., Peiris, J.S.M., Poon, L.L.M., Kung, H.-F., and Huang, J.-D. (2003). The severe acute respiratory syndrome (SARS) coronavirus NTPase/helicase belongs to a distinct class of 5' to 3' viral helicases. *J. Biol. Chem.* *278*, 39578–39582.

Tanner, J.A., Zheng, B.-J., Zhou, J., Watt, R.M., Jiang, J.-Q., Wong, K.-L., Lin, Y.-P., Lu, L.-Y., He, M.-L., Kung, H.-F., et al. (2005). The adamantane-derived bananins are potent inhibitors of the helicase activities and replication of SARS coronavirus. *Chemistry & Biology* *12*, 303–311.

Taylor, R., Kotian, P., Warren, T., Panchal, R., Bavari, S., Julander, J., Dobo, S., Rose, A., El-Kattan, Y., Taubenheim, B., et al. (2016). BCX4430 – A broad-spectrum antiviral adenosine nucleoside analog under development for the treatment of Ebola virus disease. *Journal of Infection and Public Health* 9, 220–226.

Tchesnokov, E.P., Feng, J.Y., Porter, D.P., and Götte, M. (2019). Mechanism of inhibition of Ebola virus RNA-dependent RNA polymerase by remdesivir. *Viruses* 11, 326.

Te, H.S., Randall, G., and Jensen, D.M. (2007). Mechanism of action of ribavirin in the treatment of chronic hepatitis C. *Gastroenterology Hepatology* 1–8.

Tejero, H., Montero, F., and Nuño, J.C. (2016). Theories of lethal mutagenesis: From error catastrophe to lethal defection. *Curr. Top. Microbiol. Immunol.* 392, 161–179.

Terrault, N.A., Lok, A.S.F., McMahon, B.J., Chang, K.M., Hwang, J.P., Jonas, M.M., Brown, R.S., Bzowej, N.H., and Wong, J.B. (2018). Update on prevention, diagnosis, and treatment of chronic hepatitis B: AASLD 2018 hepatitis B guidance. *Hepatology* 67, 1560–1599.

Thompson, A.J.V., Ayres, A., Yuen, L., Bartholomeusz, A., Bowden, D.S., Iser, D.M., Chen, R.Y.M., Demediuk, B., Shaw, G., Bell, S.J., et al. (2007). Lamivudine resistance in patients with chronic hepatitis B: Role of clinical and virological factors. *J. Gastroenterol. Hepatol.* 22, 1078–1085.

Totura, A.L., and Bavari, S. (2019). Broad-spectrum coronavirus antiviral drug discovery. *Expert Opin Drug Discov* 14, 397–412.

Twu, S.-J., Chen, T.-J., Chen, C.-J., Olsen, S.J., Lee, L.-T., Fisk, T., Hsu, K.-H., Chang, S.-C., Chen, K.-T., Chiang, I.-H., et al. (2003). Control measures for severe acute respiratory syndrome (SARS) in Taiwan. *Emerging Infectious Diseases* 9, 1–3.

Urakova, N., Kuznetsova, V., Crossman, D.K., Sokratian, A., Guthrie, D.B., Kolykhalov, A.A., Lockwood, M.A., Natchus, M.G., Crowley, M.R., Painter, G.R., et al. (2017). β -D-N4-Hydroxycytidine is a potent anti-alphavirus compound that induces high level of mutations in viral genome. *J. Virol.* 92, 491.

van der Hoek, L., Pyrc, K., Jebbink, M.F., Vermeulen-Oost, W., Berkhout, R.J.M., Wolthers, K.C., Wertheim-van Dillen, P.M.E., Kaandorp, J., Spaargaren, J., and Berkhout, B. (2004). Identification of a new human coronavirus. *Nature Medicine* 10, 368–373.

Van Rompay, A.R., Johansson, M., and Karlsson, A. (2000). Phosphorylation of nucleosides and nucleoside analogs by mammalian nucleoside monophosphate kinases. *Pharmacology & Therapeutics* 87, 189–198.

Velthuis, te, A.J.W., Arnold, J.J., Cameron, C.E., van den Worm, S.H.E., and Snijder, E. (2009). The RNA polymerase activity of SARS-coronavirus nsp12 is primer dependent. *Nucleic Acids Research* 38, 203–214.

- Velthuis, te, A.J.W. (2014). Common and unique features of viral RNA-dependent polymerases. *Cell. Mol. Life Sci.* *71*, 4403–4420.
- Venkataraman, S., Prasad, B.V.L.S., and Selvarajan, R. (2018). RNA dependent RNA polymerases: Insights from structure, function and evolution. *Viruses* *10*, 76.
- Vere Hodge, R.A., and Field, H.J. (2013). Antiviral agents for herpes simplex virus. In *Antiviral Agents*, (Elsevier), pp. 1–38.
- Vernekar, S.K.V., Qiu, L., Zhang, J., Kankanala, J., Li, H., Geraghty, R.J., and Wang, Z. (2015). 5'-silylated 3'-1,2,3-triazolyl thymidine analogues as inhibitors of West Nile virus and dengue virus. *J. Med. Chem.* *58*, 4016–4028.
- Visher, E., Whitefield, S.E., McCrone, J.T., Fitzsimmons, W., and Lauring, A.S. (2016). The mutational robustness of influenza A virus. *PLoS Pathog* *12*, e1005856.
- Wainberg, M.A., Rooke, R., Tremblay, M., Li, X., Parniak, M.A., Gao, Q., Yao, X.J., Tsoukas, C., Montaner, J., Fanning, M., et al. (1991). Clinical significance and characterization of AZT-resistant strains of HIV-1. *Can J Infect Dis* *2*, 5–11.
- Wainberg, M.A., Drosopoulos, W.C., Salomon, H., Hsu, M., Borkow, G., Parniak, M.A., Gu, Z., Song, Q., Manne, J., Islam, S., et al. (1996). Enhanced fidelity of 3TC-selected mutant HIV-1 reverse transcriptase. *Science* *271*, 1282–1285.
- Walsh, E.E., Shin, J.H., and Falsey, A.R. (2013). Clinical impact of human coronaviruses 229E and OC43 infection in diverse adult populations. *J Infect Dis* *208*, 1634–1642.
- Wang, M., Ng, K.K.S., Cherney, M.M., Chan, L., Yannopoulos, C.G., Bedard, J., Morin, N., Nguyen-Ba, N., Alaoui-Ismaili, M.H., Bethell, R.C., et al. (2003). Non-nucleoside analogue inhibitors bind to an allosteric site on HCV NS5B polymerase. *J. Biol. Chem.* *278*, 9489–9495.
- Wang, Q., Vlasova, A.N., Kenney, S.P., and Saif, L.J. (2019). Emerging and re-emerging coronaviruses in pigs. *Curr Opin Virol* *34*, 39–49.
- Wang, Y., Sun, Y., Wu, A., Xu, S., Pan, R., Zeng, C., Jin, X., Ge, X., Shi, Z., Ahola, T., et al. (2015). Coronavirus nsp10/nsp16 methyltransferase can be targeted by nsp10-derived peptide in vitro and in vivo to reduce replication and pathogenesis. *J. Virol.* *89*, 8416–8427.
- Warren, T.K., Jordan, R., Lo, M.K., Ray, A.S., Mackman, R.L., Soloveva, V., Siegel, D., Perron, M., Bannister, R., Hui, H.C., et al. (2016). Therapeutic efficacy of the small molecule GS-5734 against Ebola virus in rhesus monkeys. *Nature* *531*, 381–385.
- Warren, T.K., Wells, J., Panchal, R.G., Stuthman, K.S., Garza, N.L., Van Tongeren, S.A., Dong, L., Retterer, C.J., Eaton, B.P., Pegoraro, G., et al. (2015). Protection against filovirus diseases by a novel broad-spectrum nucleoside analogue BCX4430. *Nature* *508*, 402–405.

- Wilm, A., Aw, P.P.K., Bertrand, D., Yeo, G.H.T., Ong, S.H., Wong, C.H., Khor, C.C., Petric, R., Hibberd, M.L., and Nagarajan, N. (2012). LoFreq: a sequence-quality aware, ultra-sensitive variant caller for uncovering cell-population heterogeneity from high-throughput sequencing datasets. *Nucleic Acids Research* *40*, 11189–11201.
- Wilson, L., Gage, P., and Ewart, G. (2006). Hexamethylene amiloride blocks E protein ion channels and inhibits coronavirus replication. *Virology* *353*, 294–306.
- White House (2005). The national strategy for pandemic influenza. 1–17.
- Woo, P.C.Y., Lau, S.K.P., Chen, Y., Wong, E.Y.M., Chan, K.-H., Chen, H., Zhang, L., Xia, N., and Yuen, K.-Y. (2018). Rapid detection of MERS coronavirus-like viruses in bats: Potential for tracking MERS coronavirus transmission and animal origin. *Emerg Microbes Infect* *7*, 18–7.
- Woo, P.C.Y., Lau, S.K.P., Chu, C.-M., Chan, K.-H., Tsui, H.-W., Huang, Y., Wong, B.H.L., Poon, R.W.S., Cai, J.J., Luk, W.-K., et al. (2005). Characterization and complete genome sequence of a novel coronavirus, coronavirus HKU1, from patients with pneumonia. *J. Virol.* *79*, 884–895.
- Woo, P.C.Y., Lau, S.K.P., Yip, C.C.Y., Huang, Y., and Yuen, K.-Y. (2009). More and more coronaviruses: Human coronavirus HKU1. *Viruses* *1*, 57–71.
- Woo, P.C.Y., Wang, M., Lau, S.K.P., Xu, H., Poon, R.W.S., Guo, R., Wong, B.H.L., Gao, K., Tsui, H.-W., Huang, Y., et al. (2007). Comparative analysis of twelve genomes of three novel group 2c and group 2d coronaviruses reveals unique group and subgroup features. *J. Virol.* *81*, 1574–1585.
- World Health Organization (2018). Managing epidemics. 1–260.
- Wray, S.K., Gilbert, B.E., Noall, M.W., and Knight, V. (1985). Mode of action of ribavirin: Effect of nucleotide pool alterations on influenza virus ribonucleoprotein synthesis. *Antiviral Research* *5*, 29–37.
- Wu, C.-Y., Jan, J.-T., Ma, S.-H., Kuo, C.-J., Juan, H.-F., Cheng, Y.-S.E., Hsu, H.-H., Huang, H.-C., Wu, D., Brik, A., et al. (2004). Small molecules targeting severe acute respiratory syndrome human coronavirus. *Proc Natl Acad Sci USA* *101*, 10012–10017.
- Xia, S., Liu, Q., Wang, Q., Sun, Z., Su, S., Du, L., Ying, T., Lu, L., and Jiang, S. (2014). Middle East respiratory syndrome coronavirus (MERS-CoV) entry inhibitors targeting spike protein. *Virus Research* *194*, 200–210.
- Xing, Y., and Proesmans, M. (2019). New therapies for acute RSV infections: where are we? *Eur J Pediatr* *178*, 131–138.
- Xu, X. (2003). Molecular model of SARS coronavirus polymerase: Implications for biochemical functions and drug design. *Nucleic Acids Research* *31*, 7117–7130.

- Xu, X., Zhai, Y., Sun, F., Lou, Z., Su, D., Xu, Y., Zhang, R., Joachimiak, A., Zhang, X.C., Bartlam, M., et al. (2006). New antiviral target revealed by the hexameric structure of mouse hepatitis virus nonstructural protein nsp15. *J. Virol.* *80*, 7909–7917.
- Yang, D., and Leibowitz, J.L. (2015). The structure and functions of coronavirus genomic 3' and 5' ends. *Virus Research* *206*, 120–133.
- Yang, H., Xie, W., Xue, X., Yang, K., Ma, J., Liang, W., Zhao, Q., Zhou, Z., Pei, D., Ziebuhr, J., et al. (2005). Design of wide-spectrum inhibitors targeting coronavirus main proteases. *PLoS Biol.* *3*, e324.
- Yang, Y., Du, L., Liu, C., Wang, L., Ma, C., Tang, J., Baric, R.S., Jiang, S., and Li, F. (2014). Receptor usage and cell entry of bat coronavirus HKU4 provide insight into bat-to-human transmission of MERS coronavirus. *Proc Natl Acad Sci USA* *111*, 12516–12521.
- Yang, Y.-M., Hsu, C.-Y., Lai, C.-C., Yen, M.-F., Wikramaratna, P.S., Chen, H.-H., and Wang, T.-H. (2017). Impact of comorbidity on fatality rate of patients with Middle East respiratory syndrome. *Scientific Reports* *7*, 11307.
- Yoon, J.-J., Toots, M., Lee, S., Lee, M.-E., Ludeke, B., Luczo, J.M., Ganti, K., Cox, R.M., Sticher, Z.M., Edpuganti, V., et al. (2018). Orally efficacious broad-spectrum ribonucleoside analog inhibitor of influenza and respiratory syncytial viruses. *Antimicrob. Agents Chemother.* *62*, 1427.
- Yoon, J.-S., Kim, G., Jarhad, D.B., Kim, H.-R., Shin, Y.-S., Qu, S., Sahu, P.K., Kim, H.O., Lee, H.W., Wang, S.B., et al. (2019). Design, synthesis, and anti-RNA virus activity of 6'-fluorinated-aristeromycin analogues. *J. Med. Chem.* *62*, 6346–6362.
- Yount, B., Curtis, K.M., Fritz, E.A., Hensley, L.E., Jahrling, P.B., Prentice, E., Denison, M.R., Geisbert, T.W., and Baric, R.S. (2011). Reverse genetics with a full-length infectious cDNA of severe acute respiratory syndrome coronavirus. *Proc Natl Acad Sci USA* *100*, 12995–13000.
- Yount, B., Denison, M.R., Weiss, S.R., and Baric, R.S. (2002). Systematic assembly of a full-length infectious cDNA of mouse hepatitis virus strain A59. *J. Virol.* *76*, 11065–11078.
- Yu, M.-S., Lee, J., Lee, J.M., Kim, Y., Chin, Y.-W., Jee, J.-G., Keum, Y.-S., and Jeong, Y.-J. (2012). Identification of myricetin and scutellarein as novel chemical inhibitors of the SARS coronavirus helicase, nsP13. *Bioorganic & Medicinal Chemistry Letters* *22*, 4049–4054.
- Zaki, A.M., van Boheemen, S., Bestebroer, T.M., Osterhaus, A.D.M.E., and Fouchier, R.A.M. (2012). Isolation of a novel coronavirus from a man with pneumonia in Saudi Arabia. *N England J Med* *367*, 1814–1820.
- Zeng, J., Wang, H., Xie, X., Yang, D., Zhou, G., and Yu, L. (2013). An increased replication fidelity mutant of foot-and-mouth disease virus retains fitness in vitro and virulence in vivo. *Antiviral Research* *100*, 1–7.

Zeng, Z.-Q., Chen, D.-H., Tan, W.-P., Qiu, S.-Y., Xu, D., Liang, H.-X., Chen, M.-X., Li, X., Lin, Z.-S., Liu, W.-K., et al. (2018). Epidemiology and clinical characteristics of human coronaviruses OC43, 229E, NL63, and HKU1: a study of hospitalized children with acute respiratory tract infection in Guangzhou, China. *Eur. J. Clin. Microbiol. Infect. Dis.* *37*, 363–369.

Zhang, R., Li, Y., Cowley, T.J., Steinbrenner, A.D., Phillips, J.M., Yount, B.L., Baric, R.S., and Weiss, S.R. (2015). The nsp1, nsp13, and M proteins contribute to the hepatotropism of murine coronavirus JHM.WU. *J. Virol.* *89*, 3598–3609.

Zhao, L., Rose, K.M., Elliott, R., Van Rooijen, N., and Weiss, S.R. (2011). Cell-type-specific type I interferon antagonism influences organ tropism of murine coronavirus. *J. Virol.* *85*, 10058–10068.

Zhou, N., Pan, T., Zhang, J., Li, Q., Zhang, X., Bai, C., Huang, F., Peng, T., Zhang, J., Liu, C., et al. (2016). Glycopeptide antibiotics potently inhibit cathepsin L in the late endosome/lysosome and block the entry of Ebola virus, Middle East respiratory syndrome coronavirus (MERS-CoV), and severe acute respiratory syndrome coronavirus (SARS-CoV). *J. Biol. Chem.* *291*, 9218–9232.

Zhu, Z., Chakraborti, S., He, Y., Roberts, A., Sheahan, T., Xiao, X., Hensley, L.E., Prabakaran, P., Rockx, B., Sidorov, I.A., et al. (2007). Potent cross-reactive neutralization of SARS coronavirus isolates by human monoclonal antibodies. *Proc Natl Acad Sci USA* *104*, 12123–12128.

Zumla, A., Chan, J.F.W., Azhar, E.I., Hui, D.S.C., and Yuen, K.-Y. (2016). Coronaviruses - drug discovery and therapeutic options. *Nature Reviews Drug Discovery* *15*, 327–347.